GES 653–756

ISSN 0003–2654

ROYAL SOCIETY
OF
CHEMISTRY

The Analyst

A monthly international journal dealing with all branches of the theory and practice of analytical chemistry, including instrumentation and sensors, and physical, biochemical, clinical, pharmaceutical, biological, environmental, automatic and computer-based methods

Vol.114 No.6 June 1989

The Analyst

The Analytical Journal of The Royal Society of Chemistry

Editorial Manager, Analytical Journals
Judith Egan

Editor, The Analyst
Janet Dean

Assistant Editors
Paul Delaney, Mandy Mackenzie, Harpal Minhas

Editorial Office: The Royal Society of Chemistry, Thomas Graham House, Science Park, Milton Road, Cambridge CB4 4WF. Telephone 0223 420066. Telex No. 818293 ROYAL. Fax 0223 423623.

Advertisements: Advertisement Department, The Royal Society of Chemistry, Burlington House, Piccadilly, London, W1V 0BN. Telephone 01-437 8656. Telex No. 268001.

The Analyst (ISSN 0003–2654) is published monthly by The Royal Society of Chemistry, Burlington House, London W1V 0BN, England. All orders accompanied with payment should be sent directly to The Royal Society of Chemistry, The Distribution Centre, Blackhorse Road, Letchworth, Herts. SG6 1HN, England. 1989 Annual subscription rate UK £200.00, Rest of World £230.00, USA $460.00. Purchased with *Analytical Abstracts* UK £432.50, Rest of World £490.00, USA $963.00. Purchased with *Analytical Abstracts* plus *Analytical Proceedings* UK £510.00, Rest of World £580.00, USA $1142.00. Purchased with *Analytical Proceedings* UK £254.00, Rest of World £292.00, USA $584.00. Air freight and mailing in the USA by Publications Expediting Inc., 200 Meacham Avenue, Elmont, NY 11003.
USA Postmaster: Send address changes to: *The Analyst*, Publications Expediting Inc., 200 Meacham Avenue, Elmont, NY 11003. Second class postage paid at Jamaica, NY 11431. All other despatches outside the UK by Bulk Airmail within Europe, Accelerated Surface Post outside Europe. PRINTED IN THE UK.

Information for Authors

Full details of how to submit material for publication in *The Analyst* are given in the Instructions to Authors in the January issue. Separate copies are available on request.

The Analyst publishes papers on all aspects of the theory and practice of analytical chemistry, fundamental and applied, inorganic and organic, including chemical, physical, biochemical, clinical, pharmaceutical, biological, environmental, automatic and computer-based methods. Papers on new approaches to existing methods, new techniques and instrumentation, detectors and sensors, and new areas of application with due attention to overcoming limitations and to underlying principles are all equally welcome. There is no page charge.

The following types of papers will be considered:

Full papers, describing original work.

Short papers: the criteria regarding originality are the same as for full papers, but short papers generally report less extensive investigations or are of limited breadth of subject matter

Communications, which must be on an urgent matter and be of obvious scientific importance. Rapidity of publication is enhanced if diagrams are omitted, but tables and formulae can be included. Communications receive priority and are usually published within 5–8 weeks of receipt. They are intended for brief descriptions of work that has progressed to a stage at which it is likely to be valuable to workers faced with similar problems. A fuller paper may be offered subsequently, if justified by later work.

Reviews, which must be a critical evaluation of the existing state of knowledge on a particular facet of analytical chemistry.

Every paper (except Communications) will be submitted to at least two referees, by whose advice the Editorial Board of *The Analyst* will be guided as to its acceptance or rejection. Papers that are accepted must not be published elsewhere except by permission. Submission of a manuscript will be regarded as an undertaking that the same material is not being considered for publication by another journal.

Regional Advisory Editors. For the benefit of potential contributors outside the United Kingdom, a Panel of Regional Advisory Editors exists. Requests for help or advice on any matter related to the preparation of papers and their submission for publication in *The Analyst* can be sent to the nearest member of the Panel. Currently serving Regional Advisory Editors are listed in each issue of *The Analyst.*

Manuscripts (three copies typed in double spacing) should be addressed to:
The Editor, *The Analyst,*
Royal Society of Chemistry,
Thomas Graham House,
Science Park,
Milton Road,
CAMBRIDGE CB4 4WF, UK

Particular attention should be paid to the use of standard methods of literature citation, including the journal abbreviations defined in Chemical Abstracts Service Source Index. Wherever possible, the nomenclature employed should follow IUPAC recommendations, and units and symbols should be those associated with SI.

All queries relating to the presentation and submission of papers, and any correspondence regarding accepted papers and proofs, should be directed to the Editor, *The Analyst* (address as above). Members of the Analytical Editorial Board (who may be contacted directly or via the Editorial Office) would welcome comments, suggestions and advice on general policy matters concerning *The Analyst.*

Fifty reprints of each published contribution are supplied free of charge, and further copies can be purchased.

Research and Development of Biosensors*

A Review

Frieder Scheller, Florian Schubert, Dorothea Pfeiffer, Rainer Hintsche, Ina Dransfeld, Reinhard Renneberg, Ulla Wollenberger, Klaus Riedel, Mariana Pavlova, Manfred Kühn and Hans-Georg Müller
Central Institute of Molecular Biology, Academy of Sciences of the GDR, 1115 Berlin-Buch, GDR
Pham minh Tan and Werner Hoffmann
Central Institute of Nuclear Research, Academy of Sciences of the GDR, 8101 Dresden-Rossendorf, GDR
Werner Moritz
Humboldt University Berlin, Section of Chemistry, 1040 Berlin, GDR

Keywords: *Biosensors; research and development; review*

Introduction

Selectivity is a problem of paramount importance in analytical chemistry and it is generally achieved by means of selective chemical reactions. Extraordinarily selective and versatile reagents are provided by nature in the form of enzymes, antibodies and receptors.

Enzyme technology has exploited the use of biological components in analytical systems by the development of immobilised enzymes and immunocomponents which may be re-used. The invention of enzyme test strips by Free and Free[1] has opened the way for simplification of the analytical procedure: the sample is merely dropped on to the test strip, thus avoiding the need to dilute or take aliquots of the sample and reconstitution of the reagents. However, test strips are one-way materials and the reagents may not be re-used after enzyme immobilisation. Another breakthrough in the application of immobilised enzymes to analytical chemistry was made by Clark and Lyons[2] in 1962. Based on the principle of their membrane-covered oxygen electrode, an enzyme solution was entrapped by a semi-permeable membrane placed in front of the indicator electrode. This step provided a reusable enzyme and hence represented the birth of the first biosensor.

Biosensors are devices which use immobilised biomolecules combined with transducers to detect or respond to specific interactions with environmental chemicals.[3] In order to achieve optimal signal transfer, the immobilised biocomponent is in close physical contact with the transducer unit (Fig. 1).

Types of Biosensor

Basically there are two types of biosensor differing in the mode of signal generation (Fig. 1). Direct bioaffinity sensors utilise a binding event to detect substances. The binding of the incoming analyte to the complementary immobilised bioligand results in a change in the conformation of the biomolecule and/or physical changes in the immobilisation medium such as changes in charge, thickness, temperature or optical parameters (colour or fluorescence). By analogy with

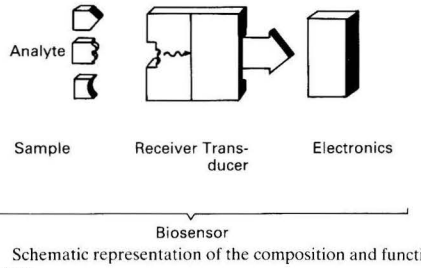

Fig. 1. Schematic representation of the composition and function of a biosensor

* Invited lecture presented at the International Bio Symposium, Nagoya 88, Nagoya, Japan, 10–13 March, 1988.

affinity chromatography, well known complementary pairs of analyte and bioligand are used for molecular recognition in bioaffinity sensors (Table 1). The second basic sensor type is the enzymatic/metabolic biosensor. Here recognition of the substrate by the immobilised receiver (enzymes on different levels of integration, *i.e.*, purified enzymes, organelles, micro-organisms or tissue slices) is followed immediately by chemical conversion to the corresponding product, which is detected.

A combination of both principles, binding of the analyte without its chemical conversion and signal generation by converting an auxiliary substance, is realised in "catalytic" biosensors for the determination of prosthetic groups and inhibitors, and in enzyme immunosensors.

State of Development of Test Strips and Enzyme Electrodes

Dry Reagent Tests

Providing a reagent in dry form for rapid use is by no means novel; litmus paper, which dates back to the 19th century, is an example. The first major impact of dry chemistry on clinical testing was the introduction in the 1950s of the Ames Clinistix[4] for the indication of urinary glucose. The further development of dry reagent chemistry has been the cumulation of several technologies; typically, a reagent zone consisting of several different layers is fixed above a reflective zone constructed with pigments such as TiO_2 or $BaSO_4$ on a support layer. For removing corpuscular particles, *e.g.*, red blood cells, the sample is dropped on to a separation layer at the top of the test strip. The chemical reactions are monitored typically by diffuse reflectance, whereas measurements of light transmission or fluorescence are less frequent occurrences. With the first approach, any light not absorbed by the products in the reaction layer is reflected to the detecting system from the underlying reflective zone. The analyte concentration is derived relative to known (reflectance) standards with a non-linear concentration dependence. As the enzyme layer and the optical transducer are separate entities, test strips cannot be classed as biosensors. However, they may be considered to form the basis of optoelectronic biosensors (optrodes).

Dry reagent test systems have been described for serum metabolites, enzymes, serum electrolytes and therapeutic drugs.[4] Dry reagent assays for nearly all commonly measured blood metabolites, namely glucose, blood urea nitrogen, uric acid, cholesterol, triglycerides, creatinine and bilirubin, are available commercially. In their highly complex, layered reaction systems, conversion of the analyte either releases hydrogen peroxide or causes a change in pH. Subsequently, a colour-producing peroxidase-catalysed reaction or the absorbance change of a pH-indicator is evaluated.

Sophisticated dry reagents are also available for the determination of serum enzymes such as creatine kinase, lactate dehydrogenase, transaminases, γ-glutamyltransferase, α-amylase and alkaline phosphatase. Ion-selective membranes, combined with either potentiometric or spectrometric detection, are used for the determination of K^+, Na^+, Cl^- and CO_2 in serum. The K^+ electrode consists of a base support and an Ag - AgCl layer, which is covered with a hydrophobic membrane containing the ionophore valinomycin. The sample is deposited on the ion-selective layer and the potential difference is measured *versus* an identical reference electrode system loaded with a KCl solution of known concentration. Therapeutic drugs are accessible by the competitive protein binding assay based on substrate-labelled fluorescence immunoassays. Using this principle, theophylline can be determined in the concentration range 1–5 μg ml^{-1}.

Generations of Biosensors

Whereas dry chemistry research focuses more on commercial applications, it is the phenomenological and fundamental aspects that are under intensive investigation in the field of biosensors. From an integrational point of view, biosensors may be subdivided into three generations.[5] The simplest approach is based on membrane-entrapped or membrane-bound biocomponents (first generation). Clark and Lyons[2] used a highly concentrated enzyme solution held in a reaction chamber by a membrane placed in front of the slightly recessed indicator electrode and thus created the enzyme electrode. This represents the unit consisting of dialyser, reactor and electrochemical transducer and has led to considerable simplification of the experimental set-up compared with that of conventional analysers. The direct adsorptive or covalent fixation of biocomponents at the transducer surface leads to the elimination of inactive membrane layers. Additional covalent coupling of the cosubstrate[6] is a pre-condition of reagentless measuring regimes (second generation). In this variant no reagent has to be added to the sample. This approach has been continued by immobilising the cofactor[7] or electron relays[8] in the neighbourhood of the active centre of the enzyme. A more recent principle of sensor integration is the combination of molecular recognition and signal processing at the biocomponent level.[9] This results in "high quality" chemical information at the transducer surface. Finally, immobilisation of the biocomponent directly on an electronic element (third generation), *e.g.*, on the gate of a field-effect transistor (FET), which directly senses and amplifies changes in surface properties, integrates biospecific recognition and electronic signal processing.[10,11] This permits differential elimination of disturbances and statistical evaluation with multi-gate sensors.

Various patents and scientific publications describe biosensors of the first and second generation for the determination of about 120 different parameters including substrates, cofactors, prosthetic groups, hormones, antigens and enzyme activities. Among biosensors, biospecific electrodes are at the forefront with respect to the number of measurable substances, the body of published data and the degree of commercialisation.

Table 1. Types of biosensor

Analyte	Bioaffinity ligand	Signal-generating step	Sensor type
Substrate analogues	Enzymes	Binding of the analyte	Binding sensor (pure)
Antigens, Haptens	Antibodies		
Viruses, Cells, Glycoproteins	Lectins		
Prosthetic groups	Apoenzymes	Conversion of an auxiliary substance	Catalytic biosensor
Inhibitors	Enzymes		
Enzyme-labelled antigens	Antibodies		
Substrates	Enzymes	Chemical conversion of the analyte	Metabolic/enzymatic sensor
	Organelles		
Cofactors	Microbes		

Substrates Measured With Biosensors

Amino acids. D-Alanine, L-arginine, L-asparagine, L-aspartic acid, L-cysteine, L-glutamine, L-glutamate, glutathione, L-histidine, L- and D-leucine, L-lysine, L- and D-methionine, *N*-acetylmethionine, L- and D-phenylalanine, sarcosine, serine, L-tyrosine, L-tryptophan and D-valine.

Gases. NH_3, H_2, CH_4, SO_2, NO, O_2, CO and CO_2.

Cofactors. Adenosine monophosphate (AMP), adenosine triphosphate (ATP), pyridoxalphosphate (PLP), pyridine nucleotides (NADPH), flavin adenine dinucleotide (FAD), H_2O_2, thiamine pyrophosphate (TPP) and phosphoenolpyruvate (PEP).

Carbohydrates. Amygdaline, lactose, galactose, maltose, glucose, sucrose, glucose 6-phosphate, starch and fructose.

Amines, amides and heterocyclic compounds. Adenosine, aminopyrine, aniline, aromatic amines, acetylcholine, choline, phosphatidylcholine, creatinine, creatine, guanidine, guanosine, penicillin, spermine, uric acid, urea, xanthine and hypoxanthine.

Organic acids or their salts. Acetate, formate, malate, gluconate, glyoxylate, D-isocitrate, L- and D-lactate, maleic acid, glycolate, nitrilotriacetic acid, oxalate, oxaloacetate, pyruvate and succinate.

Alcohols and phenols. Bilirubin, catechol, cholesterol, cholesterol esters, ethanol, glycerol, glycerol esters, methanol, phenol and 2,4-dinitrophenol.

Inorganic ions. Fluoride, nitrite, nitrate, phosphate, sulphate, sulphide, sulphite, Hg^{2+}, Zn^{2+} and Cu^{2+}.

Enzymes and proteins. Thyroxine, human albumin, proinsulin, immunoglobulin G, α-fetoprotein, human choriogonadotropin, peroxidase, α-amylase, glucoamylase, cholinesterase, creatine kinase, pyruvate kinase, lactate dehydrogenase, transaminases and pullulanase.

Miscellaneous. Antibiotics, blood groups, assimilable substances, volatile substances, biochemical oxygen demand, meat freshness, mutagenicity, vitamins, peptides, theophylline and testosterone.

Analytical Parameters of Enzyme Electrodes

Linear calibration graphs of enzyme electrode based analysers usually extend over 2–3 decades of concentration, with a detection limit of 10–100 μM. This sensitivity is sufficiently high to determine the previously mentioned compounds, using 10–100-μl sample volumes. The precision of the measurements is reflected by coefficients of variation of about 1%. The most evident advantage of enzyme electrodes is their negligible enzyme consumption; it is typically in the order of 10^{-3} U per sample.

At present, the sample throughput of enzyme electrode based analysers is limited to a maximum of about 100 samples h^{-1}. For example, the application of a glucose electrode containing the enzyme in a polyurethane layer in a stirred measuring cell permits a sampling frequency of 120 samples h^{-1}.[12] In a flow injection (FI) system for which the measuring time at 1% carry-over is only 12 s, a throughput of 300 samples h^{-1} is possible. The response is linear from the detection limit of 10 μM up to 100 mM glucose. The relative standard deviation for 25 successive injections of 1 mM glucose solution is 0.5%. This highly effective FI system has also been extended to the measurement of lactate[13]; 200 lactate samples h^{-1} can be measured with good precision and negligible carry-over. Such a high sample throughput is realised even with double-membrane type sensors. Therefore, application of biosensors of the second or third generation will speed up the measuring process further. Actually, amperometric enzyme microelectrodes for glucose and enzyme FETs for urea characterised by response times for the steady-state signal of only 3–4 s have been developed by Japanese workers.[11,14,15] The combination of these biosensors with optimised FI devices should permit the determination of 700 samples h^{-1}, a value recently reported for an FI system using soluble enzyme reagents.[16]

Both for measuring undiluted samples and for continuous monitoring of biologically active substances (*e.g.*, in the blood-stream, fermenters or wastewater), the measuring range of biosensors has to be adapted to the respective analyte concentration. In blood or fermentation broths the concentration of metabolites generally exceeds the upper limit of the calibration graph of enzyme electrodes (Fig. 2). For continuous *in vivo* monitoring of metabolites such as glucose or lactate, the linear measurement region has to be extended to higher concentrations; this can be done by decreasing the diffusion-controlled substrate flow to the enzyme layer[17,18] or by exploiting mediator chemically modified electrodes.[19–23] On the other hand, the concentration of many hormones, drugs or toxins is several orders of magnitude below the limit of detection of enzyme electrodes. Immunoelectrodes permit the specific determination of these substances in the picomolar range. However, so far, the applicability of many immunosensors is restricted by their extremely long measuring time.

If substrate concentrations in the nanomolar range are to be detected, the sensitivity of enzyme electrodes can be enhanced using substrate amplification by two enzymes.[5] Operational conditions have to be adjusted in such a way that one enzyme catalyses regeneration of the substrate of the second enzyme (Fig. 3). This has been achieved by coupling dehydrogenases with oxidases or transaminases, or by coupling kinases. For a lactate sensor, using lactate oxidase (LOD) and lactate dehydrogenase (LDH) immobilised in poly(vinyl chloride), Mizutani *et al.*[24] obtained a maximum amplification factor of 250 for the steady-state current. Using a very thin enzyme layer of co-immobilised LOD and LDH, a much higher amplification, up to 4100-fold, is possible.[25] Theoretical considerations demonstrate that the maximum amplification obtained in the latter system is a realistic value for the parameters of the enzyme membrane used, namely, the characteristic diffusion time and the first-order rate constant. However, application of these recycling systems to "real" samples is restricted by their sensitivity to both substrates of the enzymatic cycle, in this instance lactate and pyruvate. For example, the determination of lactate in plasma using this method requires the endogenous pyruvate to be removed first.

By combining glucose oxidase (GOD) and glucose dehydro-

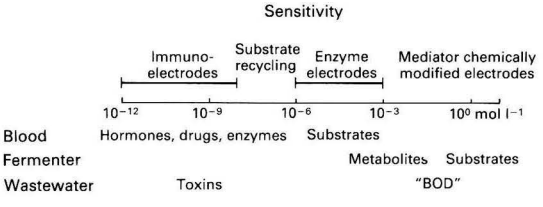

Fig. 2. Measuring range of biosensors compared with typical analyte concentrations

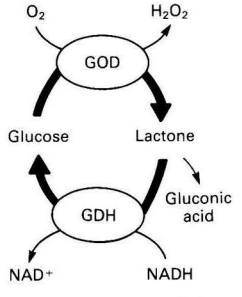

Fig. 3. Diagram of two-enzyme cycles for the increase in cosubstrate conversion for signal amplification in biosensors

genase the sensitivity of a glucose sensor has been increased by a factor of 10.[26] This enzyme system seems more promising for, in physiological media, the second substrate, gluconolactone, is not present; therefore, the enhanced signal is only related to the glucose concentration.

For signal amplification in the determination of the cofactors adenosine triphosphate (ATP) and adenosine diphosphate (ADP), hexokinase (HK) and pyruvate kinase (PK) were co-immobilised with LDH and lactate mono-oxygenase(LMO).[27] The last two were used to transduce pyruvate formation sequentially into oxygen consumption. In the presence of an excess of glucose and phosphoenolpyruvate, the nucleoside phosphate is shuttled between the kinases. Pyruvate is formed in much higher amounts than the amount of cofactor in the enzyme layer. The linear range of the sensor extends up to 6 μM ADP with a 200-fold increase in sensitivity compared with the unamplified signal in the absence of glucose.

By combining the amplification system for ADP with that for pyruvate using LOD and LDH, "double amplification" for ADP should be possible. In this system the excess of pyruvate formed in the kinase cycle enters the second cycle, where it is amplified further.

Recently a patent was taken out for an amplification scheme differing from those discussed so far in that the recycling is effected by only one enzyme[28]: LDH normally catalyses the establishment of the reaction equilibrium between pyruvate and nicotinamide adenine dinucleotide (NADH) to give lactate and the oxidised cofactor. On the other hand, in the presence of NAD^+, LDH catalyses the oxidation of the unusual substrate glyoxylate to oxalate with concomitant formation of NADH (Fig. 4). If both reactions are conducted simultaneously, *i.e.*, in the presence of pyruvate, glyoxylate and limiting amounts of NADH, the cofactor is shuttled between them. Thus a 170-fold increase in lactate is formed over the reaction without glyoxylate, leading to a detection limit for NADH of 50 nM. This type of "monoenzymatic recycling" might facilitate the design of novel and simple enzymatic amplification systems.

Application in the Clinical Laboratory

The measurement of glucose dominates the application of enzyme electrodes. Significant problems in the "pre-analytics" of blood glucose determination are the complete inhibition of the glucose-consuming glycolytic reactions and the glucose contained in erythrocytes. The latter problem has been neglected by several manufacturers of analysers prescribing the use of undiluted blood samples. The Gluco 20 A analyser (Fuji, Tokyo, Japan), using 20 μl of undiluted whole blood, gives good correlation with the hexokinase method only for serum. The glucose values measured in whole blood are 13% too low.[29] The same tendency has been reported for the Auto Stat GA-1100 (Daiichi, Kyoto, Japan) and for the analyser from Yellow Springs Instruments, Yellow Springs, OH, USA.[30] A comparison between undiluted blood and 1 + 10 pre-diluted samples has been conducted using the Glukometer GKM manual analyser (ZWG, Berlin, GDR).[31] With direct injection of undiluted blood the glucose values are 18.8% lower than those obtained for pre-diluted samples. This difference shows that the transport of glucose from the red blood cells into the bulk solution is incomplete during the response time (4 s). In contrast, the results obtained with pre-diluted samples agree well with those of the GOD - peroxidase method. Recently the problem of glucose degradation during sample storage and transport has been solved. Neither storage at 4 °C nor addition of the aldolase inhibitor fluoride resulted in acceptable stability. However, blood dilution (1 + 50) in a hypotonic buffer gave excellent stability and also good correlation with established methods.[31]

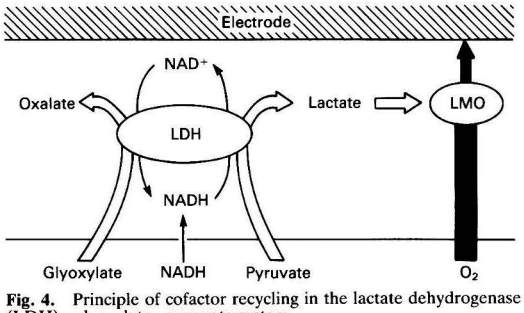

Fig. 4. Principle of cofactor recycling in the lactate dehydrogenase (LDH) - glyoxylate - pyruvate system

The problems that have been discussed also present serious challenges to the application of test strips. It is well known that the values measured with aqueous standard solutions, serum and blood differ substantially. Therefore the procedure for calibration of the strips for blood glucose measurement is laborious.

The first biosensor of the second generation has been made commercially available by Genetics International, Abingdon, UK.[32] This blood glucose sensor is based on the ferrocene-mediated glucose oxidation developed by groups in Cranfield and Oxford. The device consists of a pen-sized instrument coupled with a small, disposable strip electrode. The patient has to apply a drop of fresh blood to the sensor, push a single button and wait for the result, which appears after 30 s. Comparison with an automatic analyser yields the regression line $y = 1.04x + 4.9$ mg dl^{-1}. The serial precision for capillary or venous blood is reflected by coefficients of variation of 8.1% at 53.9 mg dl^{-1} and 3.9% at 85.8 mg dl^{-1}. Obviously these values do not compete with those of laboratory analysers. By comparison with alternative devices for measuring blood glucose at home the sensor has the following advantages: (i) a response time of only 30 s; (ii) a much simpler operating procedure; and (iii) small size and portability. The sensor will allow diabetics to control their diet, insulin injection and intake of oral antidiabetic drugs.

An important parameter for the diagnosis of kidney disease and for the control of artificial kidney dialysis is the concentration of urea in serum. For the determination of urea, urease-based potentiometric sensors are well established. Further, an amperometric urea sensor based on the pH-dependent anodic oxidation of hydrazine has been described.[33] The advantages of this method are a linear calibration graph, in contrast to the logarithmic response of potentiometric sensors, excellent reproducibility, a sample throughput of 40 samples h^{-1} and a measurement range of 1–80 mmol $^{-1}$ in the sample. Combined with the Glukometer this amperometric urea sensor has been applied successfully to urea monitoring in dialysis patients. Such process control results in a considerable decrease in cost and a reduction in the patient's discomfort.

For the sequential determination of lactate and pyruvate, an enzyme electrode with co-immobilised LDH and lactate mono-oxygenase has been developed.[34] Owing to optimum enzyme loading and the equality of the diffusion coefficients of the two substrates, this sensor is characterised by having identical sensitivities towards lactate and pyruvate. Therefore it is suitable for the sequential determination of lactate and pyruvate, the ratio of which is important diagnostically. The same electrode has also been used to measure glutamate pyruvate transaminase activity in blood serum and pyruvate kinase activity in red blood cells.[35]

Direct measurement of cholinesterase activity in serum samples is possible using the Glukometer. The rate of formation of thiocholine from butyrylthiocholine iodide is evaluated electrochemically[36] and the esterase activity is indicated only 20 s after injection of the sample. Also, inhibitors of this enzyme are easily measured: 40 s after

addition of the respective compound to the pooled serum sample of a given cholinesterase activity the degree of inhibition is reflected by the remaining activity. This inherent kinetic measuring principle is an important advantage over other methods, *e.g.*, the use of test strips, where a given time regime has to be followed very closely.

By analogy with the optimisation of exercise control in sportsmen, the fitness of race horses has been checked by measuring the blood lactate level.[37]

The lactose content in the urine of cows is of economic importance. During the acute phase of the udder disease mastitis the lactose concentration exceeds 10 mM[38] (Fig. 5). Therefore, typically, lactose concentrations are monitored to screen for this disease.

Fermentation

Biotechnologists already take advantage of process control in setting the conditions for fermentations: temperature, stirrer speed and pH are controlled by closed-loop circuits. In addition to these parameters the concentrations of several nutrients, *e.g.*, carbohydrates and amino acids, and, most importantly, those of the final products have to be controlled. The cost of growth media is extremely high, particularly for cell cultures. Therefore the consumption of the key nutrients, such as glucose, glutamine and other amino acids, has to be monitored in order to reconstitute the medium by feeding the appropriate substances. To control nutrient consumption and lactate formation in a cell fermenter producing human growth hormone (hGH) the Glukometer analyser has been used either in conjunction with an enzyme electrode for glucose or lactate, respectively, or with a microbial sensor (Fig. 6). The increase in the number of cells is paralleled by a decrease in the nutrient concentration as reflected by the signals of the glucose electrode and the microbial sensor. On the other hand, lactate in the medium is observed to increase.

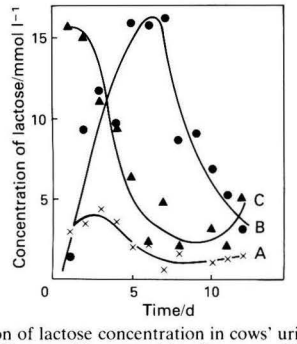

Fig. 5. Variation of lactose concentration in cows' urine with time. A, Healthy cow; B, cow with acute udder disease; and C, recovery of normal lactose level after mastitis

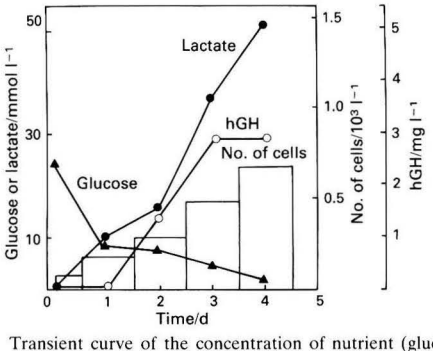

Fig. 6. Transient curve of the concentration of nutrient (glucose) and of metabolite (lactate) measured by enzyme electrodes and of human growth hormone (hGH) produced by fermentation during the cultivation cycle of human cells

Whereas the determination of high relative molecular mass fermentation products (*e.g.*, hGH) using biosensors is not yet possible, such instruments have been developed for measuring the concentration of lysine, ethanol, gluconic acid and penicillin in diluted samples of the fermentation broth.[39]

The number of reports in the field of *in situ* fermenter control is relatively small owing to the following peculiarities: (i) sterilisation of the fermenter denatures the biocomponent of the sensor; (ii) elevated temperatures during operation decrease functional stability; and (iii) the analyte concentrations exceed the dynamic range of the sensor. Nevertheless, the *in situ* application of enzyme electrodes has been studied for the measurement of penicillin, glucose and ethanol.

An autoclavable enzyme electrode for penicillin was developed by Enfors and Nilsson.[40] After the heat-sterilisation process a β-lactamase solution is pumped into the reaction chamber placed in front of a flat glass electrode. This arrangement also allows the enzyme to be exchanged during the fermentation process; hence an extended sensor lifetime is achieved. In order to eliminate disturbances caused by a drift in pH in the fermenter, an enzyme-free pH electrode is combined with the enzyme electrode in the differential mode. The requirements for operation in a suitable concentration range are partly fulfilled. Measurement in the fermentation broth yields a linear response up to 30 mM, whereas in penicillin, fermentation concentrations of up to 50 mM are produced.

The concentration of carbohydrates, such as glucose, in the fermentation broth generally exceeds the measuring range of "normal" enzyme electrodes. Cleland and Enfors[41] extended the linear response of a GOD-based sensor by electrolytic generation of oxygen in the enzyme layer and internal dilution of the sample inside the sensor housing. Thus the linear response has been extended up to 0.5 M glucose and the electrode can be used in completely anaerobic media.

Using an oxygen-independent ferrocene-modified GOD electrode Brooks *et al.*[42] have been able to extend the measuring range to 70 mM glucose. With continuous use of the electrode its half-life is about 6 d. To study the short-term kinetics of alcoholic fermentation by aerobic yeast an alcohol oxidase based electrode was developed by Verduyn *et al.*[43] The dissolved oxygen tension in the fermenter was kept between 95 and 100% by vigorous stirring and aeration. Fluctuations in this value were compensated for by an enzyme-free reference oxygen electrode. In the future, continuous measurement of biomacromolecules by immunosensors will offer an attractive alternative to the existing discontinuous methods for the detection of gene products such as interferons, insulin and monoclonal antibodies.

Commercialisation

Dry chemistry has made great inroads in clinical laboratories. Instrumentation ranges in size from hand-held to large free-standing devices. Examples of hand-held instruments are the Glucometer reflectance photometer (Ames Division, Miles, Elkhart, IN, USA) and the Reflocheck (Boehringer Mannheim, Mannheim, FRG). Bench-top manual instrumentation is available for handling more than one analyte, *e.g.*, the Seralyzer system from Ames Division with a specific module for each test. Here the analysis time ranges from 30 s to 5 min.

Fully automated analysis is possible with the Ektachem 400 (Eastman Kodak, Rochester, NY, USA), which is capable of 500 tests h^{-1} and has ten different assays available at present. The operator only has to provide the sample and select the desired tests.

Because biosensors perform non-destructive measurements on a "real-time" basis their application results in almost revolutionary advantages of cost-saving automation and data

Table 2. Enzyme electrode based analysers

Company	Model	Analyte	Range of measurement/ mmol l^{-1}	Sample throughput/ samples h^{-1}	Coefficient of variation, %	Stability
Yellow Springs Instruments, Yellow Springs, OH, USA	23A	Glucose	1–45	40	<2	300 samples
	23L	Lactate	0–15	40		
	27	Ethanol	0–60	20	<2	
		Lactose, Galactose, Sucrose	0–55	20	2	
Zentrum für Wissenschaftlichen Gerätebau (ZWG), Berlin, GDR	Glukometer	Glucose	0.5–50	60–90	1.5	>1000 samples
		Uric acid	0.1–1.2	40	2	10 d
Fuji Electric, Tokyo, Japan	Gluco 20	Glucose	0–27	80–90	1.7	>500 samples
		α-Amylase		30	4–5	
	UA-300A	Uric acid		50–60	3	
Daiichi, Kyoto, Japan	Auto Stat GA-1120	Glucose	1–40	60–120	1	
Radelkis, Budapest, Hungary	OP-GL-7110S	Glucose	1.7–20	40	5–10	240 d
Ferment, Vilnius, USSR	ExAn	Glucose	2.5–30	20	3	
La Roche, Basle, Switzerland	LA 640	Lactate	0.5–12	20–30	<5	40 d
Omron Tateisi, Kyoto, Japan	HER-100	Lactate	0–8.3		<5	10 d
Seres, Aix-en-Provence, France	Enzymat	Glucose	0.3–22	60		
		Choline	1.0–29	60		
		L-Lysine	0.1–2	60		
		D-Lactate	0.5–20	60		
Tacussel, Lyon, France	Glucoprocesseur	Glucose	0.05–5	90	<2	>2000 samples
Prüfgeräte-Werk (PGW), Medingen, GDR (Eppendorf, FRG)	ADM 300	Glucose	1–100	80	<2	>2000 samples
	ECA 20 (ESAT 6660)	Glucose	0.6–60	120–130	<1.5	10 d
		Lactate	1–30	120	<2	14 d
		Uric acid	0.1–1.2	80	<2	10 d

Table 3. Analytical characteristics of routinely used biospecific electrodes

Analyte	Enzyme*	Range mmol l^{-1}	Range μmol l^{-1} s^{-1}	Sample throughput/ samples h^{-1}	CV, %	Lifetime/ d	Correlation
Lactate	LMO	1–40	—	60	1	55	$y = -0.1 + 1.03x$ $r = 0.998$ ($n = 30$, plasma)
Pyruvate + lactate	LDH - LMO	0–7	—	20	2	55	—
Glucose	GOD	0.4–44	—	120	2	10	$y = -0.015 + 1.003x$ $r = 0.99$ ($n = 196$, blood) $y = 0.32 + 1.047x$ $r = 0.990$ ($n = 100$, serum) $y = 0.149 \pm 1.105 + (0.958 \pm 0.009)x$ $r = 0.995$ ($n = 20$, urine)
Lactose	GOD - β-gal.	1–150	—	100	1.5	20	—
Maltose	GOD - GA	1–50	—	60	2	14	—
Sucrose	GOD - MR - IN	1–44	—	40	1.5	5	—
Glutamate	GLOD	0.04–40	—	40	1.5	10	—
Uric acid	Uricase	0.1–1.2	—	40	1.6	10	$y = 0.0198 + 19.8x$ $r = 0.995$ ($n = 30$)
Urea	Urease	0.8–50	—	40	1	15	$y = 0.125 + 0.9912x$ $r = 0.997$ ($n = 67$, dialysate)
Phosphate	GOD - AcP	2–24	—	12	2	—	—
Lactate dehydrogenase	LMO	—	1–20	15	2	55	$y = 0.29 + 1.11x$ $r = 0.999$ ($n = 30$, serum)
Pyruvate kinase	LDH - LMO	—	1–14	15	3	55	$y = 0.002 + 1.003x$ $r = 0.984$ ($n = 20$)
Creatine kinase	PK - LDH - LMO	—	5–80	10	—	14	—
Acetylcholine esterase	—		20–400	40	2	21	$y = 1.70 + 0.986x$ $r = 0.993$ ($n = 205$, serum)
Alanine aminopeptidase	—	—	0.1–1	—	—	—	$y = 0.064 + 0.973x$ $r = 0.994$ ($n = 32$, serum)

* LMO = lactate mono-oxygenase; LDH = lactate dehydrogenase; PK = pyruvate kinase; GOD = glucose oxidase; GLOD = glutamate oxidase; β-gal. = β-galactosidase; GA = glucoamylase; MR = mutarotase; IN = invertase; and AcP = acid phosphatase (potato slice).

handling. In particular, monitoring of therapeutic drug levels, office testing and implantable devices will benefit from the development of biosensors. A recent study[44] estimated the 1986 US market for biosensors at $70 million and predicted that US sales would rise to $500 million by 1990 with major applications in the clinical laboratory and to drug monitoring. Further, it was concluded that biosensors would become the dominant sensor technology by the end of the century. Candidates for wide clinical use include sensors for glucose (artificial pancreas), urea (haemodialysis) and, perhaps, creatinine and cholesterol. To date, self-contained enzyme electrode based devices for the determination of 11 different analytes including glucose, sucrose, lactate, uric acid, lysine and α-amylase have been made commercially available (Table

2), starting in 1976 with the La Roche lactate analyser (Basle, Switzerland) and the YSI Model 23A (Yellow Springs Instruments). These analysers use the enzyme immobilised in the membrane and as such represent the first generation of sensors. In 1981 development of the Glukometer analyser was completed. Currently about 400 such devices are being used in clinical laboratories for whole blood glucose measurement.

The analyser has also been applied to the determination of ten other substrates and six enzyme activities (Table 3). The enzyme membranes used contain up to three interacting enzymes. They are incorporated in gelatin, which generally provides excellent functional stability,[45] or in synthetic carrier material such as polyurethane. These enzyme membranes ensure high stability and the short diffusion time allows a sampling rate of 120 samples h^{-1}.

Based on the routine application of the Glukometer and results of recent flow injection experiments[12,13] the ECA 20 Enzyme Chemical Analyzer (PGW, Medingen, GDR) was developed. It uses an optimised flow cell and a GOD - polyurethane membrane. Operation and maintenance are extremely straightforward; a built-in microcomputer conducts the measuring process including calibration and printing of the measured values.

The largest immediate market for biosensors is for clinical and health care applications. Important economic advantages, however, may be gained by exploiting novel sensors in process engineering. Owing to the extremely high cost of growth media for human cell cultivation, process control is in high demand. Control Equipment (Lowell, MA, USA) uses the Yellow Springs glucose sensor in a flow injection device for process control in cell cultivators. The sample is injected automatically into the carrier stream after filtration. Analogous process analysers have been developed by Nippon General Trading (Tokyo, Japan) for the measurement of eight different metabolites and by Seres for the parallel determination of glucose, lactate and glutamine.[46]

Research Fields

In order to achieve broad acceptance in routine analytical operations the following fields of sensor research are under investigation on a world-wide scale.

Multi-functional Sensing

Until now, enzyme electrode based analysers have been one-parameter devices. However, it would be desirable to measure several different substances in parallel using a single analyser, without changing the electrode membrane. One such approach involves the simultaneous application of different enzyme sensors to the same sample solution.

Mascini[47] installed three enzyme electrodes (for glucose, lactate and pyruvate) in a flow line of an artificial pancreas. Hence the levels of these important metabolites in the blood of critical-care patients could be controlled simultaneously during treatment.

An alternative approach towards simultaneous multi-parameter determinations is the integration of several independently working enzymes in one membrane, *e.g.*, glutamate, tyrosine and lysine oxidases used for the simultaneous determination of glutamate, tyrosine and lysine, respectively. By sweeping the potential between −600 and +600 mV, a current - potential graph with three distinct steps is obtained; these reflect oxygen consumption by tyrosinase, hydroquinone formation, which indicates the concentration of glutamate, and the formation of hexacyanoferrate(II), which is related to the concentration of lysine. All three analyte concentrations can be quantified by comparing the three signals.[48] This example demonstrates that the measuring procedure can be simplified significantly as the determination of several parameters is possible without changing any part of the enzyme sensor.

Alternatively, different enzymes, *e.g.*, for glucose, urea and lipids, have been fixed at the sensitive regions of a multiple sensors chip.[11] Thus multi-functional sensing has been realised using fabrication technologies for the mass production of microelectronic elements.

Further, several substances are accessible using only one biosensor and coupled enzyme reactions. Glucose 6-phosphate (G6P), glucose, $NADP^+$, ATP and fructose have all been quantified using a hexokinase - glucose 6-phosphate - dehydrogenase (HK - G6P - DH) sequence sensor.[49] Both glucose and fructose are converted by HK to the respective monosaccharide phosphates and G6P is subsequently dehydrogenated by G6P - DH in the presence of $NADP^+$ to produce NADPH. Therefore the NADPH oxidation current at a modified electrode reflects the rate of glucose conversion. At a constant glucose concentration, the addition of fructose results in a decreased NADPH signal with the current decreasing linearly up to a fructose concentration of 1.0 mM. The sequential reaction of HK and G6P - DH is the basis of the response of the sensor to glucose, $NADP^+$ and ATP and, by changing the experimental conditions, five different substances can thus be measured using two enzymes (Fig. 7).

Miniaturisation

The goals of miniaturising biosensors are reduction of the required sample volume, multi-component analysis of complex chemical substances by multiple microsensors and cost reduction by mass production. Three basic types of microsensor have been used so far: (i) ion-sensitive field effect transistors (ISFETs); (ii) gas-sensitive metal oxide semiconductor (MOS) capacitors; and (iii) thin-film electrodes. These sensors are now fabricated by microelectronic production technologies, which allow the production of low-cost, reproducible, small-scale electronic devices. Such technologies, *e.g.*, thick- and thin-film deposition, photolithography and chemical and plasma etching, permit well delineated patterning of metallic, insulating and semiconducting surface layers. Hence arrays of identical or different electrochemical sensors can be produced, enhancing the reliability, repeatability and versatility of the sensor. Most problems arise from the manufacturing technique used for the formation of the immobilised biomembrane.

Using enzyme entrapment in a polyurethane layer, enzyme FETs for glucose and urea have been developed. The basic sensor is a pH-sensitive FET possessing a multiple Si_3N_4 gate structure. These microbiosensors are characterised by a typical response time of 1 min for the steady-state value, a lifetime of about 30 d and a calibration graph slope (in 0.1 mM phosphate buffer) of 30 mV per concentration decade (Fig. 8). In order to avoid interferences due to changes in the sample buffer capacity, a fluoride-sensitive FET based on LaF_3 has been used. This FET is covered by an enzyme layer containing

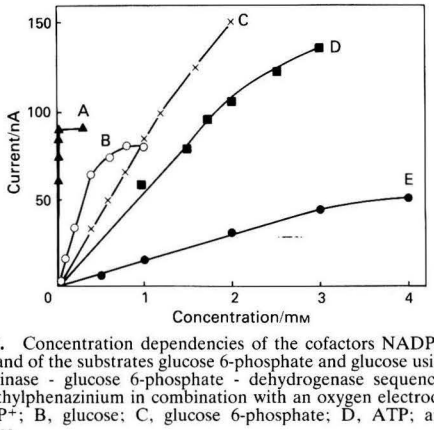

Fig. 7. Concentration dependencies of the cofactors $NADP^+$ and ATP and of the substrates glucose 6-phosphate and glucose using the hexokinase - glucose 6-phosphate - dehydrogenase sequence and *N*-methylphenazinium in combination with an oxygen electrode. A, $NADP^+$; B, glucose; C, glucose 6-phosphate; D, ATP; and E, fructose

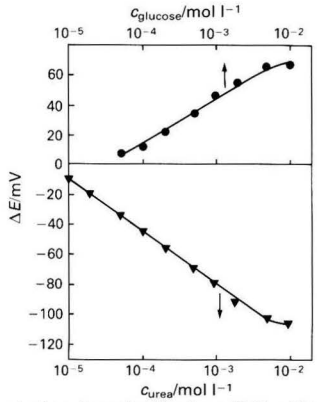

Fig. 8. Concentration dependencies for a Si_3N_4 pH-sensitive field effect transistor covered with glucose oxidase and urease, respectively

peroxidase (POD) and GOD. In the presence of the POD substrate pentafluorophenol, glucose can be determined at levels of between 0.05 and 1.0 mM with a sensitivity of 42 mV per decade.

For the microbiosensor to realise its potential, it is necessary to develop an enzyme-layer fabrication method which meets the following requirements: (i) the membrane must be deposited precisely on to the sensitive region of the basic electronic element; (ii) the deposited layer must not peel off in use; and (iii) the enzyme covering should be compatible with the integrated circuit (IC) process.

Two alternative procedures have been proposed. Nakamoto *et al.*[50] masked the passive region of the wafer with a positive photoresist. The enzyme molecules are fixed in the uncovered area by typical immobilisation methods, *e.g.*, a combination of aminopropyl-silanisation of the surface and enzyme adhesion by glutaraldehyde. The enzyme layer has a typical thickness of 1 μm and the minimum width and line separation are both 1.5 μm.

In contrast, Shiono *et al.*[15] deposited the enzymes only at the sensitive region, *e.g.*, at the gate of ISFETs, from an enzyme solution in a negative photoresist. Thus ISFET-biosensors for glucose, urea and lipids with a response time of 4 s and a sensitivity of 85% after 2000 measurements have been developed. When this enzyme FET is in a flow-through cell, which ensures both isolation and electrical connection of the conductive fields to the measuring device, it can be used without any polymeric encapsulation or wire bonding. This technique promises to reduce the cost per sensor.

Inducible Recognition Systems

Typically, the optimum operating conditions are specific for each enzyme; hence, with multi-enzyme sensors, a compromise is necessary which deviates from the standard operational parameters of a simple enzyme sensor. Therefore it seems obvious to use organelles, whole cells or tissue sections from animal or plant sources as biocatalytic packages. These structural entities contain all the necessary components in an environment optimised by evolution. Almost 60 biosensors of this type have been reported[51] but the possible number is considerably higher in view of the thousands of strains and tissues available.

Microbial sensors offer several advantages over conventional enzyme electrodes, *e.g.*, the enzyme preparation step is eliminated, the lifetime is increased compared with isolated enzymes and processes requiring enzyme sequences or cofactors are easy to achieve. However, one disadvantage of microbial sensors is their low specificity in comparison with enzyme electrodes. This is especially true for glucose (the main nutrient for microbes in fermentations), which interferes with the determination of other substances by microbial sensors. To improve the selectivity of microbial sensors undesired metabolic pathways and transport mechanisms might be blocked or inhibited whereas appropriate metabolic activities might be induced. The latter was demonstrated with a microbial glutamic acid sensor using *Bacillus subtilis*.[52] When a sample solution containing glutamic acid or glucose was injected into the measuring cell, the substrate was taken up by the micro-organisms. The respiration rate therefore increased and oxygen consumption by *B. subtilis* resulted in a decrease in the dissolved oxygen signal; the electrode current decreased with time until a steady state was reached. It is not possible to determine glutamic acid in the presence of glucose with this sensor. A sensor using *B. subtilis* cells grown in a medium without glucose shows a higher, although not sufficient, specificity for glutamic acid over glucose.

A decrease in the glucose signal, without changing the glutamic acid signal, is obtained by treatment of *B. subtilis* cells with a relatively low concentration of chloromercuribenzoate (CMB) for 20 min. The effect of CMB is irreversible. A further reduction in the glucose signal is obtained using NaF, which is an inhibitor of the enzyme enolase. However, the action of NaF at pH 6.8 is reversible and, therefore, the solutions being measured must always contain NaF. The decrease in the glucose signal by CMB is probably due to the uptake of glucose being blocked.

The concept described here for the determination of glutamic acid opens up possibilities for the development of microbial sensors with higher specificities. Further, to improve the sensitivity of microbial sensors, special cell systems, responsible for transport and assimilation of the substance of interest, can be induced by adding the respective substrate to the growth medium. For example, the rate of assimilation of maltose or aspartame by *B. subtilis* has been increased substantially by inducing the respective enzyme systems.[53] The "induced bacteria" are used for the determination of α-amylase activity or the dipeptide sweetener aspartame. By analogy, the sensitivities of microbial sensors using *Nocardia erythropolis*[54] or *Hansenula anomala*[55] for cholesterol and lactate, respectively, have been improved considerably when the respective enzymes, cholesterol oxidase and cytochrome b_2, have been induced. By using tolerant plant structures that possess induced enzyme systems, herbicides and pesticides might be measured.[56]

Group-effect Sensing

As already outlined, microbial sensors suffer from the multi-receptor behaviour of intact cells, which results in decreased substrate specificity. On the other hand, this ability to recognise a group of substances is exploited in sensors for complex variables such as the sum of biodegradable compounds. This method of determining the biological oxygen demand (BOD) has provided an impetus to environmental control.[4] The conventional BOD test takes 5 d and, therefore, it is unsuitable for process control. Rapid BOD determinations are only possible using microbial sensors, in which immobilised micro-organisms and dissolved oxygen electrodes are combined. Different microbial BOD sensors using activated sludges and cells of *Trichosporon cutaneum, Hansenula anomala, Clostridium butyricum, Pseudomonas* sp. and *Escherichia coli* have been developed.[57–60] These sensors have response times of 15–20 min. A rapid-response BOD sensor consisting of *B. subtilis* or *T. cutaneum* cells immobilised in poly(vinyl alcohol) and based on the measurement of the acceleration of respiration or of the change in current, *i.e.*, on a kinetic measurement regime, has also been developed.[61] The change in current is linearly related to a glucose - glutamic acid standard in the range 0–22 mg l^{-1} of BOD using *B. subtilis* and in the range 0–100 mg l^{-1} of BOD using *T. cutaneum*. The limits of detection are 2 and 4 mg l^{-1} of BOD

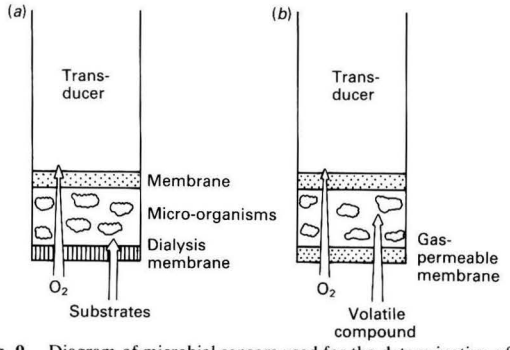

Fig. 9. Diagram of microbial sensors used for the determination of (*a*) volatile substances and (*b*) the biological oxygen demand where the separation of substances is governed mainly by the type of membrane, whereas the microbes generate an almost unspecified oxygen consumption

with the *B. subtilis* and *T. cutaneum* sensors, respectively. The signal is reproducible to within 5% for a series of ten standard solutions containing 22 mg l^{-1} of BOD. The main advantage of these sensors is the short response times (15–30 s). Other types of microbial sensor (Fig. 9) can indicate the carbohydrate content, the mutagenicity of substances, the presence of volatile compounds, over-all toxicity and vitamin action.[4,51,62]

Receptrodes

The chemical senses of living organisms provide exceptional selectivity, sensitivity and response dynamics. For example, certain insects respond to just a few molecules of stimulant and several marine animals can sense amino acids in water at below picomolar concentrations. As electrochemical processes are involved in the neuronal signals of the chemical senses, it is possible to apply the principle of chemoreception to a further type of biosensor, the receptrode. Two complementary directions are currently being pursued, these being the development of sensors using isolated receptors and sensors based on complex chemoreceptor structures.

The purified form of the nicotinic acetylcholine receptor from the electric organ of *Torpedo california* has been used in an acetylcholine sensor.[63] The molecule consists of five sub-units containing both the agonist binding sites and the ion channels. In the absence of acetylcholine the channels are closed whereas on binding of the agonist the channels open and a flux of sodium ions is started. A purified receptor preparation and the lipid lecithin have been deposited on the gate of a metal insulator semiconductor FET (MISFET). The Si_3N_4 layer of the gate is sensitive to protons, sodium ions, potassium ions and surface charge and the receptor-covered MISFET exhibits a specific response to acetylcholine and sodium ions. Obviously, the lipid membrane prevents sodium ions in the solution from reaching the Si_3N_4 gate and, therefore, a concentration gradient is formed. The ion flux through the receptor channel is reflected by the change in the gate potential on the addition of acetylcholine. This effect is only found with the active receptor preparation whereas other proteins, *e.g.*, bovine serum albumin or the heat-denatured receptor, are ineffective. This principle may be extended to other receptors or channels.

Because isolated receptors appear to retain their function only for a very short time such investigations are far from yielding actual biosensors. On the other hand, the isolation, reconstitution and immobilisation of receptors are eliminated when intact receptor structures are used as the recognition elements of the biosensor. The antennules of blue crabs were excised and the neural fibres coupled to micropipette electrodes in such a manner that the impulses generated in the recognition process could be recorded and accumulated.[64] This arrangement was adapted from typical neurophysiological techniques and it is useful for detecting extremely low concentrations of amino acids, down to 10^{-13} M, with surprising selectivity.

Immunosensors

The bulk molecular structure of an antibody is fairly constant. Local differences, however, result in specific antigen binding and, consequently, sensors embodying a wide range of antibodies could use a common transduction mechanism to detect very different analytes.

Immunological interactions of the antibody - antigen or complement-mediated type do not usually involve electroactive reactants. Hence enzyme labelling[65,66] or ionophores[56] have been used to mediate between immunological and electrochemical processes in the biosensor. Enzyme immunosensors are prepared by attaching antibodies to the surface of a Clark oxygen electrode. An enzyme such as catalase or GOD is attached either to a second antibody (two-site test) or to an antigen (competition configuration). The assay involves either the attachment of the enzyme to, or its displacement from, the electrode in the presence of the antigen. After washing, a substrate is added causing a change in current which is either directly or inversely related to the antigen concentration. Sensors of this type have been described for insulin and albumin,[67] immunoglobulin,[68] thyroxine,[69] human chorionic gonadotropin,[70] α-fetoprotein[71] and the hepatitis B surface antigen.[72,73]

Because the operation of these enzyme immunosensors necessarily involves the use of reagents admixed with the analyte they cannot be seen as stages in the development of "probe" immunosensors. Nevertheless the detection of sub-nanomolar concentrations of antigens within seconds is a realistic goal.

Currently an extremely wide range of pure monoclonal antibodies can be produced each of which is to the first approximation selective for an individual analyte (antigen). Monoclonal antibodies are especially attractive as molecular recognition elements for antigen monitoring. Bush and Rechnitz[74] developed a completely reversible biosensor, using monoclonal antibodies so that a potentiometric signal was produced as a result of the antigen - antibody interaction. In this sensor, monoclonal antibodies to the hapten 2,4-dinitrophenol (DNP) are entrapped in front of the sensing tip of a DNP-responsive membrane electrode by a collagen membrane. This membrane has a molecular cut-off that retains the antibodies but allows the passage of low relative molecular mass antigens. Hence, the entire antibody - antigen reaction takes place in the chamber in front of the sensor tip. Competition between binding of the entrapped antibody to either the constant level of antigen at the surface of the sensing membrane or to the changing sample antigen concentration results in variations in the trans-membrane potential. The dynamic response of the probe (the steady state is achieved in approximately 15 min) is limited by the slow antibody - antigen reaction. Dissociation of the complex, achieved by immersing the sensor in DNP-free buffer between measurements, restores the base-line potential within 15–20 min. After more than 50 cycles of binding and dissociation there is found to be no loss of sensor response, the lifetime of the sensor being about 17 d. Hence the sensor is a re-usable probe requiring only small amounts of the expensive monoclonal antibody. It seems likely that this concept will be extended to other small haptens.

Conclusions

So far the practical application of biosensors has been limited almost completely to oxidase-based amperometric enzyme electrodes. However, in dry chemistry, hydrolytic and coupled enzyme reactions have also been widely used and hence it seems plausible that the coupling of enzyme reactions could

also lead to an extension of applicability and result in improved analytical performance of the biosensor. Important results might be obtained using chemically and genetically modified enzymes and, further, the "site to site" oriented fixation of artificially coupled enzymes could improve the characteristics of sequential substrate conversion. In this way the effectiveness of evolution-optimised natural systems could be surpassed. Also the biosensor field might be expanded by the adaptation of complex biological recognition elements.

As electrochemical processes are involved in the neuronal signals of the chemical senses, it is possible to apply chemoreception to recognition, processing and signal transduction in biosensors. Potentially, chemical signals related to olfaction or taste might be quantified using these receptrodes.

Finally, the gap between metabolic and binding biosensors might be closed by the design of enzymatically active antibodies.

References

1. Free, A. H., and Free, H. M., *Gastroenterologia*, 1953, **24**, 414.
2. Clark, L. C., and Lyons, C., *Ann. N.Y. Acad. Sci.*, 1962, **102**, 29.
3. Aizawa, M., *in* Seyama, T., Fueki, K., Shiokawa, J., and Suzuki, S., *Editors*, "Proceedings of the International Meeting of Chemical Sensors, Fukuoka, 1983," Elsevier, Amsterdam, 1983, p. 683.
4. Walters, B., *Anal. Chem.*, 1983, **55**, 498A.
5. Scheller, F., Schubert, F., Renneberg, R., Müller, H.-G., Jänchen, M., and Weise, H., *Biosensors*, 1985, **1**, 135.
6. Blaedel, W. J., and Jenkins, R. A., *Anal. Chem.*, 1976, **48**, 1240.
7. Torstensson, A., Johansson, G., Hansson, M.-O., Larsson, P., and Mosbach, K., *Anal. Lett.*, 1980, **13**, 837.
8. Heller, A., and Degani, Y., *J. Electrochem. Soc. Rev. News*, 1987, **134**, 494C.
9. Scheller, F., Schubert, F., Pfeiffer, D., and Renneberg, R., *Enzyme Eng.*, 1987, **8**, 240.
10. Janata, J., *J. Am. Chem. Soc.*, 1975, **97**, 2914.
11. Karube, I., *Sci. Technol. Jpn.*, 1986, July/September, 32.
12. Olsson, B., Lundbäck, H., Johansson, G., Scheller, F., and Nentwig, J., *Anal. Chem.*, 1986, **58**, 1046.
13. Scheller, F., Schubert, F., Olsson, B., Gorton, L., and Johansson, G., *Anal. Lett.*, 1986, **19**, 1691.
14. Ikariyama, Y., Yamauchi, S., Yukiashi, T., and Ushioda, H., *Anal. Lett.*, 1987, **20**, 1791.
15. Shiono, S., Hanazato, Y., Nakako, M., and Maeda, M., *GBF Monogr.*, 1987, **10**, 291.
16. Mottola, H. A., *Analyst*, 1987, **112**, 719.
17. Mullen, W. H., Churchouse, S. J., and Vadgama, P. M., *Analyst*, 1985, **110**, 925.
18. Scheller, F., and Pfeiffer, D., *Z. Chem.*, 1978, **18**, 50.
19. Cenas, N. K., and Kulys, J. J., *Bioelectrochem. Bioenerg.*, 1981, **8**, 103.
20. Frew, J. E., and Hill, H. A. O., *Philos. Trans. R. Soc. London, Ser. B*, 1987, **316**, 95.
21. Albery, W. J., Bartlett, P., and Cass, A. E. G., *Philos. Trans. R. Soc. London, Ser. B*, 1987, **316**, 107.
22. D'Costa, E. J., Higgins, I. J., and Turner, A. P. F., *Biosensors*, 1986, **2**, 71.
23. Ikeda, T., Miki, K., Fushimi, F., and Senda, M., *Agric. Biol. Chem.*, 1987, **51**, 747.
24. Mizutani, F., Yamanaka, T., Tanabe, Y., and Tsuda, K., *Anal. Chim. Acta*, 1985, **177**, 153.
25. Scheller, F., Wollenberger, U., Schubert, F., Pfeiffer, D., and Bogdanovskaya, V. A., *GBF Monogr.*, 1987, **10**, 39.
26. Schubert, F., Kirstein, D., Schröder, K.-L., and Scheller, F., *Anal. Chim. Acta*, 1985, **169**, 391.
27. Wollenberger, U., Schubert, F., Scheller, F., Danielsson, B., and Mosbach, K., *Anal. Lett.*, 1987, **20**, 657.
28. Schubert, F., and Scheller, F., *DDR Pat.*, WP C 12Q/315 7391, 1988.
29. Niwa, M., Itoh, K., Nagata, A., and Osawa, H., *Tokai J. Exp. Clin. Med.*, 1981, **6**, 403.
30. Mason, M., paper presented at Biotec 87, Düsseldorf, 1987.
31. Hanke, G., Scheller, F., and Yersin, A., *Zentralbl. Pharm.*, 1987, **126**, 445.
32. McCann, J., *World Biotech. Rep.*, 1987, **1**, Part 2, 41.
33. Kirstein, D., Kirstein, L., and Scheller, F., *Biosensors*, 1985, **1**, 117.
34. Weigelt, D., Schubert, F., and Scheller, F., *Fresenius Z. Anal. Chem.*, 1987, **328**, 259.
35. Weigelt, D., Schubert, F., and Scheller, F., *Anal. Lett.*, 1988, **21**, 225.
36. Gruss, R., and Scheller, F., *Z. Med. Lab.-Diagn.*, 1987, **28**, 333.
37. Turner, A. P. F., paper presented at the Ciba Foundation Meeting, "Biosensors," London, 1986.
38. Pfeiffer, D., Ralis, E. V., Makower, A., Meiske, C., and Scheller, F., *J. Chem. Technol. Biotechnol.*, 1989, **43**, in the press.
39. Scheller, F., *Stud. Biophys.*, 1987, **119**, 221.
40. Enfors, S.-O., and Nilsson, H. J., *Enzyme Microb. Technol.*, 1979, **1**, 260.
41. Cleland, V., and Enfors, S.-O., *Anal. Chem.*, 1984, **56**, 1880.
42. Brooks, S., Ashby, R., Turner, A. P. F., Calder, M., and Clarke, D. J., *Biosensors*, 1987/88, **3**, 45.
43. Verduyn, C., Zomerdijk, T., van Dijken, J., and Scheffers, W., *Appl. Microbiol. Biotechnol.*, 1984, **19**, 181.
44. "Biosensors: Today's Technology, Tomorrow's Products," Technical Insights Incorporated, Lee, NJ, USA.
45. Bertermann, K., Scheller, F., Pfeiffer, D., Jänchen, M., and Lutter, J., *Z. Med. Lab.-Diagn.*, 1981, **22**, 83.
46. Romette, J. L., *GBF Monogr.*, 1987, **10**, 81.
47. Mascini, M., *GBF Monogr.*, 1987, **10**, 87.
48. Pfeiffer, D., Wollenberger, U., Scheller, F., Risinger, L., and Johansson, G., *Stud. Biophys.*, in the press.
49. Schubert, F., Kirstein, D., Scheller, F., Abraham, M., and Boross, L., *Anal. Lett.*, 1986, **19**, 2155.
50. Nakamoto, S., Kimura, J., and Kuriyama, T., *GBF Monogr.*, 1987, **10**, 289.
51. Karube, I., and Suzuki, S., *Ion-Sel. Electrode Rev.*, 1984, **6**, 15.
52. Riedel, K., and Scheller, F., *Analyst*, 1987, **112**, 341.
53. Renneberg, R., Riedel, K., and Scheller, F., *Appl. Microbiol. Biotechnol*, 1985, **21**, 180.
54. Wollenberger, U., Scheller, F., and Atrat, P., *Anal. Lett.*, 1980, **13**, 825.
55. Vincké, B. J., Devleeschouwer, M. J., and Patriarche, G. J., *Anal. Lett.*, 1985, **18**, 593.
56. Rechnitz, G. A., *GBF Monogr.*, 1987, **10**, 3.
57. Karube, I., Matsunaga, T., Mitsuda, S., and Suzuki, S., *Biotechnol. Bioeng.*, 1977, **19**, 1535.
58. Hikuma, M., Suzuki, H., Yasuda, T., Karube, I., and Suzuki, S., *Eur. J. Appl. Microbiol. Biotechnol.*, 1979, **8**, 289.
59. Kulys, J. J., and Kadziauskiene, K.-V., *Biotechnol. Bioeng.*, 1980, **22**, 221.
60. Strand, S. E., and Carlson, D. A., *J. Water Pollut. Control Fed.*, 1984, **56**, 464.
61. Riedel, K., Renneberg, R., Kleine, R., Krüger, M., and Scheller, F., *Appl. Microbiol. Biotechnol.*, 1988, **28**, 316.
62. Riedel, K., Renneberg, R., Wollenberger, U., Kaiser, G., and Scheller, F., *J. Chem. Technol. Biotechnol.*, 1989, **44**, 85.
63. Gotoh, M., Tamiya, E., Momoi, M., Kagawa, Y., and Karube, I., *Anal. Lett.*, 1987, **20**, 857.
64. Belli, S. L., and Rechnitz, G. A., *Anal. Lett.*, 1986, **19**, 403.
65. Aizawa, M., *Philos. Trans. R. Soc. London, Ser. B*, 1987, **316**, 121.
66. Aizawa, M., *GBF Monogr.*, 1987, **10**, 217.
67. Mattiasson, B., and Nilsson, H., *FEBS Lett.*, 1977, **78**, 251.
68. Aizawa, M., Morioka, A., and Suzuki, S., *J. Membrane Sci.*, 1978, **4**, 221.
69. North, J., *Trends Biochem. Sci.*, 1985, **3**, 180.
70. Robinson, G. A., Cole, V. M., Rattle, S. J., and Frost, G. C., *Biosensors*, 1986, **2**, 45.
71. Aizawa, M., Morioka, A., and Suzuki, S., *Anal. Chim. Acta*, 1980, **115**, 61.
72. Boitieux, J. L., Desmet, G., and Thomas, D., *Clin. Chem.*, 1979, **25**, 318.
73. Boitieux, J. L., Thomas, D., and Desmet, G., *Anal. Chim. Acta*, 1984, **163**, 309.
74. Bush, D. L., and Rechnitz, G. A., *Anal. Lett.*, 1987, **20**, 1781.

Paper 8/04772C
Received December 2nd, 1988
Accepted December 16th, 1988

Oxygen-sensitive Reagent Matrices for the Development of Optical Fibre Chemical Transducers

Philip Y. F. Li and Ramaier Narayanaswamy*
Department of Instrumentation and Analytical Science, University of Manchester Institute of Science and Technology, P.O. Box 88, Manchester M60 1QD, UK

A number of chemically-sensitive media were investigated for their suitability in the development of an oxygen-sensitive optical fibre transducer. The reagent phase is the heart of the transducer, where oxygen is measured by collisional quenching of the immobilised fluorescent indicator by oxygen. Fluorescence quenching is a rapid and reversible process and can be appropriately incorporated in an optical fibre oxygen transducer. The analytical system employed for measuring the fluorescence response to oxygen is described and the underlying reasons behind the selection process for the most suitable reagent matrix are discussed.

Keywords: *Chemically-sensitive reagent phase; oxygen measurement; optical fibre sensors; fluorescence quenching; coumarin dyes*

A suitable reagent phase for the direct measurement of oxygen levels is needed for the development of an oxygen-sensitive optical fibre transducer. The reagent phase should ideally be sensitive to fluorescence quenching by oxygen and have a high quantum yield such that the fluorescence emission is sufficiently intense to provide a measurable signal.

Optical sensors have been developed for the measurement or determination of a wide variety of chemical variables or species, such as pH,[1] metal ions[2] and glucose,[3] and also for the measurement of oxygen in blood[4] and as bioreactors.[5] Optical fibres are used for sensor fabrication because they are small in physical size, flexible, low in cost and easy to fabricate, which would enable these sensors to be considered as disposable. The optical nature of transducers offers immunity from electrical interference and their passiveness resulting from their electrical isolation means that they are inherently safe. Remote measurements in hazardous environments are possible owing to their rugged construction and reliability. These advantages can be incorporated in an optical fibre oxygen transducer through a suitable method of oxygen detection.

The principle of oxygen measurement is based on the efficient oxygen quenching of the fluorescence from a large number of fluorescent organic indicators. This phenomenon was used here for the development of a suitable reagent phase which can be incorporated on an optical fibre for the detection of oxygen. The reagent phase consists of a polymeric support matrix on which an oxygen-sensitive fluorescent indicator is physically adsorbed. The three fluorescent indicators selected for the studies were the coumarins 1, 102 and 153 and this choice was based on their availability, sensitivity and stability, respectively. These indicators were immobilised on organic polymeric support matrices (XAD resins) and on an inorganic adsorbent (silica gel).

The important areas of investigation were the interaction of the immobilised indicators with oxygen and the subsequent evaluation of their performance characteristics. In this paper the results of initial studies on the use of oxygen-sensitive media for the development of an optical fibre oxygen transducer are reported.

Fluorescence quenching is a photochemical process in which a chemical quenching species can interact with a fluorophore by decreasing its fluorescence intensity. The quenching process involves a collisional encounter between the fluorescent indicator and the oxygen molecule. The degree of collisional quenching of a fluorophore is expressed as a linear dependence on the oxygen level present by the Stern - Volmer equation[6]

$$I_0/I = 1 + kt[Q] = 1 + K[Q] \quad \ldots \quad (1)$$

where I_0 and I are the fluorescence intensities in the absence and presence of the quencher (Q), respectively, k is the bimolecular quenching constant, t is the lifetime of the fluorophore in the absence of the quencher, [Q] is the concentration of the quencher and $K = kt$.

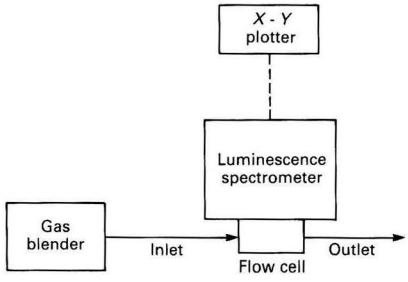

Fig. 1. Schematic diagram of the analytical system

Experimental

Instrumentation

A schematic diagram of the analytical system used is shown in Fig. 1. The Perkin-Elmer Model LS-5 luminescence spectrometer was equipped with a xenon discharge lamp, pulsed at a line frequency of 50 Hz, as the excitation source. The source produces a band of energy with a width at half the peak intensity of less than 10 μs. The incident monochromatic light enters through the silica glass window and irradiates the reagent phase contained inside a powder sample holder which is mounted on the front surface accessory. The powder sample holder was modified into a flow cell which allowed the controlled passage of gases.

The fluorescence signal was measured at the emission wavelength (Table 1) by the detector system. When operating in the fluorescence mode, a second gating period occurs shortly before the next pulse of light. The second emission signal is subtracted from the first to correct for any contribution from dark current and from any phosphorescence with a lifetime greater than 20 ms. Fluorescence spectra were recorded on a Hitachi Model 057 X - Y recorder.

* To whom correspondence should be addressed.

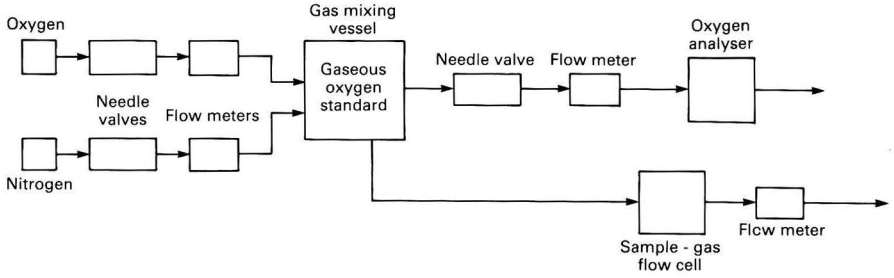

Fig. 2. Block diagram of the oxygen gas blender

Table 1. Excitation and emission wavelength maxima of the various reagent phases analysed

	Indicator					
	Coumarin 1		Coumarin 102		Coumarin 153	
Matrix	$\lambda_{ex.}$/nm	$\lambda_{em.}$/nm	$\lambda_{ex.}$/nm	$\lambda_{em.}$/nm	$\lambda_{ex.}$/nm	$\lambda_{em.}$/nm
XAD-4	373	405	385	422	405	460
XAD-8	375	415	385	422	415	468
Silica gel . .	335	434	281	336	310	392

Reagents

The fluorescent indicators coumarin 102 and coumarin 153 were purchased from A.G. Electro-optics. Coumarin 1 was supplied by Aldrich. The coumarin indicators are a group of widely used laser dyes which fluoresce in the blue - green region of the spectrum. Coumarin dyes are derived from coumarin by substitution with either an amino or a hydroxy group in the 7-position.[7]

The inorganic support matrix used was silica gel and the organic polymeric support matrices employed were Amberlite XAD-4 and XAD-8 resins. Whereas Amberlite XAD-4 is a styrene - divinylbenzene copolymer matrix and is hydrophobic in nature, XAD-8 and silica gel are hydrophilic adsorbents; XAD-8 is composed of a polymethacrylate copolymer. Preparation of the XAD resins for use involved washing the resins consecutively with dilute acid, water and methanol followed by drying. The inorganic adsorbent was used as supplied. The 5×10^{-5} M indicator solutions were prepared by dissolving the appropriate mass of coumarin dye in methanol (HPLC grade).

Immobilisation Procedure

The method of immobilisation involved adding 5.0-ml aliquots of a 5×10^{-5} M solution of the coumarin derivatives in methanol to 1.0 g of the polymer support matrices. A period of up to 16 h was allowed for the indicator to be adsorbed on the support matrices. Excess of the indicators was removed and the samples were washed thoroughly with doubly distilled water before being dried.

Gas Blending System

The oxygen gas standards used for calibrating the oxygen responses from the reagent phase were generated by a gas blender (Fig. 2). Oxygen and the inert diluent gas nitrogen were supplied from cylinders. The gas standards were produced by controlling the ratio of the flow-rates of the two gases entering the mixing chamber. The gas mixture was divided into two streams, one stream passing into a Munday reference cell oxygen analyser (Servomex, Model OA500) and the second into the flow cell containing a sample of the reagent phase.

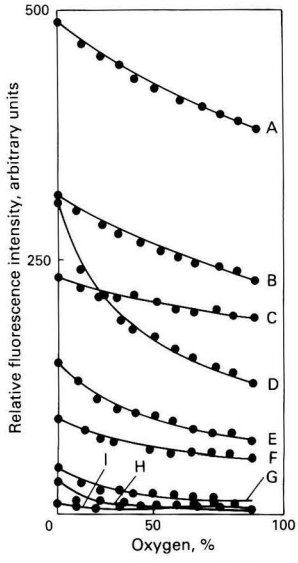

Fig. 3. Fluorescence response of the reagent phases to oxygen in the 0–100% range. A, Coumarin 1 - XAD-8; B, coumarin 102 - XAD-8; C, coumarin 153 - XAD-8; D, coumarin 102 - XAD-4; E, coumarin 1 - XAD-4; F, coumarin 153 - XAD-4; G, coumarin 1 - silica gel; H, coumarin 102 - silica gel; and I, coumarin 153 - silica gel

Sample Analyses

Samples of the reagent phase were introduced into the powder holder in amounts sufficient to cover the fused-silica window of the powder holder. The powdered sample was sandwiched between the window and the screw-cap with the gas inlet and outlet tubing. The gas inlet receives the gas mixture supplied from the gas blender. The sample holder was mounted on the front surface accessory of the luminescence spectrometer. Fluorescence from the sample was measured at different oxygen levels. The excitation wavelength maximum of the adsorbed indicator was isolated in order to irradiate the sample. The fluorescence thus produced was measured at the emission wavelength maximum.

Results and Discussion

The responses of the immobilised indicators to oxygen levels, introduced in increments of approximately 10%, were obtained by measuring the fluorescence intensities at the emission maxima (Fig. 3 and Table 1). A calibration graph can be used to relate the degree of fluorescence quenching to the oxygen level present.

The pore sizes and surface areas of the support matrices are the important physical factors affecting the performance of the reagent phase.[8] The results in Fig. 3 demonstrate that the

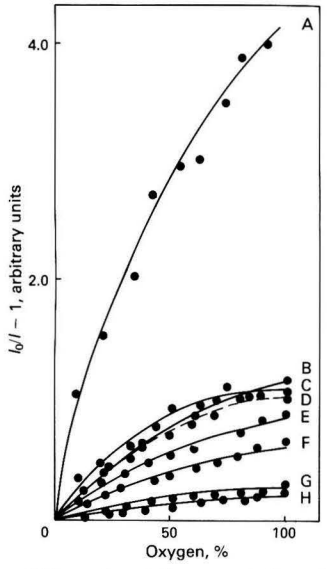

Fig. 4. Stern - Volmer plot of the reagent phases investigated, showing their sensitivities to oxygen. A, Coumarin 102 - silica gel; B, coumarin 1 - silica gel; C, coumarin 153 - silica gel; D, coumarin 102 - XAD-4; E, coumarin 1 - XAD-4; F, coumarin 153 - XAD-4; G, coumarin 102 - XAD-8; and H, coumarin 1 - and 153 - XAD-8

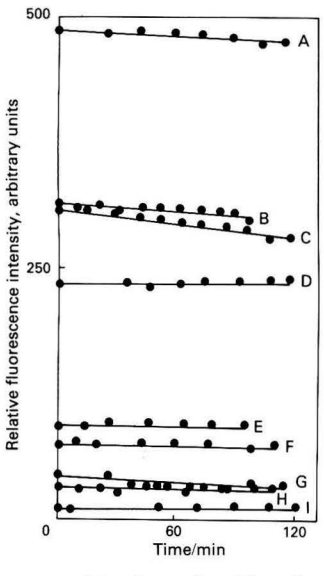

Fig. 5. Fluorescence intensity monitored from the reagent phases over a period of 2 h in the absence of oxygen. A, Coumarin 1 - XAD-8; B, coumarin 102 - XAD-8; C, coumarin 153 - XAD-8; D, coumarin 102 - XAD-4; E, coumarin 1 - XAD-4; F, coumarin 153 - XAD-4; G, coumarin 1 - silica gel; H, coumarin 102 - silica gel; and I, coumarin 153 - silica gel

emission intensity from the adsorbed indicator in the absence of an oxygen quencher is related to the range of pore sizes found in the support matrices (ranging from 4.0 to 25.0 nm for the XAD matrices). The larger the pore size in the matrix, the greater is the fluorescence emission and this observation is in agreement with the results of a similar study reported recently.[9] The highest unquenched emission intensities were measured for the three indicator dyes adsorbed on XAD-8 and were compared with the values obtained with the other adsorbents. The presence of silanol functional groups on the surface of the silica gel will reduce the amount of hydrophobic indicator being adsorbed and would account for the lower emission signal observed.

The oxygen sensitivity of the reagent phase was generally higher for indicators adsorbed on silica gel than for those adsorbed on XAD matrices. These findings are illustrated by the Stern - Volmer plots in Fig. 4. A linear Stern - Volmer relationship is generally indicative of a single class of fluorophore population, the members of which are all equally accessible to oxygen quenching. However, the experimental quenching data in Fig. 4 show a negative deviation from the Stern - Volmer relationship, which does not conform to the linear Stern - Volmer expression shown in equation (1). The negative deviation observed has been reported to be due to the presence of two fluorophore populations in the reagent phase, in which a fraction of the fluorophore is unquenched due to its inaccessibility to oxygen, while the remaining fraction of fluorophores is quenched in the normal manner.[10]

The surface area of the organic matrices can be correlated with the oxygen sensitivity of the reagent phase. The support matrix XAD-4 has a larger surface area (725 $m^2\ g^{-1}$) than XAD-8 (140 $m^2\ g^{-1}$). The results showed a correspondingly higher oxygen sensitivity for the indicator adsorbed on XAD-4. The increase in surface area exposes a proportionately larger amount of the immobilised fluorescent dye to collisional quenching by oxygen and causes an apparent increase in sensitivity. Oxygen sensitivity is also influenced by the type of coumarin indicator dye immobilised. Coumarin 102 showed the highest oxygen sensitivity on the support matrices studied (Figs. 3 and 4).

The unquenched fluorescence intensity from the samples was measured periodically over a period of approximately 2 h (Fig. 5). The degree of instability observed was dependent on the intensity and wavelength of the excitation radiation, the period of irradiation, the species of coumarin indicator and the support matrix used. Generally, the most stable response was observed for the immobilised coumarin 153. The largest drift in signal with time was observed for coumarin 102 adsorbed on XAD-4, where a 25% decrease in the fluorescence intensity was recorded over a 2-h period of continuous irradiation. The photochemical stability of the coumarin dyes in solution has been studied by several workers.[11,12] The 4-trifluoromethyl group in coumarin 153 was reported to stabilise the molecule by resisting photo-oxidation, whereas the 4-methyl group present in coumarins 1 and 102 is susceptible to photo-oxidation.[11] The 4-methyl group in coumarin 1 was reported to be oxidised photochemically to give five products, of which one was a carboxylic acid responsible for the absorption at the excitation wavelength, thus causing an over-all reduction in the fluorescence intensity.[12]

This study has demonstrated that sensitivity, high signal intensity and stability cannot be obtained from a single indicator - matrix combination. What has emerged is the necessity to select a reagent phase that is a compromise between these desirable parameters. The collisional quenching of the immobilised indicator by oxygen involves no chemical reaction and is completely reversible, without the need to replenish or regenerate the reagent phase. The above considerations have indicated that coumarin 102 adsorbed on the XAD-4 support matrix would be the reagent phase most suitable as an oxygen-sensitive medium for the development of a sensitive and reversible optical fibre oxygen sensor. The results of these studies will be reported in a subsequent paper.[13]

We thank the Science and Engineering Research Council, the Department of Trade and Industry and a consortium of industrial members of the Optical Sensors Research Unit (OSRU) for the financial support of this work.

References

1. Kirkbright, G. F., Narayanaswamy, R., and Welti, N. A., *Analyst,* 1984, **109**, 1025.
2. Zhang, Z., and Seitz, R. W., *Anal. Chim. Acta,* 1985, **171**, 251.
3. Shultz, J. S., Mansouri, S., and Goldstein, I. J., *Diabetes Care,* 1982, **5**, 245.
4. Peterson, J. I., Fitzgerald, R. V., and Buckhold, D. K., *Anal. Chem.,* 1984, **56**, 62.
5. Kroneis, H. W., and Marsoner, H. J., *Sensors Actuators,* 1983, **4**, 587.
6. Stern, O., and Volmer, M., *Phys. Z.,* 1919, **20**, 183.
7. Kubin, R. F., and Fletcher, A. N., *Chem. Phys. Lett.,* 1983, **99**, 49.
8. Pirotta, M., *Angew. Makromol. Chem.,* 1982, **109/110**, 197.
9. Wyatt, W. A., Poirier, G. E., Bright, F. V., and Hieftje, G. M., *Anal. Chem.,* 1987, **59**, 572.
10. Lakowitz, J. R., "Principles of Fluorescence Spectroscopy," Plenum Press, New York, 1983, p. 257.
11. Schimitschek, E. J., Trias, J. A., Taylor, M., and Celto, J. E., *IEEE J. Quantum Electron.,* 1973, **QE-9**, 781.
12. Winters, B. H., Mandelburg, H. I., and Mohr, W. B., *Appl. Phys. Lett.,* 1974, **25**, 723.
13. Li, P. Y. F., and Narayanaswamy, R., *Analyst,* 1989, in the press.

Paper 8/04607G
Received November 21st, 1988
Accepted February 14th, 1989

Isotopic Determination of Selenium in Biological Materials With Inductively Coupled Plasma Mass Spectrometry

Bill T. G. Ting, Christine S. Mooers and Morteza Janghorbani*
Clinical Nutrition Research Center, Department of Medicine, The University of Chicago, Chicago, IL 60637, USA

A method for the isotopic determination of selenium in biological matrices is described. The method is based on hydride generation inductively coupled plasma mass spectrometry (ICP-MS). The development is specifically related to the requirements of stable isotope tracer studies in human subjects. The method is based on isotope dilution using ^{82}Se as the *in vitro* spike and can quantify the ^{74}Se and ^{77}Se contents of samples. It involves wet oxidation (HNO_3 - H_2O_2 or HNO_3 - $HClO_4$) of the ^{82}Se-spiked matrix, reduction to selenite by boiling with HCl followed by measurement of the isotope ratios ($^{82}Se/^{77}Se$ and $^{74}Se/^{77}Se$) in the gas stream (H_2Se) generated from on-line reduction of the sample selenite with $NaBH_4$. Compared with the isotopic signal resulting from a selenite solution containing 5 ng ml^{-1} of Se, the total sample blank contributions at $m/z = 74$, 77 and 82 were less than 5% of the respective isotope signal. Worst-case absolute detection limits were 0.2–0.9 ng of Se, depending on the isotope used. Ion beam intensity ratios were measured with an over-all precision [relative standard deviation (RSD)] of 1% for both isotope pairs. Measured ratios ($MR_{a/b}$) were stable during a given day's operation within the expected precision of the measurements but varied for different days. The magnitude of $MR_{a/b}$ was generally independent of the nature of the matrix. Highly linear relationships were found between ion beam intensity ratios ($MR_{a/b}$) and the corresponding true isotope ratios for calibration solutions whose isotope ratios had been altered by as much as one order of magnitude. The precision/accuracy of the isotopic analysis was established by replicate measurements of the Se content of several biological matrices [National Bureau of Standards Standard Reference Material (NBS SRM) 1577a Bovine Liver, human plasma, red blood cells and human urine], and comparison of the results with independent measurements obtained using hydride generation atomic absorption spectrometry (AAS). The following data were obtained (mean ± SD, $n = 3$–5; first result, hydride generation ICP-MS; second result, hydride generation AAS): NBS SRM 1577a Bovine Liver, 0.697 ± 0.002, 0.69 ± 0.01 μg g^{-1}; plasma, 0.098 ± 0.001, 0.135 ± 0.008 μg g^{-1}; red blood cells, 0.211 ± 0.002, 0.216 ± 0.012 μg g^{-1}; and urine, 0.0473 ± 0.0003, 0.0489 ± 0.0003 μg ml^{-1}. It was concluded that the proposed method could be used as the measurement method for studies of Se metabolism in human subjects using the concept of stable isotope tracers. Compared with other available methods of isotopic analysis, this method possesses the added advantage of requiring no chemical separation steps as the hydride generation is sufficient for removal of any potential matrix-related interferences.

Keywords: *Stable isotopes; selenium; inductively coupled plasma mass spectrometry; hydride generation*

Since the first report of the feasibility of the stable isotope tracer approach to investigations of selenium metabolism in man,[1] a number of successful applications have been reported.[2,3] At the heart of this approach is the need for analytical methods permitting quantitative measurement of the relevant stable isotopes of Se in matrices derived from human metabolic studies (foods, faeces, urine and blood) with the required precision and accuracy.[4] At present, two methods are available: radiochemical neutron activation analysis (NAA)[4] and gas chromatography - mass spectrometry (GC - MS).[5] Both of these methods have been applied to a number of metabolic problems.[2,3,6]

Inductively coupled plasma mass spectrometry (ICP-MS) has been shown to be an important tool for stable isotope tracer investigations.[7,8] Conditions have been established for its routine application to metabolic tracer studies of Fe,[9] Zn and Cu,[10,11] Li,[12] Br[13] and Mg.[14] A number of metabolic applications have also been reported.[15–17]

The development of a suitable approach using ICP-MS for stable isotopes of Se has been hampered owing to two major difficulties: a lack of sufficient ion beam intensity for the available sample sizes; and the relatively large ion beam backgrounds resulting from the argon plasma in the region where these measurements are made. Preliminary observations[17] have indicated that of the six stable isotopes of Se, three (^{74}Se, ^{77}Se and ^{82}Se) could potentially be amenable to this approach as far as the argon plasma background is concerned. In another paper,[18] we have compared these two issues (background and sensitivity) for two modes of sample introduction, *viz.*, pneumatic nebulisation (the standard method employed with commercial instruments) and hydride generation. The data demonstrated that whereas the pneumatic nebulisation method provided sufficient ion beam intensities for the three stable isotopes ^{74}Se, ^{77}Se and ^{82}Se in matrices such as human urine, it did not possess the necessary sensitivity for other matrices such as plasma or in those situations resulting from Se deficiency experiments. In contrast, the hydride generation approach possessed worst-case absolute detection limits ($3\sqrt{B}$) within the range 0.6–1.8 ng of elemental Se.[18] This paper describes the use of hydride generation ICP-MS for the routine and accurate isotopic determination of the three stable isotopes ^{74}Se, ^{77}Se, and ^{82}Se in relation to the requirements of stable isotope tracer investigations in human subjects.

Experimental

Instrumentation

Hydride generation ICP-MS

The ICP-MS instrument employed in these studies was an Elan Model 250 system (SCIEX, Thornhill, Ontario, Canada). The distance from the load coil to the sampler was

* To whom correspondence should be addressed. Present address: Department of Medicine, Box 223, The University of Chicago, 5841 South Maryland Avenue, Chicago, IL 60637, USA.

fixed at 27 mm. The length of the outer coolant tube of the torch (distance from the end of the auxiliary gas tube to the end of the outer coolant tube) was 36 mm. The torch was placed in a fixed position as close to the sampler as possible. Vertical and horizontal positions of the torch with respect to the sampler were adjusted to provide maximum ion beam intensity, using a solution of 5 ng ml^{-1} of Se (^{77}Se, abundance 7.38%).

Argon gas was obtained from liquified argon (industrial high purity, A & R Welding Supply, Alsip, IL, USA) and supplied all the requirements of the instrument via stainless-steel and high-density polyethylene tubing.

The hydride generation system consisted of a two-channel peristaltic pump (Rabbit, Rainin Instrument Co., Woburn, MA, USA) which pumped both the analyte and the reagent ($NaBH_4$) solutions into the mixing chamber of a commercial hydride generator (PS Analytical, Questron Corporation, Princeton, NJ, USA). The output of the mixing chamber flowed into the gas - liquid separator of the hydride generator. The output of the latter was connected to the water-jacketed (25 °C) spray chamber of the Elan spectrometer (nebuliser removed) by means of approximately 120 cm of PTFE tubing 2.5 mm i.d.). All the tubing used between the reagent - sample containers and the gas - liquid separator consisted of flexible PTFE with an i.d. of <1 mm, with the exception of the small sections of plastic tubing that were necessary for the two channels of the peristaltic pump. Reagent - sample flow-rates were regulated by the settings of the peristaltic pump, which had been calibrated previously. The three argon stream flow-rates (plasma, auxiliary and carrier gases) were monitored using either the flow-meters installed with the instrument (plasma and auxiliary gases) or a mass flow-meter (carrier gas, Model 8200, Matheson Gas Products, E. Rutherford, NJ, USA).

Data acquisition was in the (peak hopping) isotope ratio mode, using the multi-channel data acquisition capability of the system, details of which have been described previously.[19] For the investigations reported here, the following settings of the software parameters were employed: resolution, M; measurements per peak, 3; scanning mode, I; measurement mode, M; measurement time, 1.000 s; repeats per integration, 5–10; dwell time, 10 ms; and cycle time, 0.200 s.

A schematic diagram of the hydride generation ICP-MS system employed has been given previously.[18] The optimised operating parameters used in this investigation are summarised in Table 1.

Hydride generation atomic absorption spectrometry

In order to establish the accuracy of isotopic analyses with hydride generation ICP-MS, we compared our results (expressed in elemental terms) with those obtained using a hydride generation atomic absorption spectrometry (AAS) system. This system consisted of a batch-type hydride generator (MHS-10, Perkin-Elmer, Norwalk, CT, USA) and an atomic absorption spectrometer (Model 5000, Perkin-Elmer). Hydrogen selenide (H_2Se) was generated by introducing a solution of $NaBH_4$ (1% *m/m*, 0.25% NaOH) at a constant rate into a 10-ml aliquot of the sample digest. Argon gas at 27 lb in^{-2} was used for this purpose. The H_2Se stream was carried into the heated quartz cell (165 mm long, 12 mm i.d.) which was fitted over the standard burner head. A Se electrodeless discharge lamp was used. The other parameters of this system were: absorption wavelength, 196.0 nm; slit width, 2.0 mm; and air and acetylene flow-rates, 15.5 and 2 l min^{-1}, respectively. Data were acquired with a PRS-10 printer with a 0.2-s cycle time starting at the time of the introduction of $NaBH_4$ into the reaction vessel and continuing until five data points had been obtained corresponding to the plateau of the absorption plot. The five data points were averaged and used for calculations. All determinations employed the method of standard additions with four points (three spike levels). Certified solutions (Fisher) of Se standards were used for spiking purposes.

Table 1. Optimised operating parameters for the hydride generation ICP-MS system

Gas flow-rates	Plasma gas, 11.0; auxiliary gas, 2.3; and carrier gas, 1.4 l min^{-1}
ICP settings	Incident power, 1100 W; spray chamber temperature, 25 °C
Interface parameters	See text
Mass spectrometer parameters	Adjusted for maximum intensity
Hydride generation parameters	Reagent flow-rate, 3.0 ml min^{-1}; sample solution flow-rate, 10.0 ml min^{-1}

Chemicals

All chemicals used were of analytical-reagent grade and were used without further purification. The stable isotopes employed were purchased as the elemental powder (Oak Ridge National Laboratory, Oak Ridge, TN, USA), which was dissolved in the minimum volume of HNO_3. The resulting selenite solution was added incrementally to solutions of selenite of natural isotopic composition in order to provide working standards of known isotope ratio covering the range of interest. The preparation of such standard solutions has been described previously for a number of other trace elements.[11–14] These standard solutions will be referred to as stable isotope ratio calibration solutions. Sodium tetrahydroborate(III) solution (1% *m/V*) was prepared in 1–2-l batches before use (2.5 g of NaOH plus 10 g of $NaBH_4$ diluted to 1 l). The resulting solution was filtered to remove any undissolved matter.

Chemical Procedure

The sample preparation procedure employed for both the hydride generation ICP-MS and the hydride generation AAS systems was as follows. Samples were wet-ashed according to previously described procedures,[4] using HNO_3 - H_2O_2 (plasma, red blood cells, faeces and foods) or HNO_3 - $HClO_4$ (urine) as the oxidant mixture, followed by boiling for 10 min with concentrated HCl in order to convert the Se content into selenite. Any insoluble residue was filtered off and the

Table 2. Details of Experiment 1

Run time/min	Sample	No. of replicates
0	Standard, 2 ng ml^{-1} of Se	1
4	Standard, 5 ng ml^{-1} of Se	1
10	10% HCl	1
14–35	Procedural blank	6
39	Standard, 2 ng ml^{-1} of Se	1
44–52	Plasma	3
56–65	NBS SRM 1577a Bovine Liver	3
69–77	Red blood cells	3
81	10% HCl	1
85–102	Standard, 2 ng ml^{-1} of Se	2
106	10% HCl	1
110–119	Urine	3
123	10% HCl	1
127	Standard, 2 ng ml^{-1} of Se	1
131–148	Isotope calibration standards	—
152–160	Spiked plasma	3
164–169	10% HCl	2
173	Standard, 2 ng ml^{-1} of Se	1
178–194	10% HCl	5
199–208	Spiked NBS SRM 1577a Bovine Liver	3
212–221	Spiked red blood cells	3
225–233	Spiked urine	3

resulting solution was diluted to the final volume (25–50 ml) with 10% HCl. The sample sizes used were: urine, 2–10 ml; plasma, 1–5 ml; red blood cells, 0.5–2 ml; faeces, 0.1% of daily output; and foods, 0.1% of composite daily intake. These were equivalent to 100–500 ng of Se. If only isotope ratio measurements were required, no spike was included, otherwise the sample was spiked with $^{82}SeO_3^{2-}$ (level of spike, 3–5 times the expected sample content of the isotope). For the hydride generation AAS system, aliquots of the digest were spiked with accurate amounts of Se from certified solutions of Se standard (four points).

For background correction for the hydride generation ICP-MS system, the use of both 10% HCl and a true procedural blank was investigated. The background corrected ion beam intensity ratios ($MR_{74/77,c}$ and $MR_{82/77,c}$) were converted to the expected true isotope ratios ($MIR_{74/77}$ and $MIR_{82/77}$, *m/m* basis) by means of stable isotope ratio calibration standards.

Individual Experiments

In order to investigate various aspects of this work, several experiments were carried out. These are described briefly below.

Basic experiments

A number of basic experiments were performed with the hydride generation ICP-MS system in order to determine its performance parameters (signal to background levels, ion beam intensity stability, precision of isotope ratio measurements, detection limits, etc.). For these experiments, solutions of Se (2–5 ng ml^{-1}) or stable isotope ratio calibration solutions were employed.

Experiment 1

The purpose of this experiment was to establish the analytical characteristics of the system for the matrices of interest. Various samples (Table 2, both unspiked or spiked with ^{82}Se) were processed as described under Chemical Procedure. Six complete procedural blanks were also prepared; these were analysed together with standard solutions of Se and 10% HCl in the sequence given in Table 2.

Experiment 2: inter-method comparison

Sub-samples from a well mixed pool of the biological matrices of interest [National Bureau of Standards Standard Reference Material (NBS SRM) 1577a Bovine Liver, human plasma, red blood cells and urine] were processed for quantitative isotopic analysis (hydride generation ICP-MS; isotope dilution analysis) or elemental analysis (hydride generation AAS; method of standard additions) as described under Chemical Procedure.

Results and Discussion

Human metabolic investigations employing the concept of stable isotope tracers impose certain requirements on the analytical method of isotopic measurement. A clear understanding of these requirements is essential for the appreciation of the measurement methodology. In the simplest experiments of this type, a single isotope (highly enriched ^{74}Se is the preferred choice, referred to as the *in vivo* tracer) is administered to the subject in an appropriate manner (orally or intravenously). Timed samples (urine, blood and faeces) are then obtained. Generally, the samples are analysed quantitatively for two stable isotopes (^{74}Se and a reference isotope, in this instance ^{77}Se). In order to perform quantitative isotopic analysis with ICP-MS the preferred method is based on *in vitro* stable isotope dilution (*in vitro* SID). For this, enriched ^{82}Se is used in the form of selenite.

Terminology

We have adopted the following terminology: $MR_{a/b}$ is the measured ion beam intensity ratio for an isotope pair *a* and *b*; $MR_{a/b,c}$ is the corresponding ratio corrected for background contributions; and $MIR_{a/b}$ is the corresponding true isotope ratio in the sample (μg of isotope *a* to μg of isotope *b*). A stable isotope ratio calibration plot is a plot of the observed relationship between $MR_{a/b,c}$ and $MIR_{a/b}$ for a set of stable isotope ratio calibration standards.

Factors Affecting Analytical Performance

The over-all objective of the measurement method is the accurate determination of ^{74}Se and ^{77}Se in the sample. This requires accurate measurement of two isotope ratios ($MIR_{74/77}$ and $MIR_{82/77}$). Therefore, the fundamental measurement criteria are related to the accuracy with which $MIR_{74/77}$ and $MIR_{82/77}$ can be determined.

Two types of performance criteria were evaluated for these analyses: the fundamental analytical performance of the hydride generation ICP-MS instrumentation and the aspects related to its application to biological materials.

Fundamental Aspects of Hydride Generation ICP-MS

We have previously compared the basic characteristics of the hydride generation ICP-MS system employed in this work with pneumatic nebulisation, which is the standard mode of sample introduction with the current ICP-MS devices.[18] The optimised parameters leading to the lowest detection limit for the three stable isotopes of Se are given in Table 1. The fundamental factors determining the over-all capabilities and limitations of this method for the accurate measurement of stable isotopes of Se in relation to tracer studies are signal to background considerations, time stability of ion beam ratios, achievable precision of measurement for isotope ratios, matrix-related systematic biases in the ion beam intensity ratios, memory effects and factors related to isotope calibration methods.

Signal to background considerations

The signal to background intensities obtained in Experiment 1 were plotted as a function of time for all matrices investigated; the results are shown in Fig. 1. Data for the ion beam intensities I_{77} were normalised to a Se concentration of 1 ng ml^{-1} based on a knowledge of the true Se concentration of the samples (determined using the *in vitro* SID procedure; spiked samples, Table 2). These data clearly demonstrate a reasonably stable ion beam intensity during the 4 h of this run. The ion beam intensities (I_{77}) for different matrices were [ions s^{-1}, mean ± 1 standard deviation (SD), normalised to 1 ng ml^{-1} of Se]: standard solution, 5250 ± 460; plasma, 6600 ± 490; NBS SRM 1577a Bovine Liver, 6490 ± 170; red blood cells, 7600 ± 650; and urine, 5600 ± 210. The intra-matrix variations [relative standard deviation (RSD)] were within the

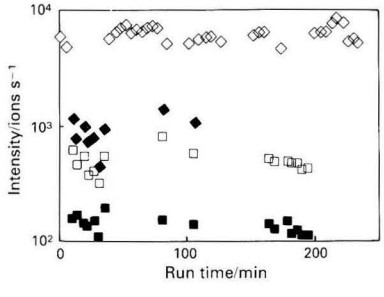

Fig. 1. Ion beam intensities (I_{77}) for all samples, normalised to a Se content of 1 ng ml^{-1}, and blank contributions for the three stable isotopes plotted against run time (see Table 2 for run details). ◇, All samples; ◆, I_{82} (all blanks); □, I_{77} (all blanks); and ■, I_{74} (all blanks)

Table 3. Signal to background data for the hydride generation ICP-MS system. Each data point corresponds to the mean ± 1 SD for ten sequential measurements

Date	I_{74}	I_{77}	I_{82}	I_{74}	I_{77}	I_{82}
Within-day measurements—*						
	10% HCl			Procedural blank		
27/6/88 (1) ..	160 ± 27	624 ± 54	1146 ± 57	163 ± 49	458 ± 80	784 ± 87
27/6/88 (2) ..	149 ± 30	797 ± 275	1347 ± 357	140 ± 10	555 ± 74	960 ± 124
27/6/88 (3) ..	139 ± 25	574 ± 67	1044 ± 64	133 ± 8	374 ± 55	727 ± 56
27/6/88 (4) ..	128 ± 25	474 ± 32	—	149 ± 23	397 ± 42	783 ± 81
27/6/88 (5) ..	113 ± 23	424 ± 20	—	110 ± 40	312 ± 10	437 ± 26
27/6/88 (6) ..	112 ± 18	431 ± 16	—	190 ± 21	554 ± 16	938 ± 20
Between-day variations—						
	10% HCl			2 ng ml^{-1} of Se		
19/4/88	87 ± 2	395 ± 10	1279 ± 26	1137 ± 13	9431 ± 97	14 009 ± 223
20/4/88	101 ± 14	1331 ± 209	1435 ± 260	1257 ± 28	11 031 ± 458	15 122 ± 255
11/5/88	97 ± 28	380 ± 140	719 ± 170	1303 ± 48	11 201 ± 424	16 332 ± 801
30/5/88	110 ± 13	676 ± 92	1732 ± 117	2977 ± 9	25 409 ± 273	35 291 ± 84
20/6/88	72 ± 3	327 ± 8	810 ± 21	1713 ± 24	14 306 ± 240	19 914 ± 490

* Ion beam intensities for 2 ng ml^{-1} of Se on 27/6/88: I_{74} 1490, I_{77} 11 700 and I_{82} 15 500.

range 3 (SRM 1577a)–9% (standard solution or red blood cells). In comparison, the mean value of I_{77} (normalised to 1 ng ml^{-1} of Se) for each matrix differed from that for the standard solution within the range 7 (urine)–44% (red blood cells), reflecting potential matrix effects on the generation of H_2Se.[20–22]

An understanding of the background intensities is important in the light of the between-day variations in the instrument parameters and other uncontrollable factors. We have investigated this by observing both within-day variations, using either 10% HCl solutions or complete procedural blanks, and between-day variations (Table 3). Background intensities (combined data for all 10% HCl and procedural blanks) during the entire run on a particular day (27/6/88) (Experiment 1) were (mean ± 1 SD): m/z = 74, 141 ± 24; m/z = 77, 498 ± 131; and m/z = 82, 907 ± 264 counts s^{-1}. This corresponded to 10, 4 and 5% of the ion beam intensities resulting from a 2 ng ml^{-1} solution of Se. Although the background count rates at m/z = 82 were higher for the 10% HCl solutions compared with procedural blanks, there did not seem to be a marked difference for the other two isotopes. Comparative data for the between-day variations for 10% HCl solutions and a standard solution of Se (2 ng ml^{-1}) on a number of occasions are summarised in Table 3. Although between-day variations in the background were observed, the background count rate was, on all but one occasion (20/4/88 for I_{77}), less than 10% of the corresponding count rate for a solution of 2 ng ml^{-1} of Se.

Calculated detection limits for Se based on the experimental SD of the six measurements carried out during a 4-h period [only three measurements for $I_{82,10\%\ HCl}$ (Table 3)] were 0.9, 0.30 and 0.2 ng of Se for 10% HCl and ^{74}Se, ^{77}Se and ^{82}Se, respectively. The corresponding values using the procedural blank data were 0.9, 0.3 and 0.3 ng of Se. For these calculations, we have assumed a total solution requirement of 50 ml. Such a solution volume would readily permit the acquisition of ten isotope ratio data points and provide sufficient solution for the necessary wash-out to minimise any memory effects due to a previous sample.[18] Hence, these detection limits correspond to conservative estimates.

The data presented here for background count rates and their between-day variations clearly demonstrate that the background can readily be reduced to a few per cent. of the signal intensity for the three stable isotopes if the Se concentration of the analyte solution is about 5 ng ml^{-1}. This would necessitate 250 ng of Se under the conditions of 50-ml solution volume requirements. The most size-limited matrix in human metabolic studies corresponds to plasma for which the normal Se concentration is about 100 ng ml^{-1}. Therefore, it is clear that this method readily meets the sample size requirements of these investigations.

We have previously investigated the effects of instrument operating parameters (IOPs) such as argon gas flow-rates or incident power on the magnitude of the signal to background ratio.[19] Over the range of optimum IOPs for stable isotopes of Se using the hydride system,[18] the signal to background ratio does not vary markedly. However, other potentially important factors such as the spray-chamber temperature could play a more marked role and these require further investigation.

Precision and time stability of $MR_{a/b}$

The measured ion beam intensity ratios vary under different operating conditions.[12–14] These variations can be accounted for by the use of appropriate calibration procedures.[12–14] However, within a particular day's run, unacceptably large variations cannot be tolerated. Therefore, it is necessary to establish that the measured ion beam intensity ratios are sufficiently constant during any particular day of operation such that the stable isotope ratio calibration procedure can be used. That this is true for stable isotopes of Se, as has been shown for a number of other isotopes,[9,11–14] can be seen from the stability data given in Fig. 2. These data were obtained by continuous measurements on a single solution of a Se standard (5 ng ml^{-1}), each data point corresponding to the mean of ten sequential data acquisitions. The data demonstrate a more stable ion beam intensity over the 4 h of observation than is characteristic of the current design of our instrument.[9,11–14] The data given in the bottom part of Fig. 2 indicate that the measured ion beam intensity ratios did not deviate outside the expected random variations corresponding to a ±1% RSD. There were no systematic changes in these values, consistent with previous observations for other stable isotopes even under conditions of much less stable ion beam intensities than those observed here.[9,11–14] Therefore, it is evident that the within-day stability of the ion beam intensity ratios is sufficient to permit the use of stable isotope ratio calibrations for the calculation of the expected true ratios.

Matrix effects

Data relating to $MR_{a/b}$ for various matrices used in Experiment 1 are summarised in Table 4. For all the matrices

investigated, the intra-matrix precision (±1 RSD) was better than 1.4% for $MR_{74/77,c}$ and better than 1.0% for $MR_{82/77,c}$. Similarly, the absolute value of $MR_{74/77,c}$ for all the matrices investigated was within 1.1% of the value for the standard solution (2 ng ml^{-1}), whereas that of $MR_{82/77,c}$ varied from the standard solution value by less than 2.7%. Although the intra-matrix precision of the ion beam intensity ratios was consistently about 1–1.4% for both isotope ratios, a small systematic bias was apparent in the $MR_{82/77,c}$ for NBS SRM 1577a Bovine Liver (+2.7%) and red blood cells (+2.2%). The reasons for this are not yet understood, but are most likely due to a positive bias in $I_{82,c}$. This could originate from molecular interferences specific to the nature of these matrices, similar to previously reported situations,[13] or could result from changes in the argon-related background at m/z = 82 arising from unknown matrix influences.

Memory effects

We have previously reported on the over-all "memory effect" of ICP-MS using the pneumatic nebulisation sample introduction system for Li[12] and Br.[13] The results indicated that this effect is not a limiting factor in the practical application of the method to accurate isotopic analysis. In a previous paper, comparing the pneumatic nebulisation and hydride generation methods for the isotopic determination of Se,[18] we found that the memory effect could be significant for the hydride method if sequential solutions had large differences in isotope ratios and if the solutions were run in the order of decreasing isotope ratio. Fig. 3 shows the speed with which ion beam intensities are reduced when a solution highly enriched with respect to ^{82}Se (corresponding to a natural Se concentration of 20 ng ml^{-1}) is replaced with 10% HCl. The data show that about 10 min after the introduction of HCl, $I_{82,c}$ was less than 1% of its original value. Because of the desirability of short wash-out times in routine isotopic analysis, the effect of relatively short wash-out times on the accuracy of isotope ratio measurements was studied. The results are presented in Fig. 4. The data given in Fig. 4 (filled diamonds) were obtained by switching (time 0) from a solution of Se of natural isotopic composition ([Se] ≈ 2 ng ml^{-1}, $MIR^0_{82/77}$ 1.291) to a solution of similar Se concentration but enriched to a small extent with respect to ^{82}Se ($MIR_{82/77}$ 1.351). The data shown as open squares were obtained when these two solutions were run in the reverse sequence (prior to running the solution with $MIR_{82/77}$ = 1.351, a solution of higher isotopic enrichment, $MIR_{82/77}$ = 1.410, had been run).[18] A 60-s wash-out with 10% HCl had also been incorporated in the latter run, as shown in Fig. 4. Several important points should be noted from the data given in Fig. 4 and from the more extensive information provided else-

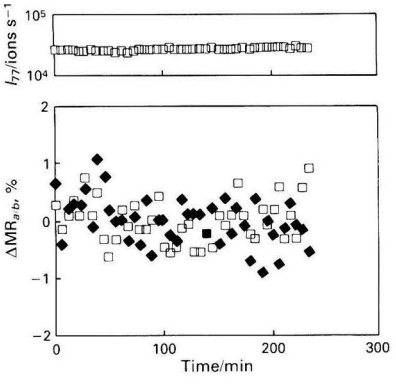

Fig. 2. Data establishing time invariance of $MR_{a/b}$ for stable isotopes of Se. Data are for continuous measurement on a Se standard solution (5 ng ml^{-1} of Se). □, $MR_{82/77}$; and ◆, $MR_{74/77}$

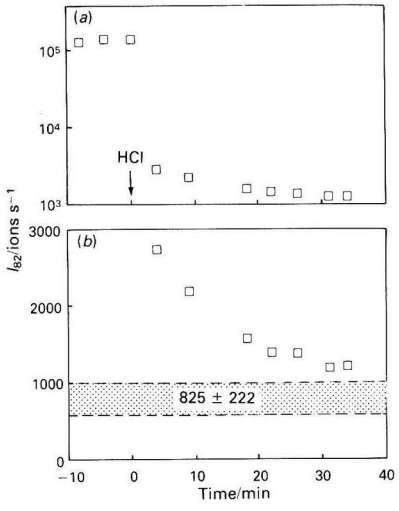

Fig. 3. Decay pattern of I_{82} for a solution of 20 ng ml^{-1} of Se replaced with 10% HCl. Fig. (*b*) shows the expanded vertical scale for the same data

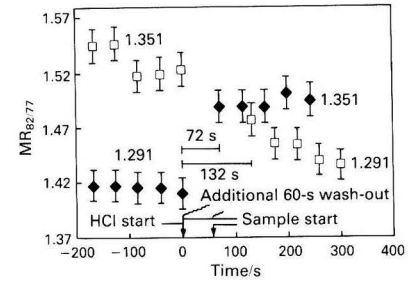

Fig. 4. "Memory effect" when solutions with different isotope ratios are run (see text for details). ◆, Order of increasing ratio; and □, order of decreasing ratio

Table 4. $MR_{a/b,c}$ for different biological matrices (data are from Experiment 1)

Matrix	No. of replicates	$MR_{74/77,c}$*	Δ,%†	$MR_{82/77,c}$*	Δ,%†
Standard, 2 ng ml^{-1} of Se	5	0.1176 ± 0.0017	0	1.284 ± 0.0074	0
Plasma	3	0.1176 ± 0.0015	0	1.302 ± 0.012	+1.4
NBS SRM 1577a Bovine Liver	3	0.1189 ± 0.0016	+1.1	1.319 ± 0.013	+2.7
Red blood cells	3	0.1176 ± 0.0005	0	1.313 ± 0.0049	+2.2
Urine	3	0.1165 ± 0.0006	−0.9	1.285 ± 0.0040	0

* Mean ± SD for *n* independently prepared sub-samples.
† Percentage difference from that for 2 ng ml^{-1} of Se.

where.[18] First, comparing the measured ion beam intensity ratios ($MR_{82/77}$) with the corresponding true ratios ($MIR_{82/77}$), the two values are not identical. This is a consistent feature of ICP-MS and has been observed on numerous occasions both for Se and other elements.[7,9,11–14] The extent of the deviation of $MR_{a/b}$ from the corresponding true ratios depends on the specific settings of the IOPs. This highlights the need for suitable isotope calibration procedures (see next section). Second, when the order of analysis is from low to high isotope ratios (filled diamonds) the sequential data obtained for the high-ratio solution reach a plateau reasonably rapidly. However, when the order of sample introduction is reversed (high to low ratio, open squares) there is a consistent decrease in the measured ratio for the low-ratio solution, indicating a significant memory effect of the previous (high-ratio) solution. Although the actual reasons for this are not clear, they probably relate to residual Se from the previous solution contaminating the low-ratio solution. We are currently attempting to pin-point the location of this memory effect. Therefore, in the current design of the system and until the source of this problem has been located and suitable design modifications implemented, accurate isotopic analysis necessitates that samples be run in the sequence of increasing isotope ratio.

Linearity of isotope ratio calibration plots

Fig. 5 shows the relevant data for stable isotope ratio calibration solutions used to convert the ion beam intensity ratios into the estimates of true isotope ratios. The data presented are for $^{82}Se/^{77}Se$ (left-hand side) and $^{74}Se/^{77}Se$ (right-hand side). For each isotope pair, both ion beam intensities and their ratios (corrected for blank) are presented.

The data given in Fig. 5(*c*) and (*d*) for each isotope pair show the degree of variability in the ion beam intensities that are sometimes observed (*cf.* Fig. 2). In this particular run (actual run time 3 h), I_{77} varied by about 40%. This is also reflected in the deviations from linearity observed for both I_{74} and I_{82} [Fig. 5(*a*) and (*b*)]. The ion beam intensity ratio ($MR_{a/b,c}$) did not show any of these fluctuations [Fig. 5(*e*) and (*f*)], as expected. Highly linear correlations were obtained for both isotope pairs over the entire range of ion beam intensity ratios involved. The linear regression equations for the two calibration plots were $MR_{74/77,c} = -0.0023 + 1.071(MIR_{74/77})$ ($r^2 = 0.9982$) and $MR_{82/77,c} = 0.098 + 1.036(MIR_{82/77})$ ($r^2 = 0.9992$).

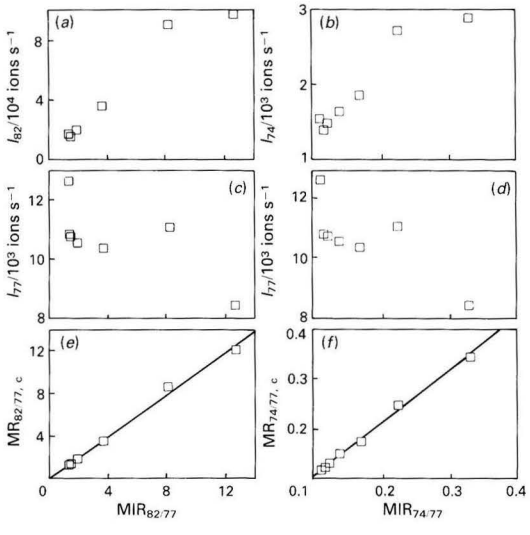

Fig. 5. Ion beam intensities and their background-corrected ratios for stable isotope ratio calibration solutions

The linear regression parameters for a single set of calibration solutions obtained on several occasions are summarised in Table 5. These data clearly demonstrate the highly linear nature of these plots. The intercept is close to zero in all instances, but the slope does not appear to be invariably unity. Whether this is related to the effect of operating parameters on mass discrimination is not yet understood; this point needs to be investigated further.

Precision/Accuracy and Practical Aspects of Routine Isotopic Analysis

In order for these methods to be suitable for routine isotopic analyses in relation to metabolic investigations, two important criteria must be satisfied: (1) the precision/accuracy in relation to the requirements of the experiment; and (2) a sample throughput consistent with the requirements of the investigations.

Precision/accuracy

Two types of isotopic analyses may be involved in metabolic investigations: those requiring only isotope ratio measurements; and investigations requiring quantitative isotopic analyses. Precision requirements of isotopic measurements vary widely for different chemical elements and for various aspects of the metabolic issues being addressed.[23] With specific reference to studies with Se, an isotope ratio measurement precision of 1–5% has been shown to be adequate for exploring many of the issues of current interest.[1] Both NAA[4] and GC - MS[5] has been reported to possess the necessary capability in this respect.

The data given in Fig. 2 and Table 4 demonstrate the capabilities of the present method in relation to this requirement. Hence, it is clear that this method can provide isotope ratio data for a variety of biological materials with a measurement precision of about 1% for routine analysis, including measurement of the ratio involving the least abundant stable isotope (^{74}Se). In particular circumstances, it may be possible to achieve a measurement precision of better than 1%, but this is not yet possible for routine analyses.

The data given in Table 4 indicate that for $MR_{74/77}$ no inter-matrix bias is present. The measurement ratios for various biological matrices are within the expected value for standard solutions of selenite. In contrast, the data given for $MR_{82/77}$ in red blood cells and NBS SRM 1577a Bovine Liver, although precise to the extent of 1%, show a positive bias of 2.2 and 2.7%, respectively. The reasons for this have not yet been identified, but are probably related to positive bias from some as yet unknown interferent in I_{82}. Such biases have been reported previously for ^{74}Se (FeO^+) in red blood cells using the pneumatic nebulisation method of sample introduction[7]

Table 5. Observed between-day variations in regression parameters for the stable isotope ratio calibration plots; $MR_{a/b} = a(MIR_{a/b}) + b$

Date of run	*a*	*b*	r^2
$MR_{82/77,c}$ versus $MIR_{82/77}$—			
28/1/88	0.916	0.134	0.998
17/2/88	1.162	0.162	0.9991
11/3/88	1.371	−0.174	0.9999
15/3/88	1.073	0.180	0.9990
16/3/88	1.050	0.172	0.9990
27/6/88	1.036	−0.098	0.9992
$MR_{74/77,c}$ versus $MIR_{74/77}$—			
28/1/88	1.057	−0.010	0.9997
17/2/88	1.099	−0.011	0.9999
11/3/88	1.165	−0.016	0.9999
27/6/88	1.071	−0.002	0.9982

Table 6. Inter-isotope comparison for isotope dilution analysis

Sample	*n*	Se/μg g^{-1} ^{82}Se/^{77}Se	Se/μg g^{-1} ^{82}Se/^{74}Se
Red blood cells	3	0.199 ± 0.008	0.196 ± 0.008
Plasma	3	0.0857 ± 0.005	0.0864 ± 0.005
Urine	3	0.0411 ± 0.0005*	0.0402 ± 0.0004*

* Values in μg ml^{-1}.

Table 7. Inter-method comparison between hydride generation ICP-MS and hydride generation AAS

Matrix	Se/μg g^{-1} Hydride generation ICP-MS*	Se/μg g^{-1} Hydride generation AAS†
NBS SRM 1577a Bovine Liver	0.697 ± 0.002	0.69 ± 0.01
Human plasma	0.098 ± 0.001	0.135 ± 0.008
Human red blood cells	0.211 ± 0.002	0.216 ± 0.012
Human urine	0.0473 ± 0.0003‡	0.0489 ± 0.0003‡

* n = 5; the isotope pair employed in the calculations was ^{82}Se/^{77}Se.
† n = 3.
‡ Values in μg ml^{-1}.

and for ^{81}Br (SO_3H^+) in urine.[13] Because of the complex nature of the biological materials and the ICP process, these interferences are likely to be much more significant than has been realised so far.

The over-all accuracy of quantitative stable isotope analysis was investigated by carrying out *in vitro* SID (spike: ^{82}Se) on the samples of interest and on NBS SRM 1577a Bovine Liver. For the isotope pair used in the calculations, both ^{82}Se/^{77}Se and ^{82}Se/^{74}Se were employed. In addition, independent elemental analyses on sample replicates were performed with hydride generation AAS using the method of standard additions. The results of these analyses, expressed in terms of elemental content (to permit ready comparison), are summarised in Tables 6 and 7.

The data given in Table 6 show the degree of agreement obtained in the *in vitro* SID procedure using either ^{82}Se/^{77}Se or ^{82}Se/^{74}Se as the isotope pair (^{82}Se as spike for both experiments) for the analyses. Although such an agreement would not necessarily indicate accuracy, it does show that no systematic biases are introduced into the analyses because of isotope-specific interferences. Comparative data for hydride generation ICP-MS and hydride generation AAS, indicating the true accuracy of the two methods, are summarised in Table 7. The Se content of NBS SRM 1577a Bovine Liver obtained with both methods agreed well with the certified value of 0.7 ± 0.07 μg g^{-1}. Inter-method agreement to within their combined measurement precision was observed for all the matrices, except plasma for which a difference of 30% was found.

As expected, the *in vitro* SID method provided analytical data with considerably better precision than the hydride generation AAS procedure. The over-all precision of the hydride generation ICP-MS method for quantitative analysis was generally similar to the expected measurement precision of the ion beam intensity ratios (Fig. 2 and Table 4), demonstrating the validity of the assumption that this method has greater analytical precision because it relies primarily, but not exclusively, on the measurement precision of the underlying ratios.

Practical aspects of isotopic analysis

A major feature of the proposed method is its accuracy under the conditions of high sample throughput. All the methods of isotopic analysis reported for mineral/trace elements[4,5,9–14] require chemical separation, the extent of which varies considerably depending on the specific method, the isotopes in question and the nature of the matrix. Methods based on thermal ionisation mass spectrometry generally require the most extensive chemical separations, and this requirement constitutes one of the major limiting factors in the development of this technique for stable isotope tracer studies. In this respect, ICP-MS has allowed a considerable degree of simplification, but in all the instances reported to date some degree of chemical separation has been required.[7,9–14]

For Se, both NAA[4] and GC-MS[5] require the use of separation techniques. We have previously attempted to develop the method of ICP-MS for Se isotopes in the pneumatic nebulisation sample introduction mode and have found that it also requires multi-step chemical separation procedures with potentially serious interference problems.[7] The proposed hydride generation ICP-MS method obviates this requirement completely. The method only requires that Se be present as selenite prior to its reaction with $NaBH_4$, a common requirement for all current methods of isotopic analysis for this element.[4,5] The removal of the need for chemical separation is, of course, due to the selective separation capability inherent in the hydride generation process.

The method described here permits the preparation of at least 20 samples per day up to the point of mass spectrometric analysis. If the measurement precisions reported here are sufficient for a specific application, about 100 analyte solutions can be readily processed per 8-h working day for the two isotope ratios, including the necessary blanks and calibration standards. Therefore, it is clear that this method represents an important addition to the analytical methodology that is currently available for stable isotope tracer investigations.

This work was supported by NIH R01-CA38943 and DK26678-09.

References

1. Janghorbani, M., Christensen, M. J., Nahapetian, A., and Young, V. R., *Am. J. Clin. Nutr.*, 1982, **35**, 647.
2. Janghorbani, M., and Young, V. R., *in* Combs, G. F., Jr., Spallholz, J. E., Levander, O. A., and Oldfield, J. E., *Editors*, "Selenium in Biology and Medicine, Third International Symposium," Van Nostrand Reinhold, New York, 1987, pp. 450–471.
3. Swanson, C. A., Reamer, D. C., Veillon, C., King, J. C., and Levander, O. A., *Am. J. Clin. Nutr.*, 1983, **38**, 169.
4. Janghorbani, M., Ting, B. T. G., and Young, V. R., *Am. J. Clin. Nutr.*, 1981, **34**, 2816.
5. Reamer, D. C., and Veillon, C., *J. Nutr.*, 1983, **113**, 786.
6. Swanson, C. A., Reamer, D. C., Veillon, C., and Levander, O. A., *J. Nutr.*, 1983, **113**, 793.
7. Janghorbani, M., *in* Date, A. R., and Gray, A. L., *Editors*, "Applications of ICP-MS," Blackie, London, 1989, pp. 115–141.
8. Houk, R. S., *Mass Spectrom. Rev.*, 1988, **7**, 425.
9. Janghorbani, M., Ting, B. T. G., and Fomon, S. J., *Am. J. Hematol.*, 1986, **21**, 277.
10. Serfass, R. E., Thompson, J. J., and Houk, R. S., *Anal. Chim. Acta*, 1986, **188**, 73.
11. Ting, B. T. G., and Janghorbani, M., *Spectrochim Acta, Part B*, 1987, **42**, 21.
12. Sun, X. F., Ting, B. T. G., Zeisel, S. H., and Janghorbani, M., *Analyst*, 1987, **112**, 1223.
13. Janghorbani, M., Davis, T. A., and Ting, B. T. G., *Analyst*, 1988, **113**, 405.
14. Schuette, S., Vereault, D., Ting, B. T. G., and Janghorbani, M., *Analyst*, 1988, **113**, 1837.
15. Woodhead, J. C., Drulis, J. M., Rogers, R. R., Ziegler, E. E., Stumbo, P. J., Janghorbani, M., Ting, B. T. G., and Fomon, S. J., *Pediatr. Res.*, 1988, **23**, 495.
16. Fomon, S. J., Janghorbani, M., Ting, B. T. G., Ziegler, E. E., Rogers, R. R., Nelson, S. E., Ostedgaard, L. S., and Edwards, B. B., *Pediatr. Res.*, 1988, **24**, 20.

17. Janghorbani, M., Ting, B. T. G., and Zeisel, S. H., *in* Prasad, A. S., *Editor*, "Essential and Toxic Trace Elements in Human Health and Disease," Alan R. Liss, New York, 1988, pp. 545–556.
18. Janghorbani, M., and Ting, B. T. G., *Anal. Chem.*, 1989, **61**, 701.
19. Ting, B. T. G., and Janghorbani, M., *J. Anal. At. Spectrom.*, 1988, **3**, 325.
20. Welz, B., and Melcher, M., *Analyst*, 1984, **109**, 569.
21. Thompson, M., Pahlavanpour, B., Walton, S. J., and Kirkbright, G. F., *Analyst*, 1978, **103**, 705.
22. Pettersson, J., Hansson, L., and Olin, A., *Talanta*, 1986, **33**, 249.
23. Janghorbani, M., *Prog. Food Nutr. Sci.*, 1984, **8**, 303.

Paper 8/03818J
Received September 27th, 1988
Accepted January 11th, 1989

Inductively Coupled Plasma Mass Spectrometric Determination of the Absorption of Iron In Normal Women

Paul G. Whittaker and Tom Lind
University Department of Obstetrics and Gynaecology, Princess Mary Maternity Hospital, Newcastle, Tyne and Wear NE2 3BD, UK

John G. Williams and Alan L. Gray
ICP-MS Unit, Department of Chemistry, University of Surrey, Guildford GU2 5XH, UK

The determination of iron isotope ratios in blood, without prior sample preparation, using inductively coupled plasma mass spectrometry (ICP-MS) with sample introduction by electrothermal vaporisation (ETV) is described. Following oral administration of 5 mg of enriched $^{54}FeSO_4$ and intravenous administration of 200 μg of $^{57}FeSO_4$ to non-pregnant women, the $^{54}Fe:^{56}Fe$ and $^{57}Fe:^{56}Fe$ isotope ratios in serum were measured reliably within 20 min per sample in quintuplicate. Changes in the fractional absorption of iron during human pregnancy could therefore be assessed.

Keywords: *Inductively coupled plasma mass spectrometry; iron; stable isotopes; women; absorption*

Assessment of the extent to which oral iron absorption increases during normal pregnancy can help to resolve the issue of whether normal pregnant women need routine iron supplements. This is important not only because oral iron can cause gastrointestinal upsets in many pregnant women but also because the absorption of other elements, such as magnesium and zinc, may be affected. The resulting therapy is also a considerable financial burden on the National Health Service, costing millions of pounds annually.

Although mass spectrometric methods have been available to investigate the absorption of trace minerals,[1–4] there are few reports of this technique having been used to study human pregnancy.[5] Until inductively coupled plasma mass spectrometry (ICP-MS) became commercially available, the determination of stable isotope ratios was carried out using techniques such as neutron activation analysis or thermal ionisation mass spectrometry, where measurement was both complex and time consuming and sample preparation often difficult.

This paper describes the use of ICP-MS to determine iron isotope ratios with sample introduction by electrothermal vaporisation (ETV) without prior sample preparation. The use of two enriched isotopes was considered most suitable for the studies relating to pregnancy, and because of polyatomic ion interferences ETV was used as a means of sample introduction.

Experimental

Chemicals

Enriched ^{54}Fe and ^{57}Fe were obtained as iron(II) sulphate from the UK Atomic Energy Authority at Harwell; a mass analysis is shown in Table 1. Both iron(II) sulphate preparations were dissolved in doubly distilled, de-ionised water with 3 mg ml^{-1} of ascorbic acid (final pH, 2.9) and then 5-ml aliquots of each solution were sealed under nitrogen in glass ampoules. The ampoules for oral administration contained 5.23 mg of total iron, equivalent to 5.01 mg of ^{54}Fe and those for intravenous (IV) administration contained 196 μg of total iron, equivalent to 187 μg of ^{57}Fe.

Table 1. Mass analysis of enriched isotope preparations

Enriched isotope	At.-%			
	54	56	57	58
$^{54}FeSO_4$	95.6	4.31	0.014	0
$^{57}FeSO_4$	0	3.00	95.10	1.9

Patients

Four normal healthy women were recruited to assist in the study. All women had the routine haematological and biochemical tests performed to assess their iron status and all were found to be without evidence of anaemia or other medical disorders. All were non-smokers and none took oral contraceptive preparations. Ethical approval was obtained from the Newcastle District Health Authority.

Patient Protocol

Subjects attended the Newcastle research unit at 9.00 a.m. having fasted overnight for at least 10 h. An 8-ml basal blood sample was obtained by venepuncture and the IV cannula was left *in situ*. The IV dose of ^{57}Fe was then administered, followed 5 min later by the oral dose, washed down with 60 ml of tap water. Further blood samples were obtained from the other arm 15, 30, 45, 60, 90, 120, 150, 180, 240, 300 and 360 min after the IV dose. A light breakfast was given after the 30-min blood sample and lunch after the 180-min sample, so that any effects of the increase in nausea and hunger during pregnancy could be minimised. The blood samples were allowed to clot at room temperature and the serum was separated and stored at −20 °C until required for analysis.

ICP-MS Isotope Ratio Determination

The combination of an atmospheric inductively coupled plasma and a quadrupole mass spectrometer was first described by Houk *et al.*[6] The sampling of ions from the plasma into the mass spectrometer is achieved with differentially pumped vacuum regions. The ICP-MS system used for these studies is described in detail elsewhere.[7] The technique has been used successfully to carry out isotope ratio determinations of several elements in a variety of materials, for example, Br, Li, Fe and Zn in biological materials,[8–11] Pb and Re in geological materials[12,13] and U in nuclear materials.[14]

The determination of the entire range of iron isotope ratios by ICP-MS with sample introduction by conventional nebulisation is prone to significant error as ^{54}Fe and ^{56}Fe suffer from severe polyatomic ion interferences by $^{40}Ar^{14}N^+$ and $^{40}Ar^{16}O^+$, respectively. Fig. 1 shows the blank spectrum of

this mass region, with 10 ng ml^{-1} of ^{55}Mn as a reference. As ^{54}Fe and ^{56}Fe were two of the three isotopes under investigation (the third being ^{57}Fe), a method was required to determine isotopes of Fe in the absence of these interfering ions which are produced as the result of ion - molecule reactions between the plasma gases (Ar, H, O and N) in the interface region. Each, apart from Ar, is derived mainly from the water introduced with pneumatic nebulisation.

Sample introduction with ETV instead of the normal nebuliser - spray chamber arrangement[12] (Fig. 2) significantly reduces the levels of certain polyatomic ion interferences as samples are introduced in the absence of any accompanying solvent. Fig. 3 shows the blank spectrum of the mass region 53–58 u in the absence of water, with the peaks at 54 and 56 u reduced almost to background levels.

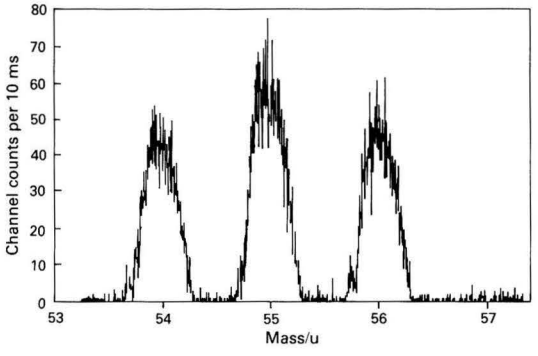

Fig. 1. Iron spectrum of the solution blank with 10 ng ml^{-1} of ^{55}Mn. Integrated counts: 54 u, 3900; 55 u, 5300; 56 u, 4300; and 57 u, 5

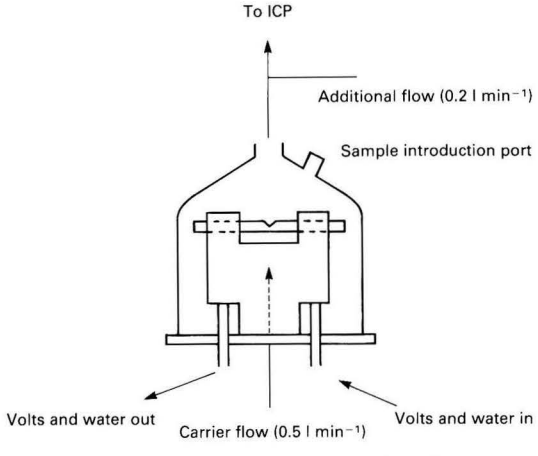

Fig. 2. Schematic diagram of the electrothermal system

An ETV system allows gentle heating of the sample on a graphite rod, causing the solvent content of a sample to be driven off, leaving only a dry coating of the sample on the rod. Further ashing, at a higher temperature, can be carried out to "burn off" the organic matrix, followed by a 5-s high-temperature vaporisation to drive off the remaining material, containing the elements of interest. As vaporisation commences, data acquisition is initiated, in the knowledge that the peaks occurring at 54 and 56 u can only be due to iron. In addition, an ETV sample introduction system allows only very small volumes of sample to be introduced, in this instance 5 μl. This is particularly useful in biomedical studies, where there is often only a minimal volume of sample available.

The ICP-MS operating conditions are summarised in Table 2. With a dwell time of 100 μs (100 sweeps), 1024 channels of the multi-channel analyser (MCA) were used; the scanning mode was in the range 53–58 u. Following data acquisition on the MCA, the data were stored and peak integration was carried out on an IBM-PC portable computer using "in-house" software. Isotope ratio calculations, including blank subtractions, were carried out using commercial spreadsheet software.

The ICP-MS system (ion optics, plasma-sampling cone alignment) was optimised for a dry aerosol by first monitoring the signal for $^{12}C^+$ (which could easily be generated from a blank firing of the ETV, but which was also present as a CO_2 impurity in the argon), then by fine tuning the ion optics using the signal for $^{114}Cd^+$, which was volatilised slowly from the rod.[12] In the absence of a system for measuring the rod temperature, the applied voltage settings for drying and ashing were determined by trial and error. The optimum vaporisation temperature was determined by carrying out repeated iron standard vaporisations, each at a high rod setting, until the maximum signal response was obtained. Isotope ratio accuracy was assessed with aqueous solutions of natural iron (1 μg ml^{-1}) and the solutions of known enrichment from Harwell. On each day of analysis, the natural ratios were checked with a basal serum sample from each patient, hence enabling the level of background interferences to be assessed. In addition, before each sample was analysed, the interference levels were determined from a blank rod vapori-

Table 2. ICP-MS operating conditions

Plasma power	1300 W
Reflected power	<10 W
Coolant Ar flow-rate	14 l min^{-1}
Auxiliary flow-rate	0.5 l min^{-1}
Carrier flow-rate—	
ETV unit	0.5 l min^{-1}
By-pass	0.2 l min^{-1}
Sampling cone orifice diameter	1 mm
Skimmer cone orifice diameter	0.7 mm

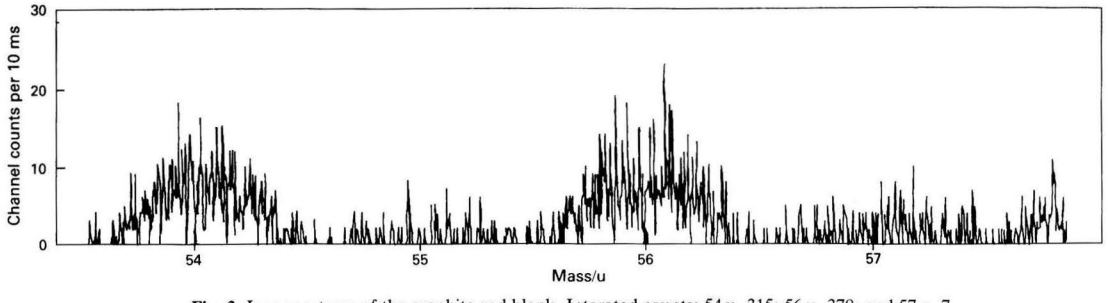

Fig. 3. Iron spectrum of the graphite rod blank. Intgrated counts: 54 u, 315; 56 u, 378; and 57 u, 7

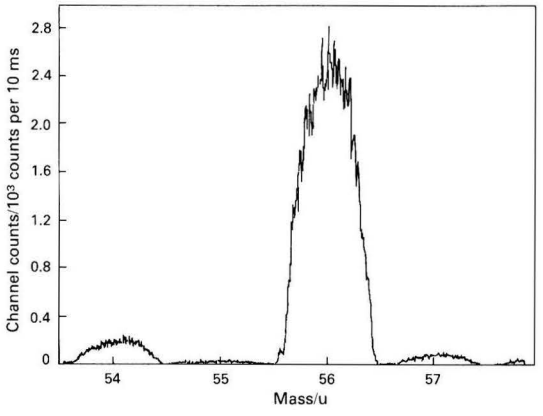

Fig. 4. Iron spectrum of the basal serum. Integrated counts: 54 u, 24100; 56 u, 321000; and 57 u, 10300

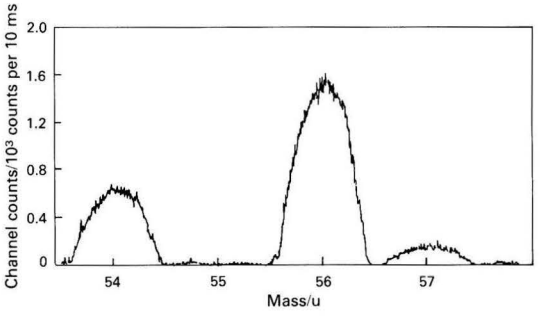

Fig. 5. Iron spectrum of the enriched serum at $t = 60$ min. Integrated counts: 54 u, 88200; 56 u, 205000; and 57 u, 18400

sation. Each 5-μl serum sample was subjected to at least five replicate analyses and between each sample the graphite rod was "cleaned" by performing several maximum-voltage vaporisations. Each set of samples for a given patient test occasion was analysed within 1 d in order to reduce variability. A basal quality control serum sample (*i.e.*, with natural Fe isotope ratios) was analysed each day to assess the across-assay variability.

Pharmacokinetic Analysis

The commonly used method for calculating absorption is to calculate the total area under the curve (AUC) of the logarithm of the enrichment in isotope ratio *versus* time[15] for the oral $^{54}Fe:^{56}Fe$ (AUC_{oral}) and the intravenous $^{57}Fe:^{56}Fe$ (AUC_{IV}). The ratio of these areas after intravenous and oral administration of equal doses of a compound is equivalent to the fraction absorbed.[16] When different doses are given, then

$$\text{oral absorption} = (AUC_{oral}/AUC_{IV})(dose_{IV}/dose_{oral})$$

Results and Discussion

For the solution blank the polyatomic peak at 54 u has a count equivalent to about 50 pg (Fig. 1) and the use of ETV reduces this background by one order of magnitude (Fig. 2). The spectrum from a basal (*i.e.*, not enriched) serum sample is shown in Fig. 4 and that of an enriched sample in Fig. 5. These signals were generated from 3–5 ng or iron in 5 μl of serum; in basal samples this corresponds to about 2–300 pg of ^{54}Fe. From Fig. 4 it can be seen that the isotope ratios are 0.0705 for $^{54}Fe:^{56}Fe$ and 0.0306 for $^{57}Fe:^{56}Fe$. Sixty minutes into the test $^{54}Fe:^{56}Fe$ has increased to 0.4044 and $^{57}Fe:^{56}Fe$ to 0.1004. The assay reproducibilities and limits of detection are shown in Table 3. The precision of the measurement of isotope ratios was calculated over ten assays. For $^{54}Fe:^{56}Fe$ the average within-sample coefficient of variation (CV) was 2.9% [0.9% standard deviation (SD)]. Hence, for the average basal or natural sample $^{54}Fe:^{56}Fe$ was 0.0694 with an SD of 0.0020, and a sample with an isotope ratio >3SD, *i.e.*, above 0.0754, was significantly different. The limit of detection of enrichment was, therefore, 0.0060. For $^{57}Fe:^{56}Fe$, the average basal ratio was 0.0289, the within-sample CV 3.8% (1.5% SD) and the limit of detection of enrichment 0.0033. Across-assay variation was 5.1% for $^{54}Fe:^{56}Fe$ and 8.7% for $^{57}Fe:^{56}Fe$. For a clinical assay, the precision was good. Calculation of the effect of within-sample variation showed that typically it would give a CV of 6.4% in the final absorption measurement. Fig. 6 shows the time course of the enrichment in Fe ratios over the period of study in one non-pregnant individual. The absorption of a 5-mg oral dose of iron(II) sulphate over 6 h was 9.0% in this subject and 8.4, 8.9 and 17.2% in three other non-pregnant women (geometric mean 10.4%). A further nine women have now been studied throughout pregnancy and the results are still being analysed.

Table 3. Assay reproducibility. $n = 10$

	$^{54}Fe:^{56}Fe$	$^{57}Fe:^{56}Fe$
CV* within-sample, % . .	2.9	3.8
CV across-assay, %	5.1	8.7
Limit of detection of enrichment (3SD)	0.0060	0.0033

* CV = coefficient of variation.

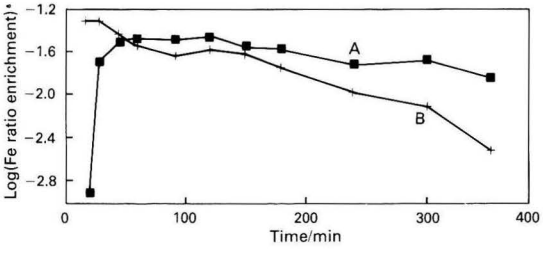

Fig. 6. Time course of Fe ratio enrichment in serum after A, oral ^{54}Fe and B, intravenous ^{57}Fe administration to a non-pregnant woman

Conclusion

Past studies using radioactive isotopes[17] have suggested that the absorption of iron increases during human pregnancy. However, reports differ widely about the degree of absorption, probably because of the variation in clinical and analytical techniques, the doses used and the small number of subjects studied. The use of a whole body counter 2 weeks after the administration of ^{55}Fe and ^{59}Fe suggested that the mean oral absorption of 3 mg of the iron(II) salt was 35% (but with a range of 17–45%) in eight healthy non-pregnant women.[18] Ethical considerations now prevent repetition in healthy subjects even using low doses. Stable isotope studies had until recently involved costly and complicated methodologies but the advent of ICP-MS promises to simplify these important investigations. The existence of polyatomic ion interferences particularly at 54 and 56 u had initially restricted the scope of these studies. Janghorbani *et al.*[10] investigated the ingestion of one stable isotope of iron (^{58}Fe) to determine iron availability in infants and children. However, the relatively rare ^{58}Fe isotope is particularly expensive and requires a long sample counting time to achieve adequate precision. Further,

although the patient protocol was simple, requiring only one sample of red blood cells 2 weeks after ingestion, erythrocyte analysis requires assumptions to be made about the level of oral iron incorporation in erythrocytes, which may not be applicable during pregnancy. This study has chosen to use the double-isotope approach to assess short-term iron absorption, two concomitant tracers being held to give greater accuracy[19] and blood samples allowing a more simple patient protocol than the faecal collection used by Ting and Janghorbani.[20]

This work shows that the interferences from polyatomic ions can be overcome, hence opening up the potential for dual tracer techniques for the study of iron absorption. A further consideration is the dose required for successful tracer studies. The IV dose had to be sufficiently low not to harm the patients as a result of saturating their iron binding capacity, while being sufficiently high to be detected accurately. This work shows that 200 μg of ^{57}Fe given intravenously will increase the natural ^{57}Fe : ^{56}Fe ratios from 0.030 to 0.100 with a limit of detection at an enrichment of 0.003; samples were still above this level 6 h post injection. Five milligrams of ^{54}Fe is well within the average daily dietary intake of our normal subjects (about 10–15 mg) and, with a non-pregnant mean of 10% absorption in our 6-h study (about 500 μg absorbed into the serum), again allows a precise determination of isotope ratio enrichment.

This new adaptation of ICP-MS offers excellent scope for studies of iron absorption during normal pregnancy and those complicated by anaemia and malabsorption.

The authors are grateful to the charity Birthright for financial support of the clinical project. The ICP-MS unit (Surrey) is an NERC analytical facility. J. G. W. acknowledges additional support from the MoD (DQA).

References

1. King, J. C., Raynolds, W. L., and Margen, S., *Am. J. Clin. Nutr.*, 1978, **31**, 1198.
2. Miller, D. D., and van Campen, D., *Am. J. Clin. Nutr.*, 1979, **32**, 2354.
3. Janghorbani, M., Ting, B. T. G., and Young, V. R., *J. Nutr.*, 1980, **110**, 2190.
4. Johnson, P. E., *J. Nutr.*, 1982, **112**, 1414.
5. Dyer, N. C., and Brill, A. B., "Nuclear Activation Techniques in the Life Sciences," IAEA, Vienna, 1972, pp. 469–477.
6. Houk, R. S., Fassel, V. A., Flesch, G. D., Svec, H. J., Gray, A. L., and Taylor, C. E., *Anal. Chem.*, 1980, **52**, 2283.
7. Date, A. R., and Gray, A. L., *Analyst*, 1983, **108**, 159.
8. Janghorbani, M., Davies, T. A., and Ting, B. T. G., *Analyst*, 1988, **113**, 405.
9. Sun, X. F., Ting, B. T. G., Zeisel, S. H., and Janghorbani, M., *Analyst*, 1987, **112**, 1223.
10. Janghorbani, M., Ting, B. T. G., and Fomon, S. J., *Am. J. Hematol.*, 1986, **21**, 277.
11. Serfass, R. E., Thompson, J. J., and Houk, R. S., *Anal. Chim. Acta*, 1986, **188**, 73.
12. Date, A. R., and Cheung, Y. Y., *Analyst*, 1987, **112**, 1531.
13. Linder, M., Leich, D. A., Borg, R. I., Russ, G. P., Bazan, J. M., Simons, D. S., and Date, A. R., *Nature (London)*, 1986, **320**, 246.
14. Russ, G. P., Bazan, J. M., and Date, A. R., *Anal. Chem.*, 1987, **59**, 984.
15. Gibaldi, M., and Perrier, D., "Pharmacokinetics," Marcel Dekker, New York, 1982, pp. 444–449.
16. Gibaldi, M., and Perrier, D., "Pharmacokinetics," Marcel Dekker, New York, 1982, pp. 169–175.
17. Heinrich, H. C., Bartels, H., Heinsch, B., Hausmann, K., Kuse, R., Humke, W., and Mauss, H. J., *Klin. Wochenschr.*, 1968, **46**, 199.
18. Sandberg, B., *Acta Obstet. Gynecol. Scand., Suppl.*, 1975, **48**, 43.
19. Werner, E., Hansen, C., Wittmaack, K., Roth, P., and Kaltwasser, J. P., *Inserm. Symp. Ser. (Paris)*, 1983, **113**, 201.
20. Ting, B. T. G., and Janghorbani, M., *Anal. Chem.*, 1986, **58**, 1334.

Paper 8/04872J
Received December 19th, 1988
Accepted February 16th, 1989

Secondary Ion Mass Spectrometric Determination of Impurities in Aluminium Oxide

Hisashi Morikawa, Yoshinori Uwamino and Toshio Ishizuka
Analytical Chemistry Division, Chemistry Department, Government Industrial Research Institute, 1-1 Hirate-cho, Kita-ku, Nagoya 462, Japan

Impurities in aluminium oxide (alumina) were determined by secondary ion mass spectrometry (SIMS), which enabled the sample powder to be analysed without time-consuming pre-treatment stages. The difficulty of acquisition of standard samples associated with quantitative SIMS was overcome by preparing chemically the standard samples in powder form and applying the calibration graph method. The four elements (Ca, Fe, Ga and Ti) in an alumina reference material and commercial alumina samples were determined successfully and the results agreed well with those of inductively coupled plasma atomic emission spectrometry. The procedures are described and experimental results presented.

Keywords: *Secondary ion mass spectrometry; determination of impurities; aluminium oxide*

Aluminium oxide (alumina) is one of the advanced ceramics which are currently of importance in the progress of materials technology. The physical, electrical, thermal, mechanical and optical properties of the material enable it to be used widely in various fields of industry.[1] As most of these properties are affected significantly by impurities present in the alumina powder, their determination is important in the characterisation of alumina.

The impurities present in alumina have been determined successfully by several methods, particularly atomic absorption spectrometry[2–5] and inductively coupled plasma atomic emission spectrometry (ICP-AES).[6–8] Both these methods, however, require the sample powder to be converted into solution, requiring special care and much time. On the other hand, other instrumental techniques, *e.g.*, neutron activation analysis[9] and X-ray fluorescence spectrometry,[10] which do not require sample dissolution, have been reported for alumina. Secondary ion mass spectrometry (SIMS) has the potential to analyse a solid sample directly with high sensitivity and the capacity to detect all the elements from H to U while also providing lateral and in-depth distributions.[11]

In quantitative analysis by SIMS, there are several quantification algorithms including a calibration graph method, a thermodynamic approach based on a local thermal equilibrium model and a matrix ion species ratio method based on the calculation of a series of sensitivity factors of elements, generated as a function of the sample chamber oxygen pressure.[12] Each method has been applied successfully in certain instances.[13–16] The calibration graph method is recognised as a valuable technique. However, the acquisition of standards having the same matrix as the sample to be analysed is the limiting factor for practical applications owing to the matrix effects on the secondary ion yields of the elements. Hence, the preparation of standards for the calibration was studied first. The operating conditions, relative sensitivities of the elements, detection limits, analytical precision and applications will be discussed in the following sections.

Experimental

Apparatus

The quantitative analysis of alumina was conducted using an Hitachi IMA-2 secondary ion mass spectrometer equipped with a duoplasmatron primary ion source. High-purity oxygen was used in the ion source, producing the primary O_2^+ ion beam. The ions were accelerated to 7 keV relative to the sample potential and focused to 170–1000 μm in diameter on the sample surface. Instrumental parameters are summarised in Table 1. Charge build-up effects at the surface due to ion bombardment were eliminated by mixing spectroscopic grade graphite powders (SP-1, National Carbon) with the sample powders.

Table 1. Instrumental parameters

Primary ion—	
Source	O_2^+
Energy	7 keV
Current	2–4 μA
Spot size	170–1000 μm
Secondary ion—	
Polarity	Positive
Accelerating voltage	3 kV
Vacuum conditions—	
Primary ion column	5×10^{-3} Pa
Sample chamber	3×10^{-5}–4×10^{-5} Pa
Detector—	
Electron multiplier	

Reagents

A stock solution of Al (2% *m/V*) was prepared by dissolving Al metal (99.999% pure, Soekawa Chemicals) in 1 M nitric acid. Commercial standard solutions for atomic absorption spectrometry (1 mg g^{-1}, Wako Pure Chemical) were also used as the stock solutions for Ga and Fe, and Titrisol (Merck) for Ti. The stock solutions of other elements were prepared from their nitrates. All other chemicals were of analytical-reagent grade.

Samples

The National Bureau of Standards Standard Reference Material (NBS SRM) 699 Alumina was used as a reference standard. Kanto Chemical (01173), Katayama Chemical (01-2810) and Wako Chemical (012-01965) alumina powders were analysed.

Preparation of Calibration Standards

The calibration standards were prepared by two distinct methods, *i.e.*, chemical and physical. The chemical preparation was as follows: mixtures of the stock solutions of the elements and the Al stock solution were evaporated to dryness and then ignited at 1200 °C in alumina crucibles (99.9%) for conversion to the corresponding oxides. The physical stan-

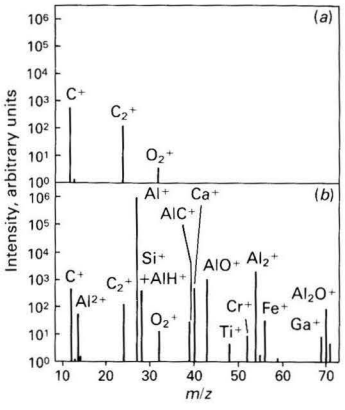

Fig. 1. Secondary ion mass spectra of (*a*) graphite powders and (*b*) NBS SRM 699 Alumina mixed with graphite powders. Alumina content is given in Table 2

dards were obtained by thorough mixing of the oxide powders of the elements with the alumina powders in a mixer/mill (Spex 8000). Two series of standards were prepared to prevent the interference from CaO on Fe at *m/z* 56. The first series consisted of Ca, Cr, Cu, Fe, Ga, Mg and Mn, each at concentrations of 10, 50, 250 and 500 μg g^{-1}, and the second of Fe and Ti, each at concentrations of 1.25, 50 and 250 μg g^{-1}.

Procedure

The sample was powdered with an agate pestle in an agate mortar after which it was mixed well with graphite powder (sample - graphite, 2 + 1 *m/m*) and the mixture pressed at 200 kg cm^{-2}. A sheet of PTFE (1 mm thick) was placed between a tungsten platen and the sample powder to prevent contact of the powder with the platen. The sample was obtained in the form of a pellet 10 mm in diameter and about 1 mm thick. This was then mounted on a sample holder and introduced into the sample chamber.

Prior to analysis, pre-sputtering was performed for 10 min to clean the sample surface. This removed contaminants of monolayer coverage efficiently.

Results and Discussion

Background Signals

The presence of a background signal in SIMS, as in any form of spectrometry, is a nuisance. As the sample was mixed with graphite powder, the intensities of the cluster ion, C_2^+, and the molecular ion, AlC^+, were not negligible and these ions produced backgrounds which interfered with the Mg^+ and K^+ signals, respectively (Fig. 1). No other cluster ions or molecular ions contributed to the background because their mass numbers did not correspond to those of the elements of interest.

Homogeneity of the Prepared Samples for Standards

The homogeneity of the standard samples was investigated and the deviations of a few ion intensity ratios obtained for chemically and physically prepared standards and for the NBS SRM were compared. The elements measured were Ca and Fe owing to their higher content in the NBS SRM. Each sample was analysed between five and eight times at five different points. The ion intensity ratios Ca/Al and Fe/Al are shown in Fig. 2. The matrix ions Al^+, AlO^+, Al_2^+, Al_2O^+ and their combinations were measured and Al^+ was selected for

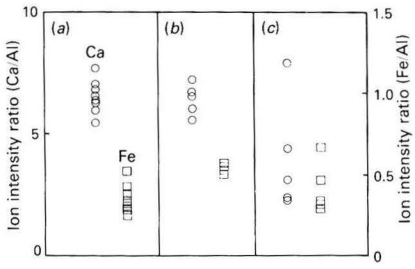

Fig. 2. Reproducibility of the ion intensity ratios Ca/Al and Fe/Al in the alumina powders. (*a*) NBS SRM 699 Alumina; (*b*) chemically prepared alumina; and (*c*) physically prepared alumina. Amount of Ca: (*a*), 257 μg g^{-1}; (*b*) and (*c*), 250 μg g^{-1}. Amount of Fe: (*a*), 91 μg g^{-1}; (*b*) and (*c*), 250 μg g^{-1}

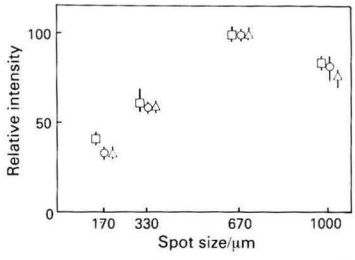

Fig. 3. Relative secondary ion intensities of Al, Ca and Fe as functions of the spot size of the primary ion beam. Error bars represent the range of values from five measurements. □, Fe; ○, Al; and △, Ca

normalisation purposes because of the minimum fluctuation in its signals; the other ions were relatively more sensitive to slight variations in the operating conditions.

The relative standard deviations of the Ca/Al intensity ratios were 9.1, 9.4 and 60.6% for the NBS SRM 699 Alumina, the chemically prepared and the physically prepared samples, respectively. As a result of tests on the lateral homogeneities of NBS SRM Glass and Clay powder samples (89, 91, 93a and 98), Morgan and Werner[14] reported that a relative secondary ion current was reproducible to better than 20%. This indicates that the chemically prepared sample is as homogeneous as the NBS SRM 699 Alumina and hence suitable for use as the standard for quantitative SIMS.

Spot Size of the Primary Beam

The current transmission of an ion optical system and the maximum transmittable ion current in an optimally matched secondary ion mass spectrometer depend on the spot size of the primary beam. It has been shown[17] that a high transmission can easily be achieved for a small primary beam diameter. However, the smaller spot size results in a lower sensitivity owing to the smaller area analysed and the lower primary ion current.

In this work the relationship between the spot size of the primary beam and the secondary ion intensity was studied. A spot size of 670 μm was found to be optimum for collecting secondary ions efficiently and gave the most reproducible ion intensity ratios with our instrument (Fig. 3). The ion intensity ratios were found to be independent of the spot size of the primary beam.

Relative Sensitivities

The chemically prepared sample containing 250 μg g^{-1} of each element was bombarded with a 7-keV O_2^+ beam. Fig. 4 shows

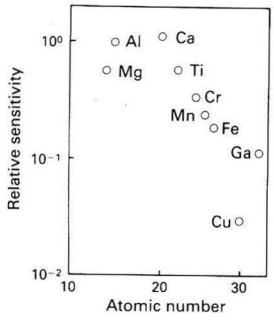

Fig. 4. Relative sensitivities of several elements in alumina. Aluminium is taken as unity

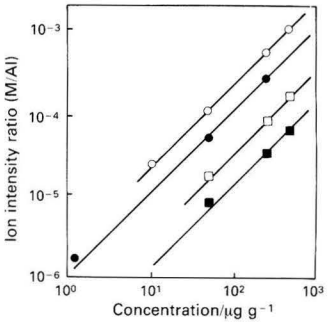

Fig. 5. Calibration graphs for ○, Ca; □, Fe; ■, Ga; and ●, Ti in alumina

a plot of relative sensitivity against atomic number for eight elements (Mg, Ca, Ti, Cr, Fe, Mn, Cu and Ga). Each value was corrected for the natural abundance of the isotope, and the value for Al was taken to be unity. These results are similar to those for NBS SRM 466 Low-Alloy Steel.[18]

Detection Limits

The detection limits for Ca, Cr, Cu, Fe, Ga, Mg, Mn and Ti were 4, 10, 10, 23, 1, 14, 3 and 1 μg g^{-1}, respectively, and were defined as the concentrations producing signals equal to three times the background fluctuations. The detection limits for Cr and Fe were higher than might have been expected from the relative sensitivities compared with the other elements studied (Fig. 4). This may be due to background formations arising from sputtering of instrument components (stainless steel) by scattered ions (O^+, O_2^+, etc.) or the neutral molecule O_2.

Calibration Graphs

The relationships between the concentrations of the elements in alumina and the ion intensity ratios M/Al were examined. Fig. 5 shows the calibration graphs obtained for Ca, Ti, Fe and Ga; these were linear in the concentration range 1–500 μg g^{-1}. The linear range extends over a further two orders of magnitude of concentration. This wide dynamic range is a further advantage of SIMS.

Analytical Precision

When the sample surface was sputtered continuously, changes occurred in the surface topography, surface electrical states and the intensity of the primary ions. The ultimate reproducibility [coefficient of variation (CV)] of the secondary ion intensity ratios was calculated to be within 35%; this allows for some sample inhomogeneity and instrumental variations over the time during which data were collected. Even allowing for such changes, however, the deviation (CV) in secondary ion intensity ratios was <10% for a cycle of measurements.

Table 2. Analytical results for NBS SRM 699 Alumina

Element	SIMS*/ μg g^{-1}	ICP-AES*/ μg g^{-1}	Certified value/μg g^{-1}
Ca	237 ± 8	257 ± 1	257
Cr	<10	<1	1.4
Cu	<10	1.5 ± 0.1	4
Fe	113 ± 14	96 ± 0.6	91
Ga	72 ± 7	75 ± 0.6	74
Mg	<14	2.7 ± 0.02	3.6
Mn	<3	3.3 ± 0.02	3.9
Si	−†	69 ± 7.5	65
Ti	5 ± 1	3.6 ± 0.1	6

* Mean content ± standard deviation for five determinations.
† Not determined.

Table 3. Analytical results for practical alumina samples

Element	Kanto*/μg g^{-1}	Katayama*/μg g^{-1}	Wako*/μg g^{-1}
Ca	27 ± 4 (29)	45 ± 2 (49)	29 ± 1 (29)
Cr	<10 (<1)	<10 (<1)	<10 (<1)
Cu	<10 (<1)	<10 (<1)	<10 (<1)
Fe	68 ± 4 (67)	71 ± 4 (78)	62 ± 2 (62)
Ga	72 ± 8 (64)	55 ± 8 (51)	55 ± 4 (49)
Mg	<14 (0.6)	<14 (2.6)	<14 (1.7)
Mn	<3 (0.4)	<3 (0.4)	<3 (0.2)
Ti	17 ± 1 (16)	21 ± 2 (19)	24 ± 4 (18)

* Mean content ± standard deviation for five determinations. Values in parentheses were obtained by ICP-AES.

Applications

The NBS SRM 699 Alumina was analysed by the proposed method; the results are given in Table 2 with the reference values determined by ICP-AES. The good agreement between these values provided some evidence that, in addition to ICP-AES, the SIMS method is also reliable.

Impurities in the commercial samples of alumina were also determined by the proposed method. The results are given in Table 3, from which it can be seen that the values for some of the elements in the sample powders were in good agreement with ICP-AES measurements.

Conclusion

The comparison between SIMS and ICP-AES shows that SIMS is the inferior technique in terms of accuracy, sensitivity and reproducibility. However, this study has emphasised one of the advantages of SIMS, namely its capacity to analyse intractable materials without the difficulties associated with sample dissolution or decomposition.

References

1. Gitzen, W. H., *Editor*, "Alumina as a Ceramic Material," American Ceramic Society, Columbus, OH, 1970.
2. Khavezov, I., and Tamnov, B. K., *Fresenius Z. Anal. Chem.*, 1978, **290**, 299.
3. Palmer, T. A., and Winkler, J. M., *Anal. Chim. Acta*, 1980, **113**, 301.
4. Nikolova, B., and Iordanov, N., *Talanta*, 1982, **29**, 861.
5. van der Walt, T. N., and Strelow, F. W. E., *Anal. Chem.*, 1985, **57**, 2889.
6. Ishizuka, T., Uwamino, Y., Tsuge, A., and Kamiyanagi, T., *Anal. Chim. Acta*, 1984, **161**, 285.

7. Morikawa, H., Iida, Y., Ishizuka, T., and Yokota, F., *Bunseki Kagaku,* 1986, **35**, 636.
8. Harada, Y., and Kurata, N., *Bunseki Kagaku,* 1986, **35**, 641.
9. Foner, H. A., *Analyst,* 1984, **109**, 1469.
10. Bennett, H., Oliver, G. J., and Holmes, M., *Trans. J. Br. Ceram. Soc.,* 1977, **76**, 11.
11. Grasserbauer, M., Stingeder, G., Wilhartitz, P., Schreiner, M., and Traxlmayr, U., *Mikrochim. Acta,* 1984, **III**, 317.
12. Benninghoven, A., Rudenauer, F. G., and Werner, H. W., *Editors,* "Secondary Ion Mass Spectrometry," Wiley-Interscience, New York, 1987, p. 287.
13. Ishizuka, T., *Anal. Chem.,* 1974, **46**, 1487.
14. Morgan, A. E., and Werner, H. W., *Anal. Chem.,* 1977, **49**, 927.
15. Ganjei, J. D., Leta, D. P., and Morrison, G. H., *Anal. Chem.,* 1978, **50**, 285.
16. Andersen, C. A., and Hinthorne, J. R., *Anal. Chem.,* 1973, **45**, 1421.
17. Benninghoven, A., Rudenauer, F. G., and Werner, H. W., *Editors*, "Secondary Ion Mass Spectrometry," Wiley-Interscience, New York, 1987, p. 455.
18. Tsunoyama, K., Ohashi, Y., and Suzuki, T., *Anal. Chem.,* 1976, **48**, 832.

Paper 8/04136I
Received October 18th, 1988
Accepted January 13th, 1989

Reconstruction of Constituent Spectra for Individual Samples Through Principal Component Analysis of Near-infrared Spectra

Ian A. Cowe, James W. McNicol and D. Clifford Cuthbertson
Scottish Crop Research Institute, Mylnefield, Invergowrie, Dundee DD2 5DA, UK

Compound component weights for a specific constituent were combined with near-infrared spectra of individual samples to produce a form of spectral reconstruction which highlighted the influence of individual absorbance bands in the estimation of a fitted value for the constituent. The technique is illustrated using a set of wheat flour spectra with corresponding values for protein and moisture. For moisture, all samples exhibited variation at two points in the spectrum where absorbance bands for moisture are known. There was little variation between samples in the relative responses of these bands. For protein, however, individual samples exhibited as few as two and as many as six sources of variation which were used by the model to estimate the protein content of the sample. Not all these sources of variation related to known protein bands, indicating that the model was sensitive to the presence of other constituents such as starch. "Null" points, where adjacent absorbance effects were always in balance, were identified for both moisture and protein. Variation in particle size of samples was shown to distort reconstructed spectra. A simple algorithm using "null" points for protein was shown to reduce this distortion and enabled absorption effects to be more clearly observed.

Keywords: *Principal components; near infrared; graphics; particle size; wheat flour*

Data compression techniques, such as Fourier analysis,[1,2] partial least squares[3,4] and, in particular, principal component analysis[5–7] have all been shown to be useful for relating near-infrared diffuse reflectance (NIR) spectra to the composition of samples. Each of these techniques involves a transformation of the original data to new variables which have better properties than the raw spectra. While all involved increased computation, the time required to produce a regression model that adequately predicts composition may in fact be reduced, as fewer combinations of variates need be examined. In addition, many of these compression techniques provide additional information which can give greater confidence that the model is indeed predicting the constituent of interest, rather than some other correlated variate.

In previous publications[7–9] we have shown that principal component weights can be plotted in the same way as spectra. Using such plots, absorption bands relating to individual constituents can be identified, as can effects relating to physical factors such as particle size variation. Taken one stage further, component weights can be combined with regression coefficients to produce compound component weights,[10] a form of spectral reconstruction that exhibits characteristics similar to the spectrum of the constituent to which the regression is related.

Compound weights are derived from an analysis of the spectral variation of all the samples in a calibration set. They represent an "average" response. A spectral analogue profiling the response of an individual sample, with respect to a specific constituent such as moisture or protein, would allow a study to be made of the degree by which samples vary in the expression of absorbance bands relating to that constituent. This paper presents a method that attempts to achieve these objectives using combinations of compound weights and centred spectra.

Experimental

Derivation of Sample Specific Compound Weights

The theory of principal components has been described elsewhere.[11] Previous papers have discussed the nature of principal component weights,[7] principal component scores[7] and compound weights[10] and their interpretation with respect to NIR spectra; such discussions are not repeated here. To define the variates plotted however, it is necessary to repeat the definition of compound weights.

In reference 10, equation (4) defined a regression model using principal components as follows:

$$Y = B_0 + G_1E_1 + G_2E_2 + \ldots\ldots\ldots + G_{700}E_{700} \qquad (1)$$

Here Y is the fitted chemical value, E_1 to E_{700} represent centred spectral data, where the centred value at any wavelength is the actual spectral value minus the mean value at that wavelength taken over all samples, and B_0 is the intercept coefficient; G_1 to G_{700} are compound weights, where the compound weight for the nth wavelength is defined by

$$G_n = \sum_{i=1}^{q} B_iC_{in} \qquad (2)$$

where B_1 to B_q are regression coefficients relating principal component scores to composition of samples and C_{1n} to C_{qn} are principal component weights for q selected components. Compound weights (G) therefore describe, in terms of all the samples, the relative importance of the data at each wavelength to the fitted value for the constituent of interest. Equation (1) presents a principal component regression model in its equivalent wavelength form; G_1 to G_{700} are the regression coefficients that would be obtained if all wavelengths were included in the equation.

In this paper we concentrate on an examination of the behaviour of sample specific compound weights, which are denoted by (GE). From equation (1) it can be seen that the deviation of the estimated value from the population mean (B_0) is a summation of the regression coefficients (G) times the centred energy values (E) over all wavelengths. As principal components are derived from centred energy values (the difference between the actual and mean response at any wavelength), centred values must be used in this reconstruction. By plotting G_iE_i against the corresponding wavelength i, the contribution at each wavelength to the fitted value for an individual sample can be observed.

Each set of compound weights (GE) is specific to a single sample, as each sample is defined by its spectrum (E_1 to E_{700}), and to a specific regression model for one constituent as defined by the wavelength regression coefficients (G_1 to G_{700}). A different constituent, or regression model, would involve a different set of regression coefficients. Hence for any constituent, we are able to examine the responses of individual

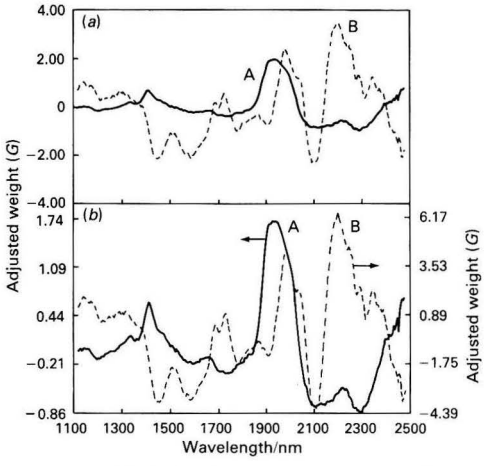

Fig. 1. Reconstructed NIR spectra for A, water and B, protein derived from samples of wheat flour. (*a*) Effects of dividing each set of compound weights by the standard deviation of the constituent values. (*b*) Compound weights scaled individually

samples to the regression model and determine the extent to which absorbance bands relating to the constituent are expressed in that sample.

Samples

A set of 39 spectra of samples of wheat flour obtained from the Flour Milling and Baking Research Association (Chorleywood, UK), with analytical values for moisture and protein was used. All spectra were collected as 700 data points at 2-nm intervals from 1100 to 2498 nm. Before derivation of the components, the first and last ten data points were discarded to avoid the influence of edge effects from the optics and a five-point moving average was used to smooth the spectra.

Adaptation from Published Method

Earlier publications detailed the shapes of the first six principal components for this sample set,[7] and of compound weights derived for two regression models,[10] the first predicting moisture content the other, protein. The graphs shown in reference 10 were scaled in terms of deviations from the mean concentration of a specific constituent and no effort was made to produce a common scale for graphs of compound weights. In fact, the scaling was chosen to emphasise the variation in weight within each graph.

For data reported in this paper, compound weights for all constituents are now scaled in the same units. To standardise the compound weights we divided, in each case, by the standard deviation of the constituent values. This standardisation produces compound weights scaled in terms of standard deviations, enabling a direct comparison of the reconstructed spectra for different constituents or for the same constituent in different samples regardless of the inherent range of concentrations found in the sample set.

Results and Discussion

Reconstructed Sample Spectra for Moisture and Protein

Fig. 1(*a*) shows reconstructed NIR spectra (compound weights *G*) for water and protein derived from 39 samples of wheat flour. In reference 10, compound weights for moisture were derived using the first three principal components and those for protein using components one, three, four and five. Here, the first five components were used to derive compound

Table 1. Reference oven dried moisture and Kjeldahl protein values together with fitted values by NIR for four of the original wheat flour samples. Regression model for moisture used components 1 and 2; for protein components 1, 3 and 4 were used

	Moisture, %		Protein, %	
Sample	Reference	Fitted	Reference	Fitted
1	12.40	12.53	13.80	13.74
3	14.30	14.36	8.40	8.84
12	14.90	14.75	13.90	14.37
16	12.00	11.83	8.90	8.51

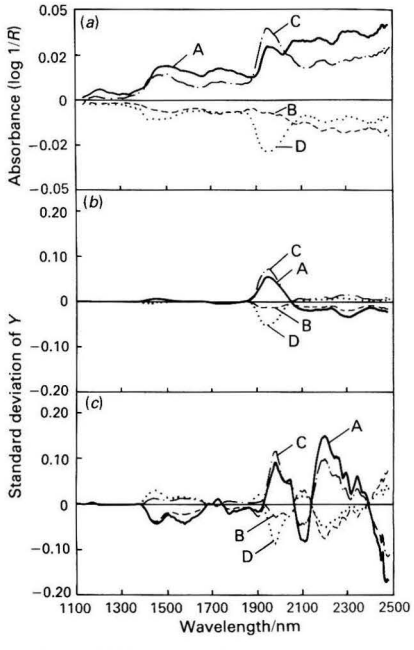

Fig. 2. (*a*) Centred NIR spectra, (*b*) reconstructed moisture spectra and (*c*) protein spectra for four typical samples of wheat flour. A, sample 1; B, sample 3; C, sample 12; and D, sample 16

weights for both moisture and protein. This combination was used to illustrate that the regression coefficients, rather than the combination of components determine the shapes of sample specific compound weights (*GE*). Comparing Fig. 1(*a*) with Fig. 1(*b*) shows the effects of standardising the scales.

Four representative samples were selected to illustrate features of sample specific compound weights. Table 1 shows values for actual and fitted moisture and protein concentrations for these samples.

Fig. 2(*a*) illustrates how the four centred spectra differ from the mean spectrum (shown as the centre line) derived using all 39 samples. In these plots, the same absorbance band may appear either as a local maximum or as a local minimum depending on whether, for that sample, the band intensity was greater or smaller than average. All four samples exhibited increasing variation towards the upper end of the spectrum. Sample 3 appeared to lack any clearly defined absorbance bands. The only absorbance effects observed in samples 12 and 16 related to water (1940 nm). For sample 1, this water band was less well defined and other bands were present in the upper part of the spectrum.

Fig. 2(*b*) shows sample specific compound weights (*GE*) for moisture. The dominant feature in these plots was the clearly

defined absorbance band centred at 1940 nm. The lower half of the spectrum was almost featureless with only small absorbance effects visible in the regions 1400–1550 and 1650–1800 nm. For all samples, the sign of the deviations in the first of these regions was always the same as that for the band at 1940 nm. In the second region the sign was always opposite to that found at 1940 nm. From 2048 to 2390 nm there was a broad region with at least two bands that acted in opposition to the band at 1940 nm. As the fitted value for any sample is the sum of all the G_iE_i values across the spectrum, it can be seen to be a weighted average of all these effects.

While the sample with the highest moisture content (sample 12) showed the greatest positive response at 1940 nm, and the sample with the lowest moisture (sample 16) had the greatest negative response, the correlation of the sample specific compound weights (*GE*) at 1940 nm with the reference moisture values for all 39 samples was low ($r = 0.35$). Similarly at 1450 nm, the correlation was 0.23. However, multiple regression using 1940 and 1450 nm gave a correlation of 0.83. This indicates that these two known moisture bands[12] represent much of the essential information required to predict moisture.

A much more complex pattern was observed for protein [Fig. 2(*c*)]. At least five distinct regions, most incorporating more than one band, were identified. The two largest effects were centred around 1980 and 2200 nm, both known protein bands.[12] The high protein samples (samples 1 and 12) both had local maxima at these points, while the low protein samples (samples 3 and 16) exhibited local minima. At 2100 nm, a band known to relate to starch,[12] high protein samples exhibited local minima, while low protein samples had local maxima. This indicates that the amount of starch present in the samples is negatively correlated with protein and is used in the prediction of protein content. Between 1400 and 1700 nm two adjacent regions of the spectrum also acted in opposition to the protein bands at 1980 and 2200 nm, as did the region between 1750 and 1900 nm.

Not all bands were present in all 39 samples. Although all the bands were highly intercorrelated ($r > 0.95$), the relative responses of bands did change from sample to sample. The four samples used in these graphs illustrate this point. Of the two high protein samples, sample 1 had the greater response at 2200 nm, but exhibited a smaller response than sample 12 at 1980 nm. For the two low protein samples the responses at 2200 nm were similar, but at 1980 nm sample 16 showed a much greater negative response than sample 3.

For the protein reconstructed spectra, the correlation of peak height with the reference protein content was uniformly low (r between 0.34 and 0.09) for all the bands. An "all possible pairs" search using the data at bands found in these reconstructed spectra showed that some combinations had correlations around $r = 0.72$. However, one combination (1980 + 2180 nm) had a multiple correlation of 0.99. The band centred on 2200 nm appears to consist of overlapping absorbance bands in the range 2180–2210 nm and any of these in combination with 1980 nm produced a high multiple correlation with reference values for protein. As the bands centred on 2200 and 1980 nm represent the largest sources of variation, and together are the only two bands which accurately predict protein in a two-term regression equation, we conclude that they provide two independent sources of information relating to protein.

One interesting feature of Fig. 2(*b*) and (*c*) was the set of points for which all 39 samples had values equal to the mean. These "null" points lie between bands where the signs of the correlations with the constituent of interest are opposite. At these points in the spectrum, opposing absorbance effects are always in balance, in effect cancelling each other out. Where two bands had the same correlation (*e.g.*, the broad bands centred on 1460 and 1580 nm) there may be a local minimum but no "null" point occurs. In Fig. 2(*b*), the "null" points on either side of the moisture band at 1940 nm were 1830 and 2048 nm. Although the latter point almost coincides with 2050 nm, a known protein band,[12] any absorbance effects relating to protein are absent.

Protein "null" points [see Fig. 2(*c*)] were found at 1356, 1682, 1746, 1930, 2066, 2144 and 2398 nm. Of these, 2144 nm is particularly interesting in that it lies between the protein band at 2180 nm and the starch band at 2100 nm. Previously, Norris and Williams[13] used first and second derivatives of log $1/R$ (R = reflectance) in the region 2170–2210 nm to predict the protein content of hard red spring wheat. These derivatives characterise the slope of the spectrum between the protein band at 2180 nm and the "null" point at 2144 nm, and will be influenced both by the protein and starch in the samples.

Effects of Particle Size on Reconstructed Spectra

Close examination of all 39 reconstructed (*GE*) spectra for both moisture and protein indicated that the magnitude of the response for any band, regardless of the sign of that response, related more to particle size influences than any absorbance effect. Whereas the compound weights (*G*) were relatively free of particle size influences, due to the fact that the first principal component has a relatively flat shape and low regression coefficient, the centred spectra (*E*) were influenced significantly by particle size [see Fig. 2(*a*)]. Sample spectra which deviated most from the mean produced reconstructed spectra (*GE*) with the largest responses at any of the absorbance bands, irrespective of the concentration of either constituent of interest.

Other workers have suggested methods to compensate for particle size variation.[13–15] The presence of "null" points suggests a simple method of adjusting for this effect. If a constituent can be found that is highly correlated with particle size and then widely separated "null" points selected where the absorbance of this constituent does not vary, then at these points in the spectrum variation between samples should relate primarily to particle size. A straight line through these points will describe approximately the influence of particle size on each individual sample. Adjusting the sample spectra so that all these straight lines are collinear will minimise particle size influences.

For these 39 wheat samples, protein was a suitable constituent for this purpose as it was highly correlated with the first component ($r = 0.70$), which in turn related to particle size. We wished to identify "null" points where the opposing effects due to absorbing constituents were likely to occur in all samples, and not just this data set. The two highest protein "null" points were 2398 and 2144 nm. The upper point was discarded as the causes of the opposing effects were unclear, although edge effects from the optics may be involved. The next "null" point (2144 nm) appeared to be ideal as it related to a balance between starch and protein absorption bands. As these constituents form most of the dry matter in wheat, the negative relationship between their concentrations is unlikely to change for any set of wheat flour samples. There were no "null" points at the lower end of the spectrum; 1120 nm was therefore selected as the lower correction point as all samples tended to have fairly constant absorbance values at this point.

Fig. 2(*a*) shows that, apart from absorbance effects relating to water, the slopes of centred spectra are relatively linear. If the slope of each centred spectrum is defined by a straight line through the energy values at 1120 and 2144 nm, then all centred spectra can be adjusted so that all slopes are superimposed on the slope of the mean sample spectrum. Similarly, individual values at each wavelength are adjusted by a factor representing the degree of rotation and translation required to superimpose the slopes.

The equation used is given by

$$E_{ai} = (E_i - E_1) - Bi \quad . . \quad . . \quad . . \quad (3)$$

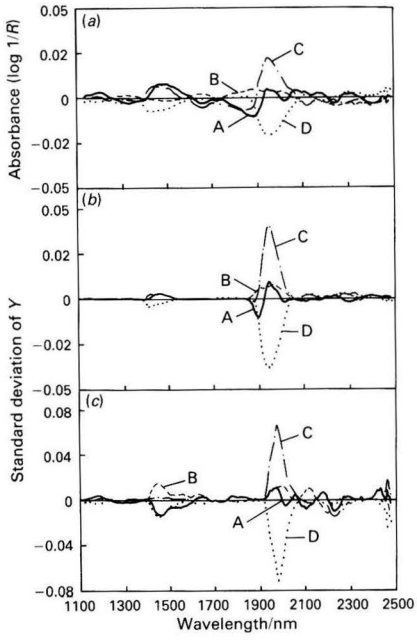

Fig. 3. (*a*) Centred NIR spectra, (*b*) reconstructed moisture spectra and (*c*) protein spectra after correction for particle size influences for four typical samples of wheat flour. A, sample 1; B, sample 3; C, sample 12; and D, sample 16

where $B = (E_u - E_l)/s$, given that E_{ai} and E_i are the adjusted and original energy values at the ith data point, E_l is the energy value at the lower correction point (1120 nm), E_u is the energy value at the upper correction point (2144 nm), B is the slope of the regression line (or the unit increase in absorbance due to particle size) and s is the number of data points between the upper and lower correction points.

Reconstructed Sample Spectra for Moisture and Protein After Correction for Particle Size Effects

Fig. 3 shows equivalent plots to Fig. 2, but after correction for particle size. The most dramatic change is in the centred spectra [Fig. 3(*a*)]. No longer is there any consistent increase in variation from the mean across the spectrum. The water bands at 1940 and 1450 nm are still the dominant features, but are much more obvious.

The reconstructed moisture spectra [Fig. 3(*b*] are very similar to those of Fig. 2(*b*), except that the variation above 2050 nm is greatly reduced. If any distortion was introduced as a result of correcting the spectra, then moisture would be the most likely constituent to be affected and would serve as a check of the distortion. Whereas the four samples still did not rank in order of moisture content, samples 1 and 3 were closer to their anticipated positions. The correlation between the individual sample compound weights (*GE*) at 1940 nm and the reference moisture values increased after correction for particle size ($r = 0.65$ compared with $r = 0.35$) and at 1450 nm ($r = 0.32$ compared with $r = 0.23$). The multiple correlation of 1940 and 1450 nm with reference moisture content values also increased (from $r = 0.83$ to 0.94) while the intercorrelation between values at 1940 and 1450 nm dropped from $r = 0.99$ to 0.92.

For protein, the shapes of the reconstructed spectra changed considerably. No longer were the greatest responses, whether positive or negative, around 2200 nm. This band virtually disappeared. Instead, the dominant band was the protein band at 1980 nm. Whereas the band centred at 1460 nm was relatively unchanged from Fig. 2(*c*), the adjacent band centred at 1580 nm did change. Correcting for particle size reduced the intercorrelation of the bands. Although some adjacent bands still correlated highly, there was now no general trend to high correlation across the spectrum.

An interesting feature of this data was the behaviour of two pairs of protein bands (1980 and 2050 nm, 2200 and 2346 nm). The band at 2050 nm appeared as a shoulder on the strong band at 1980 nm and as a consequence the two were highly correlated ($r = 0.91$). The other pair, although further apart, were also highly correlated ($r = 0.86$). There was, however, no correlation between the pairs ($r = 0.17$ between 1980 and 2200 nm was the highest correlation). Further, bands in the lower half of the spectrum could be separated into two groups, being correlated highly with one pair, but never with both. For example, the bands at 1452 and 1582 nm were both highly negatively correlated with 1980 and 2050 nm (r between -0.74 and -0.91) but showed little correlation with either bands at 2200 or 2346 nm ($r < 0.34$). The band at 1730 nm, however, was highly positively correlated with either of the higher pair ($r > 0.74$) and showed much lower correlations with 1980 or 2050 nm ($r < 0.43$). The band at 1766 nm behaved similarly, although it was negatively correlated with 2200 and 2346 nm.

These results support the suggestion that the reconstructed sample spectra for protein contained two independent sources of variation relating to protein. Whether these related to different types of protein or to different molecular groups found in all proteins is not clear. Surprisingly, now that the intercorrelation of bands had been reduced, a multiple regression using one band from each of the sources of variation had a lower correlation than before correction for particle size (r reduced from 0.99 to 0.73 for 1980 in combination with 2200 nm). This trend was opposite to that found for moisture. A comparison of Figs. 2(*b*) and 3(*b*) shows that adjusting for particle size did not change the absorbance bands relating to moisture. For protein, however, [Figs. 2(*c*) and 3(*c*)] adjusting for particle size suppressed the bands around 2200 nm. As a consequence variation around 2200 nm in the adjusted protein spectra no longer appears to complement the variation at 1980 nm.

In this paper, use of a particle size correction algorithm has been considered solely in terms of the effects on individual sample reconstructed spectra. Having shown that one algorithm breaks the intercorrelation of bands, the obvious step is to apply particle size correction algorithms to raw spectra, examine how the principal components change and determine whether regression models based on these components improve the prediction of moisture and protein content of the samples. This work will be reported in a later publication.

Conclusions

Although the reconstructed sample spectra for moisture and protein are by no means ideal solutions to the problem of revealing absorbance bands relating to constituents in the spectra of samples, they do highlight differences between samples in their response to known absorbance bands. Using the reconstructed spectra (*GE*) as a data set, measurements at two known absorbance bands for protein (1980 and 2180 nm) correlated highly with protein. This indicates the importance of these bands to regression models used to predict composition.

The identification of "null" points suggests one mechanism to overcome particle size variation. Although, in this instance, the correction for particle size was carried out on the basis of a wavelength chosen for its relevance to protein, it did not appear to distort the reconstructed moisture spectra. For protein, variation was distributed quite differently after correction for particle size.

The graphs presented in this paper still do not allow measurements at a single point in the spectrum to be directly related to either protein or moisture content of samples. For both moisture and protein there appear to be at least two distinct sources of variation which must be taken into account. The graphs do, however, provide clues as to the response of individual samples to the regression models.

References

1. McClure, W. F., Hamid, A., Giesbrecht, F. G., and Weeks, W. W., *Appl. Spectrosc.*, 1981, **38**, 301.
2. Giesbrecht, F. G., McClure, W. F., and Hamid, A., *Appl. Spectrosc.*, 1981, **35**, 210.
3. Sjostrom, M., Wold, S., Lindberg, W., Persson, J., and Martens, H., *Anal. Chim. Acta*, 1983, **150**, 61.
4. Martens, H., and Jensen, S. A., in Holas, J., and Kratochvil, J., *Editors*, "Proceedings of the 7th World Cereal and Bread Congress, Prague, June 1982," Elsevier, Amsterdam, 1983, pp. 607–647.
5. Mark, H., *Chimicaoggi*, 1987, **10**, 57.
6. Robert, P., and Bertrand, D., *Sci. Aliments*, 1985, **36**, 505.
7. Cowe, I. A., and McNicol, J. W., *Appl. Spectrosc.*, 1985, **39**, 257.
8. Cowe, I. A., McNicol, J. W., and Cuthbertson, D. C., *Analyst*, 1985, **110**, 1227.
9. Cowe, I. A., McNicol, J. W., and Cuthbertson, D. C., *Analyst*, 1985, **110**, 1233.
10. Cowe, I. A., McNicol, J. W., and Cuthbertson, D. C., *Analyst*, 1988, **113**, 269.
11. Mardia, K. V., Kent, J. T., and Bibby, J. M., "Multivariate Analysis," Academic Press, London, 1979.
12. Osborne, B. G., and Fearn, T., "Near Infrared Spectroscopy in Food Analysis," Longman Scientific and Technical, Harlow, 1986.
13. Norris, K. H., and Williams, P. C., *Cereal Chem.*, 1984, **61**, 158.
14. Murray, I., and Hall, P. A., *Anal. Proc.*, 1983, **20**, 75.
15. Ciurczak, E. W., Torlini, R. P., and Demkowicz, M. P., *Spectroscopy*, 1986, **1**(7), 37.

Paper 8/04613A
Received November 21st, 1988
Accepted January 6th, 1989

Linearity Range of Gran Plots from Logarithmic Diagrams

Carlo Maccà
Department of Inorganic, Metallorganic and Analytical Chemistry, Università di Padova, Via Marzolo 1, I-35131 Padova, Italy

Simple criteria for assessing the linearity ranges of Gran plots were implemented by the use of logarithmic diagrams of equilibrium concentrations. One-step precipitation, complexometric and acid - base titrations are considered. The graphical procedures do not require some of the approximations that are needed in order to obtain convenient and simple mathematical equations.

Keywords: *Potentiometric titration; Gran plots; logarithmic diagrams*

Simple criteria and procedures for assessing which part of a potentiometric titration curve can be used to obtain appreciably linear Gran plots[1] and an accurate extrapolation to the equivalence volume for one-step precipitation, complexation, redox and acid - base titrations were discussed in a previous paper.[2] Equations were derived for calculating the limiting or "critical" values of the experimental parameters or variables that prevent systematic titration errors higher than an assigned value. In order to ensure simplicity and convenience of use of these equations, approximations had to be introduced, thus excluding some less obvious situations from the applicability of the final equations. Although this restriction is not substantial for most of the simple titrations dealt with previously,[2] it can become a real limitation for equilibria of some complexity, for example, with some weak-acid or weak-base titrations. Moreover, it can be reasonably anticipated that for multi-step titrations (for instance, titrations of polyprotic acids or of mixtures of analytes), it would be almost impossible to obtain simple equations without introducing excessive approximations.

It is well known that logarithmic diagrams of equilibrium concentrations of titration systems represent a very convenient tool for solving complicated equilibrium problems, and provide a useful support for rationalising approximations and simplifications in the mathematical solution of the same problems.[3–6] The aim of this paper is to show that logarithmic diagrams can provide a simple, rational and correct solution to the problem of assessing the linearity ranges of Gran functions. Again, only one-step titrations will be considered. Nevertheless, it will be shown that the usefulness of the graphical approach, which does not necessarily resort to substantial approximations, increases as the complexity of the titrated system increases. Multi-step titrations will be dealt with in a subsequent paper.

Experimental

Apparatus

A Radiometer (Copenhagen) PHM 84 digital pH meter (0.1 mV, 0.001 pH), a Radiometer ABU80 motor-driven Autoburette equipped with a B282 25.00–2.500-ml burette and a Metrohm 6.1418.220 titration vessel with a circulation jacket containing water at 25.0 ± 0.1 °C were used.

Electrodes

For the titration of calcium, a Crytur (Turnov, Czechoslovakia) 09–17 fluoride ion-selective electrode and a Radiometer K711 saturated calomel reference electrode were used. For the titration of pyridinium chloride a Radiometer GK 2301 combined glass electrode was employed.

Reagents

All reagents were of analytical-reagent grade, and water was redistilled from quartz.

Principles of the Logarithmic Representation of Titration Equilibria

The graphical representation with bilogarithmic co-ordinates of the equilibrium concentrations of the species taking part in a titration[3] (the so-called logarithmic diagrams) has found wide acceptance and increasing application as an effective substitute for the conventional approach to the solution of equilibrium problems.[4–6] When used in combination with the titration error equation (according to the original approach of Bjerrum[3]), logarithmic diagrams can account for all the important properties of the titration.[7]

The extensive literature on the subject can be consulted for details of the principles, construction (by hand on graph paper) and general use of logarithmic diagrams, but only for a few basic concepts. The logarithm of the equilibrium concentration or, when convenient, of the conditional concentration[8] of any ith species taking part in the titration equilibria, $\log[i]$, is plotted against pH for acid - base titrations, against p[titrant] for complexometric and precipitation titrations and against $pE = EF/(RT\ln 10)$ for redox titrations. The only assumptions are negligible dilution during the titration, *i.e.*, a constant total analyte concentration (usually taken to be equal to the initial concentration C^0) and constant activity coefficients and side-reaction coefficients.[8] Both assumptions can be satisfied in practice. In some instances, the solution of specific problems can be made easier by introducing auxiliary curves.[5]

Linearity Criteria for Gran Plots

Extrapolation through two selected points of the Gran plot for a given titration, *viz.*, the initial point (titrant volume $V = 0$, titration ratio $f = V/V^0 = 0$) and a second point (the "critical point") satisfying the conditions represented by the equations in column 4 of Table 1 that are labelled B.E.P., gives a systematic (relative) error exactly equal to a pre-selected arbitrary value δ.[2]

When more points, evenly distributed between the initial and the critical point, are used for the linearisation, the extrapolation error decreases with respect to δ, and decreases further as the number of points increases. This allows us to exclude, if necessary, the points at the beginning of the titration (which for various reasons are frequently perturbed) and yet still to expect a systematic error no higher than δ when the last point to be used for the extrapolation is calculated from the above equations. The equations in column 5 of Table 1 that are labelled B.E.P. are approximate forms of the linearity conditions, which hold for a large number of points.

When the part of the titration following the equivalence volume is linearised, a two-point extrapolation through the point at the maximum titration ratio, f_M (the last experimental point), and the "critical point" satisfying the conditions expressed by the equations in column 4 of Table 1 that are

Table 1. Critical conditions for linearity of Gran functions

Type of titration*	Species sensed	Part of titration†	Critical condition: Higher approximation	Critical condition: Lower approximation
Isovalent precipitation				
$A + T \rightarrow AT_s$	A or T	B.E.P.	$[T] = \delta(C^0 - [A])$	$[T] = \delta C^0$
		A.E.P.	$[A] = \delta\{C^0 - [T]/(f_M - 1)\}$	$[A] = \delta C^0$
Heterovalent precipitation				
$aA + tT \rightarrow (A_aT_t)_s$	A or T	B.E.P.	$[T] = \delta(t/a)(C^0 - [A])$	$[T] = \delta(t/a)C^0$
		A.E.P.	$[A] = \delta\{C^0 - a[T]/t(f_M - 1)\}$	$[A] = \delta C^0$
Chelometric titration of metals				
$M + Y \rightarrow MY$	M	B.E.P.	$[Y] = \delta[MY]$	$[Y] = \delta C^0$
		A.E.P.	$[M] = \delta\{C^0 - [Y]/(f_M - 1)\}$	$[M] = \delta C^0$
Titration of a chelating agent with a metal				
$Y + M \rightarrow MY$	M	B.E.P.	$[M] = \delta[MY]$	$[M] = \delta C^0$
		A.E.P.	$[Y] = \delta\{C^0 - [M]/(f_M - 1)\}$	$[Y] = \delta C^0$
Strong acid with strong base				
$H^+ + OH^- \rightarrow H_2O$	H^+	B.E.P.	$[OH^-] = \delta(C^0 - [H^+])$	$[OH^-] = \delta C^0$
		A.E.P.	$[H^+] = \delta\{C^0 - [OH^-]/(f_M - 1)\}$	$[H^+] = \delta C^0$
Weak acid with strong base				
$HB + OH^- \rightarrow B + H_2O$	H^+	Initial part‡	$[H^+] - [OH^-] = \delta[B]$	$[H^+] = \delta[B]$
		B.E.P.	$[OH^-] - [H^+] = \delta[B]$	$[OH^-] = \delta C^0$
		A.E.P.	$[HB] + [H^+] = \delta\{C^0 - [OH^-]/(f_M - 1)\}$	$[HB] = \delta C^0$
Weak base with strong acid				
$B + H^+ \rightarrow HB$	H^+	Initial part‡	$[OH^-] - [H^+] = \delta[HB]$	$[OH^-] = \delta[HB]$
		B.E.P.	$[H^+] - [OH^-] = \delta[HB]$	$[H^+] = \delta C^0$
		A.E.P.	$[B] + [OH^-] = \delta\{C^0 - [H^+]/(f_M - 1)\}$	$[B] = \delta C^0$

* In some instances charges have been omitted for clarity.
† B.E.P. = before the equivalence point; A.E.P. = after the equivalence point.
‡ Negative deviations from linearity.

labelled A.E.P. [obtained by substitution of the mass balances of the reactants in equation (5) of reference 2], gives a relative extrapolation error equal to $-\delta$. A large number of experimental points and/or a relatively large value of f_M makes the approximate equations in column 5 of Table 1 valid. (For this reason, in reference 2 "exact" final equations were only shown for $f_M = 2$.)

The logarithmic diagram of a specific titration system allows us to obtain, in a simple and direct way, the equilibrium concentrations of the species corresponding to a critical point sought by finding the abscissa value for which the ordinates on the log[i] curves satisfy the relevant equation in Table 1. Therefore, as the experimentally dependent variable of the points of a titration (the electrode potential, pH or pIon) is a linear function of the logarithm of one of the equilibrium concentrations, its critical value can be obtained directly from the diagram. Hence, the value of the measured (dependent) variable at which the collection of useful titration points should stop or may begin is identified. The experimentally controlled variable is usually the added titrant volume but, for our purposes, it is conveniently substituted by the titration ratio, f

$$f = (a/t)n^t/n^0$$

or, better, by the quantity ε given by the equation

$$\varepsilon = f - 1 = \frac{(a/t)n^t - n^0}{n^0} \quad . . \quad . . \quad . . \quad (1)$$

where n^t is the total added amount, in moles, of titrant T, n^0 is the total, *i.e.*, initial, amount of analyte A and a and t are the stoicheiometric coefficients of the titration reaction

$$aA + tT \rightarrow \text{products} \quad . . \quad . . \quad . . \quad (2)$$

The quantity ε, the relative titration error (not to be confused with δ), represents the actual titration error which would result if the titration were stopped at this point.

By substitution of the equations of mass balances of solutes in equation (1), the numerator of the right-hand term becomes the sum of [i] terms. By obtaining the critical [i] values from the relevant plots on the diagram, the critical value of ε, denoted by ε_c, can be calculated. As the curve of $\log|\varepsilon|$ (the logarithm of the modulus of the titration error) is easily plotted on the logarithmic diagram,[7,9] its critical value can also be obtained directly from this plot. The critical titration ratio, f_c, is calculated as $f_c = 1 + \varepsilon_c$. Hence, the useful titration range for linear extrapolation can be identified.

The procedure for the use of logarithmic diagrams will first be discussed in detail for a very simple titration and then summarised for the other situations, Redox titrations have been discussed previously.[7]

Isovalent Precipitation Titrations

The procedure for calculating the linearity range of the Gran plots is conveniently illustrated with reference to an isovalent precipitation titration. Fig. 1 shows a diagram for the titration of a 1.0×10^{-3} M chloride solution with silver nitrate ($pK_{s0} = 9.50$ at 25 °C, ionic strength = 0.1 M).

Before the equivalence point

Exact solution. The exact solution[2] requires finding the abscissa value that satisfies the condition given by the relevant equation in Table 1, expressed in logarithmic form

$$\log[Ag^+] = \log(C^0 - [Cl^-]) + \log\delta \quad . . \quad (3)$$

For this purpose, the auxiliary curve representing $\log(C^0 - [Cl^-])$ is plotted [curve A in Fig. 1(*a*)] using the following procedure. For $[Cl^-]$ less than $0.05C^0$, *i.e.*, for $\log[Cl^-] < \log C^0 - 1.3$, the curve of $\log(C^0 - [Cl^-])$ is virtually coincident with the horizontal segment $\log C^0$. On increasing $[Cl^-]$ (*i.e.*, on increasing pAg), the value of $\log(C^0 - [Cl^-])$ rapidly decreases and approaches $-\infty$ for $[Cl^-]$ approaching C^0 (*i.e.*, for a pAg approaching the value at which precipitation of

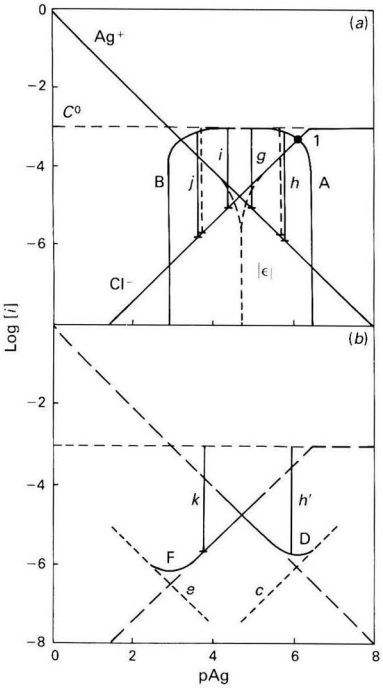

Fig. 1. Use of the logarithmic diagram log[*i*] = f(pAg) to determine the linearity limits for the Gran titration of 1.0×10^{-3} M chloride solution with silver ion ($T = 25$ °C, $I = 0.1$ M, $pK_{s0} = 9.50$). (*a*) Curve A, auxiliary curve representing $[i] = C^0 - [Cl^-]$; point 1, $\log(C^0 - [Cl^-]) = \log[Cl^-] = \log C^0 - 0.30$. Curve B, $[i] = C^0 - [Ag^+]/(f_M - 1)$ for $f_M = 2$ (only the position of the curve with respect to the pAg axis varies with f_M). (*b*) Segment *c*, $[i] = \delta[Cl^-]$; curve D, $[i] = [Ag^+] + \delta[Cl^-]$; segment *e*, $[i] = (f_M - 1)\delta[Ag^+]$, for $f_M = 5$ and $\delta = 0.2$; and curve F, $[i] = [Cl^-] + (f_M - 1)\delta[Ag^+]$. The twin specular curves marked $|\varepsilon|$ represent the modulus of the absolute titration error, $|\varepsilon|C^0$. Vertical segments represent the distances $-\log \delta$ indicated in the text (solid segments identify exact linearity limiting conditions; the dashed segments represent approximated conditions)

silver chloride begins, very near to the initial point of the titration). The downward curving part of the plot can be drawn by hand, with an approximation that is sufficient for our purpose, through the point where $[Cl^-] = C^0 - [Cl^-] = 0.5C^0$, *i.e.*, $\log[Cl^-] = \log C^0 - 0.30$ [point 1 in Fig. 1(*a*)]. For increased precision, we can make use of more points: for instance, at the pAg value where $[Cl^-] = 0.2C^0$, *i.e.*, $\log[Cl^-] = \log C^0 - 0.70$, we obtain a point with ordinate $\log(C^0 - [Cl^-]) = \log(0.8C^0) = \log C^0 - 0.10$; where $\log[Cl^-] = \log(0.8C^0) = \log C^0 - 0.1$, we obtain a point with ordinate $\log(C^0 - [Cl^-]) = \log(0.2C^0) = \log C^0 - 0.70$. The solution to equation (3) is obtained by finding the pAg value for which the vertical distance between the straight segment representing $\log[Ag^+]$ and the curve plotted as described above (curve A) equals $\log \delta$.

Alternatively, equation (3) can be written

$$\log([Ag^+] + \delta[Cl^-]) = \log C^0 + \log \delta$$

and solved by finding the pAg value for which the ordinate of the curve of $\log[i] = \log([Ag^+] + \delta[Cl^-])$ [curve D in Fig. 1(*b*)] is equal to $\log C^0 + \log \delta$. Curve D is, perhaps, more easily plotted than curve A (by connecting the straight lines representing $\log [Ag^+]$ and $\log [Cl^-] + \log \delta$, respectively, through a point lying $\log 2 = 0.3$ units above their intersection); however, at variance with A, it holds for a single value of δ. For this reason, and for brevity, this second type of solution will not be applied extensively in the next sections, although it can be used if desired.

Approximate solution. The approximate solution (Table 1, column 5) simply requires finding the point where $\log[Ag^+] = \log C^0 + \log \delta$.

Example. In the titration of a 1.0×10^{-3} M chloride solution, for $\delta = 1\%$, identical results are obtained from both the approximate and the exact equations [see the vertical segment *g* in Fig. 1(*a*)]. The critical, *i.e.*, the lowest useful, pAg is 5.00; the corresponding free chloride concentration is $10^{-4.50}$ M. If the response parameters of the indicating electrode (either a silver metal electrode or a chloride-selective electrode) are known, the critical e.m.f. of the titration cell, *i.e.*, the value at which the collection of useful experimental points must be interrupted, can be calculated. By using the mass balances

$$n^0 = n(Cl) + n(AgCl)$$

and

$$n^t = n(Ag) + n(AgCl)$$

{where $n(i)$ represents the equilibrium amount, in moles, of the *i*th species, $n(i) = (V^0 + V)[i]$} the error equation can be written

$$\varepsilon = \frac{n(Ag) - n(Cl)}{n^0} \approx \frac{[Ag^+] - [Cl^-]}{C^0}$$

(note that in order to apply logarithmic diagrams, negligible dilution must be assumed). By substitution of the critical concentration values obtained above, $\varepsilon_c = -0.02$ and $f_c = 0.98$ are obtained as the critical values of the titration error and titration ratio, respectively. The value of ε_c can also be obtained directly from the plot of the logarithm of the modulus of the titration error[7,9] [Fig. 1(*a*)].

If a systematic extrapolation error better than 0.2% ($\log \delta = -2.7$) is sought, the critical values are $[Ag^+]_c = 10^{-5.80}$ M [identified by means of segment *h* in Fig. 1(*a*) and segment *h′* in Fig. 1(*b*)], $[Cl^-]_c = 10^{-3.70}$ M, $\varepsilon_c = -0.20$ and $f_c = 0.80$ from the exact equation, (3), and $[Ag^+]_c = 10^{-5.70}$ M (broken vertical segment near to *h*), $[Cl^-]_c = 10^{-3.80}$ M, $\varepsilon_c = -0.16$ and $f_c = 0.84$ from the approximate equation. The difference is appreciable; however, the approximate result is still acceptable, particularly if a large number of experimental points are available for extrapolation.

The distance between curve A and $\log[Ag^+]$ is always smaller than 3 units; therefore, the condition for $\delta = 0.1\%$ is never attained. For this value of δ, the approximate equation gives $\varepsilon_c = -0.30$ and $f_c = 0.70$. It appears that the approximate equation is unreliable whenever it gives a critical value for the titration ratio of less than 0.80–0.85.

Fig. 1(*a*) and, perhaps more evidently, Fig. 1(*b*), show that there are two values of pAg for which equation (3) is satisfied. Of course, the second graphical solution, lying at higher pAg (and much lower *f*) is meaningless, as is the second root of the quadratic equation which represents the solution of the corresponding equation in reference 2.

After the equivalence point

After the equivalence point, f_c, the minimum value of *f* which, by a two-point extrapolation through the point at the chosen f_M, gives a systematic error equal to $-\delta$, depends on the value of f_M. The graphical solution based on the logarithmic equation

$$\log[Cl^-] = \log\left(C^0 - \frac{[Ag^+]}{f_M - 1}\right) + \log \delta$$

requires finding either the point where the distance between $\log[A]$ and the curve of $\log[i] = \log\{C^0 - [Ag^+]/(f_M - 1)\}$ [Fig. 1(*a*), curve B, for $f_M = 2$] is equal to $\log \delta$ or the point where the distance between the curve of $\log[i] = \log\{[Cl^-] + \delta[Ag^+]/(f_M - 1)\}$ [Fig. 1(*b*) curve F, for $f_M = 5$] and $\log C^0$ is equal to $\log \delta$.

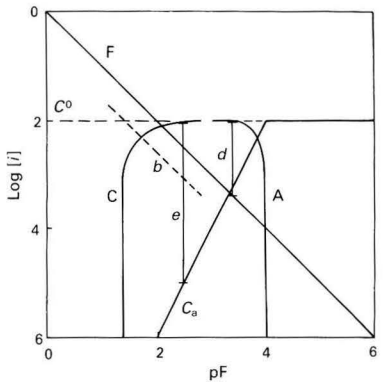

Fig. 2. Use of the logarithmic diagram log[*i*] = f(pF) for the titration of 0.010 M calcium solution with fluoride (T = 25 °C, I = 0.02 M, pK_{s0} = 10.0). Auxiliary curve A, $[i] = C^0 - [Ca^{2+}]$; segment *b*, $[i] = [F^-]/4$; curve C, $[i] = C^0 - [F^-]/4$ (the auxiliary curve for $f_M = 5$). Distance d = log(δ/2) for δ = 2%; distance e = log δ for δ = 0.1%

The approximate equation simply requires finding the point where $\log[Cl^-] = \log C^0 + \log \delta$, independently of f_M.

Example. For the titration of a 1.0 × 10^{-3} M chloride solution, with $f_M = 2$, the exact condition [Fig. 1(*a*), curve B] gives $pAg_c = 4.5$, $\varepsilon_c = +0.02$ and $f_c = 1.02$ as the critical values for δ = 1% (segment *i*), $pAg_c = 3.70$, $\varepsilon_c = 0.20$ and $f_c = 1.20$ for δ = 0.2% (segment *j*) and no solution for δ = 0.1%. The approximate solution gives $f_c = 1.02$, 1.16 and (not indicated in Fig. 1) 1.3, respectively, for the same values of δ. With f_M = 5, the critical values are $pAg_c = 3.80$, $\varepsilon_c = 0.16$ and $f_c = 1.16$ for δ = 0.2% [Fig. 1(*b*), curve F and segment *k*] and pAg_c = 3.50, ε = 0.32 and $f_c = 1.32$ for δ = 0.1% (not shown in Fig. 1) both from the exact and the approximate conditions. It is clear that on increasing f_M, the approximate equation gives results that approach the exact equation. This supports the claim[2] that, whereas the approximate solution before the equivalence point is acceptable only when it gives a critical titration ratio, f_c, higher than about 0.8–0.85, higher confidence can be placed in the approximate equation after the equivalence point, as both the titration range and the number of points can be increased as desired and the resulting f_c is valid also when appreciably higher than 1.2, provided that f_M is much greater than 2.

Heterovalent Precipitation Titrations

The linearity range before the equivalence point of heterovalent precipitation titrations is found by plotting the curve of $\log[i] = \log(C^0 - [A])$ on the logarithmic diagram of the titrated system and identifying the abscissa value for which the distance between log [T] and this curve is equal to $\log(t/a)\delta$ (see the equation for the critical condition given in Table 1).

After the equivalence point, the curve to be plotted is $\log[i] = \log\{C^0 - a[T]/t(f_M - 1)\}$ and the point where its distance from log[A] is equal to log δ must be found.

Example. The procedure is illustrated in Fig. 2 for the titration of a 1.0 × 10^{-2} M solution of calcium ion, with fluoride as the titrant (a = 1, t = 2, pK_{s0} = 10.0 and f_M = 3). The titration error is

$$\varepsilon = \frac{0.5n(F) - n(Ca)}{n^0} \approx \frac{0.5[F^-] - [Ca^{2+}]}{C^0}$$

Before the equivalence point, the exact critical condition for δ = 1%, *i.e.*, $\log[F^-] = \log(C^0 - [Ca^{2+}]) - \log 2\delta$, is never satisfied, because the distance between log[F^-] and the curve A is always smaller than 1.70. The approximate solution, $\log[T] = \log(2\delta C^0) = \log C^0 - 1.70$ (not indicated in Fig. 2), gives a value for f_c of 0.75, which is too far from 1 for the approximations on which it is based to be valid. If, however, we are content with δ = 2% (segment *d*), we can extrapolate, in principle, points up to pF = 3.4, where $\log[Ca^{2+}] = -3.2$, ε = −0.04 and $f_c = 0.96$. In contrast, after the equivalence point both the exact and the approximate conditions for $f_M = 2$ and δ = 1% (not shown in Fig. 2) are satisfied starting from pF = 3.00, $\log[Ca^{2+}] = -4.00$, ε = 0.04 and $f_c = 1.04$. With a higher f_M, higher accuracy can be reached in principle: for instance, with f_M = 5 (curve C) the condition for δ = 0.1% (segment *e*) is satisfied at pF = 2.45 and $f_c = 1.7$, giving a reasonable extrapolation range. It appears that the deviations from linearity increase as the distance from the equivalence point decreases and that this happens much more rapidly before than after the equivalence point owing to asymmetry of the titration curve.

Experimental titrations of 0.01 M calcium solutions with 0.1 M fluoride solutions monitored with a fluoride-selective electrode were indeed linear in the expected range after the equivalence point. In contrast, experimental points in the first part of the titration were useless, because of the slowness of the precipitation reaction.

It is interesting to note that the reverse titration of a 0.02 M fluoride solution with calcium (a = 2, t = 1; note that the shape of the relevant logarithmic diagram is different from that shown in Fig. 2) was not really feasible. In fact, in the first part of the titration the precipitation is again too slow (although the Gran plot satisfies in principle the condition δ = 1% up to f = 0.95). After the equivalence point, a systematic error less important than −1% is only warranted, with $f_c = 1.25$, if a relatively large f_M value is reached. Lower concentrations of fluoride (for instance, 0.01 M) cannot be titrated with reasonable accuracy.

Complexometric Titrations of Metals

The exact critical condition for linearity before the equivalence point of a complexometric titration of a metal

$$\log[Y] = \log[MY] + \log \delta \quad .. \quad .. \quad (4)$$

can be characterised on the logarithmic diagram of the titration system without plotting an auxiliary curve. Therefore, the approximate condition (see Table 1) in this particular instance offers no advantage.

In contrast, after the equivalence point the exact critical condition (see Table 1) requires that the auxiliary curve of $\log[i] = \log\{C^0 - [Y]/(f_M - 1)\}$ be plotted.

The values of ε_c, and therefore of f_c, are calculated from the equation[10]

$$\varepsilon = \frac{[Y] - [M]}{C^0}$$

Example. In Fig. 3 the logarithmic diagram for the titration of a 2.00 × 10^{-3} M solution of a cation with a conditional formation constant $K_f = 10^{5.00}$ (for instance, titration of calcium with ethylendiaminetetraacetic acid, EDTA, at about pH 5.4) is plotted. For δ = 1%, before the equivalence point, equation (4) is satisfied (segment *a*) at pY = 5.00, where $[M] = 10^{-3.00}$ M and $f_c = 0.50$, whereas the approximate solution (the next broken segment) gives the unreliable value of 0.64 for f_c. After the equivalence point, the exact condition does not allow a solution for $f_M = 2$ (not illustrated). In contrast, the approximate condition gives $f_c = 1.5$, which is not far from the "exact" value of 1.56 for f_M = 5 (the solid vertical segment and the broken segment at lower pY values, respectively).

Titration of Weak Acids

In addition to the positive deviations in the proximity of the equivalence point shown by very weak or dilute acids, Gran plots for the titration of weak acids or weak bases generally

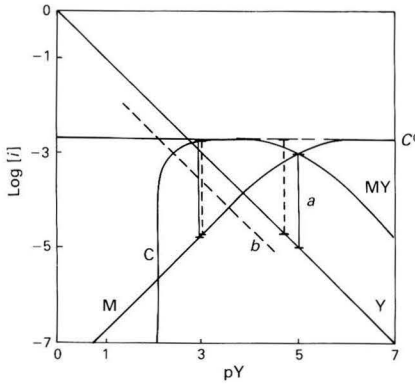

Fig. 3. Titration of a 2×10^{-3} M solution of a cation (M) with a chelating agent Y (conditional formation constant $K_f = 10^{5.00}$). Conditional concentrations are plotted. Distance *a* and the other vertical segments represent log δ for δ = 1%. Segment *b*, [Y]/4; curve C, $[i] = C^0 - [Y]/4$ (the auxiliary curve for $f = 5$)

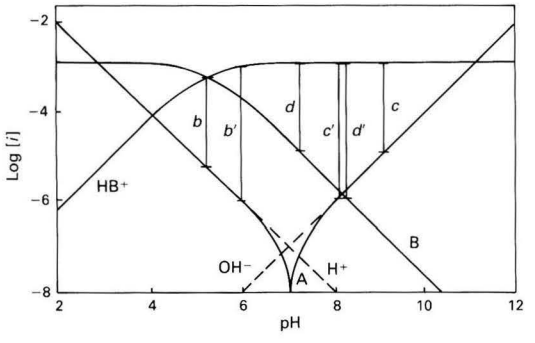

Fig. 4. Titration of 1.2×10^{-3} M pyridinium chloride solution, $pK_a = 5.25$. Auxiliary curve A: $[i] = [H^+] - [OH^-]$ at pH < 7, and $[i] = [OH^-] - [H^+]$ at pH > 7. *b*: Minimum allowed pH for linear extrapolation before the equivalence point according to equation (6) for δ = 1% and *b′*, for δ = 0.1%. *c*: Maximum pH for linear extrapolation before the equivalence point according to equation (7) for δ = 1% and *c′*, for δ = 0.1%. *d* and *d′*, Critical conditions after the equivalence point [equation (8)] for $f_M = 2$, δ as above

show negative deviations from linearity in their initial part.[2] In Table 1 the equations for critical conditions for linearity are reported for both types of deviation.

The solution of the equations in logarithmic form is supported by auxiliary curves, which can be plotted using procedures similar to those described above. For instance, the curve of $\log([H^+] - [OH^-])$ is virtually coincident with the linear segment $\log[H^+]$ at pH values lower than 6.3; at higher pH, it is represented by a curve (A in Fig. 4) that passes through a point with co-ordinates of pH = 6.85 and $\log[i] = \log[OH^-] = 7.15$ (*i.e.*, for $[H^+] = 2[OH^-]$ and $[H^+] - [OH^-] = [OH^-]$), approaching $-\infty$ at pH 7. The curve of $\log([OH^-] - [H^+])$ is symmetrical with the former.

Whereas in the other types of titration discussed earlier the approximated equations in the last column of Table 1 are obtained by introducing only one kind of approximation into the corresponding exact equations, in some of the equations for weak acids (or weak bases) two different approximations can be introduced stepwise according to the strength and concentration of the acid (or base). Only the lower approximation equations, which do not require auxiliary curves for their solution, are reported in the last column of Table 1.

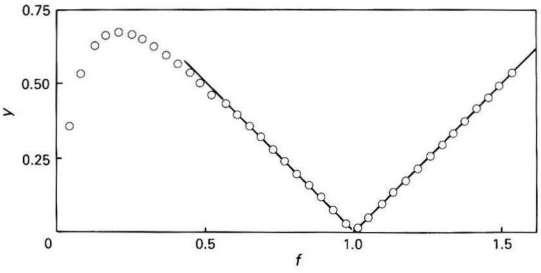

Fig. 5. Experimental Gran functions and linear extrapolation of the equivalence point for the titration of 1.16×10^{-3} M pyridinium chloride solution with 1.012×10^{-2} M sodium hydroxide solution. Co-ordinates are normalised to ±1 slopes of linear plots

The error equation for calculating ε_c and f_c is

$$\varepsilon = \frac{[OH^-] - [HB] - [H^+]}{C^0} \quad \ldots \quad (5)$$

Examples. Solutions (1.2×10^{-3} M) of pyridinium chloride ($pK_a = 5.23$ at 25 °C) were titrated with 0.01 M sodium hydroxide solution. The predictions from the logarithmic diagram (Fig. 4) were as follows. For δ = 1%, the equation

$$\log([H^+] - [OH^-]) = \log[B^-] + \log \delta \quad \ldots \quad (6)$$

in which $[OH^-]$ appears to be negligible, gives a value of 5.23 for the critical pH towards the initial part of the titration (identified by segment *b* in Fig. 4). At this pH equation (5) gives $\varepsilon_c = -0.5$ and $f_c = 0.5$. The equation

$$\log([OH^-] - [H^+]) = \log[B^-] + \log \delta \quad \ldots \quad (7)$$

gives a pH of 9.1 (segment *c*) as the critical pH value towards the equivalence point. As this pH is higher than the equivalence value (pH = 8.1), the condition sought is valid[2] up to $f = 1.00$. For δ = 0.1%, the first pH_c is 6.0 (segment *b′*), and $f_c = 0.85$, whereas the second f_c again corresponds to the equivalence point (segment *c′*). The resulting "linearity range" appears to be fairly narrow, so that the assumptions on which equation (6) is based (extrapolation through at least two points, the first of which is at, or near to, $f = 0$) could appear, at first sight, not to be valid. However, it is obvious that in situations such as this, where points near to the equivalence point can be exploited (at least in the absence of perturbations of different origin), the initial deviations are much less important.

After the equivalence point, the equation

$$\log([HB] + [H^+]) = \log\left(C^0 - \frac{[OH^-]}{f_M - 1}\right) + \log \delta \quad (8)$$

with $f_M = 2$ gives a value for pH_c of 7.23 for δ = 1% (segment *d*) and 8.23 for δ = 0.1% (segment *d′*). Both pH_c values correspond to $f_c = 1$. Note that all the approximations in the last column of Table 1 are valid. The above predictions were confirmed experimentally, as shown in Fig. 5, both before and after the equivalence point.

Fig. 6 represents the titration of a much weaker acid, *viz.*, 1.0×10^{-2} M ammonium nitrate. Auxiliary curves must be plotted, unlike the previous example. (Note that in this instance the simplifications used to obtain some of the higher approximation equations for the calculation of $[H^+]_c$ and f_c given in Table 1 of reference 2 are not strictly valid.)

As regards initial negative deviations, Fig. 6 shows that $[OH^-]$ cannot be neglected with respect to $[H^+]$ in equation (6). Nevertheless, as the linearity condition is valid starting from a pH of 6.6 for δ = 1% (segment *b*) and a pH of 7 (f = 0.005) for δ = 0.1% (segment *b′*), only the first point of the titration ($f = 0$) needs to be ignored.

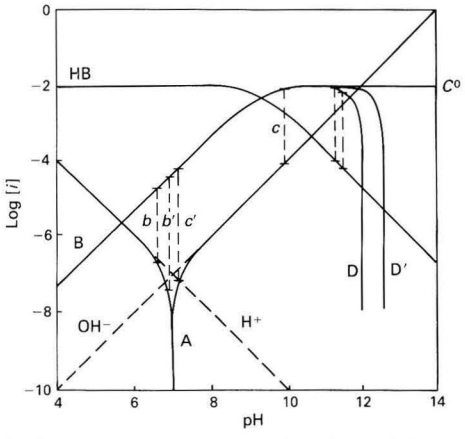

Fig. 6. Titration of 1.0×10^{-2} M ammonium nitrate solution, pK_a = 9.30. A, *b*, *b′* and *c*, *c′*, see Fig. 4; D and D′, auxiliary curves $[i] = C^0 - [OH^-]/(f_M - 1)$ for $f_M = 2$ and 5, respectively, with vertical segments characterising the critical conditions for linearity for $\delta = 1\%$ according to equation (8)

Equation (7) is satisfied with $\delta = 1\%$ (segment *c*) at pH = 9.8 and $f = 0.8$, where $[H^+]$ is negligible with respect to $[OH^-]$. However, if $\delta = 0.1\%$ is sought, all terms in equation (7) become important, and $pH_c = 7.0$ and $f_c = 0.05$ can be obtained by a graphical solution (segment *c′*). This demonstrates that the experimental Gran plot of the first part of the titration only provides a moderate degree of accuracy.

After the equivalence point, curve D in Fig. 6 shows that with $f_M = 2$ equation (8) gives $pH_c = 11.45$ and $f_c = 1.28$ for $\delta = 1\%$. With $f_M = 5$, curve D′ gives $pH_c = 11.30$ and $f_c = 1.20$ for the same δ value. For either value of f_M, equation (8) does not provide a solution for $\delta = 0.1\%$. It should be noted that $[H^+]$ is always negligible with respect to [HB], whereas $[OH^-]/(f_M - 1)$ becomes negligible with respect to C^0 only for $f_M = 5$ or higher (compare with the approximate equations given in Table 2 of reference 2).

Discussion and Conclusions

Information from equations[2] and from logarithmic plots about the linearity range and accuracy of Gran titrations have been confirmed experimentally for other systems, in addition to the two described here. In some instances, however, the agreement was poor or non-existent. Generally, deviations not predicted theoretically could be ascribed to exact causes, thereby negating the inadequacies of the approach. The adverse effect of inaccurate values of the equilibrium constants on the correctness of the estimated linearity range can be avoided by the use of reliable tables and by introducing a (rough) correction for the ionic strength. Highly inaccurate initial estimates of the unknown C^0 values can also cause erroneous predictions. For totally unknown or highly variable samples, a first estimate of C^0 obtained, for instance, by extrapolating a few points on a roughly linear portion of the titration curve (irrespective of strict linearity) is sufficient to obtain correct predictions in order to optimise the extrapolation procedure.

Causes of deviations from linearity that are different from those inherent in the titration equilibria can either produce more restrictive limits than predicted or disprove the predictions. In our experiments, many types of perturbations were not unexpected. An example of a slow reaction was discussed earlier. A frequent cause of appreciable deviations was impurities in the reagents interfering with the titration equilibria. The effect of carbon dioxide on acid - base titrations is well known.[11] Marked deviations from linearity in the initial part of weak-base titrations were found to originate from acid impurities. The effect of heavy metals is also apparent in the initial part of the complexometric titration of alkali earth metals. A non-linear dependence of the e.m.f. on the logarithm of the concentration of the sensed ion, due, for instance, to electroactive background species or to the lower response limit of the electrode being approached, can also have an appreciable effect. Experimental Gran plots should always be inspected carefully for deviations from the theoretical behaviour, as these can give very useful information about the real nature of the system under investigation.

From the above discussion, it can be predicted that the graphical approach should be particularly useful when partially overlapping equilibria are present in the titrated system.

Finally, we wish to stress that there is no rivalry between logarithmic diagrams and computer programs. Diagrams cannot compete with computers for precise, accurate and complete predictions of titrations. For instance, they do not make allowances for dilution or for variations in the ionic strength and liquid-junction potential during the titration. On the other hand, they can provide (by a rapid hand-sketch) an immediate survey of the most important properties of the system to be titrated and help in taking a rapid decision about the strategy to be followed in practice. In one respect computers must be considered to be incompatible with diagrams: it is absurd to use a sophisticated computer program to plot a logarithmic diagram giving only approximate indications, when for the same cost more exact mathematical results can be obtained (computer-plotted logarithmic diagrams should be restricted to illustrations in publications). In contrast, diagrams are compatible with computers, as they can help in the formulation of programs by providing an understanding of the system under study.

References

1. Gran, G., *Analyst*, 1952, **77**, 661.
2. Maccà, C., and Bombi, G. G., *Analyst*, 1989, **114**, 463.
3. Bjerrum, N., "Die Theorie der Alkalimetrischen und Azidimetrischen Titrierungen," Enke, Stuttgart, 1914, pp. 69–128.
4. Hägg, G., "Die Theoretischen Grundlagen der Analytischen Chemie," Birkhäuser, Basel, 1950.
5. Sillén, L. G., *in* Kolthoff, I. M., and Elving, P. J., *Editors*, "Treatise on Analytical Chemistry, Part I," Volume 1, Wiley-Interscience, New York, 1959.
6. Johansson, A., and Wänninen, E., *in* Kolthoff, I. M., and Elving, P. J., *Editors*, "Treatise on Analytical Chemistry, Part I," Volume 11, Wiley-Interscience, New York, 1975.
7. Maccà, C., and Bombi, G. G., *Fresenius Z. Anal. Chem.*, 1986, **324**, 52.
8. Ringbom, A., "Complexation in Analytical Chemistry," Interscience, New York, 1963.
9. Inczédy, J., *J. Chem. Educ.*, 1970, **47**, 769.
10. Maccà, C., *Analyst*, 1983, **108**, 395.
11. Rossotti, F. J. C., and Rossotti, H., *J. Chem. Educ.*, 1965, **42**, 375.

Paper 8/04611E
Received November 21st, 1988
Accepted January 19th, 1989

Platinum-dispersed Nafion Film Modified Glassy Carbon as an Electrocatalytic Surface for an Amperometric Glucose Enzyme Electrode

Hari Gunasingham and Chee Beng Tan
Department of Chemistry, National University of Singapore, Kent Ridge, Singapore 0511, Republic of Singapore

A Nafion film dispersed with platinum particles formed on a glassy carbon electrode combines the electrocatalytic activity of platinum with the background stability of glassy carbon. It serves as a selective and sensitive electrode surface for an amperometric glucose enzyme electrode. Details on the construction and the functional characteristics of the enzyme electrode are described. It is shown that the electrode is well suited to the determination of levels of glucose in blood by flow injection with amperometric detection.

Keywords: *Nafion; amperometric glucose enzyme electrode; flow injection; wall-jet electrode; platinum-dispersed polymer film*

Amperometric enzyme electrodes for monitoring glucose usually employ the enzyme glucose oxidase. There are essentially three categories of electrodes and these have been termed first-, second- and third-generation devices.[1] In first-generation devices, the glucose concentration is related to the amperometric current arising from the consumption of oxygen or the formation of hydrogen peroxide in the enzyme reaction.[1–5] Asperger *et al.*[5] have shown that the monitoring of the hydrogen peroxide is to be preferred because of the inherently greater accuracy of this mode.

In contrast to first-generation devices, second-generation glucose sensors employ a synthetic mediator in place of the naturally occurring oxygen,[1,6] whereas third-generation devices employ conducting organic salt electrodes.[7] Second- and third-generation devices have the advantage that the operating potential can be lowered significantly, obviating interference from electroactive species that may be present in the sample. Also, they have a wider linear range because of their insensitivity to variations in oxygen tension. However, in practical flow injection (FI) applications, first-generation devices do have the advantage of faster response times and greater stability.

An important objective of much of the development work on first-generation amperometric glucose enzyme electrodes has been the search for devices that combine high sensitivity with stability and selectivity. In general, however, these appear to be contradictory goals.

For example, platinum has been used widely as an electrode material in the construction of glucose enzyme electrodes based on both the hydrogen peroxide and oxygen consumption monitoring modes. This is because of platinum's inherently superior electrocatalytic response to oxygen and hydrogen peroxide. Unfortunately, however, platinum is also highly susceptible to electrode poisoning due to oxide formation and the adsorption of impurities.[8] The practical consequence of this is a decline in the electrode response with time which results in a loss of sensitivity and precision.

The other difficulty in monitoring glucose in physiological samples is that platinum is also sensitive to several electroactive interfering species such as ascorbic acid and paracetamol that are commonly present.

Researchers in the enzyme-electrode field have been seeking to overcome these difficulties by the use of permselective membrane films to exclude interfering species. A common approach is to sandwich the enzyme between two membranes: the top membrane (such as polycarbonate) allows the passage of glucose, whereas the bottom membrane (usually cellulose acetate) placed on the electrode allows only hydrogen peroxide through.[9]

Recently, there has been interest in the use of a number of novel ion-exchange and redox polymers in applications to electrochemical analysis in general which seek to exploit specific properties of these polymers. Of particular interest has been the Nafion ion-exchange polymer, which has the ability to exclude anionic interferences. Nafion film electrodes have been used in flowing stream analysis and high-performance liquid chromatographic detection and have been found useful, in particular for the determination of cationic neurotransmitters.[10,11]

In a previous paper we described the use of a Nafion film on glassy carbon containing dispersed platinum particles (deposited into the film electrochemically) for the determination of hydrogen peroxide.[12] Although there is some contention in the way the particles are distributed, they have been shown to be dispersed three-dimensionally in the Nafion film.[13] Similar work has been carried out with poly(4-vinylpyridine)[14] and poly(pyrole) films.[15] However, where the Nafion film differs is in its ability to reject electroactive anionic interferences such as ascorbic acid and paracetamol because of its ion-exchange properties.

In this paper, we describe the use of a platinum-dispersed Nafion electrode in the development of an enzyme electrode for the monitoring of glucose. The electrode is used in conjunction with automated flow injection for the routine determination of glucose over a wide linear range in clinical analysis.

Experimental

Buffer Solution

Phosphate buffer of pH 7.3 was used for the preparation of the enzyme solutions and glucose standards. It was also used as the carrier solution in the FI studies. The composition of the phosphate buffer was 52.8 mM Na_2HPO_4 - 15.6 mM NaH_2PO_4 - 5.1 mM NaCl - 0.01% *m/V* sodium azide - 0.15 mM disodium ethylenediaminetetraacetate.

Preparation of Platinum-dispersed Nafion Electrodes

Nafion (Du Pont) solutions (3% *m/V*) were made up in ethanol or obtained from Solution Technology, PA, USA, as solutions in ethanol.

Glassy carbon electrodes (3-mm diameter; Tokai Carbon, Tokyo, Japan) were polished to a mirror finish with diamond paste (K-5000, Kyoto Diamond Industrial, Japan). The electrodes were wiped with an ethanol-soaked tissue, rinsed thoroughly with ethanol and distilled water and then dipped in

concentrated nitric acid for 10 s. The oxidised electrodes were rinsed in distilled water and cleaned in an ultrasonic bath containing distilled water for 15 min. Finally, the electrodes were electrochemically pre-treated by potential cycling using a PAR Model 273 potentiostat (Princeton Applied Research, NJ, USA) between −0.15 and +1.1 V (scan rate, 100 mV s^{-1}) for 30 min in the phosphate buffer (pH 7.3).

After drying the glassy carbon electrodes in an oven for 30 min at 80 °C, the Nafion film was coated on the electrode surface by applying a 20-μl drop of the Nafion solution and allowing it to dry in air.

Platinum particles were deposited into the Nafion film by potential cycling between +0.7 and −0.15 V using the PAR Model 273 potentiostat in an acidic solution of K_2PtCl_6 (5 mM in 0.1 M H_2SO_4) at a scan rate of 50 mV s^{-1}.[12] The loading of the platinum was calculated from the charge consumed.[13] In this work, platinum loadings of between 100 and 150 μg cm^{-2} were used as these gave the optimum sensitivity/stability characteristics.

Preparation of Enzyme Electrodes

Glucose oxidase (E.C. 1.1.3.4. from *Aspergillus niger*, Sigma) was immobilised directly on the Pt - Nafion electrode as follows. A freshly prepared glucose oxidase solution (20 μl; 2% *m/V*) was placed on the electrode surface and allowed to dry at 4 °C overnight. Then, 10 μl of a freshly prepared mixture of equal parts of bovine serum albumin (BSA) (100% *m/V*) and gluteraldehyde (2.5% *V/V*) was added over the dried enzyme and a piece of polycarbonate membrane (Nucleopore; 1 cm^2, 0.03-μm pore size) placed immediately over the electrode. The membrane was held tightly in place with a cap. The enzyme electrodes were allowed to dry for at least 12 h at 4 °C before use.

For the interference studies, an additional cellulose acetate layer was placed over the Pt - Nafion film. This was achieved by spin coating a 10-μl drop of cellulose acetate solution (2% cellulose acetate in 50 + 50 *V/V* cyclohexanone - acetone).

Automated Flow Injection

A large-volume wall-jet detector with a Ag - AgCl reference electrode was used for the FI studies. The sample volume was 50 μl and the flow-rate was kept at 1 ml min^{-1}. For amperometric measurements, the applied potential was maintained at +0.7 V using a PAR 174A potentiostat.

Two peristaltic pumps (Eyela Model MP-3, Tokyo Rikakikai Tokyo, Japan) were used to deliver the sample and carrier streams. Two pneumatically actuated four-way valves (Model 5010, Rheodyne, CA, USA) under computer control permitted the automatic loading and injection of the sample. Unused sample was recycled into the sample reservoir, therefore minimising wastage. The flow system permitted an unattended and continuous operation.

Peak currents were digitised via a standard electronic interface and data stored in Lotus 123 files (Lotus Corporation) on the computer hard disk. The data could therefore be analysed and plotted as required.

Results and Discussion

Potential Profile

Fig. 1 shows typical peak current - potential response plots for the dispersed platinum - Nafion - glassy carbon (Pt - Nafion - GC) enzyme electrode and the solid platinum enzyme electrode for injected glucose samples (2 mM). Although the response plot for the solid platinum electrode is more sharply defined, the limiting peak currents begin at about the same potential. The electrode response varies from electrode to electrode. On average, however, the limiting peak currents for the Pt - Nafion - GC and solid platinum electrodes are comparable. For example, for 2 mM glucose, the average peak current for the Pt - Nafion - GC electrode was 0.40 ± 0.2 μA (n = 7) compared to 0.44 ± 0.2 μA (n = 7) for the solid platinum electrode.

The potential profile indicates that the Pt - Nafion - GC electrode functions in most respects as a platinum electrode with regard to its electrocatalytic activity. The detection of

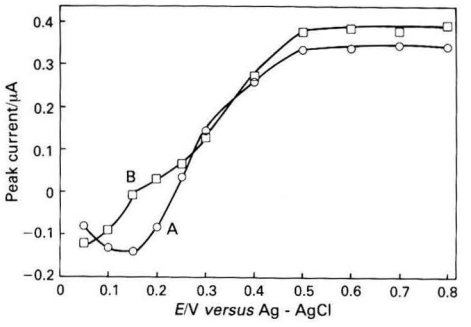

Fig. 1. Effect of applied potential on peak current for a 2 mM glucose solution. A, solid platinum enzyme electrode; B, Pt - Nafion - GC enzyme electrode. Flow-rate, 1 ml min^{-1}; carrier solution, isotonic phosphate buffer (pH 7.3) containing 0.15-mM disoduim ethylenediaminetetraacetate; sample volume, 50 μl

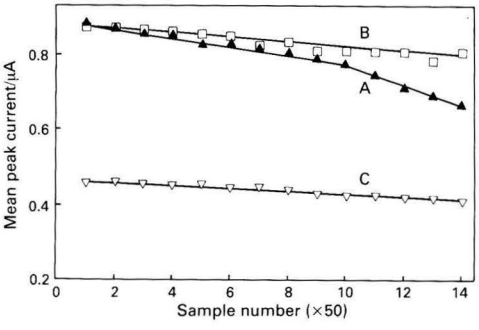

Fig. 2. Long-term behaviour of: A, solid platinum; B, Pt - Nafion - GC; and C, Pt - CA - Nafion - GC enzyme electrodes. Each point represents the mean of 50 successive injections of a 2 mM glucose solution. Working potential, +0.7 V *versus* Ag - AgCl. Other conditions as in Fig. 1

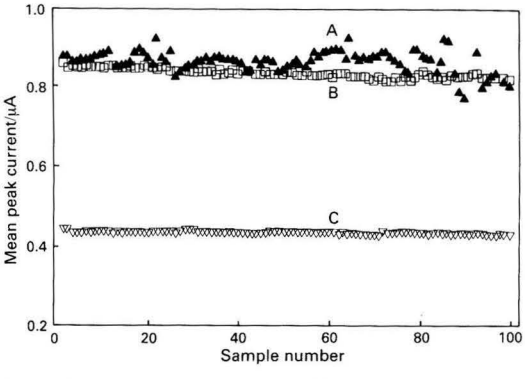

Fig. 3. Short-term behaviour of: A, solid platinum; B, Pt - Nafion - GC; and C, Pt - CA - Nafion - GC enzyme electrodes. Conditions as in Fig. 1

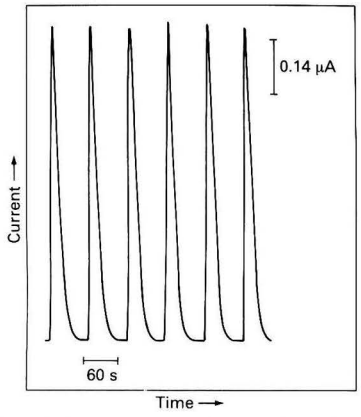

Fig. 4. FI profile for successive injections of a 2 mM glucose solution using a Pt - Nafion - GC enzyme electrode

glucose clearly depends on the current arising from the oxidation of H_2O_2 at the active platinum particles deposited in the Nafion film.

Electrode Stability

Figs 2 and 3 illustrate the long- and short-term stabilities, respectively, of the enzyme electrodes. As can be seen, in the long term, the response for the solid platinum system declines. The long-term stability is determined in terms of the over-all relative standard deviation (RSD) of the individual RSDs for every 50 injections. The over-all RSDs were 5.1, 2.3 and 1.2% for the solid platinum, Pt - Nafion - GC and dispersed platinum - cellulose acetate - Nafion - glassy carbon (Pt - CA - Nafion - GC) enzyme electrodes, respectively.

The improved stability of the Pt - Nafion - GC enzyme electrode is exemplified further in the short-term plot obtained for the first 100 sample injections. The RSDs were 4.1, 1.6 and 0.6% for the solid platinum, Pt - Nafion - GC and Pt - CA - Nafion - GC enzyme electrodes, respectively. The short-term fluctuations observed for the solid platinum electrode can be attributed in part to variations in flow as no damping was used with the peristaltic pump. The Pt - Nafion - GC enzyme electrode, however, appears to be less susceptible to fluctuations in flow.

The Pt - Nafion - GC system therefore appears to be as sensitive as a solid platinum electrode and has enhanced stability and selectivity. The stability is due in part to the Nafion film preventing electrode poisoning and in part to the underlying stability of the base glassy carbon electrode.

Linear Range

A calibration graph was constructed for the Pt - Nafion - GC enzyme electrode for which an additional cellulose acetate layer had been placed over the Pt - Nafion layer. The electrode showed a linear range between 0 and 30 mM, which covered the physiologically useful range for monitoring glucose levels in blood.

Response Time

Fig. 4 shows typical FI peak profiles for successive injections of glucose standard. The FI peak is formed in less than 60 s, giving a sample throughput of more than 60 samples per hour. With smaller sample volumes a higher throughput can be achieved.

Table 1. Effect of electroactive interferences

Interferent	Selectivity,* % Solid Pt	Pt - Nafion	Pt - CA - Nafion
Hydrogen peroxide (1 mM)	100	100	100
Ascorbic acid (1 mM)	80.6	3.6	1.2
Uric acid (1 mM)	69.9	4.3	1.0
Paracetamol (1 mM)	60.1	5.8	0.9

* Measured as the molar ratio with respect to the detection of H_2O_2.

Table 2. Comparison of the Pt - Nafion - GC enzyme electrode with the Reflolux monitor for the determination of glucose (in mM) in whole blood

Pt - Nafion - GC	Reflolux
3.0	2.8
5.8	5.2
7.5	8.3
10.5	10.6
12.2	12.3
9.0	7.4
10.3	9.9

Interferences

Table 1 shows the effect of some common electroactive interferences. Although the additional cellulose acetate membrane improves the selectivity by a few per cent., clearly Nafion is sufficient on its own. Indeed, considering the fact that normal physiological levels of interferents are much lower (*e.g.*, ascorbic acid, *ca.* 0.2 mM) the cellulose acetate membrane could be considered to be unnecessary. The effectiveness of Nafion presumably arises from its ion-exchange properties which serve to exclude anionic interferents.

Analysis of Glucose in Blood

The Pt - Nafion - GC enzyme electrode is well suited to monitoring glucose in physiological fluids as it is not prone to interferences such as ascorbic acid. This is shown in Table 2, which compares results obtained with the electrode to a standard laboratory analysis carried out with a Boehringer Refolux glucose analyser that had been previously calibrated against a Beckman Astra Analyser. The results show a good correlation.

Conclusion

The platinum-dispersed Nafion-based enzyme electrode has been shown to combine the electrocatalytic properties of platinum with the background stability of glassy carbon. At the same time, the dispersion of the platinum in the Nafion film serves to enhance selectivity such that the electrode is largely unaffected by most electroactive interferents found in physiological samples.

The platinum-dispersed Nafion system is easy to construct and reproducible results can be obtained. Also, because a relatively small amount of platinum is plated into the Nafion film, the electrode is inexpensive in comparison with a solid platinum electrode.

We gratefully acknowledge grants from the National University of Singapore and the Singapore Science Council.

References

1. Frew, J. E., and Hill, H. A. O., *Anal. Chem.*, 1987, **59**, 933A.
2. Carr, P. W., and Bowers, L. D., "Immobilized Enzymes in Analytical and Clinical Chemistry," Wiley, New York, 1980.

3. Updike, S. D., and Hicks, G. P., *Nature(London)*, 1967, **214**, 989.
4. Guibault, G. G., and Lubrano, G. J., *Anal. Chim. Acta*, 1973, **64**, 439.
5. Asperger, L., Geppert, G., and Krabisch, C. H., *Anal. Chim. Acta*, 1987, **201**, 281.
6. Cass, A. E. G., Davis, G., Francis, G. D., Hill, H. A. O., Aston, W. J., Higgins, I. J., Plotkin, E. V., Scott, L. D. L., and Turner, A. P. F., *Anal. Chem.*, 1984, **56**, 667.
7. Albery, W. J., Bartlett, P. N., and Craston, D. H., *J. Electroanal. Chem.*, 1985, **194**, 223.
8. Gunasingham, H., and Fleet, B., *in* Bard, A. J., *Editor*, "Electroanalytical Chemistry," Volume 16, Marcel Dekker, New York, 1989.
9. Guibault, G. G., "Analytical Uses of Immobilized Enzymes," Marcel Dekker, New York, 1984.
10. Wang, J., Tuzhi, P., and Golden, T., *Anal. Chim. Acta*, 1987, **194**, 129.
11. Wang, J., and Tuzhi, P., *Anal. Chem.*, 1986, **58**, 3257.
12. Tay, B. T., Ang, K. P., and Gunasingham, H., *Analyst*, 1988, **113**, 617.
13. Itaya, K., Takahashi, H., and Uchida, I., *J. Electroanal. Chem.*, 1986, **208**, 373.
14. Bartak, D. E., Kazee, B., Shimazu, K., and Kuwana, T., *Anal. Chem.*, 1986, **58**, 2756.
15. Holdcroft, S., and Funt, L. B., *J. Electroanal. Chem.*, 1988, **240**, 89.

Paper 8/03607A
Received September 19th, 1988
Accepted January 13th, 1989

Liquid Chromatographic Determination of Tetracycline Antibiotics at an Electrochemically Pre-treated Glassy Carbon Electrode

Weiying Hou and Erkang Wang*
Changchun Institute of Applied Chemistry, Chinese Academy of Sciences, Changchun, Jilin 130022, People's Republic of China

The electro-oxidation of tetracycline antibiotics has been studied by cyclic voltammetry and differential-pulse voltammetry and a liquid chromatographic method with electrochemical detection for the determination of four tetracyclines is described. The sensitivity of the electrochemically pre-treated electrode was twice that of the untreated electrode with spectrophotometric detection. With the pre-treated electrode, the limits of detection were 0.2 ng for oxytetracycline and tetracycline, 1.2 ng for chlortetracycline and 4 ng for doxycycline. The application of the method to the determination of tetracyclines in drugs is discussed.

Keywords: *Electro-oxidation of tetracyclines; electrochemically pre-treated glassy carbon electrode; liquid chromatography with electrochemical detection*

Tetracycline antibiotics (Fig. 1) are used widely in modern agricultural production. Oxytetracycline (OTC), tetracycline (TC), chlortetracycline (CTC) and doxycycline (DC) are used most frequently with respect to veterinary medicine, animal nutrition and feed additives. In Japan, more than 60% of all the antibiotics used for animals are TCs.[1] Therefore, TC monitoring is an important aspect of animal medicine and nutrition.

A variety of techniques have been utilised to detect antibiotics in clinical samples, including microbiological and non-microbiological methods.[2] Because of many disadvantages associated with both microbiological and chemical assays, high-performance liquid chromatographic (HPLC) methods for determining antibiotic concentrations have been developed. In particular, a chromatographic method with spectrophotometric detection for the determination of TCs has been reported.[3–8] In recent years, liquid chromatography with electrochemical detection (LCEC) has been shown to be a reliable method for the determination of trace amounts of electroactive compounds in complex matrices, with better selectivity than the spectrophotometric method. Moreover, the sensitivity and selectivity of electrochemical detection can be improved by applying various electrochemical techniques and LCEC has been used successfully for the determination of antibiotics.[9–13] However, there are no reports in the literature of the determination of TCs by LCEC. Although the electrochemical pre-treatment of a glassy carbon electrode in phosphate buffer solution can enhance the activity of the electrode with respect to the oxidation of electroactive components,[14–16] the possibility of utilising electrochemical pre-treatment procedures for improving the electrochemical detector response has not been seriously considered.

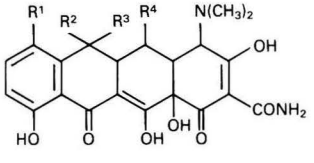

	R1	R2	R3	R4
Tetracycline (TC)	H	CH_3	OH	H
Oxytetracycline (OTC)	H	CH_3	OH	OH
Chlortetracycline (CTC)	Cl	CH_3	OH	H
Doxycycline (DC)	H	CH_3	H	OH

Fig. 1. Tetracycline structures

This paper describes how the separation and quantification of four tetracyclines was achieved by LCEC, and the response sensitivity improved after electrochemical pre-treatment of the electrode. The proposed method for the determination of TCs extends the scope of analysis by LCEC and is shown to improve on the sensitivity and selectivity of the existing method.

Experimental

Apparatus

A laboratory-built FA-1 type cyclic voltammeter and a Polarecord E 506 differential-pulse voltammeter (Metrohm, Herisau, Switzerland) were used. A three-electrode cell system with a glassy carbon working electrode, an Ag - AgCl (1 M KCl) reference electrode and a platinum auxiliary electrode was employed.

The LC system consisted of a Model 510 pump, a U6K injection valve and a Model 481 variable wavelength detector (Waters Chromatography, Milford, MA, USA). The injection volume was 20 μl and the wavelength of measurement 350 nm. A Nucleosil C_{18} (20 cm × 5 mm i.d.; 5 μm) column prepared by the Dalian Institute of Chemical Physics (Dalian, China) was used as the stationary phase and a thin-layer Model TL-5A electrochemical cell (Bioanalytical Systems, W. Lafayette, IN, USA) and a laboratory-built bipotentiostat[17] were used for the amperometric detection. An Ag - AgCl (saturated KCl) reference electrode was used. All experiments were performed at ambient temperature (20 ± 2 °C) and a flow-rate of 1.5 ml min^{-1} was applied during the chromatographic analysis.

Reagents

All chemicals were of analytical-reagent grade, unless stated otherwise. All solutions were prepared in doubly distilled water. A national standard of OTC ($C_{22}H_{24}O_9N_2.HCl.2H_2O$, 882 U mg^{-1}) and a temporal standard of DC ($C_{22}H_{24}O_8N_2.HCl$, 354 U mg^{-1}) were provided by the Institute of Pharmaceutical and Biological Product Inspection, Health Ministry, Beijing, China. National standards of TC ($C_{22}H_{24}O_8N_2.HCl$, 978 U mg^{-1}) and CTC ($C_{21}H_{21}N_2O_8Cl.HCl$, 962 U mg^{-1}) were provided by the Institute of Chinese Pharmaceutical and Biological Product Inspection and the Beijing Institute of Biological Product Inspection (Beijing, China), respectively. The OTC (840

* To whom correspondence should be addressed.

U mg^{-1} by microbiological assay) and TC (844.5 U mg^{-1} by microbiological assay) powders were provided by the Jilin Institute of Pharmaceutical Inspection (Changchun, China).

Procedures

Standard samples of OTC and TC were dissolved separately in 0.1 M hydrochloric acid and each solution was diluted with doubly distilled water to 1 mg ml^{-1}. The solution pH was maintained at about 2.5 for OTC and about 2.0 for TC. Chlortetracycline was dissolved in doubly distilled water and diluted further to 1 mg ml^{-1}. The DC was dissolved in 1% KH_2PO_4 solution (pH 6.0) to a concentration of 1 mg ml^{-1}. All solutions were stored at <5 °C. The DC standard solution could be kept for at least 2 weeks and the others for at least 1 week. Just before the actual analysis, an aliquot was taken and diluted to the appropriate concentration. The same procedures were used for the preparation of the sample solutions.

Treatment of the Glassy Carbon Electrode

The glassy carbon electrode was polished with 0.3- and 1-μm α-Al_2O_3 powder. The polished electrode was ultrasonicated in doubly distilled water for 30 s. This electrode was referred to as the fresh untreated electrode (GCE). The GCE was anodised in 0.1 M KH_2PO_4 (pH 7.0) at +1.80 V for 5 min and then cathodised at −1.20 V for 10 s; the resulting electrochemically pre-treated electrode was referred to as the PGCE. When the detector response was lowered, the electrode was re-polished and again pre-treated electrochemically, as described previously.

Results and Discussion

Electrochemical Behaviour of Four Tetracyclines

The electrochemical behaviour of four TCs was studied at a glassy carbon working electrode. Fig. 2 shows the cyclic voltammograms of the four TCs in a conventional electrochemical cell. Each yields irreversible oxidation waves, the first being at about 1.0 V; the remaining waves were indistinct. With increasing pH, the peak potential (E_p) of each TC shifts to a more negative potential.

The differential-pulse voltammetric curves were also recorded in a conventional electrochemical cell (Fig. 3). It can be seen that the four TCs each yield three oxidation waves. At the GCE, the oxidation waves are at about 0.99, 1.14 and 1.35 V for OTC, 0.98, 1.13 and 1.37 V for TC, 0.93, 1.10 and 1.38 V for CTC and 0.93, 1.14 and 1.36 V for DC. At the PGCE, the sensitivities of the first wave of both OTC and TC and the first two waves of both CTC and DC were obviously increased compared with the waves obtained at the GCE. The first wave of both OTC and TC appeared at about 1.0 V, while the positions of the other waves were unclear. Oxidation waves appeared at 0.93, 1.10 and 1.33 V and 0.93, 1.10 and 1.35 V, for CTC and DC, respectively.

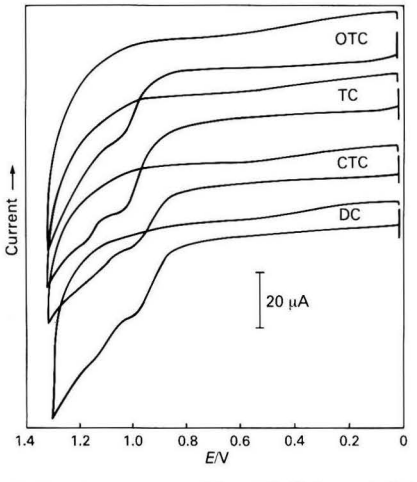

Fig. 2. Cyclic voltammograms of four TCs (0.2 mg ml^{-1}) in 0.1 M phosphate buffer at the GCE (pH 2.5). Scan rate, 100 mV s^{-1}

Liquid Chromatographic Separation and Detection

Chromatograms were obtained for CH_3CN - 0.1 M KH_2PO_4 (1 + 3 *V/V*) acidified with orthophosphoric acid to different pH in the range 2.5–4.0. With increasing pH, the peaks broadened and the response sensitivity and peak recognition decreased. At low pH, better peak separation was obtained. Below pH 2.5, peak separation was improved further. However, as the effective column life might be reduced when operated at high acidity during continuous analysis, the pH of the mobile phase was chosen to be 2.5.

Fig. 4 shows the influence of CH_3CN content in the mobile phase on the capacity ratio k'. With increasing CH_3CN

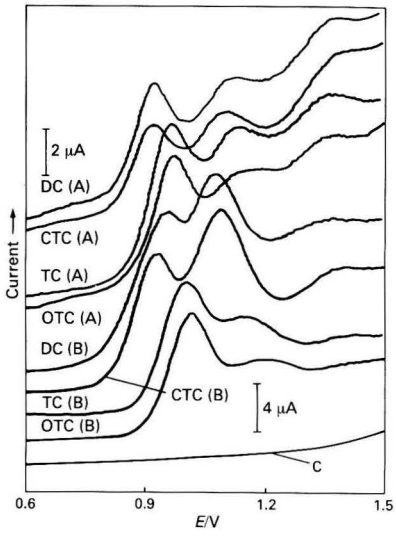

Fig. 3. Differential-pulse voltammograms of TCs (0.2 mg ml^{-1}) at A, the GCE; and B, the PGCE. C, Blank. CH_3CN (23% *V/V*) - 0.1 M KH_2PO_4 (pH 2.5); scan rate, 7.5 mV s^{-1}; ΔE, 50 mV; pulse interval, 0.1 s

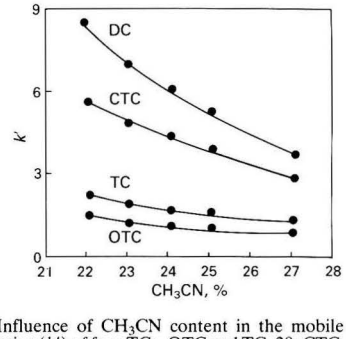

Fig. 4. Influence of CH_3CN content in the mobile phase on the capacity ratios (k') of four TCs. OTC and TC, 20; CTC, 30 and DC, 40 mg l^{-1}. Mobile phase, CH_3CN - 0.1 M KH_2PO_4 (pH 2.5); *E*, 1.25 V; flow-rate, 1.5 ml min^{-1}; and injection volume, 20 μl

Table 1. Determination of OTC and TC in drug powder

Sample	LCEC/U mg^{-1} GCE	LCEC/U mg^{-1} PGCE	Microbiological method/U mg^{-1}	Relative deviation,*% GCE	Relative deviation,*% PGCE
OTC	843.5 ± 12.28	842.9 ± 31.74	840	0.42	0.35
TC	852.2 ± 14.70	844.0 ± 20.59	844.5	0.91	−0.06

* The results were compared with those given by a microbiological assay performed by the Jilin Institute of Pharmaceutical Inspection.

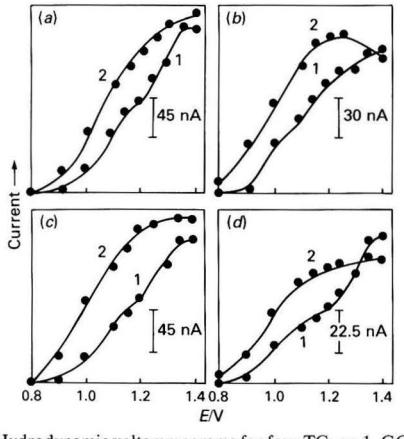

Fig. 5. Hydrodynamic voltammograms for four TCs on 1, GCE and 2, PGCE. (*a*) OTC, 5 mg l^{-1}; (*b*) TC, 10 mg l^{-1}; (*c*) CTC, 15 mg l^{-1}; and (*d*) DC, 20 mg l^{-1}. Mobile phase, 23% *V/V* CH_3CN - 0.1 M KH_2PO_4 (pH 2.5)

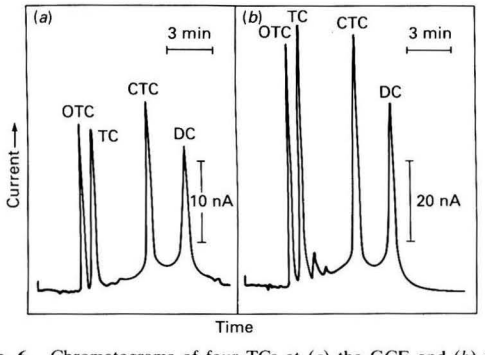

Fig. 6. Chromatograms of four TCs at (*a*) the GCE and (*b*) the PGCE. OTC and TC, 2.5; CTC, 10; and DC, 12.5 mg l^{-1}. *E*, 1.20 V; mobile phase, 23% *V/V* CH_3CN - 0.1 M KH_2PO_4 (pH 2.5); flow-rate, 1.5 ml min^{-1}; and injection volume, 20 µl

content, the *k'* values of CTC and DC decreased, whereas those of OTC and TC were influenced only slightly. As a result the CH_3CN content was fixed at 23% *V/V* for LCEC experiments, and good separations were obtained in 12 min.

In order to determine the optimum potential for electrochemical detection, hydrodynamic voltammograms were obtained at both the GCE and PGCE (Fig. 5) by injecting fixed volumes of the standard solutions and varying the potential between 0.8 and 1.4 V. Fig. 5 shows that at the GCE, the plateau currents of the four TCs became stable at about 1.15 V. For OTC and TC the currents then began to increase again at about 1.2 V and further plateau currents were obtained at 1.35 V. At the PGCE, the plateau currents of OTC and TC became stable at 1.2 V; the plateau currents of CTC and DC were also obtained at this potential. Operation at high potentials would be disadvantageous for LCEC analysis owing to the higher background current, hence a potential of 1.2 V was selected for the determination of the four TCs at the GCE and PGCE. In addition, the TC response was increased at the PGCE compared with the GCE.

The four TCs were well separated and satisfactorily determined in 23% *V/V* CH_3CN - 0.1 M KH_2PO_4 buffer (pH 2.5) at 1.2 V and a flow-rate of 1.5 ml min^{-1} (Fig. 6). It can be seen that the peak currents at the PGCE are about twice as high as those obtained at the GCE.

Eight replicate injections of the standard solution containing 10 mg l^{-1} each of OTC and TC, 30 mg l^{-1} of CTC and 40 mg l^{-1} of DC were carried out to determine the precision of the method. At the GCE, the coefficients of variation for the peak current were 3.93, 4.78, 1.68 and 2.44% for OTC, TC, CTC and DC, respectively. At the PGCE, the coefficients of variation for the peak current were 1.84, 1.47, 3.15 and 4.23% for OTC, TC, CTC and DC, respectively.

The stabilities of the GCE and PGCE were examined by comparing peak currents after a certain period of operation. The results indicated that both the GCE and PGCE can be used for at least 1 week (the coefficients of variation for the peak current were <5%) if the LCEC system is washed with doubly distilled water after each LCEC experiment.

With the GCE, linear calibration graphs were obtained for 0.6–800 ng of OTC and TC, 4 ng–3 µg of CTC and 10 ng–3 µg of DC. The correlation coefficients were better than 99.97%. The limits of detection are 0.6 ng of OTC and TC, 4 ng of CTC and 10 ng of DC (signal to noise ratio *S/N* = 3). With the PGCE, the calibration graphs were linear for 0.2–400 ng of OTC and TC, 1.2 ng–1.6 µg of CTC and 4 ng–2 µg of DC. The limits of detection are 0.2 ng of OTC and TC, 1.2 ng of CTC and 4 ng of DC (*S/N* = 3). With spectrophotometric detection (λ = 350 nm) under the same LC conditions, the limits of detection are 0.7 ng of OTC and TC, 6 ng of CTC and 8 ng of DC (*S/N* = 3). Hence it is seen that the sensitivities of the TC determination with spectrophotometric detection and with the GCE are comparable and that the selectivity of the PGCE method is twice as high as that employing spectrophotometric detection. In addition, the electrochemical pre-treatment procedure is simple and rapid.

The proposed LCEC method for the determination of TCs is not only sensitive but also selective, and absorbable and non-electro-oxidised components do not interfere. The method is twice as high as that employing spectrophotometric detection. In addition, the electrochemical pre-treatment procedure is simple and rapid.

We have determined OTC and TC in drug powder by the proposed method with detection at both the GCE and PGCE and compared the results with those of a microbiological method (Table 1). The results compared favourably although the relative deviation obtained for detection at the PGCE was lower than that for detection at the GCE (six replicate analyses).

Support from the National Natural Science Foundation of China is gratefully acknowledged.

References

1. Ministry of Agriculture, Forestry and Fisheries Japan, *Ann. Rep. Natl. Assay Lab.*, 1983, **20**, 50.
2. Ristuccia, P. A., *J. Liq. Chromatogr.*, 1987, **10**, 241.

3. Hon, J. Y. C., and Murray, L. R., *J. Liq. Chromatogr.*, 1982, **5**, 1973.
4. Oka, H., Matsumoto, H., and Uno, K., *J. Chromatogr.*, 1985, **325**, 265.
5. Oka, H., Ikai, Y., Kawamura, N., Uno, K., Yamada, M., Harada, K.-I., Uchiyama, M., Asukabe, H., and Suzuki, M., *J. Chromatogr.*, 1987, **393**, 285.
6. George, D. M., and Raymond, B. A., *J. Chromatogr. Sci.*, 1978, **16**, 93.
7. Nelis, H. J. C. F., and de Leenheer, A. P., *J. Chromatogr.*, 1980, **195**, 35.
8. Eksborg, S., and Ekqvist, B., *J. Chromatogr.*, 1981, **209**, 161.
9. Croteau, D., Vallee, F., Bergeron, M. G., and LeBel, M., *J. Chromatogr.*, 1987, **419**, 205.
10. Riley, C. M., Runyan, A. K., and Graham-Pole, J., *Anal. Lett.*, 1987, **20**, 97.
11. Riley, C. M., and Runyan, A. K., *J. Pharm. Biomed. Anal.*, 1987, **5**, 33.
12. van der Lee, J., van der Lee, H., Rysbergen, U., Tjaden, L., and van Bennekom, W. P., *Anal. Chim. Acta.*, 1983, **149**, 29.
13. Smyth, M. R., and Egan, A. M., *Anal. Proc.*, 1986, **23**, 87.
14. Ravichandran, K., and Baldwin, R. P., *J. Liq. Chromatogr.*, 1984, **7**, 2031.
15. Iriyama, K., Iwamoto, T., and Yoshiura, M., *J. Liq. Chromatogr.*, 1986, **9**, 955.
16. Iriyama, K., Iwamoto, T., and Yoshiura, M., *J. Chromatogr.*, 1987, **400**, 263.
17. Ji, H., and Wang, E., *Chin. J. Chromatogr.*, 1988, **6**, 139.

Paper 8/02984I
Received July 22nd, 1988
Accepted January 1st, 1989

Water-promoted Formation of Phenylboronates of 1,3-Diols During Gas - Liquid Chromatographic Analysis: Application to the Assay of Meprobamate

R. J. Flanagan and M. W. J. Chan*
Poisons Unit, Guy's Hospital, St Thomas' Street, London SE1 9RT, UK

A simple method for the assay of the hypnotic drug meprobamate (2-methyl-2-propylpropane-1,3-diol dicarbamate) in plasma has been developed. Hydrolysis to the 1,3-diol was followed by extraction into an organic solvent and, after mixing with phenylboronic acid in methanol - water (2 + 1), a portion (1–2 μl) of the extract was analysed directly by gas - liquid chromatography with flame ionisation detection using a column packed with 3% *m/m* OV-101 at 160 °C. Mebutamate (2-methyl-2-*sec*-butylpropane-1,3-diol dicarbamate) was used as a reactive internal standard. The limit of accurate measurement was 5 mg l^{-1} [intra-assay coefficient of variation 5.2% (n = 10)] and the assay calibration was linear up to 200 mg l^{-1}. The inter-assay coefficient of variation was 3.7% at 60 mg l^{-1} (n = 10). The finding that water acts to promote phenylboronate formation under the conditions described may prove useful when analysing other 1,2- and 1,3-diols and, possibly, other polar bifunctional compounds by gas - liquid chromatography.

Keywords: *Meprobamate assay; plasma; boronate derivatives; simple diols; gas - liquid chromatography*

Spectrophotometric methods for the measurement of the hypnotic drug meprobamate (2-methyl-2-propylpropane-1,3-diol dicarbamate) lack selectivity, whereas direct high-performance liquid chromatography is inappropriate because chromophores or oxidisable moieties are absent. Packed-column gas - liquid chromatography (GLC) is unreliable because of on-column breakdown although this can be minimised by using a capillary column.[1] Direct derivatisation cannot be performed, but meprobamate can be hydrolysed to the 1,3-diol which has been derivatised using *N,O*-bis(trimethylsilyl)acetamide,[2] benzoyl chloride[3] or butylboronic acid.[4] In the last method, the sample (1 ml), after hydrolysis (pH 14, 100 °C, 10 min), was extracted (10 min) with chloroform (5 ml) containing an internal standard (2-ethyl-2-methylpropane-1,3-diol) and, after centrifugation (10 min), 4 ml of the extract were dried over anhydrous sodium sulphate and taken to dryness. The residue was suspended (15 min) in *N,N*-dimethylformamide (25 μl) containing butylboronic acid (50 mmol l^{-1}) prior to analysis by GLC with flame ionisation detection (FID). This is clearly a lengthy procedure and is unsuitable for emergency work. In addition, the internal standard was added only after the hydrolysis step.

Cyclic alkyl- and aryl-boronates such as those formed from butyl- and phenyl-boronic acids are valuable for the GLC analysis of polar bifunctional compounds such as 1,2- and 1,3-diols, α- and β-hydroxyacids and 1,2- and 1,3-hydroxyamines.[5–7] Many such derivatives either form readily in aqueous media or are relatively stable to hydrolysis,[8,9] but preparation in the absence of water and/or the use of a dehydrating reagent are often recommended. Strong acid catalysis is required to promote the solvolysis of water with one of the commonly used reagents, 2,2-dimethoxypropane.[10] However, this requirement is often omitted and yet boronate formation still proceeds satisfactorily even with propane-1,3-diol, as evidenced by GLC,[11] even though this diol is not thought to react with phenylboronic acid in aqueous solution at room temperature.[9]

It is well known that boronate derivates can be formed on-column. This has been exploited in the structural elucidation of *cis*-diols by co-injection of the diol and an excess of boronic acid[12–15] and in the investigation of boronic acid mixtures by serial injection of the mixture and propane-1,3-diol.[16] Studies on the GLC of ethane-1,2-diol using propane-1,3-diol as the internal standard confirmed that the reaction with phenylboronic acid was apparently virtually instantaneous even in the presence of water and this, together with other evidence, suggested that the reaction was occurring largely on-column.[17] In contrast, other workers[4,18,19] have reported that, under anhydrous conditions and at room temperature, up to 15 min are required for boronation of ethane-1,2- and propane-1,3-diols to proceed to completion as assessed by GLC.

These observations suggest that water or water vapour promotes the on-column boronation of simple diols and this has been exploited in simplifying the meprobamate assay described above[4] for use in the diagnosis of acute poisoning. Aqueous solutions of meprobamate and 2-methyl-2-propylpropane-1,3-diol (MPPD) were used to study the hydrolysis and extraction/derivatisation conditions, respectively, and propane-1,3-diol (PD) and 2,2-dimethylpropane-1,3-diol (DMPD) were used as additional reference compounds as appropriate. In the assay procedure developed, hydrolysis of meprobamate to MPPD was followed by liquid - liquid extraction into methyl *tert*-butyl ether and derivatisation with phenylboronic acid in methanol - water (2 + 1). Mebutamate [2-methyl-2-*sec*-butylpropane-1,3-diol (MBPD) dicarbamate] was used as a reactive internal standard.

Experimental

Materials and Reagents

Meprobamate was obtained from Wyeth (Maidenhead, UK) and PD, DMPD, MPPD and mebutamate were supplied by Aldrich (Gillingham, UK). Phenylboronic acid (PBA) was purchased from BDH (Poole, UK) and methanol and methyl *tert*-butyl ether (MTBE) (both of HPLC grade) were obtained from Rathburn Chemicals (Walkerburn, UK). 2,2-Dimethoxypropane (2,2-DMP) was purchased from Aldrich. Other compounds, including water, were of analytical-reagent grade (BDH) unless stated otherwise.

Gas - Liquid Chromatography

A Pye Series 204 gas chromatograph was used. The column

* Present address: Beecham Pharmaceuticals Research Division, Medical Research Centre, The Pinnacles, Coldharbour Road, Harlow, Essex CM19 5AD, UK.

oven temperature was 160 °C and the injector and detector oven temperatures were 250 °C. A glass column (1.5 m × 2 mm i.d.) packed with 3% *m/m* OV-101 on GasChrom Q, 80–100 mesh (Chromatography Services, Hoylake, UK), was used with a carrier gas (nitrogen) flow-rate of 50 ml min^{-1}. The hydrogen and oxygen inlet pressures (FID) were 15 and 10 lb in^{-2}, respectively. The column was conditioned overnight at 250 °C with a carrier gas flow before use. On-column injections were performed using a 5-μl gas chromatographic syringe (SGE) fitted with an 11.5-cm needle. The detector sensitivity was 3.2 × 10^{-10} A f.s.d. Retention times were measured from the leading edge of the solvent front.

Optimisation of Assay Conditions

To study the effect of water on the derivatisation reaction, MPPD solutions (1.00 g l^{-1}) were prepared in water, chloroform, butyl acetate and MTBE. A solution of PBA containing PD (0.5 g l^{-1}) in acetonitrile (300 μl) was added to portions (100 μl) of the MPPD solutions in 60 × 5 mm i.d. glass test-tubes (Dreyer tubes; Samco, Old Woking, UK). After vortex-mixing (15 s), *ca.* 2 μl of each mixture were analysed by GLC after 10 and again after 30 min.

To establish the minimum amount of water needed for the derivatisation reaction, MPPD (1.00 g l^{-1}) in either water or heparinised bovine plasma (100 μl) was added to analyte-free water or plasma (300 μl) in a Dreyer tube. Methyl *tert*-butyl ether (100 μl) was added and, after vortex-mixing (30 s) and centrifugation (9950 *g*, 2 min; Eppendorf Model 5412), a portion (50 μl) of the MTBE extract was transferred into a second tube. 2,2-Dimethylpropane-1,3-diol (1.00 g l^{-1}) in MTBE (30 μl) and the derivatising reagent [15 g l^{-1} of PBA in methanol - water (2 + 1)] (20 μl) were added and additional portions of PBA-free methanol - water (2 + 1) were added to further tubes. After vortex-mixing (15 s), 2 μl of each mixture were analysed at 2 and again at 60 min.

A number of solvents [isoamyl alcohol (IAA) - MTBE (1 + 9), chloroform, cyclohexane - dichloromethane (1 + 1), 2,2,3,3,4,4,4-heptafluorobutan-1-ol (HFB) - MTBE (1 + 9), hexane, MTBE and light petroleum (b.p. 40–60 °C)] were compared for the extraction of MPPD from water. Hence the solvent (200 μl) was added to 200 μl of aqueous MPPD solution (1.00 g l^{-1}) in a Dreyer tube. After vortex-mixing (*ca.* 15 s) and centrifugation (9950 *g*, 2 min), a portion (50 μl) of the organic extract was transferred into a second tube. Propane-1,3-diol (0.5 g l^{-1}) in acetonitrile (200 μl), PBA (15 g l^{-1}) in 2,2-DMP (100 μl) and water (50 μl) were added and, after vortex-mixing (*ca.* 15 s), portions (2 μl) of each mixture were analysed.

Procedure Used in Sample Analyses

A solution of the internal standard (0.50 g l^{-1} aqueous mebutamate; 50 μl), sample or standard (200 μl) and 12.5 mol l^{-1} sodium hydroxide solution (200 μl) were placed in a Dreyer tube. The contents of the tube were vortex-mixed (*ca.* 15 s), heated in a boiling water-bath (5 min) and cooled under tap water. Methyl *tert*-butyl ether (100 μl) was added and, after vortex-mixing (30 s) and centrifugation (9950 *g*, 2 min), a portion (*ca.* 50 μl) of the extract was transferred into a second Dreyer tube. The derivatising reagent [15 g l^{-1} of PBA in methanol - water (2 + 1); 20 μl] was added and, after vortex-mixing (*ca.* 15 s), 1–2 μl were injected on to the GC column. Sample analyses were performed in duplicate.

Assay Calibration Procedure

Solutions of meprobamate (5, 10, 50, 100 and 200 mg l^{-1}) were prepared in water and in analyte-free heparinised bovine plasma by dilution of an aqueous stock solution of meprobamate (1.00 g l^{-1}). A quality assurance sample containing meprobamate (60 mg l^{-1}) was prepared in heparinised bovine plasma by dilution of a separate stock solution and was analysed in duplicate together with each specimen.

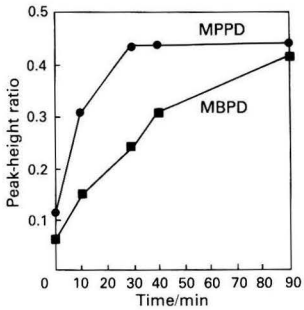

Fig. 1. Effect of derivatisation time on the formation of the phenylboronates of the meprobamate (MPPD) and mebutamate (MBPD) alkaline hydrolysis products in the absence of water. Aqueous solutions (1 ml) of meprobamate and mebutamate (each 1.00 g l^{-1}) were boiled (10 min) with 12.5 mol l^{-1} sodium hydroxide solution (1 ml) and cooled. Hydrolysate was extracted with chloroform (5 ml), evaporated to dryness and reconstituted in PD (0.5 g l^{-1}) in acetonitrile (200 μl) + PBA (15 g l^{-1}) in 2,2-DMP (300 μl). Results given as peak-height ratios relative to PD phenylboronate; 2-μl injections

Table 1. Effect of water on the formation of MPPD phenylboronate. For details see text. Results given as peak-height ratios (means of duplicate analyses) relative to DMPD phenylboronate

Additional methanol - water (2 + 1) added to MTBE extract/μl	Derivatisation time/min			
	2	60	2	60
	Aqueous standard		Plasma standard	
0	0.35	0.31	0.31	0.29
10	0.35	0.35	0.31	0.29
20	0.35	0.36	0.30	0.31
30	0.36	0.36	0.30	0.29

Results and Discussion

Choice of Assay Conditions

Although carbamates may be hydrolysed at acidic or basic pH it was found that in this instance alkaline (pH 14) rather than acidic (pH 2) hydrolysis was more efficient. However, when employing methodology similar to that used to assay ethane-1,2-diol by GLC,[17] derivatisation with PBA was impaired in aqueous alkaline as opposed to acidic solution. The diols were therefore extracted prior to the derivatisation step. However, when extracted both compounds showed an increase in response with time (up to 90 min with MBPD) when mixed with a solution of PD and derivatising reagent in the absence of water (Fig. 1).

To study the effect of water on the derivatisation reaction, MPPD solutions prepared in water and in organic solvent were analysed after 10 and again after 30 min. The results (peak-height ratios of MPPD relative to those of PD phenylboronate: 0.38, 0.07, 0.10 and 0.08 after 10 min; 0.39, 0.10, 0.15 and 0.12 after 30 min for aqueous, chloroform, butyl acetate and MTBE solutions, respectively) showed that a much greater response was obtained with the aqueous solution after 10 min and that this response did not increase with time. By adding water (50 μl) and re-analysing the organic solutions, the response increased to that obtained for the aqueous solution.

Table 2. Extraction of MPPD from aqueous solution using various solvents. For details see text. Results given as peak-height ratios (means of duplicate analyses) relative to PD phenylboronate

Solvent	Peak-height ratio
HFB - MTBE (1 + 9)	0.35
IAA - MTBE (1 + 9)	0.32
MTBE	0.28
Chloroform	0.25
Cyclohexane - dichloromethane (1 + 1)	0.05
Hexane	<0.01
Light petroleum (b.p. 40–60 °C)	<0.01

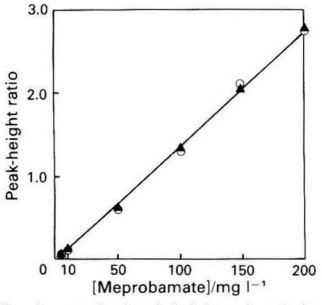

Fig. 2. Calibration graphs (peak-height ratio relative to the internal standard) obtained on analysis of the standard (▲) aqueous and (○) bovine plasma meprobamate solutions (each point is the mean of duplicate analyses). For details see text

These results clearly showed that water should be added to the meprobamate hydrolysate extract to catalyse the reaction with MPPD. However, the mechanism of this effect is not clear, although the presence of water vapour could inhibit adsorption on to the GC column thus making the diols available for derivatisation. After studying other solvents (ethanol, acetone and propan-2-ol), it was found that methanol was a suitable water-miscible solvent for PBA, but that the highest proportion of water which could be incorporated while retaining miscibility with MTBE was 33% *V/V*. However, 20 µl of methanol - water (2 + 1) containing PBA (15 g l^{-1}) were found to be sufficient for catalysing the reaction (Table 1).

Of the solvents studied, MTBE, alone or together with HFB or IAA, gave the best recovery of MPPD from water (Table 2) and had the additional advantage of forming the upper layer thus simplifying removal of the extract. The absolute efficiency of the MTBE extraction was studied using aqueous and heparinised bovine plasma solutions (200 µl) of MPPD (10, 50 and 200 mg l^{-1}). Control MPPD solutions were prepared in MTBE and analysed directly. The recovery was found to be in the range 90–99% for both the aqueous and bovine plasma solutions. This relatively high recovery of a water-soluble diol was attributed to the use of 12.5 mol l^{-1} sodium hydroxide solution (200 µl) in the procedure, which probably exerted a "salting-out" effect. Finally, the effects of changes in the volume of sodium hydroxide solution used (100, 200 or 300 µl with a hydrolysis time of 5 min) and in the hydrolysis time (5, 10, 20 or 30 min with 200 µl of sodium hydroxide solution) on the hydrolysis of meprobamate and mebutamate were studied. No major differences were observed although slight decreases in peak heights were noted after the addition of 300 µl of sodium hydroxide solution and after a hydrolysis time of 30 min.

Application of the Assay

On analysis of the standard meprobamate solutions the ratio of the peak height of derivatised MPPD to that of the internal standard, when plotted against meprobamate concentration, was linear over the concentration range studied. The calibration graphs obtained for the standard aqueous and bovine plasma solutions were identical (Fig. 2). The intra- and inter-assay coefficients of variation (CV) obtained for standard meprobamate solutions are given in Table 3. The limit of accurate measurement was 5 mg l^{-1}. After a single 400-mg oral dose the mean plasma meprobamate concentration was reported to be 7.7 mg l^{-1} after 2 h[20] whereas in 57 acute poisoning cases, concentrations in the range 10–310 mg l^{-1} [mean (± standard deviation), 60 ± 62 mg l^{-1}] were observed.[21]

Table 3. Assay of meprobamate by GLC; assessment of intra- and inter-assay reproducibilities using standard solutions prepared in heparinised bovine plasma. For details see text

	Meprobamate/ mg l^{-1}	Coefficient of variation, % (n = 10)
Intra-assay	5	5.2
	60	3.4
	200	2.9
Inter-assay*	60	3.7

* Inter-assay coefficient of variation calculated by performing duplicate analyses of the quality assurance sample on ten separate days and taking the mean result.

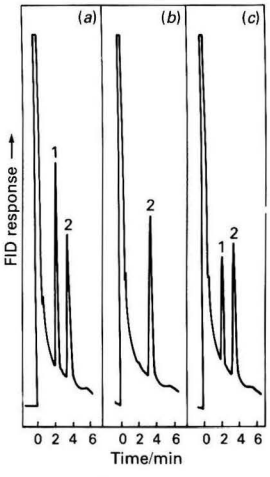

Fig. 3. Chromatograms obtained using the GLC meprobamate assay. Specimens: (*a*) bovine plasma standard containing 100 mg l^{-1} of meprobamate; (*b*) meprobamate-free bovine plasma; and (*c*) plasma from a meprobamate overdose patient (meprobamate concentration 45 mg l^{-1}). 1, MPPD phenylboronate; and 2, MBPD phenylboronate. Injection volume, 2 µl. For details see text

Mebutamate proved to be an ideal reactive internal standard. This compound, or other dicarbamates, are unlikely to be encountered in clinical samples because they are used less frequently than meprobamate itself. However, the method could be used to measure mebutamate using meprobamate as the internal standard if necessary. Some other carbamates, notably carisoprodol and tybamate, also give rise to MPPD on hydrolysis and hence could interfere. The risk of interference from other drugs is not high because few compounds which would be extracted under the conditions of the assay attain concentrations above 5 mg l^{-1} even after overdosage. No endogenous sources of interference were encountered (Fig. 3).

Meprobamate is metabolised to 2-methyl-2-(2-hydroxypropyl)propane-1,3-diol dicarbamate and also to an *N*-glucu-

ronide which is thought to be the principal urinary metabolite.[22] There is no information on the occurrence of these compounds in plasma after overdosage, but the hydroxypropyl metabolite is unlikely to interfere because, even if extracted, the corresponding 1,3-diol would still contain an underivatisable hydroxy group. Although the *N*-glucuronide would give rise to meprobamate and thence to MPPD on hydrolysis, the plasma concentrations of this metabolite are likely to be very low because glucuronides are very water soluble and are normally excreted rapidly by the kidneys. However, the method could only be used for the analysis of meprobamate in urine if a procedure such as solvent extraction was used prior to the hydrolysis to minimise interference from this source.

In conclusion, the assay described has advantages in that only a small sample volume is needed, sample preparation is relatively rapid (*ca.* 10 min) and both GLC with FID and the OV-101 column used are readily available in clinical toxicology laboratories. The finding that water acts to promote phenylboronate formation may prove useful when analysing other 1,2- and 1,3-diols and, possibly, other polar bifunctional compounds by GLC.

We thank M. Ruprah, Poisons Unit, for her help and advice.

References

1. Debruyen, D., Moulin, M. A., Camsonne, R., and Bigot, M.-C., *J. Pharm. Sci.*, 1980, **69**, 835.
2. Martis, L., and Levy, R. H., *J. Pharm. Sci.*, 1974, **63**, 834.
3. Gupta, R. N., and Eng, F., *J. High Resolut. Chromatogr. Chromatogr. Commun.*, 1980, **3**, 419.
4. Johansson, B., and Fromark, I., *J. Chromatogr.*, 1985, **341**, 462.
5. Brooks, C. J. W., and Maclean, I., *J. Chromatogr. Sci.*, 1971, **9**, 18.
6. Poole, C. F., and Zlatkis, A., *J. Chromatogr.*, 1980, **184**, 99.
7. Kossa, W. C., *in* Frei, R. W., and Lawrence, J. F., *Editors*, "Chemical Derivatisation in Analytical Chemistry," Plenum Press, New York, 1981, pp. 99–123.
8. Kuivila, H. G., Keough, A. H., and Soboczenski, E. J., *J. Org. Chem.*, 1954, **19**, 780.
9. Bowie, R. A., and Musgrave, O. C., *J. Chem. Soc.*, 1963, 3945.
10. Critchfield, F. E., and Bishop, E. T., *Anal. Chem.*, 1961, **33**, 1034.
11. Porter, W. H., and Auansakul, A., *Clin. Chem.*, 1982, **28**, 75.
12. Belvedere, G., Pantarotto, C., and Frigerio, A., *Res. Commun. Chem. Pathol. Pharmacol.*, 1975, **11**, 221.
13. Pantarotto, C., Cappellini, L., Negrini, P., and Frigerio, A., *J. Chromatogr.*, 1977, **131**, 430.
14. Frigerio, A., Lanzoni, J., Pantarotto, C., Rossi, E., Rovei, V., and Zanol, M., *J. Chromatogr.*, 1977, **134**, 299.
15. Pantarotto, C., Cappellini, L., De Pascale, A., and Frigerio, A., *J. Chromatogr.*, 1977, **134**, 307.
16. Rose, M. E., Longstaff, C., and Dean, P. D. G., *J. Chromatogr.*, 1982, **249**, 174.
17. Flanagan, R. J., Dawling, S., and Buckley, B. M., *Ann. Clin. Biochem.*, 1987, **24**, 80.
18. Robinson, D. W., and Reive, D. S., *J. Anal. Toxicol.*, 1981, **5**, 69.
19. Smith, N. B., *Clin. Chim. Acta,* 1984, **144**, 273.
20. Meyer, M. C., Melikian, A. P., and Straughn, A. B., *J. Pharm. Sci.*, 1978, **67**, 1290.
21. Bailey, D. N., *Am. J. Clin. Pathol.*, 1981, **75**, 102.
22. Ludwig, B. J., Douglas, J. F., Powell, L. S., Meyer, M., and Berger, F. M., *J. Med. Pharm. Chem.*, 1961, **3**, 53.

Paper 8/04580A
Received November 17th, 1988
Accepted February 20th, 1989

Determination of Trace Amounts of Molybdate in Soil by Ion Chromatography

Harish C. Mehra and William T. Frankenberger, Jr.*
Department of Soil and Environmental Sciences, University of California, Riverside, CA 92521, USA

Trace amounts of molybdate (MoO_4^{2-}) in soil were determined by single-column ion chromatography (SCIC). The method is based on the chromatographic separation of MoO_4^{2-} from other inherent ions (Cl^-, NO_3^-, PO_4^{3-} and SO_4^{2-}) and was characterised in terms of time of analysis, detection limits and column efficiency. Separation of the anions was compared with the use of resin-based and polymethacrylate (PMA) gel analytical columns with 5 mM *p*-hydroxybenzoic acid (pH 8.25) as the mobile phase. The analytes were quantified by conductimetry with a detection limit of 45 μg l^{-1} of MoO_4^{2-} (signal to noise ratio = 3). The SCIC method for the determination of MoO_4^{2-} with the PMA column gave good separation and the results were comparable to those obtained with inductively coupled plasma optical emission spectrometry.

Keywords: *Ion chromatography; high-speed ion determination; ion high-performance liquid chromatography; anion chromatography*

Molybdenum is an essential element to plants and animals. It is a constituent of several metalloflavin enzymes (*e.g.*, NADPH nitrite reductase), including those involved in nitrogen fixation and reduction of nitrate.[1] The Mo content of soil usually resembles that of the parent rocks but is also dependent on the degree of weathering and organic matter content. In igneous and sedimentary rocks, the Mo content (mg kg^{-1}) is approximately 1.5 (igneous rocks), 2.6 (shales), 0.2 (sandstones) and 0.4 (limestone).[1] Molybdenum also enters the environment through industrial smoke, fugitive dust and the application of sewage sludge. The Mo content in soils ranges from 0.05 to 40 mg kg^{-1} with a mean of 1.5 mg kg^{-1}.[2] The availability of Mo for uptake by plants is highly dependent on soil pH; the average Mo content in land plants is 0.9 mg kg^{-1}.[1] However, Mo toxicity (molybdenosis) in ruminants can occur with high levels of Mo in forage in Mo-rich soils.[3] Deficiencies in Mo can also occur at levels of less than 0.1 mg kg^{-1} within plant tissue.[4,5] For the determination of Mo in solid matrices, spectrophotometric procedures such as the thiocyanate and dithiol methods are commonly used.[6] Such procedures require pre-concentration techniques or organic extraction and are subject to interferences by other ions. Atomic absorption spectrometry (AAS) and inductively coupled plasma optical emission spectrometry (ICP-OES)[7,8] have been used for the determination of Mo in soils, but are subject to matrix interference and involve organic extraction procedures in order to obtain high sensitivity.

Ion chromatography (IC) is a rapid, sensitive and selective multi-element technique for analysing complex solutions of ionic species. In the field of soil analysis, IC has received relatively little attention. The first application of IC to soil analysis employed suppressed ion chromatography (SIC) for the simultaneous determination of NO_3^- and SO_4^{2-}.[9] Single-column ion chromatographic (SCIC) procedures have been developed for the determination of various common soil anions,[10,11] ammonium, alkali metals and alkaline earth metal cations[12] and trace oxoanions such as those of selenium,[13–15] arsenic[16] and tungsten.[17]

In this work, SCIC was evaluated for the simultaneous on-line determination of MoO_4^{2-} in soils together with other common anions. A routine and inexpensive method for the detection of trace levels of MoO_4^{2-} in soils with high accuracy and precision and with minimum sample preparation was developed. Further, two analytical columns were evaluated for their suitability for the determination of MoO_4^{2-}. Little information is available on the use of polymethacrylate (PMA) gel columns for the separation of solutes by IC. This work has shown that a PMA column is superior to silica- and resin-based columns for the determination of MoO_4^{2-} in soil extracts.

* To whom correspondence should be addressed.

Experimental

Apparatus

A schematic representation of the SCIC system used has been given previously.[10] The high-performance liquid chromatographic (HPLC) assembly consisted of a Beckman (Fullerton, CA, USA) Model 332 liquid chromatograph equipped with a Model 110A pump and a Model 210 sample injector. Conductimetric detection was accomplished with a Waters (Milford, MA, USA) Model 430 conductimetric detector. A Hewlett-Packard (Avondale, PA, USA) Model 3390A printer - plotter integrator with a variable input voltage was used to record the signal response. Three analytical columns were assessed for the separation and quantification of MoO_4^{2-}: a Waters analytical TSK gel IC-Pak anion column, Cat. No. 26770 (150 × 4.6 mm i.d.), containing PMA gel (10 μm) with quaternary amine functional groups; a Vydac (The Separator Group, Hesperia, CA, USA) 300 IC (250 × 4.6 mm i.d.) column containing 10-μm quaternised silica bonded with quaternary amine groups having a capacity of 0.10 mol kg^{-1}; and a Wescan (San Jose, CA, USA) anion/R (269-029) low-capacity (0.2 mequiv. g^{-1}) resin-based (250 × 4.1 mm i.d.) column. A Wescan guard column (40 × 4.6 mm i.d.) packed with pellicular anion-exchange material (269-003) preceded the analytical column with zero dead-volume fittings. To prevent drift in conductance, due to temperature variations, the column was insulated with a column heater (Eldex Laboratories, Menlo Park, CA, USA, Model III) and maintained at 25 °C. Sample injection loops of 100, 500 and 2000 μl were employed to establish the detection limits.

Reagents

Analyte solutions were prepared from analytical-reagent grade chemicals. Sodium molybdate, *p*-hydroxybenzoic acid (PHBA), potassium hydrogen phthalate, sodium borate, boric acid, glycerine, sodium gluconate and sodium benzoate were obtained from Sigma (St. Louis, MO, USA), ammonium oxalate from Aldrich (Milwaukee, WI, USA) and potassium chloride, potassium nitrate, dipotassium hydrogen phosphate and potassium sulphate from Fisher Scientific (Tustin, CA,

USA). HPLC grade water was obtained by filtering de-ionised water through the following: (*i*) an HN organic removal resin (Barnsted, Boston, MA, USA); (*ii*) an ultrapure DI exchange column (Barnsted); and (*iii*) a 0.22-μm membrane filter (Millipore, Bedford, MA, USA).

Mobile Phase

Aqueous solutions of PHBA with concentrations of 5, 6, 7, 8 and 9 mM over the pH range 8.0–9.0 (in 0.2 pH unit increments) were assessed for the separation of MoO_4^{2-} from the other anions. Various flow-rates from 1.0 to 2.5 ml min^{-1} were also tested, with optimum separation observed at 1.8 ml min^{-1}. The column inlet pressure was about 70 bar (1000 lb in^{-2}) and the detector output was 10 mV. The column conditioning procedures have been discussed elsewhere.[10]

Field Samples and Preparation

All soil samples were air-dried and passed through a 2-mm sieve. Two extraction procedures were evaluated: hot water[18] *versus* ammonium oxalate.[19] A soil extract was prepared by adding 50 ml of de-ionised water to 10-g samples and heating at 70–80 °C for 4 h. The mixture was subjected to shaking for 2 h and then filtered through Whatman No. 42 filter-paper. A second soil extract was prepared in 0.175 M ammonium oxalate solution, with a ratio of oxalate solution to soil of 5 : 1, and was subjected to shaking overnight. The extract was then filtered (Whatman No. 42 filter-paper) and a measured aliquot of the filtrate was evaporated to dryness. The residue was ignited in a crucible for 4 h at 450 °C to remove the oxalate and organic matter and then dissolved in 50 ml of de-ionised water. Both extracts were passed through a 3-ml Supelclean LC-Si (40 μm) column (Supelco, Bellefonte, PA, USA). The pH of each extract was adjusted to 8.25 with sodium hydroxide solution and the extracts were passed through a 0.22-μm membrane filter (Millipore) before the SCIC analysis.

To check the reproducibility of the method, standards were injected on seven separate occasions to determine the between-sample variation. The minimum detection limits with various sample sizes were calculated as a three-fold signal to noise ratio at the base line.

Inductively Coupled Plasma Optical Emission Spectrometry

A Jarrell-Ash Atom Comp 800 ICP spectrometer was used. The operating conditions were as follows: wavelength, 202.03 nm; torch, fassel type; forward power, 1.75 kW; viewing height, 13 mm above the coil; coolant gas (argon) flow-rate, 14.1 l min^{-1}; integration time, 17 s; and pre-integration time, 17 s.

Results and Discussion

Optimisation of Separation Conditions

The important factors in the determination of MoO_4^{2-} are the choice of eluent, the concentration of the mobile phase, the working pH and column selection; these were varied in order to optimise the resolution of MoO_4^{2-} from other anions in soils. The following eluents were tested for quantification and separation of MoO_4^{2-} with the three analytical columns: potassium hydrogen phthalate, PHBA, sodium hydroxide, borate - gluconate and sodium benzoate. The silica-based column had pH limitations and was found to be unsuitable. The resin-based and PMA columns responded well to the PHBA and borate - gluconate eluents. *p*-Hydroxybenzoic acid was selected as the optimum mobile phase for both columns because it gave excellent resolution of a mixture of Cl^-, NO_3^-, PO_4^{3-}, SO_4^{2-}, and MoO_4^{2-} ions and a reasonable time of analysis. The detection of MoO_4^{2-} was enhanced by increasing the pH. As PHBA has a high buffering capacity in the alkaline pH range, the pH of the mobile phase was varied from 7.5 to 9.0 in order to determine the optimum pH for MoO_4^{2-} separation. At pH > 9.0, the resolution (R_s) between MoO_4^{2-} and SO_4^{2-} was poor and at pH < 7.5 poor sensitivity was obtained and a longer time of analysis was required. The optimum resolution of a mixture of MoO_4^{2-} and SO_4^{2-} ions occurred at pH 8.25 (R_s = 6.14). Further studies were carried out with the PMA and resin-based columns to assess the optimum concentration of PHBA required for the determination of MoO_4^{2-}. Of the concentrations tested, 5 mM PHBA was found to give the best resolution between MoO_4^{2-} and SO_4^{2-} ions and provided a suitable time of analysis (14 min). The capacity factor k' decreased as the concentration of PHBA increased.

The pH of the sample injected also affected the sensitivity of the detection of MoO_4^{2-}. It was found appropriate to keep the sample pH the same as that of the eluent (PHBA, pH 8.25).

The PMA and resin-based columns were compared in terms of time of analysis (k'), efficiency (plate number, N) and resolution (R_s) for MoO_4^{2-} together with other inherent anions detected in the extract. With the same flow-rate, mobile phase (PHBA) and temperature, the response towards MoO_4^{2-} was excellent with the PMA column in terms of the resolution of MoO_4^{2-} - SO_4^{2-}, detection limits, efficiency (N), and time of analysis (k') (Table 1). Hence all subsequent work on the determination of MoO_4^{2-} by SCIC was performed with the PMA column.

Table 1. Chromatographic parameters of the TSK PMA gel column for the determination of MoO_4^{2-}. Conditions: eluent, PHBA (pH 8.25, 5 mM); detection, conductimetric

Anion	t_R/min	Capacity factor (k')	Plate No. (N)	R_s
Cl^-	3.33	0.39	784	4.72 (Cl^- : NO_3^-)
NO_3^-	5.96	1.48	1642	1.50 (NO_3^- : PO_4^{3-})
PO_4^{3-}	6.80	1.83	2176	2.33 (PO_4^{3-} : SO_4^{2-})
SO_4^{2-}	8.28	2.45	3136	6.14 (SO_4^{2-} : MoO_4^{2-})
MoO_4^{2-}	12.09	4.04	4712	—

Calibration and Precision

A calibration graph of peak area against ionic concentration was linear (r^2 = 0.970, n = 7) in the range 0.50–35 μg ml^{-1} of MoO_4^{2-}. The relative standard deviation (RSD) for different solutions (between-sample variation) ranged from 0.3 to

Table 2. Precision of the ion chromatographic method for the determination of MoO_4^{2-} and other anions. Conditions as in Table 1

Volume of sample injected/μl	Parameter	Anion					
		Cl^-	NO_3^-	PO_4^{3-}	SO_4^{2-}	MoO_4^{2-}	
100	Concentration/μg ml^{-1}	6.0	8.0	10.0	12.0	12	10
	RSD,* %	0.92	0.84	0.72	0.68	0.75	0.86
500	Concentration/μg ml^{-1}	4.0	2.5	3.5	4.0	5.0	7.5
	RSD,* %	1.78	2.14	3.05	2.80	3.01	2.52
2000	Concentration/μg ml^{-1}	1.5	1.0	2.5	3.0	2.0	1.0
	RSD,* %	3.02	3.24	4.13	5.02	6.21	5.55

* RSD = relative standard deviation from seven measurements.

Table 3. Comparison of SCIC and ICP-OES for the determination of MoO_4^{2-}

Sample	MoO_4^{2-}/μg g^{-1} SCIC*	ICP-OES
Soil treated with sewage sludge I (Michigan)	2.38	2.87
Soil treated with sewage sludge II (Michigan)	4.10	4.68
Soil I (California)	0.90	0.92
Soil II (California)	ND†	ND
Soil II spiked with 1.20 mg l^{-1} of MoO_4^{2-}	1.10 (91.6)‡	1.39 (115.8)
Soil III (California)	ND	ND
Soil III spiked with 6.50 mg l^{-1} of MoO_4^{2-}	6.70 (103.8)	6.98 (107.4)
Soil IV (California)	ND	ND
Soil IV spiked with 5.25 mg l^{-1} of MoO_4^{2-}	5.11 (97.1)	4.76 (90.4)

* Conditions as in Table 1.
† ND = not detected.
‡ Figures in parentheses indicate percentage recovery.

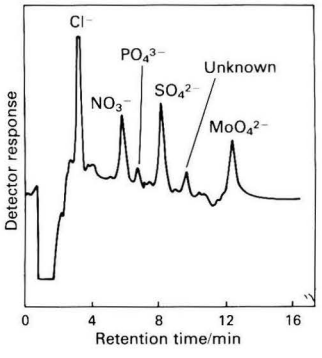

Fig. 1. Typical SCIC trace of an aqueous extract of soil treated with sewage sludge. Column, PMA; eluent, 5 mM PHBA (pH 8.25); detection, conductimetric

7.4%. The precision of the SCIC method was determined by carrying out seven replicate injections of combined standards in order to determine the within-sample variation (Table 2). The results showed that the RSD of all the analytes tested varied from 0.78 to 3.05% (MoO_4^{2-}, 2.70%) with a 500-μl loop. The precision with the 2-ml loop varied from 3.02 to 6.87% (MoO_4^{2-}, 6.87%).

Detection Limits

Limits of detection for various sample sizes were calculated as a three-fold signal to noise ratio at the base line. The ion chromatographic detection limit for MoO_4^{2-} was 45 μg l^{-1} with a 2-ml injection loop. Increasing the injection sample loop size above 2 ml resulted in decreased resolution owing to increased distortion and peak overlap.

Interferences

One of the major concerns in the analysis of soils treated with sewage sludge is the precise determination of the ion of interest in the presence of other inherent ions which could mask the signal. The ion chromatographic separation of MoO_4^{2-} by SIC[20] has been reported without reference to the common anions typically found in soil, *viz.*, Cl^-, NO_3^-, PO_4^{3-} and SO_4^{2-}. Further, it was found necessary to concentrate the sample through a Chelex resin. In the proposed SCIC method, all the above ions can be determined simultaneously with no interference in the detection of MoO_4^{2-}. In addition, studies with related transition metals (from Group VIB of the Periodic Table) indicated that CrO_4^{2-} [retention time (t_R) = 13.3 min] and WO_4^{2-} (t_R = 11.0 min) did not affect the determination of MoO_4^{2-} (t_R = 12.1 min).

Comparative Methods of Detection

A close relationship was observed between the proposed SCIC method (y) and ICP-OES (x) for the analysis of the soil extracts (spiked and unspiked) (Table 3). The relationship between the two methods was as follows: $y_{SCIC} = 0.984x_{ICP\text{-}OES} - 0.275$, $r = 0.99$ ($p < 0.001$). The regression equation gave a value for the slope of unity, demonstrating the excellent agreement between the two methods of detection. The discrepancy between the ICP-OES and SCIC methods (average 11.3%, RSD) might be due to interferences from specific cations (*i.e.*, Al^{3+} and Ca^{2+}) in the soil extracts. Manzoori[7] reported that Al^{3+} and Ca^{2+} caused a 20–25% enhancement in the intensity of the Mo emission with ICP-OES. This enhancement was thought to be due to the suppression of ionisation.

Determination of MoO_4^{2-} by SCIC

A typical chromatogram of an aqueous extract of soil treated with sewage sludge is shown in Fig. 1. Larger amounts of MoO_4^{2-} were extracted with ammonium oxalate than with hot water (2.52- to 3.16-times more), which is in agreement with the observations of Lowe and Massey.[18] The results of the soil analysis shown in Fig. 1 were as follows (μg g^{-1}): Cl^-, 29.6; NO_3^-, 16.0; PO_4^{3-}, 8.8; SO_4^{2-}, 58.2; and MoO_4^{2-}, 2.4. The ions were separated into well defined peaks with a time of analysis of 14 min. An additional peak with a retention time of 10.2 min was detected, but it could not be identified. The elution sequence of the detected anions was $Cl^- > NO_3^- > PO_4^{3-} > SO_4^{2-}$ > unknown peak > MoO_4^{2-}. The recovery of MoO_4^{2-} from soil extracts spiked with known amounts of MoO_4^{2-} was studied using SCIC and ICP-OES; the recoveries ranged from 91.6 to 103.8 and from 90.4 to 115.8%, respectively. In addition, the efficiency of the extraction of Mo spiked into sewage sludge (five samples) was determined and was found to be in the range 81–94%.

This research was partially supported by the UC Salinity and Drainage Task Force. We are grateful to Lee W. Jacobs for providing soil samples treated with sewage sludge with elevated levels of Mo and to G. Bradford for the ICP-OES analyses. We are also grateful to Waters and Wescan Instruments for the analytical columns used in this work.

References

1. Bowen, H. J. M., "Trace Elements in Biochemistry," Academic Press, New York, 1966.
2. Berrow, M. L., and Reaves, G. A., *in* "Proceedings of the International Conference on Environmental Contamination, London, July 1984," pp. 333–340.
3. Pierzynski, G. M., and Jacobs, L. W., *J. Environ. Qual.*, 1986, **15**, 323.
4. Gough, L. P., Shacklette, H. T., and Case, P. A., "Geological Survey Bulletin," 1979, No. 1466, pp. 36–38.
5. Aubert, H., and Pinta, M., "Trace Elements in Soils," Elsevier, Amsterdam, 1977, pp. 55–62.
6. Marczenko, Z., "Separation and Spectrophotometric Determination of Elements," Wiley, New York, 1986, pp. 380–391.
7. Manzoori, J. L., *Talanta*, 1980, **27**, 682.
8. Fassel, V. A., *Science*, 1978, **202**, 183.
9. Dick, W. A., and Tabatabai, M. A., *Soil Sci. Soc. Am. J.*, 1979, **43**, 899.

10. Nieto, K. F., and Frankenberger, W. T., Jr., *Soil Sci. Soc. Am. J.*, 1985, **49**, 587.
11. Karlson, U., and Frankenberger, W. T., Jr., *Soil Sci. Soc. Am. J.*, 1987, **51**, 72.
12. Nieto, K. F., and Frankenberger, W. T., Jr., *Soil Sci. Soc. Am. J.*, 1985, **49**, 592.
13. Mehra, H. C., and Frankenberger, W. T., Jr., *Chromatographia*, 1988, **25**, 585.
14. Karlson, U., and Frankenberger, W. T., Jr., *J. Chromatogr.*, 1986, **368**, 153.
15. Karlson, U., and Frankenberger, W. T., Jr., *Anal. Chem.*, 1986, **58**, 2704.
16. Mehra, H. C., and Frankenberger, W. T., Jr., *Soil Sci. Soc. Am. J.*, 1988, **52**, 1603.
17. Mehra, H. C., and Frankenberger, W. T., Jr., *Anal. Chim. Acta*, 1989, **217**, 383.
18. Lowe, R. H., and Massey, H. F., *Soil Sci.*, 1965, **100**, 238.
19. Grigg, J. L., *Analyst*, 1953, **78**, 470.
20. Ficklin, W. H., *Anal. Lett.*, 1982, **15**, 865.

Paper 8/03970D
Received October 5th, 1988
Accepted January 31st, 1989

Continuous-flow Chemiluminescence Determination of Acetaminophen by Reduction of Cerium(IV)

Ioanna I. Koukli, Antony C. Calokerinos* and Themistocles P. Hadjiioannou
Laboratory of Analytical Chemistry, University of Athens, 106 80 Athens, Greece

A rapid and precise continuous-flow method is described for the determination of acetaminophen (1.00–10.0 μg ml^{-1}) based on the chemiluminescence produced by its reaction with cerium(IV) in acidic solution. When applied to tablets, the method is relatively free from interferences from common excipients and co-existing drugs. The results obtained for the assay of commercial pharmaceutical preparations compared well with those obtained by a reference method and demonstrated good accuracy and precision.

Keywords: *Acetaminophen determination; chemiluminescence; pharmaceutical preparations; cerium(IV)*

Acetaminophen (paracetamol, *N*-acetyl-4-aminophenol) occupies a prominent position among the extensively employed antipyretic analgesics. Many methods have been described for its determination, including titrimetry,[1] chromatography,[2–4] electrochemistry[5,6] and spectrophotometry.[7–14] Most of these methods require lengthy treatments and lack the simplicity needed for routine analysis.

In recent years there has been increasing interest in the application of chemiluminescence (CL) to assays in biological systems.[15,16] Most of the reported procedures use the well known luminol,[17,18] peroxyoxalate[19,20] or lucigenin[21] CL reaction systems. Work on CL reactions of organic compounds formulated in pharmaceutical preparations is limited and an extensive evaluation of CL in drug analysis is not available. Owa *et al.*[22] have described the determination of tetracycline by oxidation with potassium persulphate and Townshend and co-workers[23,24] have described the determination of morphine and its derivatives by oxidation with potassium permanganate. The need for sensitive and selective determination procedures for existing drugs will ensure the rapid development of such CL reactions.

This work was concerned with the study of the CL generated by the oxidation of acetaminophen with cerium(IV) in an acidic medium. A flow-through detector built in this laboratory was used to develop a simple and sensitive assay procedure for acetaminophen.

Experimental

Apparatus

The continuous-flow CL analyser features two basic components, the detector housing and the flow-through system, which allow mixing of the reacting solutions just before the detector. Both were assembled from parts in our laboratory and have been described in detail elsewhere.[25]

Reagents

All solutions were prepared from analytical-reagent grade materials using de-ionised, distilled water.

Stock acetaminophen solution, 100.0 μg ml^{-1}. Dissolve 0.1000 g of acetaminophen (Serva) in water, transfer the solution into a calibrated flask and dilute to 1 l. The solution was stable for at least 1 month at 4 °C. More dilute solutions were prepared daily by the minimum number of dilution steps possible.

Cerium(IV) working solution, 2.50 × 10^{-2} M. Dissolve 3.95 g of ammonium cerium(IV) sulphate dihydrate (Merck) in 4 M perchloric acid, transfer the solution into a calibrated flask and dilute to 250 ml with 4 M perchloric acid. The solution must be prepared daily.

Procedures

Sample preparation

Not less than 20 tablets were weighed, ground into a fine powder and mixed. Approximately 200 mg of acetaminophen were weighed accurately, transferred into a 1-l calibrated flask and diluted to volume with water. The mixture was shaken mechanically for 15 min to aid dissolution and then filtered. The first 20 ml of the filtrate were discarded. An 8.00-ml volume of the filtrate was transferred into a 250-ml calibrated flask and diluted to volume with water.

Measurement procedure

The instrument was set at the optimised conditions but the sampling needle was kept in the "wash" position until the base line on the recorder had been established. The sampler was activated and the analysis proceeded automatically. The calibration graph of emission intensity (I/mV) *versus* concentration of acetaminophen (c/μg ml^{-1}) was constructed and the acetaminophen content of the samples was determined. A standard solution should be included after every 12 samples.

Results and Discussion

Optimisation of Experimental Parameters

The instrumental parameters (rate of reagent and analyte addition, sampling and wash times, etc.) were the same as described previously.[25] The cerium(IV) concentration and the nature and concentration of the acid present in the reaction solution have a marked influence on the detector response and were investigated in order to obtain the maximum emission intensity. The effect of the cerium(IV) concentration at various perchloric acid concentrations on 5.00 and 10.0 μg ml^{-1} of acetaminophen is shown in Fig. 1. The results showed that the cerium(IV) and perchloric acid concentrations should be as high as possible, the dilution efficiency and the durability of the tubing being the limiting factors. It was decided to use 4 M perchloric acid in order to avoid rapid deterioration of the tubing at higher acidities. The sensitivity deteriorated when sulphuric acid (Fig. 1) or mixtures of sulphuric and nitric acids were used instead of perchloric acid. Therefore, perchloric acid was the most suitable medium for the sensitive measurement of acetaminophen.

Analytical Parameters

Fig. 2 shows a typical recording for a series of acetaminophen standards carried out by the proposed procedure. The

* To whom correspondence should be addressed.

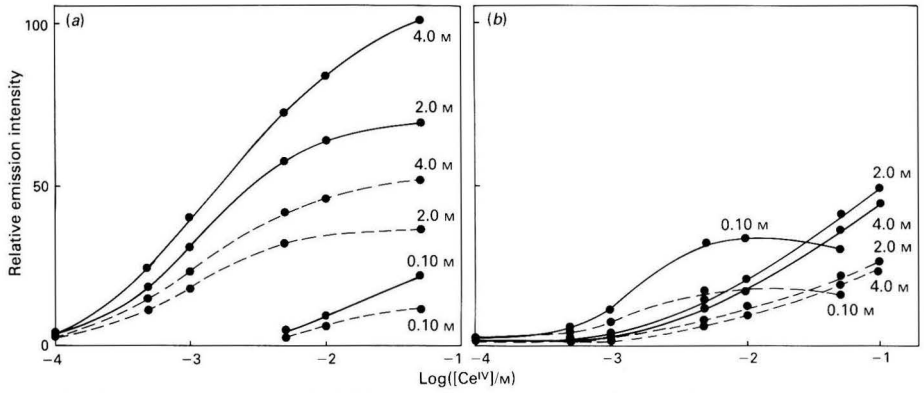

Fig. 1. Effect of cerium(IV) concentration on the CL intensity from: broken line, 5.00 and solid line, 10.0 μg ml^{-1} of acetaminophen in 0.10, 2.0 and 4.0 M (*a*) perchloric and (*b*) sulphuric acid. Conditions: photomultiplier voltage, −600 V; flow-rate of cerium(IV), 1.60 ml min^{-1}; and flow-rate of acetaminophen, 2.00 ml min^{-1}

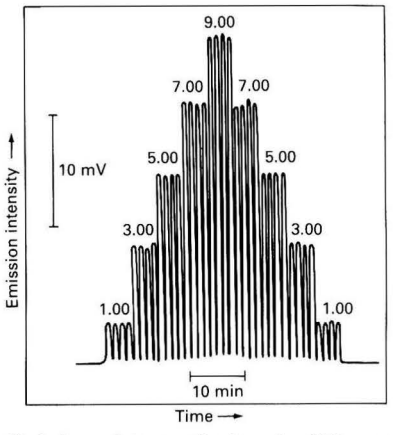

Fig. 2. Typical recorder output for the cerium(IV) - acetaminophen reaction under the recommended conditions (numbers above each set of peaks are μg ml^{-1} of acetaminophen)

calibration graph was linear in the range 1.00–10.0 μg ml^{-1} of acetaminophen [$I = 0.352 + 3.35c$; $r = 0.9997$ ($n = 10$)], which was used for all the analytical measurements. The limit of detection (signal to noise ratio = 3) was 0.070 μg ml^{-1} of acetaminophen and the coefficients of variation for 1.00 and 10.0 μg ml^{-1} of acetaminophen were 0.7 and 0.2%, respectively (n = 7). When aqueous solutions of acetaminophen (1.00–10.0 μg ml^{-1}) were analysed by the proposed procedure, the average error was ±1% (range 0.4–2.2%) and the correlation coefficient (r) was 0.9996 (n = 10).

Interference Studies

In order to assess the possible analytical applications of the CL reaction described above, the effect of some common excipients used in pharmaceutical preparations was studied by analysing synthetic sample solutions containing 5.00 μg ml^{-1} of acetaminophen and various excess amounts of each excipient. The undissolved material, if any, was filtered before measurement. The recovery results are shown in Table 1. No interference was observed from carbopol, starch, sugar, saccharin and magnesium stearate, which showed recoveries in the range 97.4–104.6%. Glucose, galactose and lactose interfere owing to their non-CL reaction with cerium(IV), but the effect is reduced by dilution. Citric acid, sodium citrate, sorbitol and propylene glycol, which are the most common excipients in elixirs, also react with cerium(IV). The interference can only be reduced by large dilutions but such dilutions would reduce the acetaminophen concentration to below the limit of detection. Hence, the method cannot be used for the determination of acetaminophen in elixirs. Gelatin probably reduces the flow-rate of the solution and EDTA interferes

Table 1. Recovery of acetaminophen (5.00 μg ml^{-1}) from various additives used as excipients

Additive	Concentration ratio (additive to acetaminophen)	Recovery, % (n = 5)
Glucose	10	90.2
	5	98.0
Galactose	10	84.4
	5	92.4
	1	97.5
Lactose	10	94.8
	5	97.4
Carbopol*	10	102.6
Starch	10	104.6
CAHP†	10	108.0
	5	97.0
Sugar	10	97.4
Sodium lauryl sulphate	10	73.2
	5	88.8
	1	100.1
Carbowax‡	10	75.8
	5	86.9
	1	95.4
Magnesium stearate	10	97.6
Saccharin	10	101.4
Gelatin	10	87.0
Citric acid	10	21.9
	5	22.7
	1	59.4
	0.1	91.8
Sodium citrate	10	25.6
	5	34.9
	1	67.0
	0.1	92.4
Sorbitol	10	53.6
	5	66.3
	1	89.3
	0.1	98.3
Propylene glycol	10	67.7
	5	80.1
	1	95.3
	0.1	98.8
EDTA	10	68.2
	5	77.7
	1	94.7

* Carboxypolymethylene.
† Cellulose acetate hydroxyphthalate.
‡ Polyethylene glycol 4000.

Table 2. Recovery of acetaminophen (5.00 μg ml^{-1}) from some co-existing drugs

Drug	Concentration ratio (drug to acetaminophen)	Recovery, % (n = 5)
Acetylsalicylic acid	10	81.5
	5	91.8
	1	98.8
Salicylamide	10	11.2
	5	20.0
	1	48.9
	0.1	88.4
Salicylic acid	10	10.8
	5	22.4
	1	64.0
	0.1	95.2
Promethazine	10	12.2
	5	19.6
	1	46.3
	0.1	93.3
Pentobarbital	10	100.3
p-Aminophenol*	10	9.9
	5	19.5
	1	55.9
	0.1	100.0

* Hydrolysis product of acetaminophen.

Table 3. Recovery experiments for acetaminophen added to sample solutions of commercial formulations

Formulation	Acetaminophen/μg ml^{-1} Initially present	Added	Recovered	Recovery, %
Depon	2.13	3.00	3.01	100.3
		6.00	6.10	101.7
Norgesic	1.45	3.00	2.98	99.3
		6.00	5.74	95.7
Lonarid	1.26	3.00	3.22	107.3
		6.00	6.21	103.5
			Mean:	101.3

owing to the formation of stable complexes with cerium(IV). The interference from Carbowax and sodium lauryl sulphate, when present at concentrations higher than that of acetaminophen, is probably due to a quenching effect.

The effect of some common co-existing drugs on the recovery of acetaminophen was studied as for excipients (Table 2). The interference from most drugs is reduced by dilution. Therefore, the high sensitivity of the method allows large dilutions of the sample solution and the reduction or elimination of interferences.

Accuracy

The accuracy of the continuous-flow CL method was examined by performing recovery experiments on solutions prepared from acetaminophen tablet formulations. A mean recovery of 101.3% was found (range 95.7–107.3%) (Table 3). Elixirs did not give satisfactory recoveries, as expected, owing to the serious interferences from their excipients.

The proposed method was also evaluated by analysing commercial formulations of acetaminophen and comparing the results with those obtained using the established nitrosation method.[9] A satisfactory agreement between the results was obtained (Table 4) with a mean relative difference of 2.2% (range 0.4–4.4%).

Conclusions

The CL reaction studied here has demonstrated the potential applicability of sensitive CL reactions to the field of drug analysis. The method described is simple, rapid, automated, fairly sensitive and sufficiently accurate and precise. The results were reproducible and showed that the method can be applied directly to solutions prepared from tablets containing acetaminophen, without any further treatment. Further, the reaction can be used for the sensitive determination of acetaminophen in complex matrices after separation of the drug from interfering substances.

Table 4. Determination of acetaminophen in commercial tablet formulations with the CL method and a reference method[9]

Formulation	Composition (mg)	Acetaminophen found/mg per tablet: CL ± SD*	Reference method[9]	Relative difference (CL—reference), %
Depon	Paracetamol (500)	477 ± 5	488	−2.3
Lonarid	Parcetamol (400) caffeine (50) codeine phosphate (10)	407 ± 3	413	−1.5
Panadol	Paracetamol (500)	511 ± 3	509	+0.4
Medamol	Paracetamol (500) codeine phosphate (10)	510 + 4	506	+0.8
Dalmin	Paracetamol (500) caffeine (20)	497 ± 8	515	−3.5
Norgesic	Paracetamol (450) orphenadrine citrate (35)	433 ± 9	453	−4.4
			Average:	2.2

* Standard deviation (n = 5).

The authors thank M. Koupparis for helpful discussions.

References

1. Srivastava, M. K., Ahmad, S., Singh, D., and Shukla, I. C., *Analyst*, 1985, **110**, 735.
2. Dechtiaruk, W. A., Johnson, G. F., and Solomon, H. M., *Clin. Chem.*, 1976, **22**, 879.
3. Plakogiannis, F. M., and Saad, A. M., *J. Pharm. Sci.*, 1977, **66**, 604.
4. Evans, M. A., and Harbison, R. D., *J. Pharm. Sci.*, 1977, **66**, 1628.
5. Miner, D. J., Rice, J. R., Riggin, R. M., and Kissinger, P. T., *Anal. Chem.*, 1981, **53**, 2258.
6. Falkowski, A., and Wei, R., *Anal. Lett.*, 1981, **14**, 1003.
7. Davis, D. R., Fogg, A. G., Burns, D T., and Wragg, J. S., *Analyst*, 1974, **99**, 12.
8. Ellcock, C. T. H., and Fogg, A. G., *Analyst*, 1975, **100**, 16.
9. Belal, S. F., Elsayed, M. A. H., Elwalily, A., and Abdine, H., *Analyst*, 1979, **104**, 919.
10. Verma, K. K., Gulati, A. K., Palod, S., and Tyagi, P., *Analyst*, 1984, **109**, 735.
11. Koupparis, M., Macheras, P., and Tsaprounis, C., *Int. J. Pharm.*, 1985, **27**, 349.
12. Issa, A. S., Beltagy, Y. A., Gabr Kassem, M., and Daabees, H. G., *Talanta*, 1985, **32**, 209.
13. El Kheir, A. A., Belal, S., El Sadek, M., and El Shanwani, A., *Analyst*, 1986, **111**, 319.
14. Sultan, S. M., Alzamil, I. Z., Alrahman, A. M. A., Altamrah, S. A., and Asha, Y., *Analyst*, 1986, **111**, 919.
15. Seitz, W. R., *CRC Crit. Rev. Anal. Chem.*, 1981, **13**, 1.
16. Kricka, L. J., and Thorpe, G. H. G., *Analyst*, 1983, **108**, 1274.
17. Huu, T. P., Marquetty, C., Pasquier, C., and Hakim, J., *Anal. Biochem.*, 1984, **142**, 467.

18. Malavolti, N. L., Pilosof, D., and Nieman, T. A., *Anal. Chim. Acta,* 1985, **170**, 199.
19. Kobayashi, S., and Imai, K., *Anal. Chem.,* 1980, **52**, 424.
20. Mahant, V. K., Miller, J. N., and Thakrar, H., *Anal. Chim. Acta,* 1983, **145**, 203.
21. Veazey, R. L., and Nieman, T. A., *J. Chromatogr.,* 1980, **200**, 153.
22. Owa, T., Masujima, T., Yoshida, H., and Imai, H., *Bunseki Kagaku,* 1984, **33**, 568.
23. Abbott, R. W., Townshend, A., and Gill, R., *Analyst,* 1986, **111**, 635.
24. Alwarthan, A. A., and Townshend, A., *Anal. Chim. Acta,* 1986, **185**, 329.
25. Koukli, I. I., Sarantonis, E. G., and Calokerinos, A. C., *Analyst,* 1988, **113**, 603.

Paper 8/02370K
Received June 14th, 1988
Accepted January 31st, 1989

Flow Injection Spectrophotometric Determination of Selenium Based on the Catalysed Reduction of Toluidine Blue in the Presence of Sulphide Ion

Carmen Martinez-Lozano, Tomás Pérez-Ruiz, Virginia Tomás and Concepción Abellán
Department of Analytical Chemistry, Faculty of Sciences, University of Murcia, Murcia, Spain

The flow injection spectrophotometric determination of selenium is described based on its catalytic effect on the reduction of Toluidine Blue by sodium sulphide. After optimisation of the measuring conditions the detection limit is 0.08 μg of selenium(IV) and the linear range is 0.2–2 μg (80-μl injections). The method is suitable for routine analysis; about 35 samples can be injected per hour. The procedure was applied to the determination of selenium in ores and pharmaceutical preparations.

Keywords: *Selenium determination; flow injection; catalytic analysis; Toluidine Blue - sulphide ion reaction*

As the toxicological and physiological importance of selenium has become more evident, there has been an increasing interest in the determination of this essential element.[1,2] The method most commonly used is based on the spectrophotometric or fluorimetric measurement of piazselenol, which is formed when selenium(IV) reacts with aromatic *o*-diamines.[3,4] Although these methods offer excellent sensitivity and specificity, the procedures are lengthy and often require careful control of pH.

Catalytic assays have also been applied. Hence, Kawashima and Tanaka[5] have determined selenium by the catalytic reduction of 1,4,6,11-tetraazanaphthacene with hypophosphorous acid; however, this method suffers from non-linear calibration. A method based on the Landolt reaction, *viz.*, the chlorate - chloride - hydrazine sulphate system, has been reported[6] and methods based on the oxidative coupling reaction of *p*-hydrazinobenzenesulphonic acid with 1-naphthylamine or *m*-phenylenediamine have been proposed.[7,8] The catalytic effect of selenium on the reduction of the Tetranitro Blue Tetrazolium ion by dithiothreitol has also been used.[9]

The reduction of Methylene Blue by sulphide ion, enhanced by elemental selenium, has been adopted as a selective and sensitive method for the detection of selenium.[10] The reaction was later developed for the determination of low levels of selenium.[11–13]

Few automatic flow techniques have been used for the determination of selenium and to date only three methods have been described that use flow injection (FI). Two of these methods employ FI combined with hydride generation atomic absorption spectrometry.[14,15] The other method uses a molecular optical technique in conjunction with FI based on the Landolt reaction.[16]

The reduction of Toluidine Blue (TB) by sulphide ion catalysed by selenium has been utilised as a sensitive and selective method for selenium.[17] In this paper, a procedure for the rapid and selective determination of selenium, involving a simple FI technique, is described. The method is based on previous studies of the TB - sulphide ion reaction.[17]

Experimental

Reagents

All chemicals used were of analytical-reagent grade and were used without further purification. Doubly distilled water was used throughout.

Selenite stock solution, 500 mg l^{-1}. Prepared by dissolving $Na_2SeO_3.5H_2O$ (Merck), previously dried, in water. Working standard solutions were prepared by appropriate dilution with water.

Alkaline sulphide solution (*ca.* 0.1 M). Prepared by dissolving 2.40 g of sodium sulphide, 2.40 g of sodium sulphite and 4 g of sodium hydroxide in 100 ml of water. This solution must be prepared daily.

Barium disodium ethylenediaminetetraacetate, 5×10^{-2} M. Prepared by dissolving the product (Merck) in water or by mixing equivalent amounts of barium carbonate and disodium dihydrogen ethylenediaminetetraacetate, dissolving in water and filtering if necessary.

Formaldehyde solution, 4%. Prepared by mixing 20 ml of formaldehyde (36–38%) with 180 ml of water.

Toluidine Blue O (CI 52040) *solution*, 30 mg l^{-1}. Prepared by dissolving the product (Merck) in water.

Alkaline sulphide solution (5×10^{-3} M) *containing barium disodium ethylenediaminetetraacetate* (10^{-2} M) *and formaldehyde* (4%). Prepared by mixing 10 ml of 0.1 M alkaline sulphide solution, 40 ml of 5×10^{-2} M barium disodium ethylenediaminetetraacetate solution, 20 ml of formaldehyde and 130 ml of water.

Apparatus

A Pye Unicam Model SP8-200 recording spectrophotometer, a Gilson Minipuls HP4 peristaltic pump, an Omnifit injection valve and a Helma 18-μl flow cell were used. Teflon tubing of 0.5 mm i.d. was used for the mixing coil and for connections.

Manifold

The FI configuration used is outlined in Fig 1; it consists of three pump lines. Toluidine Blue solution and alkaline sulphide solution containing barium disodium ethylenediaminetetraacetate (Na_2BaY) and formaldehyde are pumped at a

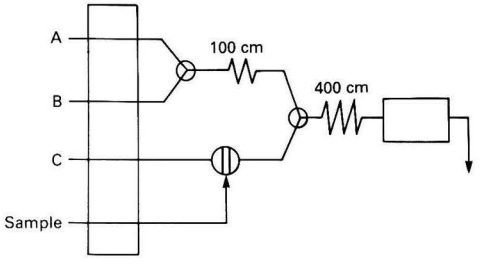

Fig. 1. Schematic diagram of the FI system. A, Toluidine Blue (30 mg l^{-1}); B, alkaline sodium sulphide (5×10^{-3} M) containing barium disodium ethylenediaminetetraacetate (10^{-2} M) and formaldehyde (4%); and C, formaldehyde (4%)

flow-rate of 0.74 ml min^{-1} and merge at a Y-piece. The mixing of the two streams is effected in a coil (100 cm). The sample solution is introduced with the aid of an injection valve with an 80-μl loop. The sample itself is introduced in a carrier consisting of 4% formaldehyde solution. The sampling valve is connected to a second Y-piece, where the carrier stream merges with the combined TB - alkaline sulphide stream. The reaction coil (400 cm) is submerged in a water-bath, the temperature of which is adjustable. A timer synchronised to the injection system allows the flow to be stopped for a given period of time. All three FI reagent solutions must be deaerated by bubbling nitrogen through them.

Recommended Procedure

A 30 mg l^{-1} TB solution and 5×10^{-3} M alkaline sulphide solution containing 10^{-2} M barium disodium ethylenediaminetetraacetate and 4% formaldehyde are each pumped at a flow-rate of 0.74 ml min^{-1}. An 80-μl sample volume containing between 0.3 and 2 μg of selenium is injected into the carrier (4% formaldehyde), which is also pumped at a flow-rate of 0.74 ml min^{-1}. The timer is programmed so that after 30 s the flow stops for 30 s and then the pump starts again. The absorbance of TB ($\lambda_{max.}$ = 620 nm) is measured and recorded.

Determination of Selenium in Ores

The dried sample (0.5–2 g) is digested with HCl and HNO_3. Under these conditions, selenium is converted into selenite. If necessary, cationic species are removed using an Amberlite IR-120 resin.

Determination of Selenium in Pharmaceutical Preparations

The sample is treated with concentrated HCl and heated nearly to dryness. Concentrated HNO_3 is added and the mixture heated nearly to dryness. After cooling, the pH is adjusted to about 6–8 with sodium hydroxide solution and the solution is diluted to volume with water in a calibrated flask.

Results and Discussion

The reaction between TB and sulphide ion occurs according to the equation

$$2TB + S^{2-} + 2H_2O \rightarrow 2HTB + 2HO^- + S$$

Selenium catalyses this reaction. The accelerating effect of selenium has been explained by the fact that in the presence of this element $[SSe]^{2-}$ ions are formed, which react much faster than sulphide ions. The selenium liberated again reacts with sulphide ion.[17,18] The reaction can be monitored spectrophotometrically, because the reduced TB (HTB) is colourless.

Effect of Chemical Reaction Variables

Previous studies on the selenium-catalysed reduction of TB with sulphide ion[17] have shown that the optimum pH range is between 9.6 and 11.5.

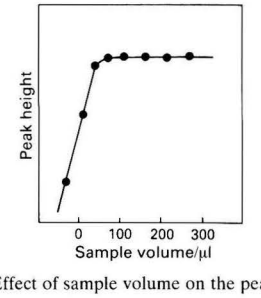

Fig. 2. Effect of sample volume on the peak height

The influence of the concentrations of TB and sulphide ion was also investigated. The best results were obtained at reagent concentrations of about 30 mg l^{-1} for TB and 5×10^{-3} M for sulphide ion.

The deleterious effect caused by the formation of polysulphides was overcome by the addition of sodium sulphite to form thiosulphate which, similar to sulphite, does not interfere with the reduction of TB.

The reduction of TB by sodium sulphide is too fast to detect the catalytic effect of selenium satisfactorily. The uncatalysed reaction was arrested by the addition of a water-miscible organic solvent. It was found that the presence of 4% formaldehyde in the reaction mixture caused a marked decrease in the rate of the uncatalysed reaction with little or no effect on the catalysed reaction rate.[17]

Increasing the temperature caused an increase in the rate of both the catalysed and uncatalysed reactions. A temperature of 30 °C was chosen as the most suitable.

The selectivity of the method was greatly improved in the presence of EDTA by complexation of the interfering ions. As a photochemical reduction of the thiazine dyes by EDTA also occurred,[19–21] it was decided to carry out the reaction in the presence of Ba^{II} - EDTA. In this situation the photochemical reaction does not take place because EDTA is forming a complex. On the other hand, the low formation constant of the Ba^{II} - EDTA complex permitted the complexation of most of the interfering ions through a displacement reaction.

The potential of the TB_{ox} - TB_{red} couple decreases with increasing pH.[21,22] In alkaline medium oxygen can oxidise HTB (colourless) to TB (blue) with a concomitant decrease in sensitivity. A thorough deaeration of the reaction mixture, by bubbling nitrogen through it, is recommended.[17]

Influence of Flow Injection Variables

Volume of sample

In flow injection measurements, the magnitude of the signal can generally be increased by increasing the injected sample

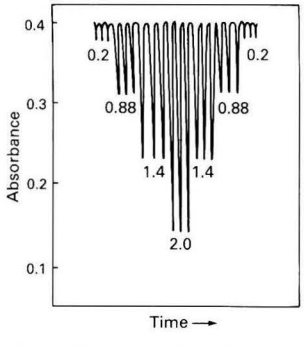

Fig. 3. Typical recording for the determination of selenium. The numbers on the peaks are micrograms of selenium injected

Table 1. Interference studies (0.5 μg of selenium)

Ion	Tolerated ratio of foreign ion to selenium
NO_3^-, Cl^-, $C_2H_3O_2^-$, PO_4^{3-}, CO_3^{2-}, F^-, MoO_4^{2-}, WO_4^{2-}, VO_3^-, AsO_4^{3-}, Mg^{2+}, Ca^{2+}, Sr^{2+}, Be^{2+}, Al^{3+}, Fe^{3+}, Cr^{3+}, TeO_3^{2-}, Ce^{3+}, Pb^{2+}	200*
Zn^{2+}, Cd^{2+}, Ni^{2+}	150
Mn^{2+}, Bi^{3+}, Hg^{2+}, Co^{2+}	100
Ag^+, Cu^{2+}	10

* Largest amount tested.

volume, the limiting factor being the degree of attainment of equilibrium. For the manifold used, this relationship is shown in Fig. 2. Above a sample volume of 80 μl, there is only a slight increase in the peak height; therefore, this sample volume can be considered to be the optimum.

Flow-rate of reactants and length of reaction tube

In the application of any catalytic kinetic reaction, the change in the absorbance depends on the residence time of the sample zone in the system, *i.e.*, on the flow-rate and the tube length. The effect of the flow-rate on peak height was studied over the range 0.4–1.8 ml min^{-1} in each stream. The lower flow-rates gave higher peaks, but at 0.4 ml min^{-1} the peak-height reproducibility was poor and the peaks broadened leading to lower sample throughput. The decrease in sensitivity was significant at a flow-rate of 1.0 ml min^{-1}, hence a flow-rate of 0.74 ml min^{-1} was selected as the best compromise between the conflicting demands of reproducibility, sensitivity and sample throughput.

Reaction coils of 1–6 m in length were tested. The peaks became higher as the length of the coil was increased from 1 to 4 m, but with longer coils the peak heights decreased. With the 4-m reaction coil and a flow-rate of 0.74 ml min^{-1}, the peak height increased if the pump was stopped when the sample plug was located in the reaction coil. A stop-time of about 30 s was sufficient to produce the maximum peak height.

Determination of Selenium

Typical peaks for the injection of 0.2–2 μg of selenium, obtained under the optimised conditions, are shown in Fig. 3. The linear plot of peak height *versus* concentration had a correlation coefficient of 0.9993. The repeatability of the method is good; the relative standard deviation (RSD) for 11 replicate injections of a 0.56-μg sample was 0.011%. The detection limit was calculated by comparing the magnitude of the signal for the analyte with the noise level, caused mainly by the uncatalysed reaction and pulsations of the peristaltic pump. For a signal to noise ratio of 2, the detection limit was 0.08 μg of Se. The sampling rate was about 35 samples per hour.

Table 2. Determination of selenium in ores

Sample	Amount found/μg g^{-1} FI method*	Piazselenol method†
Ore 1	217 ± 0.7	218
Ore 2	159 ± 0.8	158

* Average of four determinations ± SD.
† Average of two determinations.

Table 3. Determination of selenium in pharmaceutical preparations

Sample* (Source)	Amount found/g FI method†	Piazselenol method‡
Sebum selen (Llorente)	0.022 ± 0.005	0.024
Bioselenium (Uriach)	2.52 ± 0.06	2.51
Abbotselsun (Abbot)	2.42 ± 0.04	2.44
Caspiselenium (Kin)	2.40 ± 0.06	2.48

* Composition of samples. Sebum selen: selenium sulphide 0.025 g; benzalkonium chloride 0.003 g; and excipient up to 1 g. Bioselenium: selenium sulphide 2.5 g; and excipient up to 100 g. Abbotselsun: selenium sulphide 2.5 g; and excipient up to 100 g. Caspiselenium: selenium sulphide 2.5 g; and excipient up to 100 g.
† Average of four determinations ± SD.
‡ Average of two determinations.

Table 4. Recovery data for the determination of selenium in pharmaceutical preparations

Sample	Selenium in sample/mg g^{-1}	Selenium added/mg g^{-1}	Recovery, %
Sebum selen	22	10	99.3
Bioselenium	25	10	99.8
Abbotselsun	24	20	100.4
Caspiselenium	24	20	99.1

Interferences

Because of the reactivity of sulphide ion towards many cations, it was decided to use EDTA as a general masking agent. In order to eliminate the photochemical reaction between TB and EDTA,[20,21] the Na_2BaY complex was added to the alkaline sulphide solution. Table 1 lists the ions that were examined as potential interferents using the recommended procedure. An ion was considered not to interfere if it caused a variation in the peak height of selenium of less than 2%.

Applications

As examples of the application of the method to routine analysis, selenium was determined in ores and pharmaceutical preparations. Tables 2–4 show the results obtained.

This work was supported by DGICYT (project PB87-0053).

References

1. Robberecht, H., and van Grieken, R., *Talanta*, 1982, **29**, 823.
2. Robberecht, H., and Deelstra, H., *Talanta*, 1984, **31**, 497.
3. Hoste, J., and Gillis, J., *Anal. Chim. Acta*, 1958, **2**, 402.
4. Parker, C. A., and Harvey, L. G., *Analyst*, 1962, **87**, 558.
5. Kawashina, T., and Tanaka, M., *Anal. Chim. Acta*, 1968, **40**, 137.
6. Bognar, J., and Sarosi, S., *Mikrochim. Acta*, 1969, 361.
7. Kawashina, T., Nakano, S., and Tanaka, M., *Anal. Chim. Acta*, 1970, **49**, 443.
8. Kawashina, T., Kai, J., and Takashina, S., *Anal. Chim. Acta*, 1977, **89**, 65.
9. Hawkes, W., *Anal. Chim. Acta*, 1986, **183**, 197.
10. Feigl, F., and West, P. W., *Anal. Chem.*, 1947, **19**, 351.
11. West, P. W., and Ramakrishna, T., *Anal. Chem.*, 1968, **40**, 966.
12. Mesman, B. B., and Doppelmayer, H., *Anal. Chem.*, 1971, **43**, 1346.
13. Grases, F., Genestar, G., and Forteza, R., *Int. J. Environ. Anal. Chem.*, 1986, **23**, 321.
14. Yamamoto, M., Yasuda, M., and Yamamoto, Y., *Anal. Chem.*, 1985, **57**, 1382.
15. Chan, C. C. Y., *Anal. Chem.*, 1985, **57**, 1482.
16. Linares, P., Luque de Castro, M. D., and Valcárcel, M., *Analyst*, 1986, **111**, 1405.
17. Pérez-Ruiz, T., Martinez-Lozano, C., and Hernández, M., *An. Univ. Murcia*, 1982, **39**, 213.
18. Feigl, F., and Anger, V., "Spot Tests in Inorganic Analysis," Elsevier, Amsterdam, 1972, pp. 409–414.
19. Oster, G., and Watherspoon, N., *J. Am. Chem. Soc.*, 1957, **79**, 4936.
20. Faure, J., and Joussot-Dubien, J., *J. Chim. Phys.*, 1966, **63**, 621.
21. Sierra, F., Sánchez-Pedreño, C., Pérez-Ruiz, T., and Martinez-Lozano, C., *An. Quím.*, 1974, **70**, 595.
22. Bishop, E., "Indicators," Pergamon Press, New York, 1972, pp. 503–509.

Paper 8/04280B
Received October 27th 1988
Accepted January 17th, 1989

Spectrophotometric Determination of Oxytetracycline in Pharmaceutical Preparations Using Sodium Tungstate as Analytical Reagent

Milena Jelikić-Stankov and Dragan Veselinović
Institute of Analytical Chemistry, Faculty of Pharmacy, Belgrade, and Institute of Physical Chemistry, Faculty of Science, Belgrade, University of Belgrade, Yugoslavia

The formation of a complex between oxytetracycline (H_3OTC) and tungstate ion was studied in the pH range 3.0–8.0, in aqueous solution, at room temperature. Using the optimum conditions for complex formation a spectrophotometric method for the assay of H_3OTC in the concentration range 4.9–34.9 μg ml^{-1} is proposed. The detection limit of the method is 2.5 μg ml^{-1} of H_3OTC. The coefficient of variation is within the range 0.60–1.29%. The proposed method is simple and sensitive and was applied to the determination of H_3OTC in pharmaceutical preparations.

Keywords: *Oxytetracycline; sodium tungstate; spectrophotometry; pharmaceutical preparations; Geomycin capsules*

Oxytetracycline (H_3OTC) belongs to a group of tetracycline antibiotics that are characterised by the formation of stable complexes with many metals.[1,2] In addition to microbiological methods for the assay of tetracycline and its analogues, there are numerous chemical methods based on the formation of complexes with different metals.[3–7] In previous papers we studied the complexation reactions of tetracycline and doxycycline with tungstate and molybdate ions by using acidimetric, conductimetric and spectrophotometric methods.[8,9] The data reported so far have been for the application of spectrophotometric methods to the assay of tetracycline antibiotics; these methods are based on colour-forming reactions between the antibiotics and tungstate and molybdate ions,[10–12] but at elevated temperatures and in buffered solutions. The aim of this work was to establish the composition and the stability constant of the H_3OTC - WO_4^{2-} complex and to develop conditions for the application of this complexation reaction to the spectrophotometric determination of H_3OTC in pharmaceutical preparations.

Experimental

Apparatus

Spectra and absorbance measurements were recorded on a Carl Zeiss Jena Specord M-40 and a Pye Unicam SP-6-500 spectrophotometer, using glass cells with a path length of 1 cm. The pH measurements were performed with a Radiometer PHM 62 pH meter (Copenhagen) which had been previously standardised using standard buffer solutions.

Reagents

Oxytetracycline dihydrate ($H_3OTC.2H_2O$) standard (Sigma).
Sodium tungstate, p.a. (Merck).
Geomycin capsules (Pliva, Zagreb) containing 250 mg of H_3OTC.
Nitric acid, p.a. (Merck).
Sodium hydroxide, p.a. (Merck).
Sodium nitrate, p.a. (Merck).

Solutions

A fresh H_3OTC (10^{-3} M) solution was prepared by dissolving an appropriate amount of the H_3OTC standard in doubly distilled water. A standard sodium tungstate (0.101 M) solution was obtained by dissolving sodium tungstate in water and standardising the solution gravimetrically.[13] The ionic strength of the solution was kept constant (μ = 0.1 M) by the addition of 1 M sodium nitrate solution.

For the analysis of Geomycin capsules, ten capsules were powdered and the amount of sample required for the preparation of a solution containing approximately 0.496 mg ml^{-1} of H_3OTC was weighed and dissolved in water. The solution obtained was filtered and diluted to 25 ml with water. The pH of the solution was adjusted using nitric acid and sodium hydroxide solution.

Procedure for Calibration Graph

Aliquots of the 1×10^{-3} M H_3OTC solution (0.1–0.7 ml) and of a 5×10^{-3} M sodium tungstate solution (2 ml) were pipetted into a 10-ml calibrated flask. After the addition of 1 M sodium nitrate solution (1 ml) the reaction mixture was diluted to 10 ml with water. The pH of the solutions thus obtained was 6.1 ± 0.5. After shaking the solutions, the absorbance was measured at 390 nm, using H_3OTC solution as the reference.

Preparation of Samples From Capsules

To a solution prepared from Geomycin capsules (0.1–0.3 ml), 5×10^{-3} M sodium tungstate (2 ml) and 1 M sodium nitrate (1 ml) solutions were added and the mixture was diluted to 10 ml with water. The absorbances of these solutions were measured at 400 nm against water, as at this wavelength H_3OTC does not absorb over the range of concentrations investigated.

Results and Discussion

Absorption Spectra

Sodium tungstate reacts with H_3OTC in aqueous solution in the pH range 3.0–8.0 to form a yellow complex. The absorption spectra of the complex, H_3OTC and sodium tungstate were recorded in the range 350–430 nm. The complex exhibits maximum absorbance at 390 nm (pH = 6.0; μ = 0.1 M) (Fig. 1). Absorbance measurements for the determination of the composition and the stability constant of the complex and for the assay of H_3OTC were carried out at 390 and 400 nm. As the absorbance of H_3OTC is negligible at 390 and 400 nm, and as sodium tungstate does not absorb at these wavelengths, all absorbance measurements were performed by using H_3OTC solution as the reference.

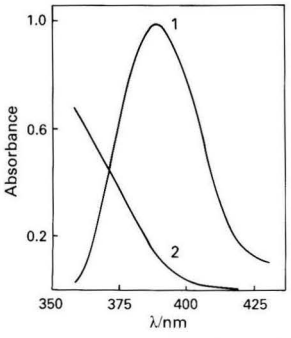

Fig. 1. Absorption spectra of 1, H_3OTC; and 2, the complex. $[H_3OTC] = 5 \times 10^{-5}$ M; $[Na_2WO_4] = 1 \times 10^{-3}$ M; pH = 6.0; and μ = 0.1 M

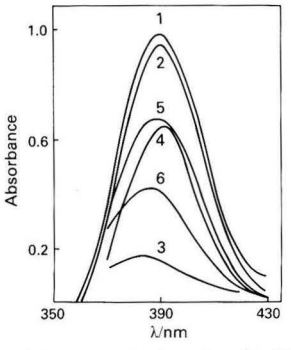

Fig. 2. Effect of pH on complex formation: $[H_3OTC] = 5 \times 10^{-5}$ M; $[Na_2WO_4] = 1 \times 10^{-3}$ M; pH = 6.0; and μ = 0.1 M. pH: 1, 6.0; 2, 7.0; 3, 3.0; 4, 8.0; 5, 5.0; and 6, 4.0

Effect of pH

Absorption spectra of mixtures of aqueous 5×10^{-5} M H_3OTC and 1×10^{-3} M sodium tungstate solutions were recorded in the pH range 3.0–8.0. At pH 3.0 the complex had an absorbance maximum at 382 nm; increasing the pH to 6.0 produced a slight shift of the absorbance maximum towards longer wavelengths; at pH 6.0 the absorbance of the complex reached a maximum ($\lambda_{max.}$ = 390 nm). On increasing the pH further, the absorbance was found to decrease, probably due to the dissociation of the complex followed by formation of sodium tungstate (Fig. 2).

Optimum Conditions for Complex Formation

From the previous section it can be concluded that the optimum pH for complex formation is 6.0. Therefore, this pH was used to determine the composition and the stability constant of the complex and for the assay of H_3OTC in Geomycin capsules. Investigations into the effect of the sodium tungstate concentration on complex formation showed that H_3OTC was converted quantitatively into the complex in the presence of a large excess of sodium tungstate, *i.e.*, increasing concentrations of sodium tungstate produced an increase in the absorbance of the complex up to a concentration of 1×10^{-3} M at which the absorbance of the complex reached a maximum. On increasing the sodium tungstate concentration further, the absorbance remained unchanged.

The colour of the complex developed instantaneously and the absorbance remained unchanged for 4 h (pH = 6.0).

The effect of the ionic strength (in the range 0.1–0.7 M) was found to be negligible.

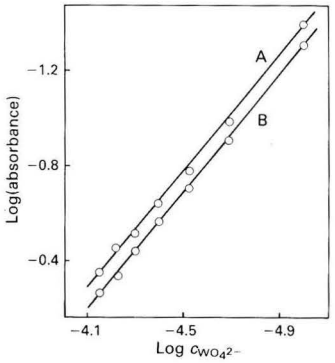

Fig. 3. Bent - French method (m): $[H_3OTC] = 6.5 \times 10^{-5}$ M; $[Na_2WO_4] = 1 \times 10^{-5}$–$7 \times 10^{-5}$ M; pH = 6.0; and μ = 0.1 M. A, 400 nm (m = 1.16); and B, 390 nm (m = 1.18)

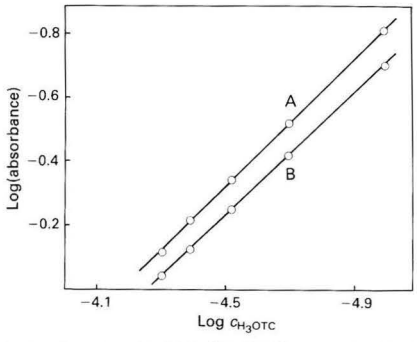

Fig. 4. Bent - French method (n): $[H_3OTC] = 1 \times 10^{-5}$–$5 \times 10^{-5}$ M; $[Na_2WO_4] = 1 \times 10^{-3}$ M; pH = 6.0; and μ = 0.1 M. A, 400 nm (n = 0.99); and B, 390 nm (n = 0.97)

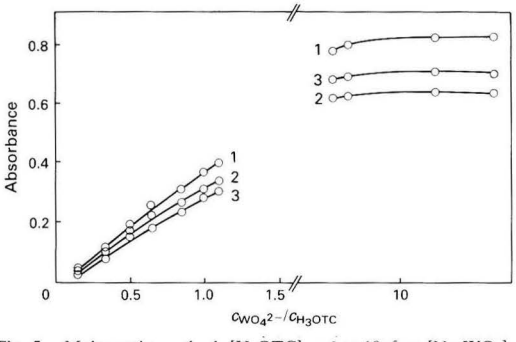

Fig. 5. Molar ratio method: $[H_3OTC] = 6 \times 10^{-5}$ M; $[Na_2WO_4] = 1 \times 10^{-5}$–$1 \times 10^{-3}$ M; pH = 6.0; and μ = 0.1 M. 1, 390; 2, 400; and 3, 380 nm

Composition of the Complex

The stoicheiometric ratio of H_3OTC to Na_2WO_4 in the complex was determined by the method of Bent and French.[14] At a constant (6×10^{-5} M) H_3OTC concentration and for various (1×10^{-5}–7×10^{-5} M) sodium tungstate concentrations, graphs having slopes (m) of 1.18 and 1.16 were obtained. For another series of solutions having a constant (1×10^{-3} M) sodium tungstate concentration and various (1×10^{-5}–5×10^{-5} M) H_3OTC concentrations, graphs with slopes (n) of 0.97 and 0.99 were obtained (pH = 6.0, μ = 0.1 M). These results point to the formation of a complex in which the stoicheiometric ratio of H_3OTC to Na_2WO_4 is 1 : 1 (Figs. 3 and 4). The application of the molar ratio method[15] to the

Table 1. Determination of the relative stability constant (β_1') of the H_3OTC - WO_4^{2-} complex. Conditions: pH = 6.0 ± 0.01; T = 20 ± 0.5 °C; and μ = 0.1 M ($NaNO_3$). n = 5

Molar ratio method (ε = 13 700 l mol^{-1} cm^{-1})—

Wavelength/nm	Log β_1'	SD*	CV,%†
390	3.87	0.011	0.28
400	3.79	0.027	0.71

Bent - French method (ε = 13 700 l mol^{-1} cm^{-1})—

Wavelength/nm	Log β_1'	SD*	CV,%†	Log β_1'	SD*	CV,%†
390	3.89	0.036	0.93	3.13	0.008	0.26
400	3.80	0.069	1.82	3.05	0.005	0.16

* SD = standard deviation.
† CV = coefficient of variation.

Table 2. Spectrophotometric determination of H_3OTC in Geomycin capsules (250 mg) (n = 10)

H_3OTC/mg ml^{-1}				
Expected	Found	SD, mg ml^{-1}	CV,%	H_3OTC in capsules, %
0.00497	0.00503	0.00003	0.60	101.21
0.00994	0.01010	0.00013	1.29	101.61
0.01491	0.01510	0.00014	0.93	101.27

determination of the composition of the complex showed that the absorbance increased, even after the formation of a complex of definite composition, until a large excess of sodium tungstate was present, after which the absorbance remained unchanged (Fig. 5).

Relative Stability Constant of the Complex

On the basis of acidimetric investigations, it has been shown that H_3OTC behaves similarly to other tetracycline analogues in the reaction with sodium tungstate.[16] In the course of the complexation reaction tungstate ion is converted into the corresponding oxide:

$$H_3OTC + Na_2WO_4 \rightleftharpoons Na_2(WO_3HOTC) + H_2O$$

As no data are reported in the literature for the equilibrium constant of the reaction

$$WO_4^{2-} + 2H^+ \rightleftharpoons WO_3 + H_2O$$

the calculated stability constant of the complex is relative and specific. The results obtained for the calculation of the stability constant of the complex by both the Bent - French and molar ratio methods are presented in Table 1. The calculated value for the molar absorptivity (ε) obtained by the molar ratio method was also used to calculate the stability constant by the Bent - French method. The results obtained for the stability constant by the application of both methods are in good agreement.

Quantification and Linearity of the Calibration Graph

Beer's law was tested at pH 6.0 (μ = 0.1 M). A linear dependence between the absorbance and the H_3OTC concentration was observed in the range 4.9–34.9 μg ml^{-1}. The regression equation obtained is y = 17 380x + 0.0275; the correlation coefficient (r) of 0.9991 (n = 10) indicates good linearity. The detection limit of the method is 2.5 μg ml^{-1} of H_3OTC.

The precision of the method was determined by using three different H_3OTC concentrations (Table 2). The results obtained show that the coefficient of variation is 0.60–1.29% for H_3OTC concentrations in the range 0.00497–0.01491 mg ml^{-1}.

Application to Capsules

The method was applied to the determination of the H_3OTC content in Geomycin capsules (Pliva). The results are presented in Table 2.

The proposed method is very simple and sensitive; it can be applied to the analysis of pure H_3OTC samples and to the assay of H_3OTC in pharmaceutical preparations and various dosage forms at room temperature, without using buffered solutions.

References

1. Albert, A., and Reese, C. W., *Nature (London)*, 1963, **172**, 201.
2. Albert, A., and Reese, C. W., *Nature (London)*, 1956, **177**, 433.
3. Hassan, S. M., Amer, M. M., and Ahmed, S. A., *Mikrochim. Acta*, 1984, **III**, 165.
4. Sultan, S. M., *Analyst*, 1986, **111**, 97.
5. Roushdi, I. M., Sebai, E., Ibrahim, B. Y. A., and Issa, A., *Pharmazie*, 1973, **28**, 236.
6. Vogt, H., *Arch. Pharmacol.*, 1956, **289**, 502.
7. Mahgoub, A. E. S., Khairy, E. M., and Kasem, A., *J. Pharm. Sci.*, 1974, **63**, 1451.
8. Jelikić, M., and Veselinović, D., *Vestn. Slov. Kem. Drus.*, 1986, **33**, 199.
9. Veselinović, D., and Jelikić, M., "Journees d'Electrochimie 1987, Abstracts and Author Index," Dijon, 1987, pp. 9–29.
10. Kakemi, K., Uno, T., and Samejima, M., *J. Pharm. Soc. Jpn.*, 1955, **75**, 194.
11. Kakemi, K., Uno, T., and Miyake, T., *J. Pharm. Soc. Jpn.*, 1955, **75**, 973.
12. Basilio, M., and Pasquole, P., *Anal. Lett.*, 1985, **18**(B15), 1865.
13. Vogel, A., "Quantitative Inorganic Analysis," Third Edition, Longmans, London, 1961, p. 439.
14. Bent, H., and French, C., *J. Am. Chem. Soc.*, 1941, **63**, 568.
15. Yoe, J., and Jones, A., *Ind. Eng. Chem. Anal. Ed.*, 1944, **16**, 111.
16. Veselinović, D., and Jelikić, M., "Journees d'Electrochimie 1985, Abstracts and Author Index," 28–31 May, Florence, 1985, pp. 8–22.

Paper 8/04035D
Received October 11th, 1988
Accepted January 23rd, 1989

Spectroscopic Investigation of the Equilibria of the Ionic Forms of Sinapic Acid

Bogdan Smyk and Regina Drabent
Institute of Physics and Food Chemistry, University of Agriculture and Technology, 10–957 Olsztyn-Kortowo, Poland

The equilibria of the ionic forms of sinapic acid (SA) in Britton - Robinson buffer at pH 1.9–11.5 and 297 K were studied using spectrophotometry and spectrofluorimetry. Three ionic forms of SA were found. Equilibrium constants and pK values were calculated. The absorption and fluorescence spectra for all the ionic forms of SA were determined.

Keywords: *Sinapic acid; ionic equilibria; absorption spectra; fluorescence spectra*

Phenolic compounds are common in the plant world, especially phenolic acids and their derivatives. They are present in most oilseeds, cereals and legume seeds.[1] Products obtained from these seeds are characterised by low organoleptic quality and nutritive value.[1–5] Sinapine (choline ester of sinapic acid) and sinapic acid (SA) seem to be the most important phenolic compounds[5–11] present in rapeseeds. Sinapic acid occurs mostly in a bound form, but it is usually liberated in the final stages of seed processing by acidic or alkaline hydrolysis. The amount of free acid that can be determined depends on the procedure used.[8,12–14] Sinapic acid has been the subject of many studies based on a variety of methods carried out under different physico-chemical conditions.

Combined methods are used to analyse phenolic compounds. For instance, gas chromatography is frequently used together with mass spectrometry,[12,14–17] UV - visible spectrophotometry[10,18] and fluorescence methods.[3,7,15,16]

Fluorescence methods have been used in many studies as they are more precise[18] and simpler than absorption methods. However, applications of these methods have usually been restricted to the identification of chromatographic spots only. Cinnamic acids (including SA) can occur in *cis* and *trans* isomeric forms and the presence of these two forms of SA has been confirmed by mass spectrometry.[9,12,13,15,19] The *trans* form is more stable; transformation to the *cis* form may be induced by UV radiation.[14,17–19]

There are few data in the literature on the spectral properties of cinnamic acids, and especially of SA under different physico-chemical conditions. Tzagoloff[20] and Austin and Wolff[21] presented partial spectral data for SA obtained from natural products in distilled water and in a buffer at pH 10. However, these data differ in location of bands in the electronic absorption spectrum: Austin and Wolff stated that the maximum of the absorption band was noted at $\lambda_{max.} = 355$ nm with a shoulder at 305 nm for a solution of pH 10, whereas Tzagoloff observed one band with $\lambda_{max.} = 305$ nm. Moreover, Austin and Wolff observed a considerable bathochromic shift as the pH of the solution increased, and this effect was found by other workers. Sabir *et al.*[3] stated that $\lambda_{max.}$ shifted from 318 to 340 nm when NaOH was added to SA solution, and with other compounds this shift was even more pronounced. Zeikel[22] found that the absorption band of *p*-hydroxycinnamic acid shifted 20–60 nm to longer wavelength as the pH increased, and stated that the absorption bands of these acids shifted more than those of the *ortho* and *meta* isomers. Rao[23] presented absorption data and pK values for cinnamic acid.

Notwithstanding the numerous papers on phenolic compounds, there is no comprehensive information in the literature on the physico-chemical properties and isomeric forms of phenolic acids. The aim of this work was to determine the effect of pH on SA and its spectral properties using molecular absorption and fluorescence spectroscopy.

Experimental and Results

Materials

Sinapic acid from Fluka, redistilled water and Britton - Robinson buffer (pH range 1.9–11.5) were used.

Methods

A 5×10^{-4} M solution of SA and buffer solutions with selected pH values were prepared. The SA solution was diluted 1 + 4 (*V*/*V*) with these buffers, giving a number of solutions with identical SA concentrations but different pH values. Each sample was prepared just before measurement. The buffer solution did not exhibit fluorescence over the entire excitation range.

Spectral Analyses

Analyses were carried out at 24 °C. The absorption spectra of SA solutions at known pH were measured with a Zeiss Specord M40 spectrophotometer in the range 235–450 nm.

Fluorescence spectra were measured using the set-up shown in Fig. 1. The sample (K) was excited at an angle to the surface of the fluorescence solution with monochromatic modulated light of frequency 62.3 Hz. Light emitted by the sample passed through the monochromator M_2 to the photomultiplier PM_2. The signal was then amplified and cleared by the selective nanovoltmeters V_2 and V_3 and transferred to the interface (I). Part of the excited light passed to the photomultiplier PM_1 as a reference beam, the signal being amplified by V_1, and transferred to the interface. From the interface both signals were transmitted to the microcomputer (MC). The spectra obtained were corrected and normalised to maximum. Corrections for reabsorption were also made.

Fluorescence spectra of SA solutions were measured for three excitation wavelengths ($\lambda_{ex.} = 300$, 333 and 365 nm). The excitation wavelength was selected so as to take into account changes in the absorption spectra at different pH values of the solutions.

Absorption Spectra

Absorption spectra of SA are presented for two pH ranges: 1.93–6.66 (Fig. 2) and 7.28–11.50 (Fig. 3). Fig. 2 shows that the spectrum shifted towards short wavelength as the pH increased and isosbestic points appeared. The absorption values at these points were constant and did not change with the pH of the solution. The wavelength corresponding to the maximum long-wavelength absorption, $\lambda^{a}_{max.}$, shifted from 322 nm at pH 1.93 to 305 nm at pH 6.66. A further increase in pH to 11.50 resulted in new bands and the old bands disappeared. Some of the absorption spectra in this pH range are shown in

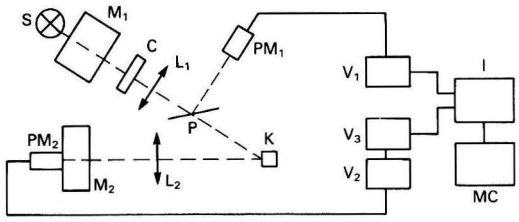

Fig. 1. Schematic diagram of the experimental set-up for the fluorescence measurements. S = Source light (450-W xenon lamp); M_1 = single monochromator (Opton M4QIII); C = chopper; L_1, L_2 = lenses; P = beam splitter; K = sample; M_2 = monochromator (SPM2, Carl Zeiss); PM_1 = photomultiplier (EMI 9558QB); PM_2 = photomultiplier (Hamamatsu R928); V_1, V_2 = lock-in amplifiers (232B); V_3 = nanoselective voltmeter; I = interface; and MC = microcomputer

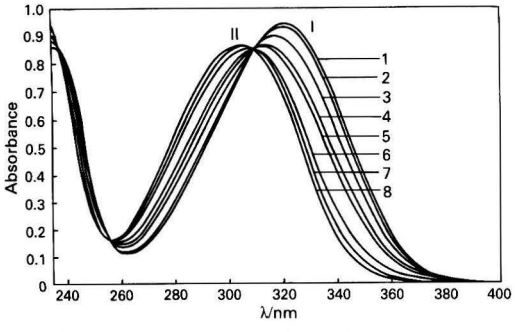

Fig. 2. Absorption spectra of SA in buffer. Path length, 0.5 cm. **I** = Undissociated form; **II** = form with carboxy group dissociated (see text). pH: 1, 1.93; 2, 3.22; 3, 4.00; 4, 4.25; 5, 4.69; 6, 5.42; 7, 5.87; and 8, 6.66

Fig. 3, where it can be seen that $\lambda^{a}_{max.}$ shifted from 305 nm at pH 7.28 to 355 nm at pH 11.50. Consequently, new isosbestic points were formed. Hence it can be stated that the ionic form remained in equilibrium with variation in the pH of the solution, other parameters remaining constant.[23] Particular ionic forms are denoted here by **I**, **II** and **III**. The spectra obtained revealed that forms **I** and **II** remained in equilibrium within the first pH range; form **I** was present at lower and form **II** at higher pH. Form **III** appeared in the second pH range, and remained in equilibrium with form **II**.

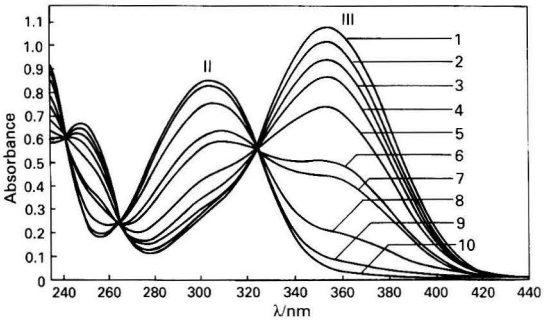

Fig. 3. Absorption spectra of SA in buffer. Path length, 0.5 cm. **II**, As in Fig. 2; **III**, form with carboxy and hydroxy groups dissociated. pH: 1, 11.50; 2, 10.98; 3, 10.37; 4, 10.00; 5, 9.40; 6, 9.10; 7, 9.00; 8, 8.50; 9, 7.80; and 10, 7.28

than 9 (see Fig. 3). On the other hand, an excitation wavelength of 300 nm resulted in fluorescence of form **II** in the middle range of pH values. In order to demonstrate the fluorescence of form **III**, excitation at 365 nm was also performed.

The fluorescence spectra were analysed taking into account changes in the pH of the solutions and the wavelength of excitation. Fig. 4 presents selected fluorescence spectra characterising the spectral changes of SA over the whole pH range studied. Samples of increasing pH excited at $\lambda_{ex.}$ = 333 nm showed maximum fluorescence at different wavelengths, $\lambda^{f}_{max.}$. The fluorescence spectra shifted first towards shorter and then towards longer wavelengths with increasing pH. Solutions of lower pH were characterised mainly by fluorescence of form **I** (Fig. 4, curve 1). At higher pH, fluorescence of form **II** appeared at shorter wavelengths (Fig. 4, curve 2). Further increases in pH resulted in shifts of the fluorescence spectra towards longer wavelengths (Fig. 4, curves 3 and 4). Form **III**, responsible for the long-wavelength fluorescence of SA, appeared in this pH range.

Fig. 5 presents fluorescence spectra for selected pH values and at different excitation wavelengths. A sample of pH 1.93, excited at two wavelengths ($\lambda_{ex.}$ = 300 and 333 nm), gave two overlapping emission spectra. This confirms an earlier suggestion (Fig. 2, curve 1) that only form **I** of SA was present in the solution. Fluorescence spectra of the samples of pH 4.25 excited at the same wavelengths revealed that two forms of SA were present, **I** and **II** [Fig. 5(*b*)]. At pH 8.50, form **III** was also present [Fig. 5(*c*) and Fig. 3]. This sample was excited at

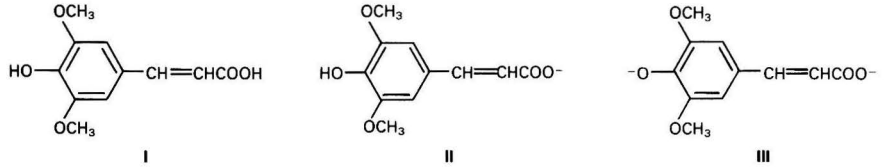

Fluorescence Spectra

When a compound that can undergo ionisation is analysed in an environment that induces dissociation, changes in the fluorescence spectra will usually parallel the changes in the absorption spectra[23] if the forms that appear are fluorescent.

Fluorescence spectra were measured for the same samples for which absorption spectra had been obtained. The excitation wavelength ($\lambda_{ex.}$) was selected so as to favour the fluorescence of particular ionic forms of SA. Hence, a wavelength of 333 nm (*i.e.*, within the absorption bands of form **I**) excited form **I** most when the pH of the solution was lower than 5. As regards solutions with higher pH, in which forms **II** and **III** were in equilibrium, a wavelength of 333 nm corresponded to strong absorption of form **III** at pH higher

three wavelengths ($\lambda_{ex.}$ = 300, 333 and 365 nm). Fig. 5(*c*) revealed a noticeable dependence between $\lambda_{ex.}$, the shape and $\lambda^{f}_{max.}$ of emission, the dependence being due to the existence of more than one emitting centre (in this instance forms **II** and **III**).

Determination of Equilibrium Constants

The structure of SA and the results of the spectral studies suggest that three different ionic forms (**I**, **II** and **III**) are present in the solutions. Moreover, it was assumed that within each pH range, SA could be treated as monoprotonic. An SA concentration of 10^{-4} M was so low that the following

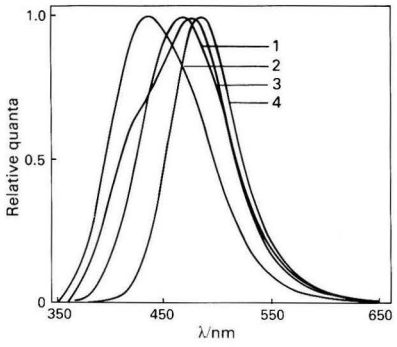

Fig. 4. Fluorescence spectra of SA in buffer. Wavelength of light excitation, $\lambda_{ex.}$ = 333 nm. pH: 1, 1.93; 2, 6.66; 3, 8.89; and 4, 11.50

equations for the apparent equilibrium constants could be used:

$$K_a^c = \frac{[H^+][S^-]}{[SH]} \quad \ldots \quad (1)$$

$$K_b^c = \frac{[H^+][S^{2-}]}{[S^-]} \quad \ldots \quad (1')$$

where [SH], $[S^-]$ and $[S^{2-}]$ are the concentrations of forms **I**, **II** and **III**, respectively.

The absorption spectra of SA obtained at different pH values were used to calculate the following linear relationships:

$$\frac{1}{K_a^c} - \frac{\varepsilon_S^-}{(\varepsilon - \varepsilon_{SH})[H^+]} = -\frac{\varepsilon}{(\varepsilon - \varepsilon_{SH})[H^+]} \quad \ldots \quad (2)$$

for forms **I** and **II** and

$$\frac{1}{K_b^c} - \frac{\varepsilon_S^{2-}}{(\varepsilon - \varepsilon_S^-)[H^+]} = -\frac{\varepsilon}{(\varepsilon - \varepsilon_S^-)[H^+]} \quad \ldots \quad (2')$$

for forms **II** and **III**, where ε, ε_{SH}, ε_S^- and ε_S^{2-} are the molar absorption coefficients of the solution and of forms **I**, **II** and **III**, respectively, for a given wavelength.

The molar absorption coefficient of form **I**, ε_{SH} (λ), was obtained experimentally. This represents the absorption spectrum of the solution with pH 1.93. Equations (2) and (2′) represent straight lines, the slopes of which and their intercepts with the ordinate axis can be used to determine ε_S^-, ε_S^{2-}, $1/K_a^c$ and $1/K_b^c$. These values were calculated using the least-squares method. Eleven curves were used in the calculations, from pH 1.93 (ε_{SH} known) to pH 5.87 and at about 30 wavelengths from 280 to 320 nm. All the results with errors caused by close positioning of the isosbestic points were eliminated. The concentration of form **II** was determined in each sample using the equation:

$$[S^-] = \frac{c \times 10^{pH - pK_a}}{1 + 10^{pH - pK_a}} \quad \ldots \quad (3)$$

where $c = 10^{-4}$ M is the initial concentration. The results are presented in Table 1.

To determine ε_S^- for the whole range of wavelengths (also at the isosbestic point), the equation

$$\varepsilon_S^-(\lambda) = \frac{c}{[S^-]}\left[\varepsilon(\lambda) - \varepsilon_{SH}(\lambda)\right] + \varepsilon_{SH}(\lambda) \quad \ldots \quad (4)$$

was used. In this way, the absorption spectrum of pure form **II** was obtained. In order to calculate the equilibrium constant for forms **II** and **III** (K_b^c), spectra for 16 samples were used, for pH from 7.23 to 11.50, and $\varepsilon_S^-(\lambda)$ obtained from the calculations. Calculations were performed similarly to those for forms **I** and **II** for 30 wavelengths from 330 to 365 nm. The absorption spectrum of form **III** [$\varepsilon_S^{2-}(\lambda)$] was also calculated using an equation similar to equation (4). All calculations were made on an 8-bit computer. Complete results are presented in Tables 1 and 2 and are shown in Fig. 6 for three forms of SA.

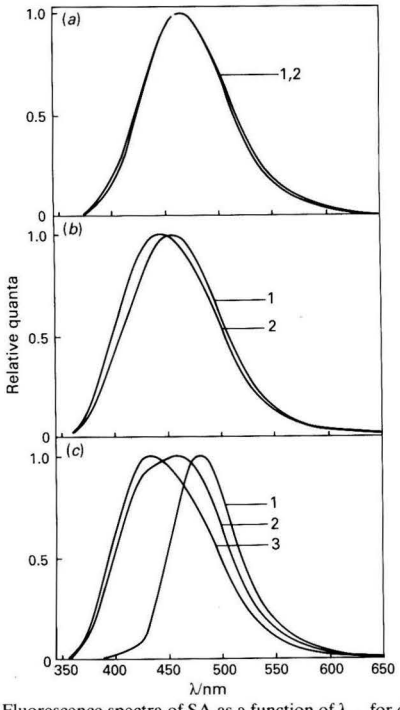

Fig. 5. Fluorescence spectra of SA as a function of $\lambda_{ex.}$ for different pH values. (*a*) pH 1.93; $\lambda_{ex.}$: 1, 300; and 2, 333 nm. (*b*) pH 4.25; $\lambda_{ex.}$: 1, 333; and 2, 300 nm. (*c*) pH 8.50; $\lambda_{ex.}$: 1, 365; 2, 333; and 3, 300 nm

Table 1. Calculated concentrations of two forms of SA

pH	$[S^-]/10^{-5}$ M	pH	$[S^{2-}]/10^{-5}$ M
1.93	0	7.28	0.115
2.98	0.310	7.80	0.374
3.22	0.527	8.23	0.946
3.44	0.845	8.50	1.63
3.79	1.71	8.68	2.27
4.00	2.51	8.89	3.23
4.25	3.73	9.00	3.75
4.69	6.21	9.19	4.88
4.93	7.40	9.40	6.07
5.42	8.98	9.70	7.55
5.87	9.61	10.37	9.35
6.26	9.84	10.98	9.83
6.66	9.94	11.50	9.95

Table 2. Data relating to the three forms of SA

Form	$K^c_{a,b}$/mol l^{-1}	$pK^c_{a,b}$	$\lambda^a_{max.}$/nm	$\varepsilon(\lambda^a_{max.})$/l mol^{-1} cm^{-1}	$\lambda^f_{max.}$/nm
I ..			322	18890 ± 50	463
II ..	$(3.35 \pm 0.10) \times 10^{-5}$	4.47 ± 0.01	305	17760 ± 50	432
III ..	$(6.16 \pm 0.30) \times 10^{-10}$	9.21 ± 0.03	355	22040 ± 150	479

Discussion

The results of these studies on the absorption and fluorescence spectra of SA in aqueous solutions in the pH range 1.93–11.50 showed that three ionic forms of this acid were present.

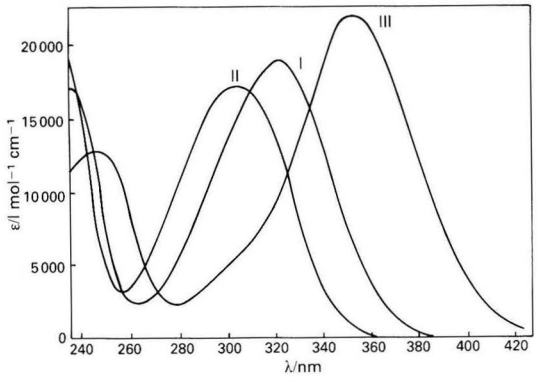

Fig. 6. Absorption spectra of ionic forms of SA. **I**, Measured; **II** and **III**, calculated

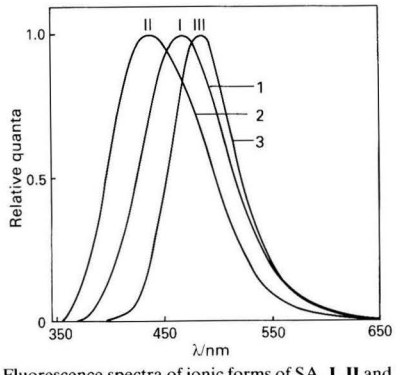

Fig. 7. Fluorescence spectra of ionic forms of SA. **I**, **II** and **III** are as in Fig. 6 (measured). 1, pH 1.93; $\lambda_{ex.}$ 333 nm. 2, pH 6.66; $\lambda_{ex.}$ 300 nm. 3, pH 11.50; $\lambda_{ex.}$ 365 nm

Calculations of the equilibrium constants of these forms (Table 2) indicate that $K_b^c/K_a^c \approx 1.8 \times 10^{-5}$. Hence, it is possible to distinguish two stages of the dissociation of SA in the pH range studied.

The results of calculations and changes in the absorption and fluorescence spectra [Fig. 5(*a*)] revealed that the ionic form **I** of SA (SH) was present at pH ≤2. In solutions of 2 < pH ≤ 6.6 two ionic forms were present in equilibrium, *viz.*, form **I** (SH) and form **II** (S^-). At pH > 6.6 form **III** (S^{2-}) appeared, being in equilibrium with form **II**. Absorption spectra of the ionic forms of SA were obtained experimentally (form **I**) or were calculated from the experimental data (forms **II** and **III**).

The results of studies on the fluorescence spectra of SA solutions of different pH suggest that all three ionic forms of SA are fluorescent. Separation of the fluorescence spectra by calculation was difficult because the fluorescence intensity was affected by deactivation of the energy of optical excitation and also by energy transfer between the ionic forms of SA. The fluorescence of particular forms may be partly eliminated by selection of a suitable wavelength of excitation.

Characteristic fluorescence spectra of SA are presented in Fig. 7. Curve 1 represents the fluorescence spectrum of form **I** (SH) with $\lambda^f_{max.}$ = 463 nm and curve 2 that of form **II** with $\lambda^f_{max.}$ = 432 nm. At pH 11.50 SA was present mostly in form **III** (see Table 1). The absorption spectrum of form **III** is shifted towards a longer wavelength so that the molar absorption coefficient at 365 nm of this form was higher than that of form **II** by one order of magnitude (Fig. 6). Also, the concentration of form **III** (9.95×10^{-5} M, Table 1) was higher than that of form **II** (5.1×10^{-7} M) by two orders of magnitude. It may be concluded that the fluorescence spectrum of a solution excited at $\lambda_{ex.}$ = 365 nm at pH 11.50 represents form **III** with $\lambda^f_{max.}$ = 479 nm (Fig. 7, curve 3). In conclusion, SA exists in three ionic forms (SH, S^- and S^{2-}) in the pH range studied (1.9–11.5), each having characteristic absorption and fluorescence spectra.

It should be noted that the differences in the absorption and fluorescence spectra of the ionic forms of SA may be of considerable importance in analytical studies based on fluorescence and absorption methods. Hence, quantitative studies on SA in buffer solutions should take into account the pH of these solutions. Moreover, when fluorescence methods are applied to chromatogram identification, great care is necessary.

The authors thank H. Kozłowska and R. Zadernowski of the Institute of Food Engineering and Biotechnology of the University of Agriculture and Technology, Olsztyn, for useful discussions. This work was supported by project CPBR 10.1.

References

1. Sosulski, F. W., *J. Am. Oil Chem. Soc.*, 1979, **56**, 711.
2. Kozłowska, H., Zadernowski, R., and Sosulski, F. W., *Nahrung*, 1983, **27**, 449.
3. Sabir, M. A., Sosulski, F. W., and Kernan, J. A., *J. Agric. Food Chem.*, 1974, **22**, 572.
4. Van Sumere, C. F., Albrecht, J., Dedonder, A., De Pooter, H., and Pé, I., *in* Harborne, J. B., and Van Sumere, C. F., *Editors*, "The Chemistry and Biochemistry of Plant Proteins," Academic Press, London, 1975, pp. 211–264.
5. Zadernowski, R., Rotkiewicz, D., Kozłowska, H., and Sosulski, F. W., *Acta Aliment. Pol.*, 1981, **7**, No. 3–4, 147.
6. Dąbrowski, K. J., and Sosulski, F. W., *J. Agric. Food Chem.*, 1984, **32**, 128.
7. Durkee, A. B., and Thivierge, P. A., *J. Food Sci.*, 1975, **40**, 820.
8. Kozłowska, H., Sabir, M. A., Sosulski, F. W., and Coxworth, E., *Can. Inst. Food Sci. Technol. J.*, 1975, **8**, 160.
9. Kozłowska, H., Rotkiewicz, D., and Zadernowski, R., *J. Am. Oil Chem. Soc.*, 1983, **60**, 1119.
10. Zadernowski, R., and Kozłoska, H., *Lebensm.-Wiss. Technol.*, 1983, **16**, 110.
11. Zadernowski, R., Kozłowska, H., and Łysakowski, H., *in* "Proceedings of the Sixth International Rapeseed Conference, Paris," Paris, 1983, pp. 1351–1355.
12. Dąbrowski, K. J., and Sosulski, F. W., *J. Agric. Food Chem.*, 1984, **32**, 123.
13. Fenton, T. W., Leung, J., and Clandinin, D. R., *J. Food Sci.*, 1980, **45**, 1702.
14. Krygier, K., Sosulski, F. W., and Hogge, L., *J. Agric. Food Chem.*, 1982, **30**, 334.
15. Krygier, K., Sosulski, F. W., and Hogge, L., *J. Agric. Food Chem.*, 1982, **30**, 330.
16. Schulz, J. M., and Herrman, K., *J. Chromatogr.*, 1980, **195**, 85.
17. Schulz, J. M., and Herrman, K., *J. Chromatogr.*, 1980, **195**, 95.
18. Zerr, W., and Funk, W., *in* "Proceedings of the Second International Symposium on Instrumental High-Performance Thin-Layer Chromatography, Interlaken," Interlaken, 1982, pp. 321–328.
19. Ribereau-Gayon, P., "Plant Phenolics," Oliver and Boyd, Edinburgh, 1972.
20. Tzagoloff, A., *Plant Physiol.*, 1963, **38**, 207.
21. Austin, F. L., and Wolff, I. A., *J. Agric. Food Chem.*, 1968, **16**, 132.
22. Zeikel, M. K., *in* Harborne, J. B., *Editor*, "Biochemistry of Phenolic Compounds," Academic Press, London and New York, 1964, pp. 34–66.
23. Rao, C. N. R., "Ultra-Violet and Visible Spectroscopy, Chemical Applications," Butterworths, London, 1975.

Paper 8/02724B
Received July 11th, 1988
Accepted November 3rd, 1988

Titrations in Non-aqueous Media

Part XVIII.* Observation of the Benzidine Rearrangement Reaction in Acetonitrile

Turgut Gündüz, Esma Kılıç and Adnan Kenar
Department of Chemistry, Faculty of Science, University of Ankara, Ankara, Turkey
S. Gül Öztaş
Graduate School of Natural and Applied Sciences, Department of Chemistry, University of Ankara, Ankara, Turkey

When titrated potentiometrically in acetonitrile 1 mol of phenylhydrazine reacts with 1 mol of perchloric acid, whereas 1 mol of 1,2-diphenylhydrazine reacts with 2 mol of perchloric acid. This is an indication that the benzidine rearrangement reaction occurs under these conditions. In order to support this view, the salts formed during the titration were filtered off and neturalised with diethylamine. The neutralised material was recrystallised from pure ethanol and was shown to be benzidine by infrared and UV - visible spectrophotometry. Benzidine is formed when 1,2-diphenylhydrazine undergoes the benzidine rearrangement reaction. Chromatographic methods were also used to explain, at least in part, the mechanism of the reaction. From the results obtained it was concluded that the benzidine rearrangement reaction was occurring and that it proceeded through a monoprotonated 1,2-diphenylhydrazine species rather than a diprotonated species as proposed by other workers. This is the first benzidine rearrangement reaction to be observed in a non-aqueous medium such as acetonitrile.

Keywords: *Benzidine rearrangement reaction; titration in acetonitrile; titration in non-aqueous media; potentiometric titration*

The titration of compounds in non-aqueous solvents such as acetonitrile, nitrobenzene, acetic acid and dimethyl sulphoxide can provide valuable information about these compounds, particularly organic compounds.[1-16] Recently, we have titrated a large number of compounds, both organic and inorganic, in non-aqueous solvents.[17-24] In this work, 1,2-diphenylhydrazine (hydrazobenzene) was titrated potentiometrically with perchloric acid in acetonitrile and a well shaped titration curve with one end-point corresponding to 2 mol of perchloric acid per mole of 1,2-diphenylhydrazine was obtained (Fig. 1). In an attempt to rationalise this observation, phenylhydrazine and benzidine were also subjected to the titration procedure (Fig. 1, curves B and C). The former gave a titration curve with one end-point corresponding to 1 mol of perchloric acid consumed, whereas the latter gave a titration curve with two end-points. Although the first of these was extremely poor each end-point corresponds to 1 mol of perchloric acid per mole of benzidine. This means that 1 mol of benzidine reacts with 2 mol of perchloric acid.

Experimental

All titrations were performed as described previously[18] unless stated otherwise.

Apparatus

The potentiometer used was identical with that described under Potentiometer and accessory in Part II.[18]

A Perkin-Elmer Model 337 spectrophotometer was used to record the IR spectra and a Hitachi Model 200-20 spectrophotometer for the UV - visible spectra.

Chemicals

Acetonitrile. Purchased from Merck [for synthesis (LAB) grade] and dried over calcium hydride overnight. The dried solvent was distilled in a tall column and the fraction distilling at 78 °C was collected.

Silica-gel coated plates. Purchased from Merck, DC, Aluefolien, Kieselgel 60 F_{254}.

1,2-*Diphenylhydrazine (hydrazobenzene).* Purchased from Fluka (puriss) and used after recrystallisation from light petroleum (b.p. 50–75 °C).

Benzidine. Purchased from Merck (analytical-reagent grade, DAB-6) and used without further purification.

Phenylhydrazine. Purchased from Schering (Berlin) (for analysis) and used without further purification.

Diethyl ether. Purchased from Merck and used after drying over sodium wire.

Diethylamine. Purchased from Merck and used without further purification.

Solutions prepared for potentiometric titrations with perchloric acid were approximately 0.001 M in acetonitrile. Solutions prepared for chromatographic experiments were approximately 0.02 M in acetonitrile.

Results and Discussion

As can be seen from Fig. 1, the curve obtained by titrating 1,2-diphenylhydrazine with perchloric acid shows only one end-point, corresponding to 2 mol of perchloric acid per mole of 1,2-diphenylhydrazine. It is extremely unlikely that 1,2-diphenylhydrazine would react with 2 mol of perchloric acid to give a diprotonated species when phenylhydrazine is known to react with only 1 mol of perchloric acid to give a monoprotonated species. This is because 1,2-diphenylhydrazine is more acidic than phenylhydrazine due to the strong electron withdrawing effect of the phenyl groups. The second phenyl group in the former compound makes the nitrogen atoms of the hydrazine moiety much more electron deficient. Hence 1,2-diphenylhydrazine cannot form a diprotonated species. The diprotonated species involved must, therefore, be a compound derived from 1,2-diphenylhydrazine and must have its two amino groups far apart from each other. This is because

* For Part XVII of this series see Gündüz, T., Kılıç, E., Atakol, O., and Köseoğlu, F., *Analyst*, 1989, **114**, 475.

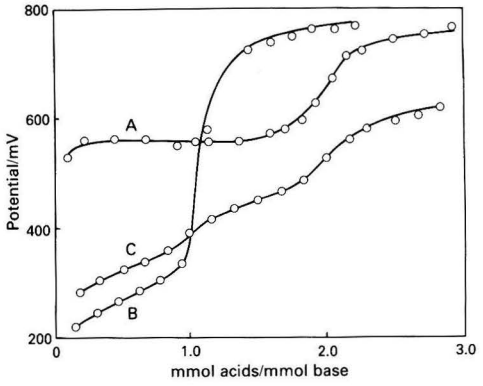

Fig. 1. Potentiometric titration curves of: A, 0.001 M 1,2-diphenylhydrazine; B, 0.001 M phenylhydrazine; and C, 0.001 M benzidine, titrated with 0.034 M perchloric acid in acetonitrile

strong electrical repulsions between two protonated sites that are close to each other prevent the hydrazine group from attracting two protons under mild conditions. It has been shown that two amino groups give only one end-point when there are at least four bond-lengths between them.[25,26] This suggests that the benzidine rearrangement reaction may be occurring under these conditions. The classical representation of this reaction is as follows:

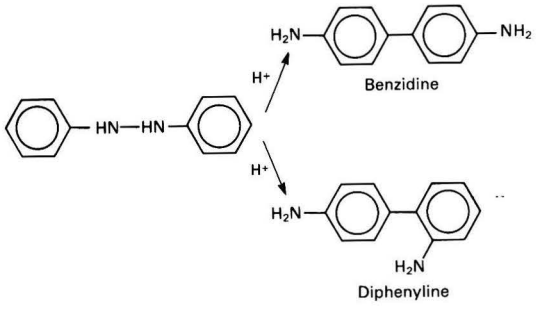

In addition to benzidine and diphenyline, semidines are also formed in trace amounts.[27,28] The major product of this reaction is benzidine (70%). Either benzidine or diphenyline can react with two protons to give a diprotonated species. In order to support the assumption that the benzidine rearrangement reaction is taking place, the following experiments were performed.

(A) Pure benzidine was titrated under the same conditions as for 1,2-diphenylhydrazine. A poorly-defined titration curve with two end-points, each corresponding to 1 mol of perchloric acid per mole of benzidine was obtained. The first end-point was extremely weak and the second fairly weak.

(B) A large excess of 1,2-diphenylhydrazine was titrated with perchloric acid in acetonitrile and the salts formed were filtered off and neutralised with diethylamine. The crude product obtained after neutralisation with diethylamine was recrystallised from ethanol and its melting-point was determined to be 125–126 °C. This compound was mixed with pure benzidine (standard) and its melting point was again found to be 125–126 °C. The thin-layer chromatograms of these two compounds were identical.

(C) The free diamine obtained during recrystallisation of the salts and a sample of pure benzidine had identical UV - visible spectra. The molar extinction coefficient at 288 nm was approximately 1.3×10^5 l mol^{-1} cm^{-1} for both compounds.

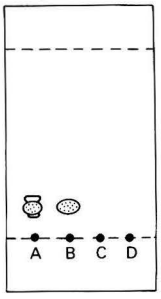

Fig. 2. Chromatograms of: A, neutralised solution; B, pure benzidine; C, perchloric acid; and D, amine. The chromatograms were obtained on a silica-gel coated plate with diethyl ether as eluent and detection at 254 and 366 nm. All the spots were purple under UV light

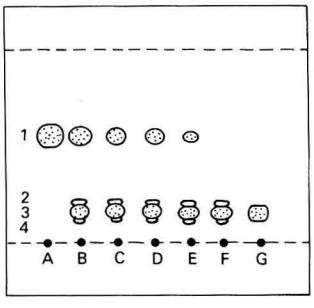

Fig. 3. Chromatograms of the solutions: A, pure 1,2-diphenylhydrazine; B, 20; C, 40; D, 60; E, 80; and F, 100% neutralised; and G, pure benzidinium perchlorate. From R_F values: 1, 1,2-diphenylhydrazine; 2, diphenyline; 3, benzidine; and 4, possibly semidines. All the spots were purple under UV light

Also, the IR spectra of both compounds were found to be identical.

(D) The thin-layer chromatographic behaviour of the onium perchlorates, pure benzidine, perchloric acid and diethylamine was also studied (Fig. 2). In order to obtain these chromatograms silica-gel coated plates were used with diethyl ether as eluent. The solutions were first applied to the plates as small spots which were then dried. Diethylamine was adsorbed on to each dry spot, except the diethylamine spot, using capillary tubing in order to free the amines from their perchlorate salts. Examination of the chromatograms showed that three spots were present in the neutralised solutions. One of these corresponded to benzidine, the second to diphenyline and the third, probably, to one of the semidines. This qualitative examination also revealed that the major product was benzidine and that the semidine was formed only in trace amounts. In experiments (A)–(C) the recrystallised reaction product was used; the results indicated that it contained only one compound and that this compound was benzidine. This means that ethanol is a good solvent for the recrystallisation of benzidine. The other compounds either dissolved more readily in ethanol or the amounts present in the crude product were very small. This observation strongly supports the results obtained from the chromatographic experiments. Experiment (D) showed that when 1,2-diphenylhydrazine was titrated with perchloric acid in acetonitrile, at least three compounds were formed: benzidine, diphenyline and a semidine.

All the experiments carried out so far have demonstrated that the reaction which occurs during the titration of 1,2-

diphenylhydrazine with perchloric acid is the benzidine rearrangement reaction. In order to explain the mechanism of the reaction, at least in part, chromatograms were obtained for a solution of pure 1,2-diphenylhydrazine, for 20, 40, 60, 80 and 100% neutralised solutions of 1,2-diphenylhydrazine and for a solution of benzidinium perchlorate. The chromatograms were obtained under the same conditions as described for experiment (D). In addition, the concentrations of the solutions used in these experiments were approximately equal (0.02 M) and the capillaries used were of the same diameter. The chromatograms obtained are shown in Fig. 3. The spots or compounds observed on these chromatograms can be designated by using the relevant letters and numbers given in Fig. 3. For example, in the upper row, the first spot can be designated as 1A and the second spot as 1B.

From a detailed examination of these chromatograms the following conclusions can be drawn.

(*a*) In the chromatogram of pure 1,2-diphenylhydrazine, there is only one spot or one compound. This indicates that the compound used was chromatographically pure; its R_F value was fairly large.

(*b*) In the chromatogram of the 20% neutralised solution of 1,2-diphenylhydrazine there are four spots or four compounds. The compound designated as 1B is 1,2-diphenylhydrazine, 2B is diphenyline, 3B is benzidine and 4B is probably a semidine. When the colours of spots 1A and 1B were compared, it was found that the colour of spot 1B was lighter than that of spot 1A. This means that a portion of the 1,2-diphenylhydrazine has undergone the benzidine rearrangement reaction to give benzidine, diphenyline and, probably, a semidine.

(*c*) In the chromatogram of the 40% neutralised solution of 1,2-diphenylhydrazine there are again four spots or four compounds. The R_F values of these compounds were identical with the R_F values of the compounds observed in the 20% neutralised solution. However, the colour of spot 1C was lighter than of spot 1B. On the other hand the colours of the spots designated 2C, 3C and 4C were darker than the colours of the spots designated 2B, 3B and 4B. Similarly, spots 2D, 3D and 4D were darker than spots 2C, 3C and 4C and spots 2F, 3F and 4F were also darker than spots 2E, 3E and 4E. In general, the spots in the bottom row of the plate darkened in going from left to right, whereas the spots in the upper row became lighter and could not be detected at the spot designated 1F. Moreover, the colour of spot 3F was almost identical with that of spot 3G. This shows that benzidine is the major component formed in the titration of 1,2-diphenylhydrazine with perchloric acid in acetonitrile. Data from these experiments demonstrated that the benzidine rearrangement reaction can proceed in acetonitrile and that the reaction proceeds proportionally with the amount of acid added. We believe that the benzidine rearrangement reaction in acetonitrile proceeds by a one-proton mechanism. Monoprotonated 1,2-diphenylhydrazine undergoes a rearrangement reaction to give a monoprotonated benzidine species. A second proton then reacts with the monoprotonated benzidine species rather than with the unprotonated 1,2-diphenylhydrazine molecule because of the more basic character of benzidine compared with 1,2-diphenylhydrazine.

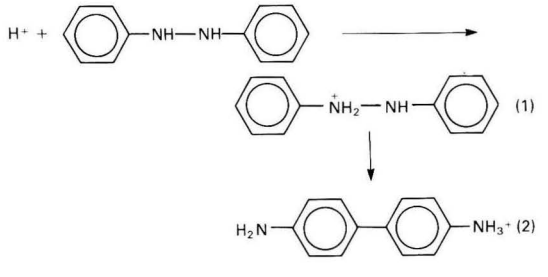

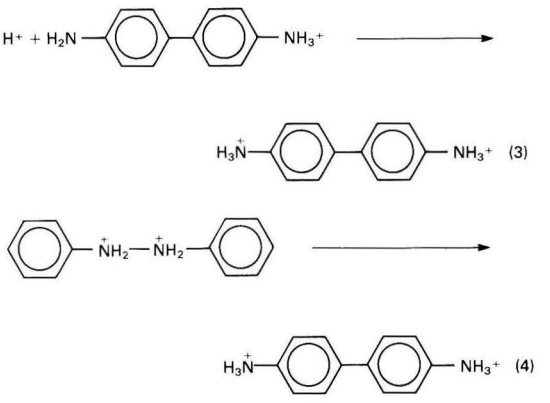

If the reaction were to proceed through a diprotonated 1,2-diphenylhydrazine species as proposed by other workers[27–31] until the half-neutralisation point was reached no benzidine would have been detected because formation of the monoprotonated 1,2-diphenylhydrazine species would be easier than formation of the diprotonated species. In fact, the presence of benzidine was detected chromatographically even with a 10% neutralisation of the 1,2-diphenylhydrazine. Very similar results were also obtained when tetrahydrofuran was used as the solvent.

Conclusions

The benzidine rearrangement reaction can proceed in a non-aqueous medium, and was observed when acetonitrile and tetrahydrofuran were used as the solvents for the titration of 1,2-diphenylhydrazine with perchloric acid.

The mechanism of the benzidine rearrangement reaction proceeds via monoprotonation of 1,2-diphenylhydrazine rather than diprotonation as proposed by other workers.

It is possible to show chromatographically that the benzidine rearrangement proceeds through a monoprotonated rather than a diprotonated 1,2-diphenylhydrazine species. This can be shown by running the chromatograms of 20, 40, 60, 80 and 100% neutralised solutions from the titration of 1,2-diphenylhydrazine with perchloric acid in acetonitrile or tetrahydrofuran.

References

1. Hall, N. F., and Conant, J. B., *J. Am. Chem. Soc.*, 1927, **49**, 3047.
2. Hall, N. F., *Chem. Rev.*, 1931, **8**, 191.
3. Fritz, J. S., *Anal. Chem.*, 1950, **22**, 578.
4. Fritz, J. S., *Anal. Chem.*, 1952, **24**, 674.
5. Fritz, J. S., and Fuldo, M. D., *Anal. Chem.*, 1953, **25**, 1837.
6. Lagowski, J. J., *Editor*, "The Chemistry of Non-aqueous solvents," Volumes I–IV, Academic Press, New York and London, 1966, 1967, 1970 and 1976.
7. Waddington, T. C., *Editor*, "Non-aqueous Solvent Systems," Academic Press, New York and London, 1965.
8. Huber, W., "Titrations in Non-aqueous solvents," Academic Press, New York and London, 1967.
9. Fritz, J. S., "Acid - Base Titrations in Non-aqueous Solvents," Allyn and Bacon, Boston, 1973.
10. Taft, R. W., *Prog. Phys. Org. Chem.*, 1983, **14**, 247.
11. Mucci, A., Domain, R., and Benoit, R. L., *Can. J. Chem.*, 1980, **58**, 953.
12. Streuli, C. A., *Anal. Chem.*, 1958, **30**, 997.
13. Streuli, C. A., *Anal. Chem.*, 1959, **31**, 1652.
14. Brown, H. C., *J. Am. Chem. Soc.*, 1945, **67**, 374.
15. Brown, H. C., *J. Am. Chem. Soc.*, 1945, **67**, 378.
16. Munson, M. S., *J. Am. Chem. Soc.*, 1965, **87**, 2332.
17. Kılıç, E., and Gündüz, T., *Analyst*, 1986, **111**, 949.

18. Gündüz, T., Gündüz, N., Kılıç, E., Kenar, A., and Çetinel, G., *Analyst*, 1986, **111**, 1099.
19. Gündüz, T., Gündüz, N., Kılıç, E., and Kenar, A., *Analyst*, 1986, **111**, 1103.
20. Gündüz, T., Gündüz. N., Kılıç, E., and Kenar, A., *Analyst*, 1986, **111**, 1345.
21. Gündüz, T., Kılıç, E., Ertüzün, V., and Çetinel, G., *Analyst*, 1986, **111**, 1439.
22. Gündüz, N., Gündüz, T., Hursthouse, M. B., Parkers, H. G., Shaw, L. S., Shaw, L. A., and Tüzün, M., *J. Chem. Soc., Perkin Trans. 2*, 1985, 899.
23. Gündüz, N., Gündüz, T., Kılıç, E., Oztaş, S. G., Tüzün, M., Shaw, L. S., and Shaw, R. A., *J. Chem. Soc., Dalton Trans.*, 1987, 925.
24. Gündüz, T., Kılıç, E., and Özkan, G., *Analyst*, 1988, **113**, 1017.
25. Gündüz, T., Gündüz, N., Kılıç, E., Kenar, A., and Atakol, O., *Analyst*, 1987, **112**, 1373.
26. Gündüz, T., Kılıç, E., Atakol, O., and Kenar, A., *Analyst*, 1987, **112**, 1735.
27. Beyer, H., and Walter, W., "Lehrbuch der Organischen Chemie," Auflage 18, S. Hirzel Verlag, Stuttgart, 1978, p. 490.
28. Bunton, C. A., and Rubin, R. J., *J. Am. Chem. Soc.*, 1976, **98**, 4236.
29. March, J., "Advanced Organic Chemistry," Wiley, New York, 1985, pp. 1034–1036.
30. Banthorge, D. V., Hughes, E. D., and Ingold, C. K., *J. Chem. Soc.*, 1964, 2864.
31. Nojima, M., Ando, T., and Tokuro, N., *J. Chem. Soc., Perkin Trans. 1*, 1976, 1504.

NOTE—References 17, 18, 19, 20, 21, 24, 25 and 26 are to Parts I, II, III, IV, V, XII, VII and IX of this series, respectively.

Paper 8/04414G
Received November 7th, 1988
Accepted January 5th, 1989

SHORT PAPERS

Separation and Determination of Inorganic Anions by High-performance Liquid Chromatography Using a Micellar Mobile Phase

Biswanath Maiti, Arvind P. Walvekar and T. S. Krishnamoorthy*
Analytical Chemistry Division, Bhabha Atomic Research Centre, Trombay, Bombay 400 085, India

The use of cetylpyridinium bromide, a cationic surfactant, added as a modifier to an aqueous acetonitrile mobile phase allowed good separation of the inorganic anions iodate, bromate, bromide, nitrite, nitrate, iodide and thiocyanate on a reversed-phase high-performance liquid chromatography column. Spectrophotometric detection at 222 nm was used for the identification and determination of the anions. The method was applied successfully to the determination of nitrite and nitrate in human saliva.

Keywords: *High-performance liquid chromatography; cationic surfactant; inorganic anions; human saliva*

Ionic surfactants have recently been used as mobile phase modifiers in order to effect the separation of inorganic ions and improve the partitioning characteristics of ionic solutes in reversed-phase liquid chromatography. Mullins and Kirkbright[1] have studied the separation of some inorganic anions using hexadecyltrimethylammonium chloride. Cassidy and Elchuk[2,3] have reported the determination of inorganic anions using tetrabutyl- and tetramethyl-ammonium salts on a stationary phase coated with cetylpyridinium chloride.

In this work the separation of iodate, nitrite, nitrate, iodide and thiocyanate on a reversed-phase column was studied using cetylpyridinium bromide (CPB) added as a modifier to the aqueous acetonitrile mobile phase. It was demonstrated that this cationic surfactant could be used to effect a good separation of inorganic anions on a reversed-phase high-performance liquid chromatography (HPLC) column. An attempt was also made to apply this technique to the determination of nitrite and nitrate in human saliva and iodide in common salt.

Experimental

Instrumentation

High-performance liquid chromatographic separations were carried out on a DuPont Model 8800 series instrument with a pump module equipped with a gradient controller, a Rheodyne 7125 valve injector, a DuPont Spectro 400 variable-wavelength UV detector and a 25 cm × 4.6 mm i.d. 5-μm particle size Zorbax octadecylsilane (ODS) (DuPont) column fitted with 2-μm removable stainless-steel frits. Retention times, peak heights and peak areas were measured using a recording integrator (Spectraphysics 4100).

Reagents and Solvents

Standard solutions of sodium or potassium nitrate, nitrite, iodate, iodide, bromate, bromide and chloride were prepared from AnalaR (BDH) or guaranteed reagent grade (Merck) chemicals. Sodium dihydrogenphosphate and sodium hydroxide were of guaranteed reagent grade and were supplied by Sarabhai Merck (India). Cetylpyridinium bromide was obtained from Fluka and was used as received.

* To whom correspondence should be addressed.

Acetonitrile. HPLC grade supplied by Spectrochem (India).

Water. De-ionised water was refluxed with alkaline $KMnO_4$ (AnalaR, BDH) and was doubly distilled in a quartz distillation apparatus.

Procedure

The aqueous mobile phases were prepared by dissolving appropriate amounts of the surfactant in a 10 mM aqueous solution of sodium dihydrogenphosphate. The pH of the solutions was then adjusted to the desired value with H_3PO_4 or NaOH.

The above aqueous solutions and acetonitrile were degassed each time before use in a DuPont series 8800 LC flotation de-gasser by evacuating the solvent reservoir to 0.63 bar or less for 15–20 min while stirring the solvent magnetically.

The composition of the mobile phase and the flow-rate were controlled by the gradient controller. An equilibration time of about 2 h or more was allowed prior to sample injection, in order to obtain reproducible retention times.

Results and Discussion

Separation of Anions

Surfactants have been added as modifiers to the mobile phase to improve the separation in reversed-phase liquid chromatography, but the exact role of surfactants is not yet understood. "Ion exchange," "ion-pair formation" and "ion interaction" are some of the mechanisms that have been postulated. The bulky hydrophobic group present in the surfactant may be contributing in some way to the improvement in the separation characteristics of the column. According to Bidlingmeyer *et al.*[4] the hydrophobic surfactant is assumed to be sorbed on the stationary phase as a primary layer with the counter ion in the secondary layer, thus establishing an electrical double layer. The primary layer is due to hydrophobic ion retention as a result of its hydrophobic centre producing a surface charge. The secondary diffused layer is composed of ions of opposite charge. The second equilibrium determines the selectivity between the ions in the diffused secondary layer and the analyte ions. Recently, the use of the tris(1,10-phenanthro-

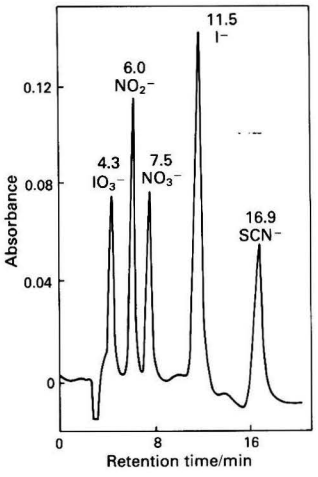

Fig. 1. Chromatogram of a synthetic mixture of anions. Conditions: column, Zorbax ODS; flow-rate, 1 ml min^{-1}; mobile phase, acetonitrile - water (35 + 65); CPB, 2×10^{-3} M; and phosphate buffer, 10 mM. Detection at 222 nm

Table 1. Separation and calibration data

Anion	Retention time/min	Detection limit/ng	Calibration range used/ng	Correlation coefficient
Iodate ..	4.3	25	250–400	0.998
Bromate ..	4.8	30	300–500	0.975
Bromide ..	5.9	35	400–600	0.995
Nitrite ..	6.0	8	100–250	0.990
Nitrate ..	7.5	19	200–350	1.008
Iodide ..	11.5	16	100–250	1.002
Thiocyanate ..	16.9	20	200–350	0.997

line)iron(III) ion as a mobile phase modifier for the separation of anions[5,6] has been reported. The separation mechanism operating in this type of ion-interaction chromatography has also been explained by the formation of an electrical double layer. However, a micellar mobile phase is different from an ion-pair forming mobile phase in the sense that the former is microscopically heterogeneous and the concentration of the surfactants is generally kept above the critical micellar concentration (CMC) (1×10^{-3} M). The concentration of CPB used was kept above the CMC in all the experiments.

Fig. 1 shows a typical chromatogram of a synthetic mixture of five different anions obtained with a mobile phase composition of acetonitrile - water (35 + 65) and at a CPB concentration of 2×10^{-3} M with 10 mM phosphate buffer. The detector was set at 222 nm, the optimum wavelength as determined from the UV spectra of the anions in the mobile phase. There is an initial dip in the chromatogram due to the inhomogeneity of the mobile phase caused by the injection of the aqueous sample. This was confirmed by injecting distilled water alone into the mobile phase. All the peaks are sharp and symmetrical and the retention times are reproducible to within 5%.

The separation characteristics of a mixture of these anions were studied using various mobile phase compositions ranging from acetonitrile - water (50 + 50) to acetonitrile - water (30 + 70). At higher acetonitrile concentrations (*e.g.*, 50%), good resolution between some of the anions, *e.g.*, nitrate and nitrite, was not obtained and the retention times were also shorter. A good base-line separation for all the anions was obtained when the mobile phase contained at least 63% water.

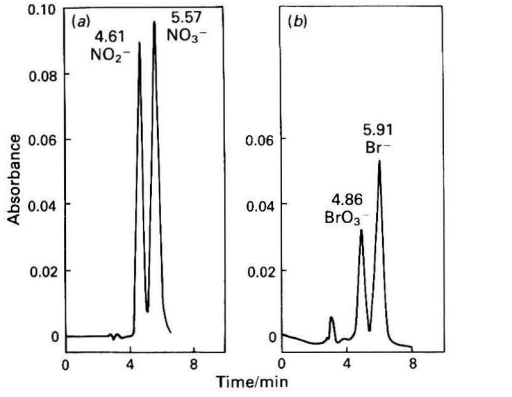

Fig. 2. Separation of (*a*) nitrate and nitrite; and (*b*) bromide and bromate. Conditions as in Fig. 1

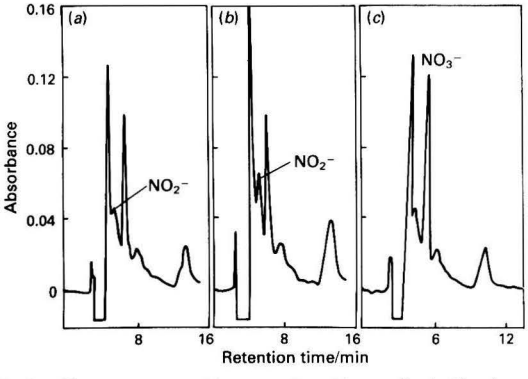

Fig. 3. Chromatograms of human saliva. (*a*) Unspiked; (*b*) spiked with nitrite; and (*c*) spiked with nitrate. Conditions as in Fig. 1

Any increase in the CPB concentration also had a similar effect and gave poor separation and shorter retention times. These could be attributed to an increase in the partial molar volume and the relative molecular mass of the micelle in the mobile phase. An increase in the micelle concentration would cause a reduction in the capacity factor and hence give poor resolution and shorter retention times. Although the resolution improved still further at higher water concentrations, the retention times also increased considerably, *e.g.*, the separation of these anions took more than 30 min when acetonitrile - water (30 + 70) was used as the mobile phase. Hence, a mobile phase of acetonitrile - water (35 + 65) was chosen as the optimum. A deviation of about ±2% from this composition can be tolerated without it affecting the separation to a significant extent. An increase in the pH of the mobile phase marginally increased the retention time of a given anion, whereas a change in the buffer ion (phosphate) concentration did not have a significant effect. A pH of 6.6 and 10 mM phosphate buffer concentration were maintained throughout this work. The order of retention of the anions on the column with CPB in the mobile phase was found to be as follows: $SCN^- > I^- > NO_3^- > NO_2^- > BrO_3^- > IO_3^-$, which is similar to the selectivity order generally found for a typical basic anion exchanger.

Table 1 summarises the experimental data. Five or six points were taken for calibration and the correlation coefficients for the least-squares lines were close to unity. Although the detection limits are much lower, a higher calibration range was used for the application described here. Between-day variations of about 15% in the detection limits, retention times

Table 2. Results of the analysis of saliva samples

Volunteer No.	Nitrite/ mg l^{-1}	Nitrate/ mg l^{-1}
1	8.9	49.0
2	6.0	30.0
3	6.0	37.5
4	6.2	34.5
5	4.0	27.0
6	3.0	18.0

and the slopes of the calibration graphs were observed. However, these variations were found to be less than 5% on any given day.

Analytical Applications

Fig. 2(*a*) and (*b*) shows the chromatograms of synthetic mixtures of nitrate and nitrite and bromate and bromide, respectively. These separations are normally difficult by conventional methods, but the use of CPB produced a good separation and allowed the quantification of these anions. The determination of nitrate and nitrite in various matrices is important because of the potentially deleterious effect of the latter. Nitrite reacts with amines and amides to form nitroso compounds, which are known to possess carcinogenic properties. In addition, nitrite exposure can lead to the development of methaemoglobinaemia in new-born babies. In general, food has a relatively higher nitrate than nitrite content, but the former can be converted to nitrite in the oral cavity and under certain conditions in the stomach. Trace amounts of nitrate are generally determined spectrophotometrically, *e.g.*, using chromotropic acid.[7] Nitrate and nitrite together or nitrate alone can be determined by diazotisation.[8] However, the simultaneous determination of nitrate and nitrite is difficult. We have applied this HPLC method successfully to the simultaneous determination of nitrate and nitrite in human saliva. Fig. 3(*a*) shows the chromatogram of a typical saliva sample recorded by injecting 20 μl of human saliva directly into the mobile phase. Fig. 3(*b*) and (*c*) shows the chromatograms of the same saliva sample spiked with a known amount of nitrite and nitrate, respectively. The enhancement of the peaks at 5.3 and 6.4 min after spiking the saliva with nitrite and nitrate, respectively, confirmed their identities. The nitrate and nitrite content could be obtained from a standard calibration graph or by the standard additions technique. The nitrate and nitrite contents in the saliva samples obtained from six different volunteers are given in Table 2. The values lie within the normal range for nitrite[9] (5–350 mg l^{-1}) and nitrate.

An attempt was also made to apply the method to the determination of iodide in commercial salt. Iodised common salt (20–40 p.p.m. of iodide) is often recommended for the treatment of goitre.[10] Owing to the broad matrix peak, small amounts of iodide, if present, could not easily be detected. The addition of about 20 p.p.m. of iodide to the common salt did not give a measurable peak. The absence of this peak confirmed the very low levels (below the recommended minimum) of iodide in the locally available common salt. However, direct quantification was not feasible. Even though the absorption of chloride ion at 222 nm is not significant, the very large excess of this ion results in an overloading of the column followed by gradual elution for a long period of time leading to the observed broad matrix peak.

References

1. Mullins, F. G. P., and Kirkbright, G. F., *Analyst*, 1984, **109**, 1217.
2. Cassidy, R. M., and Elchuk, S., *J. Chromatogr.*, 1983, **262**, 311.
3. Cassidy, R. M., and Elchuk, S., *J. Chromatogr. Sci.*, 1983, **21**, 454.
4. Bidlingmeyer, B. A., Deming, S. N., Price, W. P., Sachok, B., and Pelruesik, M., *J. Chromatogr.*, 1979, **186**, 419.
5. Rigas, P. G., and Pietrzyk, D. J., *Anal. Chem.*, 1986, **58**, 2226.
6. Rigas, P. G., and Pietrzyk, D. J., *Anal. Chem.*, 1987, **59**, 1388.
7. Fisher, P. L., Lbert, E. R., and Beckman, H. F., *Anal. Chem.*, 1958, **30**, 1972.
8. Sawicki, E., Stanley, T. W., Pfaff, J., and D'Amico, A., *Talanta*, 1963, **10**, 641.
9. Bos, P. M. J., van den Brandt, P. A., Wedel, M., and Ocktmizen, Th., *Food Chem. Toxicol.*, 1988, **26**, 93.
10. Underwood, E. J., "Trace Elements in Human and Animal Nutrition," Academic Press, London, 1977, pp. 286–289.

Paper 8/03909G
Received October 3rd, 1988
Accepted January 19th, 1989

Thiamine - Reineckate Liquid Membrane Electrode for the Selective Determination of Thiamine (Vitamin B_1) in Pharmaceutical Preparations

Saad S. M. Hassan and Eman Elnemma
Department of Chemistry, Faculty of Science, Qatar University, Doha, P.O. Box 2713, Qatar

The construction and electrochemical response characteristics of a liquid membrane electrode for thiamine (vitamin B_1) based on the formation of an ion pair between the thiamine cation and the reineckate anion in nitrobenzene are described. The electrode showed a linear response for thiamine over the concentration range 10^{-3}–10^{-6} M with a cationic slope of 31.6–mV per concentration decade and had a wide working pH range (4–8), fast response time (1–2–min), low detection limit (0.3–μg–ml^{-1}) good stability and reasonable selectivity. The direct potentiometric determination of vitamin B_1 in some pharmaceutical preparations using the proposed electrode gave an average recovery of 98.1% of the nominal values and a mean standard deviation of 1.3%, which compare fairly well with data obtained using the British and United States pharmacopoeial methods.

Keywords: *Liquid membrane electrode; thiamine-selective electrode; reineckate; vitamin B_1 determination; pharmaceutical analysis*

The United States Pharmacopeia (USP) describes a method for the determination of thiamine (vitamin B_1) based on the fluorimetric measurement of thiochrome formed by oxidation of the vitamin with potassium hexacyanoferrate(III).[1] Other oxidants such as *N*-bromosuccinimide,[2] cyanogen bromide[3] and mercury(II) oxide[4] can also be used. The application of this method to pharmaceutical preparations is restricted in the presence of excess of oxidant and by many of the pharmaceutical excipients, which quench the fluorescence. The British Pharmacopoeia (BP) method,[5] which is based on gravimetric precipitation of thiamine - silicotungstate, suffers from interference by many organic bases. Other analytical procedures including titrimetry,[6] gravimetry,[7] manometry,[8] nephelometry,[9] amperometry,[10] polarography,[11] coulometry,[12] spectrophotometry[13] and nuclear magnetic resonance spectroscopy[14] have been described. Many of these methods, however, suffer from a lack of selectivity.

Ion-selective electrodes that respond to thiamine have been advocated as more simple, direct and specific monitoring systems. In this context, liquid membrane[15–17] and graphite-based[18] electrodes incorporating thiamine derivatives of tetraphenylborate,[15,18] tetra(*m*-methylphenyl)borate[16] and picrolonate[17] as electroactive materials have been suggested. In previous work, we demonstrated the suitability of reineckate as a counter anion for the preparation of liquid and poly(vinyl chloride) membrane electrodes that are sensitive and selective for the determination of atropine[19] and lidocaine.[20] As the spectrophotometric determination of thiamine by precipitation as its reineckate derivative followed by dissolution of the precipitate in an aqueous organic solvent and measurement of the absorbance at 525 nm is considered to be a convenient and selective method for the determination of thiamine in pharmaceutical preparations,[13] it was decided to investigate the suitability of thiamine - reineckate as an electroactive material for the preparation of a thiamine ion-selective electrode. This paper describes the preparation, characterisation and application of a thiamine - reineckate liquid membrane electrode.

Experimental

Apparatus

Potentiometric measurements were made at 25 ± 1 °C with an Orion digital ion analyser (Model 701 A) and a thiamine - reineckate liquid membrane electrode in conjunction with an Orion 90-02 Ag - AgCl double-junction reference electrode, containing 10% *m*/*V* KNO_3 in the outer compartment. The thiamine - reineckate electrode was prepared using an Orion Model 92 liquid membrane electrode barrel as the electrode assembly with an Orion 92-81-04 porous membrane to separate the organic phase from the test solution. The organic liquid membrane and the internal reference solution were 10^{-3} M thiamine - direineckate in nitrobenzene and 10^{-2} M each in KNO_3 and thiamine hydrochloride, respectively. Adjustment of pH was made with an Orion 91-02 combination glass electrode. The conductivity and resistivity of the thiamine - reineckate membrane solution were measured by means of a Tacussel conductivity cell (Type CM 0.05/G) and a Prolabo conductivity meter (Type CD 6N). Fluorimetric measurements were made at 435 nm using a Beckman ratio spectrofluorimeter and an excitation wavelength of 365 nm.

Reagents

All chemicals were of analytical-reagent grade unless stated otherwise. Doubly distilled water was used throughout. Nitrobenzene, used as a membrane solvent, and 2-methylpropan-1-ol, used for the extraction of thiochrome for fluorimetric measurements, were laboratory-reagent grade and were used after two distillations.

Thiamine hydrochloride (vitamin B_1) was obtained from BDH, with a purity of not less than 98% as confirmed by the BP gravimetric procedure[5] and by assay of the chloride content potentiometrically. Aqueous 10^{-3}, 10^{-4}, 10^{-5} and 10^{-6} M thiamine hydrochloride solutions were prepared fresh by accurate dilution of a standard 10^{-2} M stock solution and were kept in brown bottles. Pharmaceutical preparations containing vitamin B_1 were obtained from local drug stores. Pure vitamin powder and pulverised tablets were dried at 60 °C for 2 h under a pressure of 40 mmHg. Aqueous silicotungstic acid, potassium hexacyanoferrate(III) and quinine sulphate solutions for the gravimetric and fluorimetric determination of vitamin B_1 were prepared as described in the BP and USP standard procedures.[1,5]

Membrane Preparation

The thiamine - direineckate ion-pair complex was prepared by adding slowly a three-fold molar excess of ammonium reineckate dissolved in the minimum volume of doubly

distilled water to 25–ml of 10^{-2}–M aqueous thiamine hydrochloride solution. The mixture was stirred for 10–min and the resulting pink precipitate was filtered on a sintered glass crucible (porosity 4), washed with water and dried at room temperature.

Electrode Calibration

The electrode was pre-conditioned by soaking it in aqueous 10^{-3} M thiamine hydrochloride solution for 24 h before use. After conditioning, the electrode was calibrated for aqueous thiamine hydrochloride in the range 10^{-2}–10^{-6} M, the e.m.f. readings being recorded to within ±1 mV.

Sample Preparation

Five tablets containing vitamin B_1 were finely powdered, mixed and weighed. A portion of the powder equivalent to a tablet was weighed, dissolved in the minimum amount of doubly distilled water and filtered. The filtrate was transferred into a 500-ml calibrated flask, made up to the mark with water and shaken. The contents of five ampoules of vitamin B_1 were transferred into a 100-ml calibrated flask, made up to the mark with water and shaken. A 10.0-ml aliquot of this solution was transferred into a 500-ml calibrated flask, made up to the mark with water and shaken.

Determination of Vitamin B_1

A 50-ml aliquot of the vitamin test solution (30–300 μg ml^{-1}) was transferred into a 100-ml beaker. The thiamine - reineckate liquid membrane electrode and the Orion double-junction Ag - AgCl reference electrode were immersed in the solution and allowed to equilibrate with stirring. The e.m.f. was recorded and compared with the calibration graph. The thiamine electrode was stored in doubly distilled water between measurements.

Results and Discussion

Electrode Characteristics

The reaction of thiamine hydrochloride (vitamin B_1) with ammonium reineckate gives a pink precipitate of thiamine direineckate. Elemental analysis and infrared spectral data of the precipitate were consistent with the formation of the ion-pair complex $[C_{12}H_{18}ON_4S]^{2+}[Cr(NH_3)_2(SCN)_4]_2^{2-}$. The complex is sparingly soluble in pure aqueous media but readily soluble in nitrobenzene. A 10^{-2} M nitrobenzene solution of thiamine - direineckate was used as a liquid ion-exchange site in an electrode responsive to vitamin B_1. This solution has an equivalent conductivity of 20.8 Ω^{-1} mol^{-1} cm^2 and an electrical resistivity of 3.7×10^4 Ω. The performance characteristics of the electrode were evaluated according to IUPAC recommendations[21] at 25 ± 1 °C. The results are summarised in Table 1.

The linear response of the electrode covers the range 10^{-3}–10^{-6} M. The slope of the linear portion of the calibration graph is 31.6 mV per concentration decade, which is almost equivalent to the Nernstian slope for a doubly-charged cation. Other previously described thiamine electrodes give a similar slope.[15,18] The reproducibility and stability of the electrode were also evaluated by constructing replicate calibration graphs (n = 10) over a period of 2 weeks. Although the absolute potential of the electrode drifted between 3 and 8 mV to more positive values, the calibration slope remained constant to within ±1 mV per concentration decade over this period.

The useful lifetime of the electrode is about 6 weeks. During this period, its response time, measured in constantly stirred thiamine hydrochloride solutions, showed a stable reading for 10^{-3}–10^{-4} M solutions in less than 60 s. With more dilute thiamine solutions, a 1.5–2.0-min period was required to obtain stable readings. The pH dependence of the electrode for 10^{-3} and 10^{-4} M thiamine hydrochloride solutions was studied over the pH range 2–10. The results indicated a working pH range of between 4 and 8. The potential readings were virtually unaffected over this pH range.

The possible effects of some other vitamins normally present with vitamin B_1 in multi-vitamin preparations, such as riboflavine (vitamin B_2), pyridoxine (vitamin B_6), folic acid, pantothenic acid, biotin, niacin, and also some substances normally used as excipients or tablet coatings such as lactose, sucrose, starch and Tween 80, were evaluated. The potentiometric selectivity coefficients ($k^{pot}_{thia,j}$) were measured using the mixed solution method.[21,22] The concentration of the interferents was fixed at 10^{-3} M and the concentration of thiamine hydrochloride was varied between 10^{-3} and 10^{-5} M. The results obtained showed that there was no adverse effect on the electrode response due to the presence of these substances, all of which have $k^{pot}_{thia,j}$ values of between 10^{-2} and 10^{-3}.

Determination of Vitamin B_1

The direct potentiometric determination of thiamine hydrochloride in pure, aqueous solutions in the concentration range 3–350 μg ml^{-1} (five replicates of each) using the thiamine - reineckate liquid membrane electrode and the calibration graph method gave an average recovery of 98.2% and a mean standard deviation (SD) of 1% (Table 2). The method was also applied to the determiantion of vitamin B_1 in some pharmaceutical tablets and ampoules. The results obtained showed an average recovery of 98.1% of the nominal values and a mean SD of 1.3% (Table 3). These data were evaluated further by comparison with those obtained using the standard BP method[5] (average recovery 98.0%, mean SD 1.4%) and the USP method[1] (average recovery 98.2%, mean SD 1.4%). The three sets of results are shown in Table 3.

The results obtained with the proposed electrode agreed fairly well with those given by the standard pharmacopoeial methods. The F-test revealed no significant differences

Table 1. Response characteristics of the thiamine - reineckate liquid membrane electrode

Parameter	Value
Slope	31.6 mV (log c)$^{-1}$
Standard deviation (SD)	0.7 mV
Correlation coefficient (r)	0.998
Intercept	228 mV
Lower limit of linear range	3×10^{-6} M
Detection limit	10^{-6} M
Membrane resistivity	3.7×10^4 Ω
Working pH range	4–8
Response time	1–2 min

Table 2. Direct potentiometric determination of thiamine hydrochloride using the thiamine - reineckate liquid membrane electrode

Thiamine hydrochloride added/μg ml^{-1}	Recovery, %*	SD, %
3.37	97.6	1.5
6.75	98.2	1.3
13.49	98.5	1.2
26.98	98.1	1.2
33.73	97.9	1.1
67.46	98.4	1.1
134.90	98.5	1.0
202.40	98.3	0.9
269.80	98.2	1.0
337.30	98.4	1.0

* Average of five measurements.

Table 3. Determination of vitamin B_1 in some pharmaceutical preparations using the thiamine - reineckate liquid membrane electrode and the BP and USP methods

Sample	Source	Labelled vitamin B_1/mg per tablet	Thiamine electrode		BP gravimetric method[5]		USP fluorimetric method[1]	
			Recovery, %*	SD, %	Recovery, %*	SD, %	Recovery, %*	SD, %
Bénerva	Hoffman La-Roche (Switzerland)	100	98.0	1.5	98.2	1.8	98.0	1.6
Benerva	Roche (UK)	50	98.5	1.4	98.1	1.5	97.8	1.5
Betaxin	Bayer (FRG)	50	97.7	1.3	98.0	1.5	98.0	1.4
Vitacid B_1	CID (Egypt)	100	98.1	1.3	98.3	1.3	98.6	1.3
B-vit	Wander (Switzerland)	100	98.0	1.2	97.8	1.3	98.5	1.3
Bivamin	Misr (Egypt)	100†	97.9	1.4	97.5	1.4	98.0	1.4
Ecavit B_1	Nile (Egypt)	100†	98.4	1.3	98.0	1.5	98.4	1.4

* Average of five measurements.
† Values quoted are mg per ampoule.

between the means and variances of the three sets of results. The electrode method, however, has the advantages of simplicity, selectivity and speed and can be applied to both turbid and coloured vitamin solutions without prior treatment. As little as 1 μg ml^{-1} of vitamin B_1 can be determined accurately compared with a sample size of at least 25 mg required for the BP procedure.[5] The proposed method is also free from many limitations and complications associated with the USP procedure,[1] caused by variation of the oxidant concentration and the presence of quenching substances. Further, the proposed electrode offers three advantages over many of the previously reported electrode systems: it has a lower limit of detection (down to 10^{-6} M), a wide working pH range (at least 2 pH units) and higher selectivity in the presence of other vitamins (particularly vitamin B_6).[15–18]

References

1. "United States Pharmacopeia XXI, National Formulary XVI," United States Pharmacopeial Convention, Rockville, MD, 1984, p. 1210.
2. Barary, M., Abdel-Hamid, M., Hassan, E., and Elsayed, M., *Pharmazie*, 1986, **41**, 483.
3. Dong, M. H., Green, M. D., and Sauberlich, H. E., *Clin. Biochem. (Ottawa)*, 1981, **14**, 16.
4. Patrick, R., and Wright, J. F. H., *Analyst*, 1949, **74**, 303.
5. "British Pharmacopoeia 1980," Volume II, University Press, Cambridge, 1980, p. 673 and 827.
6. Pifer, C. W., and Wollish, E. G., *J. Am. Pharm. Assoc.*, 1951, **40**, 609.
7. Mehta, A. K., Wadodkar, S. G., and Kasture, A. V., *Indian Drugs*, 1982, **19**, 165.
8. Malnic, G., de Silva, A. C., Giesbrecht, A. M., and de Angelis, R. C., *Rev. Hosp. Clin. Fac. Med. Univ. Sao Paulo*, 1957, **12**, 81; *Chem. Abstr.*, 1960, **54**, 24982c.
9. Bernshtein, V. N., *Zh. Anal. Khim.*, 1958, **13**, 365.
10. Calu, C., and Eugenia, E., *Rev. Roum. Chim.*, 1983, **27**, 667.
11. Skobets, V. D., and Skobets, E. M., *Ukr. Khim. Zh.*, 1959, **25**, 114; *Chem. Abstr.*, 1959, **53**, 16794h.
12. Kalinowski, K., and Sykulska, Z., *Acta Pol. Pharm.*, 1959, **16**, 111.
13. Hashmi, M.-H., "Assay of Vitamins in Pharmaceutical Preparations," Wiley, London, 1973, Chapter 4.
14. Hassan, S. S. M., *J. Assoc. Off. Anal. Chem.*, 1978, **61**, 111.
15. Ishibashi, N., Kina, K., and Maekawa, N., *Chem. Lett.*, 1973, 119.
16. Yao, S., Xu, X., and Shen, G., *Yaoxue Xuebao*, 1983, **18**, 612; *Chem. Abstr.*, 1984, **100**, 56902w.
17. Hassan, S. S. M., Iskander, M. L., and Nashed, N. E., *Fresenius Z. Anal. Chem.*, 1985, **320**, 584.
18. Wang, C., and Guo, Y., *Yaoxue Tongbao*, 1986, **21**, 143; *Chem. Abstr.*, 1986, **105**, 49142y.
19. Hassan, S. S. M., and Tadros, F. S., *Anal. Chem.*, 1984, **56**, 542.
20. Hassan, S. S. M., and Ahmed, M. A., *J. Assoc. Off. Anal. Chem.*, 1986, **69**, 618.
21. "IUPAC Analytical Chemistry Division, Commission on Analytical Nomenclature of Ion-Selective Electrodes," *Pure Appl. Chem.*, 1976, **48**, 127.
22. Ma, T. S., and Hassan, S. S. M., "Organic Analysis Using Ion-Selective Electrodes," Volumes I and II, Academic Press, London, 1982.

Paper 8/03866J
Received September 29th, 1988
Accepted January 4th, 1989

Complementary Study on the Use of the Potassium Reinecke's Salt as a Chemical Actinometer

Jerzy Szychliński, Piotr Bilski,* Kazimierz Martuszewski and Jerzy Blażejowski
Institute of Chemistry, University of Gdansk, Sobieskiego 18, 80-952 Gdansk, Poland

Aqueous solutions of $K[Cr(NH_3)_2(SCN)_4].H_2O$ (the potassium Reinecke's salt) can be used as a photochemical reference system for radiations in the visible region. The results of complementary studies on the improvement of analytical procedures, the direct synthesis of the salt and its thermal reactivity are reported. The possibilities of the application of the system are also discussed.

Keywords: *Potassium Reinecke's salt; chemical actinometer*

In 1966 Wegner and Adamson[1] proposed a chemical actinometer based on aqueous solutions of $K[Cr(NH_3)_2(SCN)_4].H_2O$ [potassium diamminetetrathiocyanatochromate(III) monohydrate (the potassium Reinecke's salt)]. An electromagnetic radiation in the region 310–650 nm initiates hydrolytic substitution at the central atom of the complex with the simultaneous release of SCN^-. The latter species can be easily assayed spectrophotometrically as a coloured complex with Fe^{3+}. Since the paper by Wegner and Adamson only a few reports describing the application of the above actinometric system have appeared.[2–4] The reasons for this lack of interest are the difficulties involved in using this actinometer, namely, the fairly lengthy synthesis of the potassium Reinecke's salt and the relatively low thermal stability of the compound in aqueous solutions. Despite these facts this system has been used to calibrate the widely recommended potassium trioxalatoferrate(III) actinometer in the visible region.[4] The actinometer based on the potassium Reinecke's salt is one of the simplest chemical systems available for the visible region. Other chemical actinometers, whose absorption extends to the visible region, have also been proposed.[5–14] However, some of these systems absorb visible radiation only over a narrow region,[6–8] others are inconvenient owing to the necessity of using gaseous reactants[5,13] that require the application of special analytical procedures[5,12,13] and lastly they usually require materials that are both costly and not readily available.[10,14] Therefore, they are used for specific purposes only.[8,9] Studies in the visible region became very popular after extensive investigations into biological photosynthesis and conversion of solar energy into chemical or electrical energy had been initiated. Chemical actinometry may be a useful tool for the examination of these problems.

In this paper the results of complementary studies on the direct synthesis of the potassium Reinecke's salt, its thermal reactivity in aqueous media and the improvement of analytical procedures are reported. In spite of the difficulties mentioned above, this system appears to be useful in the visible region.[15,16]

Direct Synthesis of $K[Cr(NH_3)_2(SCN)_4].H_2O$

The direct synthesis of the ammonium Reinecke's salt was described by Reinecke[17] and Christensen[18] in the last century. The appropriate potassium salt can be prepared by adding KNO_3 to an aqueous solution of the ammonium salt and subsequent crystallisation.[1] To avoid a two-stage process we attempted to synthesise $K[Cr(NH_3)_2(SCN)_4].H_2O$ directly. For this purpose a mixture of 0.8 M SCN and 0.1 M $KCr(SO_4)_2.12H_2O$ was heated in a shallow metallic crucible at *ca.* 410 K until a viscous, homogeneous phase was obtained. The mixture was stirred vigorously and 1.6 M NH_4HCO_3 was added in small portions. The temperature during the latter operation should not exceed 365 K. During this stage large amounts of gaseous products are evolved, which cause foaming of the mixture. It is important to remove the water, this being one of the gaseous products, almost completely to avoid the decomposition of the final product. After cooling, the crude solid product was divided into four portions, each of which was dissolved in 0.2 dm^3 of water at 330 K and then filtered quickly through a sintered glass funnel heated to the same temperature. The filtrate was immediately cooled to 273 K and left for 1 h. The resulting crystals of $K[Cr(NH_3)_2(SCN)_4].H_2O$ were separated by filtration and dried in a desiccator over KOH. Except for the first stage of the synthesis all the other procedures were peformed under red light. The over-all yield of the synthesis was greater than 30%, based on the amount of chromium potassium sulphate consumed. The identity of the final product was confirmed by volumetric and spectrophotometric analyses. In addition, the thermoanalytical behaviour of the compound was identical with that reported by Zsako *et al.*[19]

Quantum Yield of the Photohydration of $[Cr(NH_3)_2(SCN)_4]^-$ at 366 nm

Wegner and Adamson[1] have reported values for the quantum yield of SCN^- [$\phi(SCN^-)$] formation in the region 315–750 nm. A re-examination of these data revealed that the values of $\phi(SCN^-)$ decreased slightly with the wavelength of the incident radiation (λ). This dependence is not, however, linear either for λ itself or for $1/\lambda$. With the exception of the quantum yield value at 350 nm (0.39), all the other values lie between 0.27 at the longer wavelengths and 0.32 at the shorter wavelengths. As the value reported at λ=350 nm is not consistent with the other data, we performed a series of experiments in which the potassium Reinecke's salt and the potassium trioxalatoferrate(III) actinometers[1,2,8,20] were irradiated under the same conditions at 293 ± 1 K. The source of the UV radiation was a medium-pressure mercury lamp (Q400, Hannau) and the line at 366 nm was isolated by means of a combined glass filter (Schott u. Gen., Jena; $\lambda_{max.}$ = 366 nm, half-width = 20 nm). The mean value of $\phi(SCN^-)$ at 366 nm was found to be 0.32.[16] This value follows a general trend that is characteristic of the $\phi(SCN^-)$ *versus* λ dependence reported by Wegner and Adamson.[1] Taking into account that $\phi(SCN^-)$ *versus* λ can be expected to be a continuous dependence, that both points, *i.e.*, 350 and 366 nm, are located very close to each other on the wavelength scale and that no other deviations in the $\phi(SCN^-)$ values are observed, it can be concluded that the value of the quantum yield at 350 nm reported by Wegner and Adamson[1] is incorrect. In order to support this conclusion further, we determined analogously the values of the quantum yield of SCN^- formation at two

* To whom correspondence should be addressed.

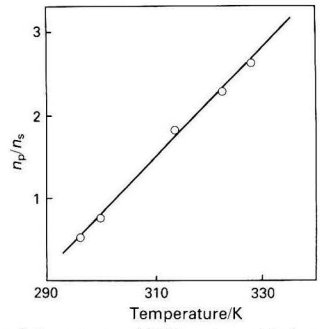

Fig. 1. Ratio of the amount of SCN^- released (n_p) to the amount of $[Cr(NH_3)_2(SCN)_4]^-$ depleted (n_s) *versus* temperature in the thermal hydration process

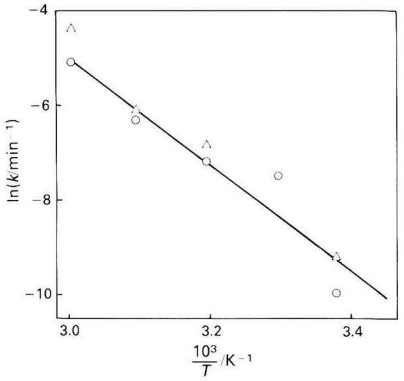

Fig. 2. Arrhenius plot for the hydration of Reinecke's salt anion. ○, depletion of $[Cr(NH_3)_2(SCN)_4]^-$; and △, formation of SCN^-. The experimental points were fitted with the equation $\ln k = \ln Z - [(E_a/R)\ (1/T)]$ (Z is the frequency factor) and the solid line corresponds to the values of the constants $Z = 7.0 \times 10^{14}$ min^{-1} and $E_a = 109 \pm 12$ kJ mol^{-1} (correlation coefficient, 0.951)

other wavelengths, namely, 313 and 415 nm. The values of the quantum yield thus obtained were in good agreement with the data reported by Wegner and Adamson[1] for the appropriate wavelength region.

Kinetics of the Hydration of the $[Cr(NH_3)_2(SCN)_4]^-$ Ion

According to Wegner and Adamson[1] and Adamson[21] the mechanism of the hydration of the Reinecke's salt anion involves several stages, depending on the acidity of the medium. The first slow step always proceeds according to the following equation and is independent of the acidity of the medium:

$$[Cr(NH_3)_2(SCN)_4]^- + H_2O \rightarrow [Cr(NH_3)_2(SCN)_3(H_2O)] + SCN^- \quad (1)$$

According to these workers this is the only reaction occurring in a neutral medium. However, in an acidic solution, a fast equilibration takes place

$$[Cr(NH_3)_2(SCN)_3(H_2O)] + H_2O \xrightarrow{H_3O^+} [Cr(NH_3)_2(SCN)_2(H_2O)_2]^+ + SCN^- \quad (2)$$

On the other hand, in a basic medium a fast reaction leading to the release of all the SCN^- ions occurs

$$[Cr(NH_3)_2(SCN)_3(H_2O)] + 3H_2O \xrightarrow{OH^-} [Cr(NH_3)_2(H_2O)_4]^{3+} + 3SCN^- \quad (3)$$

The first step, reaction (1), can also be initiated by UV - visible radiation and it is followed by the thermal processes (2) and (3), depending on the pH of the medium. Reaction (3) takes place only for the partially hydrated complex. Hence, Wegner and Adamson[1] recommended that an actinometric solution should be made alkaline after irradiation in order to increase the sensitivity of the actinometric measurements. They suggested that by keeping the photolyte in an alkaline solution for 2 h a four-fold increase in the SCN^- concentration could be expected. Because of the sensitivity of Reinecke's salt to visible radiation, all procedures must be performed in the dark. However, owing to the possibility of hydration of the compound during the thermal process [reaction (1)], an error may be introduced into the actinometric measurements. Therefore, Wegner and Adamson recommended that all spectrophotometric measurements of the SCN^- concentration should be performed relative to a sample kept in the dark.

As the thermal reactivity of the aqueous solutions of Reinecke's salt was not investigated completely by Wegner and Adamson[1] we conducted a complementary study in order to clarify some aspects of this problem. Firstly, several series of kinetic and photochemical measurements were carried out on the hydration of $[Cr(NH_3)_2(SCN)_4]^-$ in a neutral medium. In both instances the rate of formation of SCN^- (assayed spectrophotometrically as its complex with Fe^{3+}[1]) was compared with the rate of depletion of the Reinecke's salt anion. The latter was determined by measuring the absorption of a sample at 520 nm (the maximum of the charge transfer transition in $[Cr(NH_3)_2(SCN)_4]^-$[1]) relative to the absorption of a sample in which the complex anion had been removed by adding $N(CH_3)_4Cl$. The ratio of the amount of SCN^- ions released (n_p) to the amount of hydrated Reinecke's salt anion (n_s) is shown in Fig. 1. As can be seen this ratio is slightly lower than 1 at room temperature and increases markedly at higher temperatures. This clearly indicates that at higher temperatures, reactions analogous to those shown in equations (2) and (3) must also occur in a neutral medium. On the other hand, the ratio n_p/n_s is close to 1 at room temperature if the reaction is initiated photochemically ($\lambda = 366$ nm). Because the release of SCN^- ion is accelerated by heat it may be expected that in the photochemically initiated hydration of $[Cr(NH_3)_2(SCN)_4]^-$ the ratio n_p/n_s will also increase with temperature. To shed more light on this matter we compared the reaction rate constant (k) for the hydration of the Reinecke's salt anion, determined either from the depletion of $[Cr(NH_3)_2(SCN)_4]^-$ or from the formation of SCN^-. The appropriate rate equations can be written as

$$-d\{[Cr(NH_3)_2(SCN)_4]^-\}/dt = k\{[Cr(NH_3)_2(SCN)_4]^-\}^n \quad (4)$$

for the depletion of a substrate and as

$$1/\theta(d[SCN^-]/dt) = k\{[Cr(NH_3)_2(SCN)_4]^-\}^n \quad (5)$$

where $\theta = n_s/n_p$, for the formation of a product. It was found that in both instances the kinetics were first order, *i.e.*, $n = 1$. From the almost linear plot of $\ln k$ against T^{-1} (Fig. 2), an activation energy (E_a) of 109 ± 12 kJ mol^{-1} can be calculated, which agrees well with the value of 113 kJ mol^{-1} obtained by Wegner and Adamson[1] on the basis of the yield of SCN^-.

The complexity of the mechanism of the hydration of $[Cr(NH_3)_2(SCN)_4]^-$, discussed above, for both the thermal and photochemical processes implies that the quantum yield measurements must be carried out under constant conditions, *i.e.*, at constant temperature, pH, etc. Moreover, all measurements must be made relative to the non-irradiated sample, which should be treated in the same way as the irradiated solution. Nevertheless, an error can still be introduced due to the fact that secondary thermal processes can proceed differently in irradiated and non-irradiated samples. For these reasons, all the procedures, *i.e.*, exposure, analytical measurements, etc., must be carried out in as short a time as possible. However, this cannot always be accomplished,

particularly if measurements of a dose of solar radiation are to be made in the field or at sea. The problem therefore arises as to how to protect the samples from thermal side-reactions. One possibility is to remove the Reinecke's salt anion from the solution and hence to fix the effect of a photochemical process. We checked several substances for this purpose: $N(CH_3)_4Cl$ appeared to be the most promising compound as the cation of this salt forms an insoluble complex with $[Cr(NH_3)_2(SCN)_4]^-$. A sample protected in this way can be kept for 2 weeks without noticeable changes in the SCN^- ion concentration. Separation of a solution from a sediment allows a photolyte to be kept unchanged for an even longer time; similarly, the storage of a photolyte at low temperature has the same effect. In our opinion, the use of a photolyte at alkaline pH as proposed by Wegner and Adamson[1] is not to be recommended. Presumably this procedure improves the sensitivity of actinometric measurements, but, on the other hand, it can also introduce large errors.

In conclusion, the direct synthesis of the potassium Reinecke's salt, its thermal reactivity and the value of the quantum yield for its photohydration at 366 nm have been examined. In our opinion, this actinometer may be useful if a simple and readily available system for the measurement of radiation intensity in the visible region is required. Particular attention should be given to the possibility of using this system to determine the dose of absorbed UV - visible radiation. This possibility is illustrated by the fact that the quantum yield reaches values close to 0.29 J mol^{-1} in the range 320–650 nm.[1,16]

Financial support of this work by the Polish Academy of Sciences, project MR.I.15.1.4.9, is gratefully acknowledged.

References

1. Wegner, E. E., and Adamson, A. W., *J. Am. Chem. Soc.*, 1966, **88**, 394.
2. Maciejewski, A., and Wojtczak, J., "Seventh Conference on Quantum Electronics and Non-linear Optics," Poznan, Poland, April 1978, Abstracts, p.191.
3. Demas, J. N., and Blumenthal, B. H., *J. Res. Natl. Bur. Stand., Sect. A*, 1976, **80**, 409.
4. Langford, C. H., and Holubov, C. A., *Inorg. Chim. Acta*, 1981, **53**, L59.
5. Ryabov, S. E., *Khim. Vys. Energ.*, 1982, **16**, 422.
6. Leighton, W. G., and Forbes, G. S., *J. Am. Chem. Soc.*, 1930, **52**, 3139.
7. Hatchard, C. G., and Parker, C. A., *Proc. R. Soc. London, Ser. A*, 1956, **235**, 518.
8. Demas, J. N., McBride, R. P., and Harris, E. W., *J. Phys. Chem.*, 1976, **80**, 2248.
9. Sanchez-Pedreno, C., Perez-Ruiz, T., Martinez-Lozano, C., and Hernandez-Cordoba, M., *Anal. Chim. Acta*, 1978, **104**, 397.
10. Heller, H. G., and Langan, J. R., *J. Chem. Soc., Perkin Trans. 1*, 1981, 341.
11. Dressick, W. J., Meyer, T. J., and Durham, B., *Isr. J. Chem.*, 1982, **22**, 153.
12. Moan, J., Hovik, B., and Vold, E., *Photochem. Photobiol.*, 1979, **30**, 623.
13. Warburg, O., and Schocken, V., *Arch. Biochem.*, 1949, **21**, 363.
14. Schmidt, R., and Brauer, H.-D., *J. Photochem.*, 1985, **25**, 489.
15. Dulin, H. D., and Mill, T., *Environ. Sci. Technol.*, 1982, **16**, 815.
16. Szychlinski, J., Martuszewski, K., Blazejowski, J., and Bilski, P., *Stud. Mater. Oceanol. (Pol. Akad. Nauk, Kom. Badan Morza)*, 1984, **45**, 217.
17. Reinecke, A., *Justus Liebigs Ann. Chem.*, 1863, **126**, 113.
18. Chistensen, O. T., *J. Prakt. Chem.*, 1892, **45**, 213.
19. Zsako, J., Liptay, G., Varhelyi, Cs., and Brandt-Petric, E., *J. Therm. Anal.*, 1982, **23**, 123.
20. Demas, J. N., Bowman, W. D., Zalewski, E. F., and Velapoldi, R. A., *J. Phys. Chem.*, 1981, **85**, 2766.
21. Adamson, A. W., *J. Am. Chem. Soc.*, 1958, **80**, 3183.

Paper 8/03699C
Received September 21st, 1988
Accepted January 13th, 1989

Photometric and Fluorimetric Methods for the Determination of Bromate in Bread

F. García Sánchez, A. Navas Díaz and M. Santiago Navas
Department of Analytical Chemistry, Faculty of Sciences, University of Málaga, E-29071 Malaga, Spain

Kinetic methods for the determination of bromate based on the oxidation of benzyl 2-pyridyl ketone 2-quinolylhydrazone are described. The initial reaction rate is linearly related to the bromate concentration with detection limits of 0.25–6.50 μg ml^{-1} for photometric monitoring and 0.08–5.20 μg ml^{-1} when the change in the fluorescence signal is measured. Under appropriate working conditions, the photometric method was applied satisfactorily to the determination of bromate in bread.

Keywords: *Bromate determination; kinetic method; photometry; fluorimetry; bread*

The oxidation of benzyl 2-pyridyl ketone 2-quinolylhydrazone (BPKQH) by bromate to give coloured and fluorescent products could provide the basis for the kinetic determination of the latter.

The advantages and limitations of fluorescence monitoring in kinetic methods have been discussed and compared with the use of absorbance measurements.[1] The main reasons for using fluorescence in place of absorbance monitoring are that greater sensitivity and selectivity can be achieved.[2] However, absorbance monitoring improves the precision and accuracy of the methods. Also, the instrumentation required for absorbance measurements is less expensive and sophisticated than that required for fluorescence measurements. When absorbance monitoring provides adequate precision, sensitivity, selectivity and accuracy, other considerations such as speed, cost, ruggedness and ease of operation may influence the selection process.

Only a few methods have been reported for the determination of bromate[3]; most of these are based on kinetic measurements of oxidative processes involving organic reagents[4] as reductants.

Potassium bromate is used in bread-making as an oxidising agent. The applicability of the photometric method to the determination of bromate was demonstrated by determining the residual potassium bromate content in bread at the μg g^{-1} level.

Experimental

Reagents

All chemicals used were of analytical-reagent grade and distilled, de-ionised water was used throughout. The dilute solutions were prepared immediately before use, and all reagents and analyte solutions were maintained at the same temperature by means of a thermostatically controlled water-bath.

Benzyl 2-pyridyl ketone 2-quinolylhydrazone was synthesised as described previously.[5] Solutions (5×10^{-3} M) were prepared weekly in hot absolute ethanol.

A stock standard potassium bromate solution (0.1 M) was prepared by dissolving 16.701 g of $KBrO_3$ in 1 l of de-ionised water.

Apparatus and Measurement Conditions

All fluorimetric measurements were made with a Perkin-Elmer Model MPF-43A fluorescence spectrophotometer equipped with an Osram XBO 150-W xenon lamp, 1 × 1 cm quartz cells and an R-777 photomultiplier (Hamamatsu). All spectra and kinetic curves were recorded on a Perkin-Elmer 023 chart recorder. Absorbance measurements were made with a Shimadzu UV-240 Graphicord spectrophotometer.

Procedure

Transfer 1.5 ml (fluorimetric measurement) or 2.5 ml (photometric measurement) of 5×10^{-4} M BPKQH solution and an aliquot of a sample solution containing 0.39–5.20 μg ml^{-1} (fluorimetric procedure) or 1.95–6.50 μg ml^{-1} (photometric procedure) of bromate into a 25-ml calibrated flask. Add 10 ml of 2 M HCl and dilute to volume with de-ionised water. Record the signal intensity - time curve at 374 nm (absorbance) or 438 nm (emission) with excitation at 343 nm (fluorescence), at 25 °C, 60 s after the addition of HCl.

Collection and Treatment of Samples

A circular sample, 2 cm in diameter, was taken from the centre of a 15-mm thick slice of bread. It was freeze-dried under vacuum for 48 h.

Two grams of the powered sample were weighed and 20 ml of water were added. The mixture was subjected to ultrasonic extraction at 20 °C for 10 min followed by centrifugal separation. The liquid fraction was diluted with de-ionised water in a 100-ml calibrated flask. Aliquots of this solution were then treated as described under Procedure.

Results and Discussion

Absorption and Fluorescence Spectra

Fig. 1(*a*) shows the excitation and emission spectra and Fig. 1(*b*) the absorption spectra of BPKQH and its oxidation product from the reaction with bromate. Under the conditions used, BPKQH exhibited no fluorescence. The wavelengths chosen for subsequent work were 343 and 438 nm for excitation and emission, respectively, and 374 nm for absorption studies.

Effect of Reaction Variables

The effect of the reaction variables on the initial rate was studied by monitoring the reaction photometrically and fluorimetrically. Optimisation was carried out by systematically varying one parameter while keeping all the others constant. The optimum concentration was taken as that which gave a reaction order with respect to the variable concerned of zero or as close to zero as possible.

From the assays carried out it was observed that the reaction occurred at a lower acidity when a higher concentration of bromate was used. Also, when the bromate concentration was kept constant, the reaction rate increased in the order $HClO_4 < H_2SO_4 < HCl$. This suggests that the use of a high concentration of HCl should improve the sensitivity of the method for the determination of bromate.

Using concentrations of BPKQH and bromate of 1×10^{-5} M

(fluorescence measurements) or 4×10^{-5} M (absorbance measurements), a 0.8 M HCl concentration was chosen for the analytical procedure, bearing in mind that the initial reaction rate is independent of the HCl concentration for concentrations between 0.7 and 1.0 M (fluorimetric mode) and 0.64 and 0.85 M (photometric mode).

The influence of the BPKQH concentration on the initial reaction rate was also studied. The results obtained are shown in Fig. 2. The logarithmic plot showed that the reaction rate was independent of the BPKQH concentration in the range 2.5×10^{-5}–3.5×10^{-5} M (fluorimetric) and 4.0×10^{-5}–8.0×10^{-5} M (photometric). Hence, BPKQH concentrations of 3×10^{-5} and 5×10^{-5} M were selected for the fluorimetric and photometric procedures, respectively.

Because the initial reaction rate is independent of the temperature in the range 20–40 °C, a temperature of 25 °C was chosen for the procedure. The kinetic data from the logarithmic plots are summarised in Table 1.

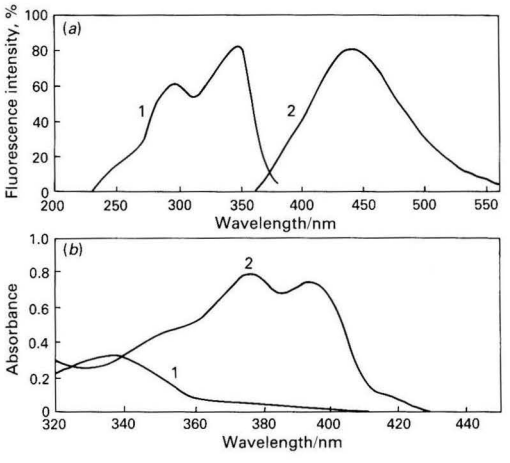

Fig. 1. (*a*) 1, Excitation; and 2, emission spectra of the BPKQH oxidation product. [BPKQH] = [$KBrO_3$] = 1×10^{-5} M; [HCl] = 0.8 M. (*b*) Absorption spectra of 1, BPKQH; and 2, its oxidation product. [BPKQH] = [$KBrO_3$] = 4×10^{-5} M

Analytical Parameters

Under optimum conditions, the initial reaction rate was found to be a linear function of the concentration of bromate over the range 0.26–5.20 μg ml^{-1} (photometric) and 0.84–6.50 μg ml^{-1} (fluorimetric) with regression coefficients of 0.9987 and 0.9994, respectively.

The sensitivities of the two methods are reported as the analytical sensitivity $S_A = s_s/m$, where s_s is the standard deviation of the analytical signal and m is the slope of the calibration graph. The limit of detection (LOD) and limit of quantification (LOQ) are reported using the definition given by IUPAC,[6] *viz.*, LOD = $3s_B/m$ and LOQ = $10s_B/m$ (where s_B is the relative standard deviation of the blank signal and m is the slope of the calibration graph). Because no blank signal is observed in the absence of analyte, s_B approaches s_s at the detection limit. The LOQ was used as the lower limit of the dynamic range.

In order to evaluate the precision of the proposed methods, two series of 11 identical bromate samples, each containing 2.60 μg ml^{-1} (fluorimetric) or 3.90 μg ml^{-1} (photometric) were analysed under the optimum conditions. Table 2 shows the results obtained.

The fluorimetric procedure has a higher sensitivity and lower LOD and LOQ values than the photometric method. Examination of Table 2 also shows that the precision of the latter is greater. Application of the *F*-test[7] indicates that the precision of both methods differs significantly, the photometric method being the more precise.

Table 1. Kinetic data

	$v = k[BrO_3^-]^{\frac{3}{2}}$
$v \propto [HCl]^{\frac{3}{2}}$ ..	[HCl] ≤ 0.69 M
$v \propto [HCl]^0$ ..	0.69 M ≤ [HCl] ≤ 0.96 M
$v \propto [HCl]^{\frac{3}{2}}$ ..	0.96 M ≤ [HCl] ≤ 1.20 M
$v \propto [BPKQH]^1$	2.5×10^{-6} M ≤ [BPKQH] ≤ 2.5×10^{-5} M
$v \propto [BPKQH]^0$	2.5×10^{-5} M ≤ [BPKQH] ≤ 3.5×10^{-5} M
$v \propto [BrO_3^-]^{\frac{3}{2}}$	3.0×10^{-6} M ≤ [BrO_3^-] ≤ 4.0×10^{-5} M
	$v = k'[BrO_3^-]^1$
$v \propto [HCl]^{\frac{3}{2}}$ ..	[HCl] ≤ 0.64 M
$v \propto [HCl]^0$ ..	0.64 M ≤ [HCl] ≤ 0.96 M
$v \propto [HCl]^{-\frac{3}{2}}$ ..	0.96 M ≤ [HCl] ≤ 1.2 M
$v \propto [BPKQH]^1$	1.0×10^{-5} M ≤ [BPKQH] ≤ 4.0×10^{-5} M
$v \propto [BPKQH]^0$	4.0×10^{-5} M ≤ [BPKQH] ≤ 7.0×10^{-5} M
$v \propto [BrO_3^-]^1$ ..	1.5×10^{-5} M ≤ [BrO_3^-] ≤ 5.0×10^{-5} M

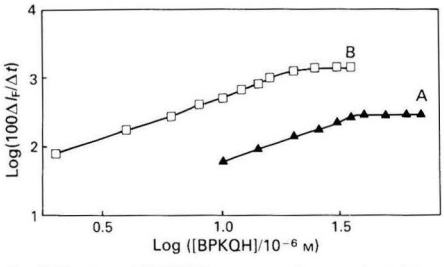

Fig. 2. Influence of BPKQH concentration on the initial reaction rate. I_F, fluorescence intensity; t, time. A, Photometric method; [HCl] = 0.8 M; [$KBrO_3$] = 4×10^{-5} M. B, Fluorimetic method; [HCl] = 0.8 M; [$KBrO_3$] = 1×10^{-5} M

Table 2. Analytical characteristics of the proposed methods

Analytical mode	Slope (m)/I_F ml μg^{-1} min^{-1}	S_A*/ μg ml^{-1}	LOD†/ μg ml^{-1}	LOQ‡/ μg ml^{-1}	LDR§/ μg ml^{-1}	Error,¶ %	RSD,‖ %
Fluorimetic ..	1.57	0.026	0.076	0.26	0.26–5.2	4.04	6.02
Photometric** ..	0.58	0.084	0.25	0.84	0.84–6.50	1.26	1.88

* S_A = analytical sensitivity.
† LOD = limit of detection.
‡ LOQ = limit of quantification.
§ LDR = linear dynamic range.
¶ Relative error = $100ts/\bar{x}n$.
‖ RSD = relative standard deviation.
** Absorbance instead of fluorescence intensity (I_F).

Table 3. Tolerance of the methods towards foreign ions

Fluorimetric monitoring		Photometric monitoring	
Tolerance ratio	Foreign ion or species	Tolerance ratio	Foreign ion or species
100	Mg^{II}, Zn^{II}, Cd^{II}, Mn^{II}, Hg^{II}, Ga^{III}, In^{III}, Cr^{III}, As^{V}, ClO_3^-, F^-, $S_2O_8^{2-}$, IO_3^-	100	Zn^{II}, Mn^{II}, Cd^{II}, Ga^{III}, IO_3^-, ClO_3^-, IO_4^-, CrO_4^{2-}, $S_2O_8^{2-}$
10	Co^{II}, Ni^{II}, Sn^{II}, Cu^{II}, IO_4^-, SO_4^{2-}, citrate, EDTA	50	EDTA
		10	Cu^{II}, citrate
5	CrO_4^{2-}	5	Fe^{III}, Ce^{IV}
1	Fe^{III}, Ce^{IV}, V^{V}	1	Ni^{II}, Co^{II}, Au^{III}, SO_3^{2-}
0.5	Pd^{II}, NO_2^-	0.5	Pd^{II}, I^-, Sn^{II}
0.25	Au^{III}, Br^-, ascorbic acid	0.25	$S_2O_3^{2-}$, V^{V}, ascorbic acid
0.16	CN^-, MnO_4^-	<0.10	NO_2^-, Fe^{II}
<0.1	Fe^{II}, $S_2O_3^{2-}$		

Table 4. Determination of bromate in bread

Sample	Bromate added/ μg ml^{-1}	Bromate found*/ μg ml^{-1}	Recovery,%	Endogeneous bromate/ μg ml^{-1}
1	—	0.606(0.021)	—	0.606
1	3.00	3.620(0.026)	100.47	0.620
2	—	0.620(0.026)	—	0.620
2	4.00	4.600(0.020)	99.50	0.600
3	—	0.620(0.020)	—	0.620
3	5.00	5.553(0.042)	98.66	0.553

* Average of three determinations. Standard deviation given in parentheses.

Selectivity Study

The effect of various potentially interfering ions on the determination of bromate at the 2.60 μg ml^{-1} level (fluorimetric method) and at the 3.90 μg ml^{-1} level (photometric method) was studied. The criterion for interference was a deviation in the analytical signal of more than t (Student) standard deviations (11 measurements) from the mean value expected for bromate alone. This criterion provides a confidence limit for concentrations ranging from 2.34 to 3.06 μg ml^{-1} (fluorimetric) and from 4.03 to 3.71 μg ml^{-1} (photometric), which are equivalent to recoveries of 118–90 and 103–95%, respectively.

The most important interferences are given in Table 3, which shows that species such as EDTA, IO_3^- and CrO_4^{2-} (photometric method) or EDTA, $S_2O_8^{2-}$, ClO_3^- and IO_3^- (fluorimetric method) do not interfere. Also, ions such as Zn^{II}, Cd^{II} and Ga^{III}, which form complexes with BPKQH, do not interfere. The only serious interferents are reductants (Br^- and NO_2^-) and cations such as Co^{II}, Fe^{II} and Pd^{II}, which form strong complexes with BPKQH even in the acidic medium of the reaction.

Analysis of Bread Samples

The proposed photometric method is superior to the fluorimetric methods; it was applied to the determination of potassium bromate in spiked bread samples. The samples, containing known amounts of bromate, were analysed by comparing the measured initial reaction rate with that of a linear calibration graph. Three individual extractions were performed and three determinations were carried out on each extraction. The results obtained, together with the percentage recoveries, are summarised in Table 4. The average bromate concentration in the bread samples analysed was found to be 381.25 μg g^{-1}, which is in good agreement with values reported in the literature.[8]

We thank the Dirección General de Investigación y Técnica (Project PB86-0247) for supporting this study.

References

1. Ingle, J. D., and Ryan, M. A., *in* Wehry, E. L., *Editor*, "Modern Fluorescence Spectroscopy," Volume 3, Plenum Press, New York, 1981, Chapter 3, p. 104.
2. Navas, A., and Sánchez Rojas, F., *Talanta*, 1984, **31**, 437.
3. Román, M., Fernández Gutierrez, A., and Muñoz de la Peña, A., *Microchem. J.*, 1984, **29**, 19.
4. García Sánchez, F., Navas, A., and Laserna, J., *Anal. Chem.*, 1983, **55**, 253.
5. Santiago, M., Navas, A., Laserna, J., and García Sánchez, F., *Mikrochim. Acta*, 1983, **II**, 197.
6. Long, G. L., and Winefordner, J. D., *Anal. Chem.*, 1983, **55**, 712A.
7. Miller, J. C., and Miller, J. N., "Statistics for Analytical Chemistry," Second Edition, Ellis Horwood, Chichester, 1988.
8. Oikawa, K., Saito, H., Sakazume, S., and Fujii, M., *Bunseki Kagaku*, 1982, **31**, E251.

Paper 8/03478H
Received August 30th, 1988
Accepted January 18th, 1989

COMMUNICATION

Material for publication as a Communication must be on an urgent matter and be of obvious scientific importance. Rapidity of publication is enhanced if diagrams are omitted, but tables and formulae can be included. Communications receive priority and are usually published within 5–8 weeks of receipt. They are intended for brief descriptions of work that has progressed to a stage at which it is likely to be valuable to workers faced with similar problems. A fuller paper may be offered subsequently, if justified by later work.

Manuscripts are usually examined by one referee and inclusion of a Communication is at the Editor's discretion.

Rapid Determination of Nitrite in Water by Flow Injection With Chemiluminescence Detection

Alexander R. Thornton and Josef Pfab*
Department of Chemistry, Heriot-Watt University, Riccarton, Edinburgh EH14 4AS, UK
Robert C. Massey
Ministry of Agriculture, Fisheries and Food, Food Science Division, Queen Street, Norwich NR2 4SX, UK

Keywords: *Chemiluminescence; nitrogen monoxide; nitrite; flow injection*

There is currently considerable interest in the determination of nitrite and nitrate in water and various foods, and this is reflected by the wide variety of techniques available for the determination of these two ions.[1] Walters *et al.*[2] introduced the chemiluminescence detection of nitrogen monoxide (NO) as a highly selective and sensitive procedure for the determination of nitrite, and improvements to this approach utilising the chemical reduction of nitrite to NO and its extension to the determination of nitrate have been reported.[2–5] Detection limits of the order of 0.1–0.5 nmol (7–35 ng as $NaNO_2$) have been achieved.[4,5] The main disadvantages of these chemical reduction techniques are peak broadening due to the dead-volume of the reaction flasks and vapour traps and the use of batch rather than continuous liquid flow operation.

We have succeeded in lowering the detection limits for the determination of nitrite in water by two orders of magnitude and have improved the speed and simplicity of operation by combining flow injection with chemiluminescence detection. Nitrogen monoxide in equilibrium with HNO_2 is separated from the aqueous flowing eluate by entrainment in Ar carrier gas and is detected with high specificity in the gas stream by the chemiluminescence associated with its reaction with ozone (O_3).

The sequence of reactions involved in the chemiluminescence determination of nitrite ion is

$$NO_2^- + H^+ \rightleftharpoons HONO \rightarrow NO$$

$$NO + O_3 \rightarrow NO_2^* \rightarrow NO_2 + h\nu$$

Experimental

A Gilson Model 303 reciprocating pump and a Rheodyne Model 7010 loop injector with a 5-μl loop were used for flow injection. The solvent was 0.1 M H_3PO_4 flowing at a rate of 1.25 ml min^{-1}. The injection port was connected to a zero dead-volume T union attached to the top of a vertically positioned water-cooled glass condenser. The third port of the T served for the introduction of the Ar carrier gas. Water accumulating at the bottom of the condenser was removed at regular intervals by suction with a water pump. The NO released under partial vacuum and entrained by the carrier gas enters the chemiluminescence analyser (modified Thermoelectron, Model 12A) via PTFE tubing (3.125 mm o.d.). Mixing of the NO containing carrier gas with gaseous O_3 from the ozone generator of the instrument leads to the well known chemiluminescence reaction producing electronically excited NO_2. The resulting emission of NO_2 in the near-infrared (IR) permits NO to be monitored with a photomultiplier tube. Typical operational parameters of the set-up used are summarised in Table 1.

Table 1. Operational parameters of the detection system for the determination of trace amounts of nitrite by flow injection using chemiluminescence detection of NO

Injection volume	5 μl
Flow-rate of aqueous solvent	1.25 ml min^{-1}
Flow-rate of Ar carrier gas	50–70 ml min^{-1}
Pressure of Ar carrier gas	230 mbar
Operating pressure of chemiluminescence chamber	5 mbar
Photomultiplier tube	Thorn EMI 9658R (cooled)

Results and Discussion

Fig. 1 shows the chemiluminescence response for NO released from the injection of 5 μl of a 5×10^{-7} M solution of $NaNO_2$ in 0.1 M H_3PO_4. We have observed qualitatively similar responses when H_3PO_4 was substituted by HCl and acetic acid and conclude that there is no pronounced dependence of the detector response on the nature of the acid. Typical peak widths at half-height are 10 s. This indicates that the detection system in its present configuration gives rise to only moderate peak broadening and can be adapted readily for chromatographic detection. We are currently investigating its use as a post-column high-performance liquid chromatographic detection system for substances releasing HNO_2, nitrite, NO_2 or NO on photolysis.

* To whom correspondence should be addressed.

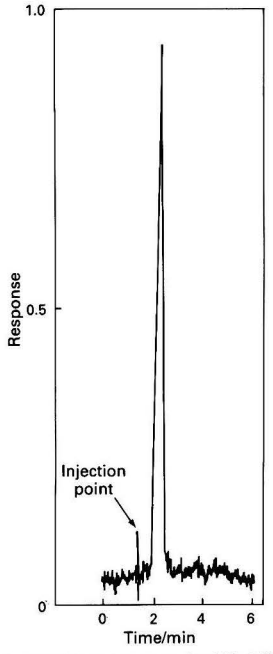

Fig. 1. Chemiluminescence response for NO following injection of 5 μl of a 5×10^{-7} M solution of $NaNO_2$ in 0.1 M H_3PO_4

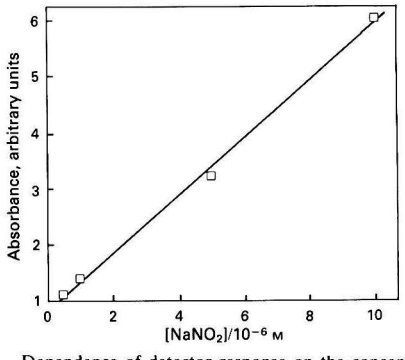

Fig. 2. Dependence of detector response on the concentration of $NaNO_2$ in the lowest concentration range studied. Note the intercept on the ordinate due to the blank response of the system

The dependence of the detector response on the concentration of $NaNO_2$ in the range 1×10^{-7}–1×10^{-3} M was examined. Linearity of response was good over a limited concentration range. Fig. 2 shows a plot of response *versus* concentration of $NaNO_2$ for the range 0–1×10^{-5} M. The positive intercept of *ca.* 0.8 is due to the blank response of the system. A detection limit of 0.14 ng or 2 pmol was evaluated following recently published recommendations.[6] No efforts were made to reduce the relatively high blank response of the system which dictates this detection limit. The magnitude of the blank response was equivalent to 0.11 ng or 1.6 pmol of $NaNO_2$ and was characterised by a relative standard deviation for the blank responses (σ_B) of 7.8%. Interference effects from *N*-nitrosoamines were found to be negligible for a wide range of such compounds, for example, *N*-nitrosodimethylamine, *N*-nitrosoproline, *N*-nitrosopipecolic acid and *N*-methyl-*N*-nitroso-*p*-toluenesulphonamide. In contrast, *S*-nitroso and *O*-nitroso compounds (alkyl thionitrites and alkyl nitrites) yield nearly equivalent responses on a molar basis, presumably due to hydrolysis. The response of nitrate ion is negligible and may be accounted for by the nitrite impurity present.

The physico-chemical principle of this technique for the determination of trace amounts of nitrite in water can be summarised briefly: HNO_2 is a weak acid and exists via its undissociated form in equilibrium with dissolved and gaseous NO and NO_2. On purging its solution at ambient temperature with Ar under partial vacuum using effective dispersion of the liquid phase, a significant fraction of the NO in equilibrium is removed. This technique has enabled the detection limits for nitrite in water to be improved by two orders of magnitude. Provided an NO_x detector is available the method can be implemented readily for the rapid determination of trace amounts of nitrite (or dissolved NO) in water and aqueous extracts. The very high specificity of the technique is well known and its extension to the determination of trace amounts of nitrate using well established reduction procedures[5] appears feasible.

References

1. Usher, C. D., and Telling, G. M., *J. Sci. Food Agric.*, 1975, **26**, 1793.
2. Walters, C. L., Downes, M. J., Hart, R. J., Perse, S., and Smith, P. L. R., *Z. Lebensm. Unters. Forsch.*, 1978, **167**, 229.
3. Doerr, R. C., Fox, J. B., Lakritz, L., and Fiddler, W., *Anal. Chem.*, 1981, **53**, 381.
4. Cox, R. D., *Anal. Chem.*, 1980, **52**, 332.
5. Walters, C. L., Gillatt, P. N., Palmer, R. C., and Smith, P. L. R., *Food Add. Contam.*, 1987, **4**, 133.
6. Analytical Methods Committee, *Analyst*, 1987, **112**, 199.

Paper 9/00837C
Received February 23rd, 1989

BOOK REVIEWS

Supercritical Fluid Chromatography

Edited by Roger M. Smith. *RSC Chromatography Monographs.* Pp. xii + 238. Royal Society of Chemistry. 1988. Price £27.50; $59. ISBN 0 85186 577 1.

This book is the product of a very successful short course in Supercritical Fluid Chromatography (SFC) held at Loughborough University in July 1986. A number of the lecturers have provided expanded versions of their contributions to the course and these have been supplemented by invited papers from other workers in the field. By and large the book is a successful follow-up to the course. It provides a good blend of theory and practice and also manages to capture the excitement of the emergence of an important new analytical technique.

The real meat of the book for chromatographers is provided by three successive chapters authored by Leyendecker, Schoenmakers and Sandra, respectively. I would recommend the book for these three chapters alone. Leyendecker provides a very comprehensive discussion of the effect of mobile phase parameters on an SFC separation and also a consideration of the choice of stationary phase. A theoretical comparison of the performance of packed and capillary columns in SFC is nicely related by Schoenmakers to practical considerations in the choice of conditions for a specific analysis. A comparison of high-temperature capillary GC and capillary SFC is well illustrated by the practical examples taken from a number of applications areas by Sandra and co-authors.

It is also a pleasure to find a comprehensive treatment of the coupling of SFC with mass spectrometry in two chapters by Games and co-authors and by Lane. The latter concentrates on applications in the pharmaceutical industry and is replete with practical examples. The last chapter in the book gives the reader an all too brief introduction to supercritical fluid extraction, an important technique which deserves far more space than can be given to it in this book.

I have no hesitation in recommending this book. It is well edited, referenced and indexed and provides a reasonably priced, practical introduction to the field.

J. R. Chapman

Electrochemical Detection Techniques in the Applied Biosciences. Volume 1: Analysis and Clinical Applications

Edited by Guy Alain Junter. *Ellis Horwood Series in Biochemistry and Biotechnology.* Pp. 306. Ellis Horwood. 1988. Price £45. ISBN 0 7458 0494 2 (Ellis Horwood); 0 470 21179 2 (Halsted Press).

This book, containing an Introduction, two Chapters, and a good Index, is a most useful survey of the application to bioscience of analytical methods employing electrochemical methods and will be of value to both the novice and expert in this field. Volume 1 is subtitled "Analysis and Clinical Applications" and is divided into two parts, the first of which is a single book and the subject of this review. The first Chapter, subdivided into five Sections, is entitled "*In vitro* Determinations" and the second, consisting of three Sections, is called "*In vivo* Determinations." Each Section has different authorship and is an expanded commentary with a generally extensive list of commendably up to date references.

Vire, Kauffmann and Patriarche are the authors of the first Section in Chapter 1 which is entitled "Conventional and Novel Electrochemical Detection Techniques in Clinical Analysis" and covers the various voltammetric techniques, their problems and applications particularly to the determination of drugs in body fluids. Metal determinations by direct voltammetry, voltammetric stripping and potentiometric stripping methods are surveyed and the Section is concluded by a useful table of relevant stripping analysis applications. The second Section by M. Porthault covers HPLC with electrochemical detection (ECD) and summarises the parameters relevant to these analyses before covering electrochemical electrode systems and techniques, miniaturisation, reaction detectors and applications. Ion-selective electrodes and bioprobes as potentiometric sensors are covered in Sections 3 and 4 of Chapter 1, the authors being P. Nabet and J. L. Romette, respectively. The approaches are essentially practical and commercial rather than theoretical, with the potential of these devices being assessed realistically. The editor of this volume, G. A. Junter, is the author of this Chapter's final Section entitled "Electrochemical Detection Techniques in Clinical Microbiology," which covers conductance and capacitance, redox, dissolved oxygen and pH measurements as indicators of the vital activity or metabolic pathways of microbiological cultures. The editor has set a good example to his co-authors because this Section is an admirable reflection of the approach of the volume as a whole: it is replete with practical examples, results and graphs from the literature, and apart from certain classic citations, most of this Section's 247 references come from the 1970s and 1980s.

Chapter 2 begins with a Section entitled "Carbon Fibre Electrodes" by J. L. Taboureau and P. Blond who start by describing neurochemical transmission and voltammetric techniques using conventional carbon electrodes *in vivo*. Discussion of miniaturisation leads to a description of the use, properties, characteristics and pre-treatment methods for carbon fibre electrodes and the Section concludes with results of some *in vivo* experiments which cause brain concentration changes of catecholamines or 5-HT (serotonin). The longest Section in the volume is "Ion Selective Microelectrodes" by D. Michel and P. Blond in which the practical details of non-commercial construction and *in vivo* use of Li^+, Mg^{2+}, Ca^{2+}, Cl^-, Na^+ and K^+ microelectrodes are described and results discussed with suggestions made about likely future developments considering present limitations. Novel designs including multi-barrel constructions and new neutral carriers are well covered. Glass, antimony and liquid ion-exchanger pH microelectrodes are described in this Section's final 13 pages. The *in vivo* Chapter concludes with "HPLC with Electrochemical Detection" by P. Blond, who concentrates initially on dialysis and perfusion methods of sample collection (including catecholamine, HVA, 5-HIAA and uric acid) and then briefly covers on-line and conventional HPLC - ECD for analysis of such samples before discussing results from the neurochemical and pharmacological literature some of which show impressive sensitivity and potential versatility.

Very rarely it is noticeable that English is not the first language of these authors, but this is a trivial point compared with the commendable quality of coverage and presentation in this very welcome volume.

J. R. Johnson

A Guide to Materials Characterization and Chemical Analysis

Edited by John P. Sibilia. Pp. x + 318. VCH. 1988. Price £25.95; DM75. ISBN 3 527 26867 7.

This is an interesting and unusual book. Staff of the Corporate Laboratories of Allied-Signal Inc. of New Jersey have tried to

produce a guide for novices, and a review for experienced investigators, on the principles and applications of modern analysis and characterisation techniques. The first reaction must be that this is an impossible goal in a book of only 318 pages. And, indeed, some methods are given very short shrift. Functional group analysis, atomic spectrometry, radiochemistry, isotachophoresis(!) and other electrochemical methods are all curiously grouped together in one chapter of only 28 pages. But in this, and most other chapters, the bare essentials are there—an outline of the physico-chemical principles and the equipment used, and some typical applications and results. Inevitably, many topics and details are omitted. The quantitative evaluation of results by statistical means is not discussed at all: the Beer-Lambert law is only covered by implication and there is an assumption that only linear calibration methods are useful. Analytical methods based on biochemical principles (enzymes, antibodies, etc.) are not covered, and fluorescence appears only as a detection method for supercritical fluid chromatography, without an explanation of why there are distinct excitation and emission wavelengths. Each section is complemented usefully by references to books or review articles, although in some instances these references are perhaps not as up to date as they should be. Other signs that some chapters or sections were written originally some years ago appear with the use of cc as a unit of volume, and an appended table that converts, for example, tons to kilograms! Other sections, such as that on ion chromatography, are by contrast very up to date.

A major merit of the book for the average analytical chemist is the coverage given to methods which many of us think about less often than we should. Microscopy (both optical and electron) has a chapter to itself, as do surface analysis (X-ray PES, Auger, SIMS, etc.) and thermal analysis. Two chapters are devoted to the characterisation of synthetic polymers, one to physical testing: all this is very useful material. A final short chapter illustrates the use of computer modelling in fluid dynamics and molecular structures. The relevance of this material is unclear: the applications of computers to simpler calculations might have been covered instead. The production of the book is very clear, with relatively few errors, although an unfortunate victim of a misprint is the Chairman of *The Analyst* Editorial Board! In summary, this is a useful book for any analytical library: I suspect I shall refer to it often, if only as a guide to more detailed sources.

James N. Miller

Spectroscopic Properties of Inorganic and Organometallic Compounds. Volume 21

Senior Reporters G. Davidson and E. A. V. Ebsworth. *A Specialist Periodical Report.* Pp. xv + 509. Royal Society of Chemistry. 1988. Price £120; $240. ISBN 0 85186 193 8.

This volume, which reviews recent literature published up to late 1987, follows exactly the same format as Volume 20 (reviewed in the *Analyst*, 1988, **113**, 1343). It also has the same contributing authors apart from D. G. Anderson who has succeeded H. E. Robertson as an author of the chapter on Gas Phase Molecular Structures Determined by Electron Diffraction. Hence, all major molecular spectroscopic techniques are covered in addition to Mössbauer spectroscopy and electron diffraction, within only slightly more pages than Volume 20. The book presents clearly, with commendably little delay, a vast amount of information, and therefore should be made available to all inorganic chemists and to spectroscopists involved with inorganic and organometallic compounds.

Alan Townshend

Nitrosamines. Toxicology and Microbiology

Edited by M. J. Hill. *Ellis Horwood Series in Food Science and Technology.* Pp. 169. Ellis Horwood. 1988. Price DM180; £64. ISBN 3527 26708 5 (VCH Verlagsgesellschaft); 0 89573 650 0 (VCH Publishers).

The chemistry and determination of *N*-nitrosamines and other *N*-nitroso compounds have been the subject of much work in the 22 years that have elapsed since Magee and Barnes published a review of *N*-nitrosamine carcinogenicity. During the intervening period the substrates considered have ranged from meat through beer and rubber teats to cosmetics and toiletries while the list of compounds considered to be of importance has grown ever longer.

There was a need for much of this hard-won information to be gathered together in a single, readable text and this new book from Ellis Horwood goes a long way towards fulfilling that need.

The title of the book is slightly misleading in that its contributed chapters cover methods of analysis for foods and human body fluids, the chemistry of *N*-nitrosation, endogeneous formation, precursors in the human environment, toxicology and the relationship of *N*-nitroso compounds to human cancer.

All the chapters are well written, with comprehensive, up to date, sets of references.

The bad news is the price, which is likely to deter many of those at whom the book is targetted.

G. M. Telling

Handbook of Basic Tables for Chemical Analysis

Thomas J. Bruno and Paris D. N. Svoronos. U.S. National Bureau of Standards, NBS1R. Pp. 929. U.S. Department of Commerce, National Technical Service. 1988. Price £133; £27 + VAT (Microfiche).

This book consists of two one-inch thick wads of paper fastened into pad form by two large staples through a flimsy yellow paper cover. The immediate response is therefore one of rejection, especially at the price. Inside the book, one's automatic response continues; it is made up of photocopied pages with the authors' names stamped on to the corners of most of the pages with a rubber stamp, and with page numbering in the original handwriting! To cap all this, the quality of photocopying in my copy left much to be desired, with odd pages fading into oblivion on one side or the other.

The multiplicity of tables have been produced in an amateurish fashion on a computer by an operator who does not know how to produce reasonable graphics, and I was surprised to see thanks to the manager of the NBS word processing facility in the preface; it lacks any feel of professional layout.

It will be seen that I was unimpressed by the quality of presentation; it falls very far short of what I would expect from so prestigious a body as the NBS, and I would not allow it from my own much more humble organisation.

Having said all that, it is a fascinating compendium of analytically useful data. Part 1 deals with chromatography, giving information on the properties of carrier gases, supports, support modifiers, stationary phases, adsorbents, derivatising agents and cryogens for gas chromatography, and then on a similarly wide range of component parts of an HPLC system. It goes on to a similar coverage of TLC and SFC, and then begins to cover UV spectrophotometry.

There is no natural break for the commencement of Part 2; it is quite obvious that the assemblers of the pads merely arranged the papers into two equal piles before wielding the

staple gun. The first page of my Part 2 was numbered by hand 470 (not that this does much good; there is no mention of page numbers in the table of contents) and consists of a set of numerical UV absorption spectra for organic solvents from 2-butanol to chloroform.

It contains a further eight pages of such spectra, then proceeds to deal with IR spectroscopy, NMR, mass spectroscopy, atomic absorption and emission and finishes off with a selection of miscellaneous data on conversion factors, physical constants, buffers, etc.

The IR data contain a few poorly reproduced IR spectra and correlation charts for wavenumber *versus* structural groups; there is then similar data for NMR and mass spectra. The atomic spectrometry section has pages on useful standards, the inevitable optimistic list of detection limits presumably culled from manufacturers' literature and then useful tables of spectral interferences for both AAS and AES.

Many modern graduates should find the pages on organic and inorganic group qualitative tests useful as it is rare to find them taught these days, but the inorganic ones in particular would have benefited from a more structured approach and the inclusion of the ammonia group before the ammoniacal hydrogen sulphide group. Nowadays too, I would have included such elements as molybdenum, the rare earths and at least some of the platinum metals.

Overall, there is no doubt that it is an exceedingly useful collection of facts; I only wish that it had been presented in a manner reflecting its value. To me, the least that should have been done, assuming that it was necessary to actually use the raw typescript in this way, was to go over it with an eraser to take out the odd handwritten bits, and to have produced it on at least 80-gm paper instead of the 60 or 70 gm actually used. It could then have been bound in a two or three ring binder at very little greater cost than the two sheets of yellow paper and a couple of staples, and the end result would have been infinitely more pleasing and certainly longer lived—even if only because the owner could have stuck reinforcing rings over the holes! The microfiche version at its much lower price would be very much better value for money assuming that one has a reader, but the logical habitat for a collection of this nature would appear to be on copies of the floppy disks from which it obviously orginated. Coupled with a free text search program it would then be both attractive and much more useful.

R. C. Rooney

ERRATUM

Uses (Proper and Improper) of Correlation Coefficients

Analytical Methods Committee

Analyst, 1988, **113**, 1469

Page 1471, left-hand column, line 21: *for* "$x = 0.1$; $y = 0.01, 0.08, 0.12$" *read* "$x = 0.1$; $y = 0.10, 0.08, 0.12$."

Page 1471, left-hand column, line 26: *for* "The fitted line is $y = 0.027 + 1.024x$" *read* "The fitted line is $y = 0.0027 + 1.024x$."

CUMULATIVE AUTHOR INDEX

JANUARY–JUNE 1989

FIRST FOLD HERE

THE ANALYST READER ENQUIRY SERVICE

For further information about any of the products featured in the advertisements in this issue, write the appropriate number on the postcard, detach and post.

FOLD HERE

THE ANALYST READER ENQUIRY SERVICE

JUNE'89

For further information about any of the products featured in the advertisements in this issue, please write the appropriate number in one of the boxes below.
Postage paid if posted in the British Isles but overseas readers must affix a stamp.

PLEASE USE BLOCK CAPITALS LEAVING A SPACE BETWEEN WORDS *Valid 12 months*

1 NAME

2 COMPANY

PLEASE GIVE YOUR BUSINESS ADDRESS IF POSSIBLE. IF NOT, PLEASE TICK HERE ☐

3 STREET

4 TOWN

5 COUNTY
POST CODE

6 COUNTRY

7 DEPARTMENT
DIVISION

8 YOUR JOB TITLE
POSITION

9 TELEPHONE NO

OFFICE USE ONLY RECD PROCD

FOLD HERE

Postage will be paid by Licensee

Do not affix Postage Stamps if posted in Gt. Britain, Channel Islands, N. Ireland or the Isle of Man

BUSINESS REPLY SERVICE
Licence No. WD 106

Reader Enquiry Service
The Analyst
The Royal Society of Chemistry
Burlington House, Piccadilly
LONDON
W1E 6WF
England

ROYAL SOCIETY OF CHEMISTRY

CHEMICAL SAFETY DATA SHEETS

Volume 1 – Solvents

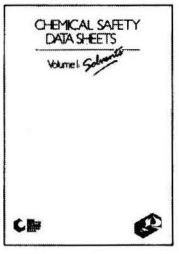

All solvents have hazardous properties, yet find ubiquitous use in industry and are among the most widely used chemicals in society.

This important new book aims to cover every aspect of the hazards of these solvents, providing invaluable information in a concise but readable format, with full references for further investigation if required.

Chemical Safety Data Sheets Volume 1 – Solvents provides up-to-date information on over 100 representative solvents. Included will be the full range of CHEMICAL, PHYSICAL AND BIOLOGICAL hazards likely to be encountered by their use, as well as safe handling, emergency precautions, safe disposal procedures and legislation governing their use regarding exposure, transportation and labelling, plus much more.

It provides a concise overview of the related hazards of compounds, in a uniform style and is fully indexed by chemical names, synonyms, class name, trade names and CAS Registry No., with a special 'flash point' index.

Brief Contents:
The data sheets are arranged in alphabetical order, and cover the following class headings: Glycols; Alcohols; Esters; Amines (including Nitro Compounds); Ethers; Chlorinated Hydrocarbons; Aromatic Hydrocarbons; Ketones.

ISBN 0 85186 903 3 **Published 1989**
Softcover 300 pages **Price £39.95 ($89.00)**

Volume 2 is scheduled for publication mid 1989 and will be entitled *Main Group Metals and their Compounds*.

SOLVENTS IN COMMON USE: HEALTH RISKS TO WORKERS

This key handbook contains essential information on ten of the most commonly used solvents and is a must for safety officers and all workers in the EEC at risk from exposure to these solvents.

The following information is given for every solvent covered: Chemical Abstracts name; synonyms and trade names; CAS Registry Number; NIOSH number; chemical and structural formulae; occurrence; spectroscopic data; measurement techniques; conditions under which the solvent is put on the market; storage, handling and use precautions; fire hazards; hazardous reactions; emergency measures in the case of accidental spillage; first aid; physio-chemical properties; toxicity; medical/health surveillance; occupational exposure limits.

The ten solvents covered are:
Acetone; Carbon Disulphide; Diethyl Ether; 1,4-Dioxane; Ethyl Acetate; Methanol; Nitrobenzene; Pyridine; Toluene; Xylene.

The information contained in this extremely useful book was compiled by an expert committee of the Royal Society of Chemistry for the Commission of European Communities.

ISBN 0 85186 088 5 **Published 1988**
Hardcover 308pp **Price £60.00 ($120.00)**

ROYAL SOCIETY OF CHEMISTRY
Information Services

For further information, please write to:
Royal Society of Chemistry,
Sales and Promotion department,
Thomas Graham House,
Science Park,
Milton Road,
Cambridge CB4 4WF. U.K.

To Order, please write to:
Royal Society of Chemistry, Distribution Centre, Blackhorse Road, Letchworth, Herts SG6 1HN. U.K.
or telephone (0462) 672555 quoting your credit card details.
We can now accept Access/Visa/MasterCard/Eurocard.

RSC Members are entitled to a discount on most RSC publications and should write to:
The Membership Manager,
Royal Society of Chemistry,
Thomas Graham House,
Science Park, Milton Road,
Cambridge CB4 4WF. U.K.

ANALAO 114(6) 653–756 (1989) June 1989

The Analyst

The Analytical Journal of The Royal Society of Chemistry

CONTENTS

Typeset and printed by Black Bear Press Limited, Cambridge, England